Antimalarial Activity of 5´,N^6- and 3´,N^6-Disubstituted Adenosines

Polymer-Assisted Synthesis, Analytical Characteristics, and Biological Evaluation

DISSERTATION

Zur Erlangung des Doktorgrades
der Universität Hamburg
Fachbereich Chemie

vorgelegt von

Claudia Herforth
aus Hamburg

Hamburg 2002

Referees: Prof. Dr. A. Link
Prof. Dr. D. Geffken

Defense of doctoral thesis: 27.11.2002

Danksagung

Die vorliegende Arbeit entstand in der Zeit von August 2000 bis Oktober 2002 am Institut für Pharmazie unter der Leitung von Herrn Prof. Dr. Andreas Link in Zusammenarbeit mit Herrn Prof. Dr. Detlef Geffken. Meinem Doktorvater, Herrn Prof. Dr. Andreas Link, möchte ich an dieser Stelle für die Überlassung des Themas, die vorbildliche Betreuung und seine stete Hilfsbereitschaft danken. Mein besonderer Dank gilt Herrn Prof. Dr. Detlef Geffken für seine großzügige Förderung, sowie für die Übernahme des Koreferats.

Sehr dankbar bin ich Herrn Dr. Stephan Franke für seine unermüdliche Hilfsbereitschaft und freundliche Unterstützung bei der Messung von Hochauflösungsspektren, sowie der Durchführung von LC/MS^n Experimenten. Bei Prof. W. A. König bedanke ich mich für die großzügig zur Verfügung gestellten Meßzeiten am Finnigan MAT XL95-Massenspektrometer.
Dr. Wolfgang Thimann, Dr. Abolfasl Golisade und Philipp Heidler möchte ich ganz herzlich für ihre fundierten Ratschläge und die nette Zusammenarbeit danken.
Danken möchte ich unseren Kooperationspartnern Jomaa Pharmaka GmbH, Gießen, Prof. Dr. Erik de Clercq, Katholike Universiteit Leuven, Belgien, Frau Prof. Dr. Christa E. Müller, Universität Bonn und Tibotec, Mechelen, Belgien für die Zusammenarbeit und die Bereitstellung der biologischen Daten.
Für die Hilfe beim Lesen der Korrekturen danke ich Deborah Roger, Dr. W. Thimann und Philipp Heidler. Des weiteren gilt mein Dank den Mitarbeitern des Instituts für Pharmazie, die zum Gelingen dieser Arbeit beigetragen haben.

Besonders danke ich der Deutschen Forschungsgemeinschaft für die finanzielle Förderung durch ein Promotionsstipendium im Rahmen des Graduiertenkollegs 464 Glycoconjugate: Darstellung, Analyse, Struktur und Funktion, unter der Leitung von Herrn Prof. Dr. Bernd Meyer.

List of Abbreviations

Ac_2O	acetic anhydride
ADP	adenosine-5´-diphosphate
AdoMet	*S*-adenosylmethionine
AdoMetDC	*S*-adenosylmethionine decarboxylase
AMP	adenosine monophosphate
ATP	adenosine-5´-triphosphate
CC_{50}	50% cytotoxic concentration
CCl_4	tetrachloromethane
CH_2Cl_2/DCM	dichloromethane
cPASP	convergent polymer-assisted solution-phase
CMR/R	complementary molecular reactivity/molecular recognition
d	doublet
δ	chemical shift
DEAD	azo dicarboxylate diethyl ester
DIC	*N*,*N*-diisopropylcarbodiimide
DIPEA	*N*,*N*,*N*-ethyldiisoproylamine (diisopropylethyl-amine)
DMAP	4-dimethylaminopyridine
DMF	*N*,*N*-dimethylformamide
DMSO	dimethylsulfoxide
DNA	deoxyribonucleic acid
DOXP	1-deoxy-D-xylulose-5-phosphate
etc.	et cetera
ESI	electrospray ionisation
EtOAc	ethyl acetate
EtOH	ethanol
FAD	flavin-adenine dinucleotide
Fmoc	9-fluorenylmethyloxycarbonyl
GAP	glyceraldehyde-3-phosphate
GAPDH	glyceraldehyde-3-phosphatedehydrogenase
h	hour
HIV	human immunodeficiency virus
HOBt	1-hydroxy-1-*H*-benzotriazole
HPLC	high performance liquid chromatography
IC_{50}	50% inhibitory concentration

IR	infrared
IPP	isopentenyl diphosphate
J	coupling constant
LC	liquid chromatography
m	multiplet
M	exact molecular mass
min	minute
MeOH	methanol
MEP	2-*C*-methyl-D-erythritol-4-phosphate
MPLC	medium pressure liquid chromatography
MS	mass spectrometry
MW	molecular weight
NAD	nicotinamide-adenine dinucleotide
NADP	nicotinamide-adenine dinucleotide phosphate
NH_4Cl	ammonium chloride
NMP	1-methylpyrrolidone
NMR	nuclear magnetic resonance
ODC	ornithine decarboxylase
PASP	polymer-assisted solution-phase
P. falciparum	*Plasmodium falciparum*
PfEMP	*Plasmodium falciparum* erythrocyte membrane proteine
PfNT	*Plasmodium falciparum* nucleoside transporter
Ph_3P	triphenylphosphine
q	quartet
RNA	ribonucleic acid
s	singlet
SPOS	solid-phase organic synthesis
SPPS	solid-phase peptide-synthesis
SPR	surface plasmon resonance
t	triplet
T. b. brucei	*Trypanosoma brucei brucei*
THF	tetrahydrofuran
TLC	thin layer chromatography
UV	ultraviolet
WHO	World Health Organization

Contents

1 Polymer-Assisted Solution-Phase (PASP) Approach for the Synthesis of Antimalarials

1.1 Introduction

According to estimations by the World Health Organization, 3.5 billion people suffer from one or more parasitic infections, with the greatest causes of morbidity being attributed to malaria[1]. The pathogen *Plasmodium falciparum*, the causative agent of malaria tropica, infects approximately 400 million individuals each year, resulting in 1-2 million deaths annually. As the parasites resistance to conventional antimalarial drugs is increasing the need for novel chemotherapeutic approaches in the fight against the multiresistant *P. falciparum* pathogen is unquestionable.

Our search for inhibitors of *P. falciparum* started from the fact that adenosine binding motifs are associated with a broad array of therapeutically significant targets in biological systems. On the one hand, adenosine is a well-known constituent of relevant bioactive molecules being involved in many physiological processes[2,3]. By this means, adenosine is related to bioactive nucleotides (e.g. ATP, ADP, AMP), coenzymes (e.g. NAD, FAD, coenzyme A), biochemical methylating agents (e.g. *S*-adenosylmethionine), second messengers (e.g. cAMP), and RNA. On the other hand, adenosine regulates various physiological functions by stimulating specific cell membrane receptors[2,4-6]. For instance, adenosine is involved in the regulation of cardiac ischemia, inflammation, neurodegeneration, asthma, psychosis, and anxiety[3,4].

Adenosine receptors, enzymes that utilize adenosyl-containing substrates, not to mention nucleoside-related targets, share the opportunity of rational design of ligands starting from the adenosine scaffold. Consequently, the systematic modification of adenosine represents a promising strategy to identify receptor ligands, enzyme inhibitors, or nucleoside function modifiers.

The adenosine molecule (**1**) consists of the heterocycle 6-aminopurine (adenine) connected to the pentofuranose ribose via a β-N-glycosidic bond between the N^9-atom and the anomeric carbon of the sugar moiety. Due to its low molecular weight and the amount of hydrogen bond donors and acceptors, adenosine represents a ´lead structure´ like compound.

Derivatizations of the adenosine molecule with retained scaffold characteristics are conceivable in the following positions (figure 1).

Figure 1. Conceivable derivatizations of adenosine.

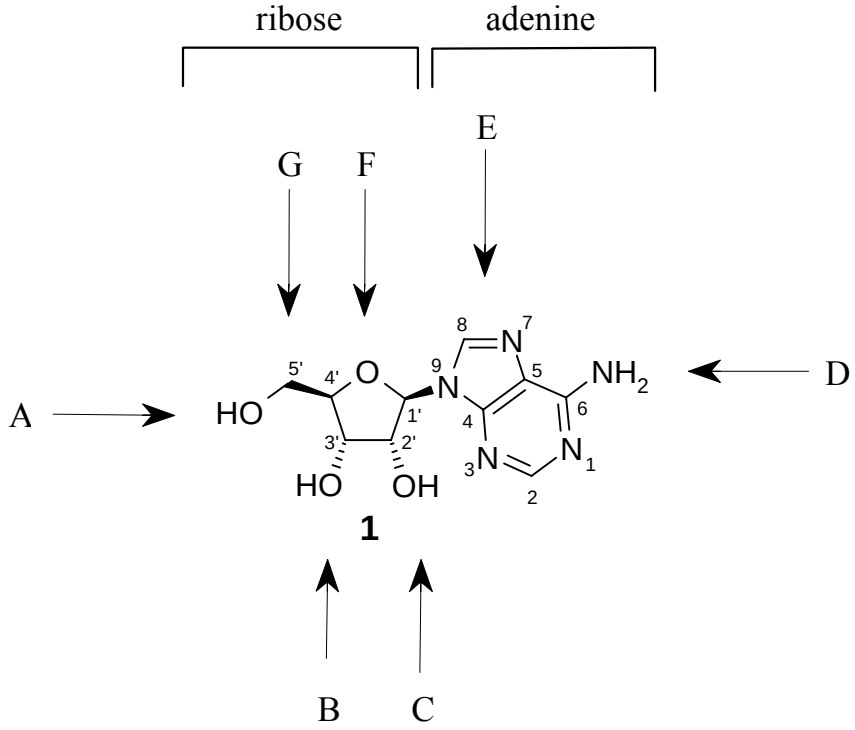

Incorporation of substituents as well as replacement by heteroatoms or carbon atoms at the N^6-position (D) increases the binding affinity in some cases and the stability of adenosine in biological systems, generally[2,3]. Attachment of substituents to hydroxyl functions (A-C) forming corresponding ethers or carboxylic acid esters leads to the loss of hydrogen bond donor characteristics. Further, the hydrogen bond donor is converted into a hydrogen bond acceptor, possibly leading to repulsion of peptidic hydrogen bonding to the hydrogen bond acceptor of the protein. To overcome these difficulties, a promising concept to conserve the hydrogen bond characteristics of adenosine represents the replacement of hydroxyl by amino functions and subsequent amido substitution.

Modifications of the heterocyclic system incorporating substituents at the C2-position (E) were already shown to enhance the binding affinity in special cases[3]. Nonetheless, this enhancement is associated with an undesirable change in the orientation of the base versus the ribose ring. Replacement of the tetrahydrofuran ring by cyclopentane or other similar heteroatoms (F) also displays an effect on the conformation and fixation of the carbohydrate ring structure leading to an altered orientation of the

substituents. Either replacement of the methylene group (G) by e.g. homologous alkyls, substitution with halogen atoms or oxidation of the primary alcohol to the corresponding carboxylic acid represents further possible modifications of the adenosine scaffold.
Approaches A-D allow for the straightforward incorporation of diversity fragments establishing nucleoside libraries of diverse adenosines. Thus, they are suited for the preparation of ´lead structure´ like adenosines, whereas modifications in E-G generally are used for the lead structure optimization on a later stage of drug design.
Approaches A-D are especially suited for incorporating lipophilic residues into the adenosine molecule intended for the exploration of hydrophobic protein pockets. Following this idea, adenosine derivatives modified in N^6- and/or 2´-position have been investigated regarding their antiparasitic effects. Nucleophilic substitution of 1-(6-chloropurin-9-yl)-β-D-1-deoxyribofuranose with various amines furnished three series of N^6-substituded adenosines, displaying moderate antimalarial activity versus the multi-resistant *P. falciparum* strain Dd2[7]. 2´-Amido-2´-deoxyadenosines proved to be inhibitors of trypanosomal glyceraldehyde-3-phosphate dehydrogenase (GAPDH)[8-10]. Additional modification in the N^6-position lead to a substantial increase in the inhibitory potency of N^6-alkyl-2´-amido-2´-deoxyadenosines against the GAPDH of the parasite *Trypanosoma cruzi*[11-14]. Thereby, the introduction of a 1-naphthylmethyl group in the N^6-position was found to be especially suited.

Within the course of this work, the polymer-assisted synthesis of nucleoside libraries of modified ´lead structure´ like 5´,N^6- and 3´,N^6-disubstituted adenosine derivatives is outlined. The in vitro antimalarial activity of 38 disubstituted adenosine derivatives and eight adenosine analogs was investigated. Conclusions along structure-activity relationships to define general structural features involved in the antimalarial activity are discussed.
Furthermore, a polymer-assisted protocol for the chemoselective biotinylation of aminonucleosides, ready to be used in a surface plasmon resonance (SPR) assay is described. Biotin labeled amino-modified adenosine derivatives analyzed by SPR can be employed for the study of molecular interactions with biological targets, revealing potential metabolic targets against the *P. falciparum* pathogen on a molecular basis.

1.2 Synthetic Approach

A simple and high yielding methodology for the preparation of a nucleoside-based library was needed. Since time-consuming protection and deprotection schemes and necessary chromatographic purification steps often hamper common syntheses in solution and since methods for generating carbohydrate-modified nucleoside-based combinatorial libraries are limited, our group established a polymer-assisted solution phase protocol for the preparation of modified adenosine analogs[8,15].
For the synthesis of diverse adenosine derivatives, first the preparation of a common scaffold is required. Appropriate nucleoside scaffolds (see exemplarily scaffold **2**, figure 2) were prepared on a larger scale in solution. Since the common scaffold can be used to prepare a large number of highly diverse derivatives, time-consuming preparation and purification are acceptable.

Figure 2. Amino-modified nucleoside template for the synthesis of 5′,N^6-disubstituted adenosine derivatives.

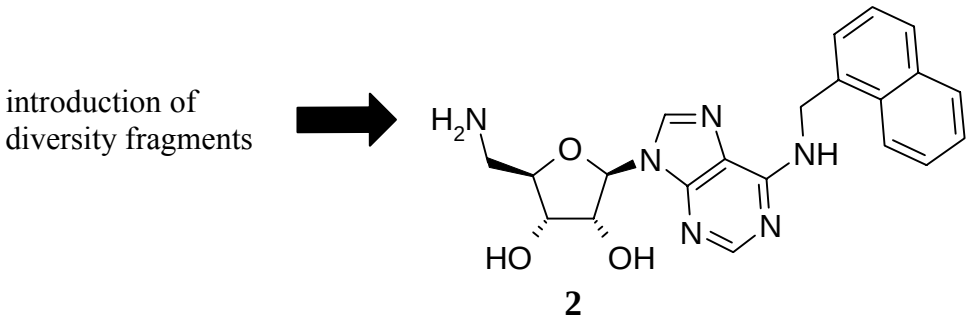

2

Currently, two strategies for the introduction of amide substituents to primary or secondary amino groups of common scaffolds can be distinguished: (A) Carbodiimide-mediated acylation in solution and (B) polymer-assisted solution-phase (PASP) acylation with appropriately acylated safety-catch resins. Both approaches have proven to be suitable for the acylation of 2′-amino-2′-deoxyadenosine derivatives in high yield and purity[8,13,15].
For the following reasons, method (B) was selected to access arrays of adenosine analogs for biological evaluation. PASP synthesis has the added benefit of merely filtering off the solid support to obtain the desired product in nearly quantitative yield and in typically greater than 95% purity as determined by HPLC, according to our earlier findings and confirmed by

Bressi et al., lately[8,13,15]. In addition, the PASP protocol allows for the chemoselective introduction of diversity fragments into the amino-deoxy-sugar moiety of the common scaffold with no protecting group operations for the hydroxyl groups necessary. Due to these advantages, additional steps needed to prepare resins of type **3**, including the incorporation of the safety-catch acylating agent and the activation step are thus tolerated.

1.2.1 Polymer-Assisted Solution-Phase (PASP) Approach for the Synthesis of Adenosine Derivatives

PASP synthesis allows for the preparation of a large scale of derivatives of a common scaffold (see exemplarily carbohydrate-modified nucleoside **2,** scheme 1) ready for biological testing without demanding purification steps. Carboxylic acid equivalents are immobilized via in situ anhydride formation to the Kenner safety-catch linker attached to aminomethylated polystyrene leading to appropriate polymer-bound N-acylsulfonamides. Subsequent activation of the sulfonamide linker by cyanomethylation with bromoacetonitrile provides polymer-bound N-cyanomethyl analogs (**3**). Activated N-cyanomethyl analogs can finally be cleaved by nucleophils (**2**) under mild reaction conditions to be chemoselectively transferred to primary or secondary amino moieties of common scaffolds yielding appropriate amides (see exemplarily acylated nucleoside **4**, scheme 1).

Scheme 1. PASP synthesis of 5′,N^6-disubstituted adenosine derivatives.

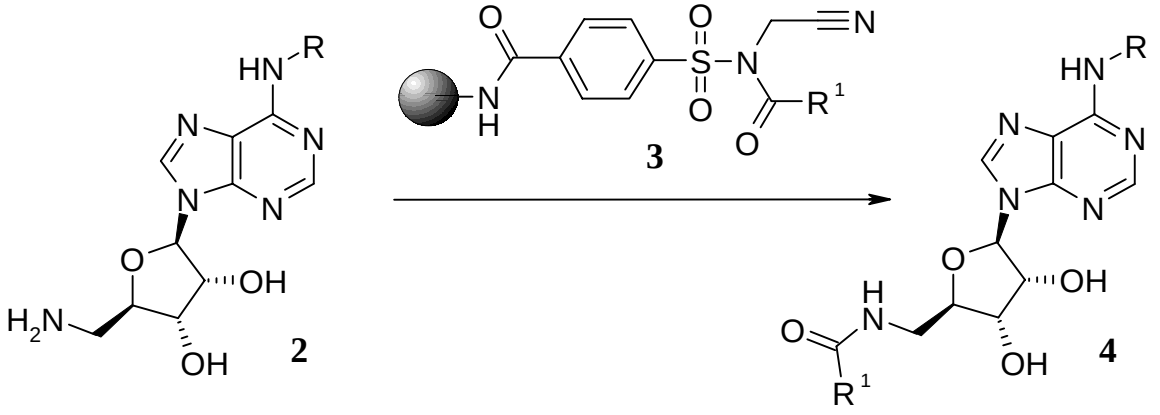

R = 1-naphthylmethyl

Three different activation methods employing diazomethane, bromo-acetonitrile and DEAD/Ph_3P, respectively, are commonly applied. In good agreement to our observations Backes et al. found that the cyanomethylated

analog of the sulfonamide linker was significantly more susceptible to nucleophilic cleavage than the corresponding methyl derivative[16]. Furthermore, when activating the Kenner linker with diazomethane in THF formation of byproducts were observed in many cases. The Mitsunobu reaction is the underlying rational of the activation with DEAD/Ph_3P[17]. However, this rational could not be established for the transfer of activated building blocks to sugar-modified nucleoside scaffolds.
Overall, PASP synthesis leads to undemanding product isolation since the excess of polymer-bound reagent (**3**) that is necessary to drive the reaction to completion can be removed by simple filtration, whereas the final compound (**4**) stays in solution. This allows for the convenient assessment of structurally highly diverse amides in a short period of time exhibiting high yields and purities.

1.2.1.1 Kenner Safety-Catch Linker

The Kenner safety-catch linker invented by Kenner[18] and modified by Backes and Ellmann[16,19,20] combines two major features: The safety-catch concept as well as N-selective acylation characteristics.
The attachment of the building block to the linker has to be reversible due to the fact that at the end of the reaction sequence the building block has to be released from the polymer support. Within the safety-catch concept the linker is maintained in a stable form during synthesis and is then activated by discrete chemical modification immediately prior to cleavage. Polymer-bound N-acylsulfonamides possess a high stability in acidic and strong nucleophilic reaction media and at elevated temperatures, and thus play a key role in the reaction pattern. This property enables to work under drastic reaction conditions so that a wide range of on-bead modifications is possible. Alkylation of the safety-catch linker with electron withdrawing cyanomethyl groups leads to a highly reactive analog that can easily be cleaved with a broad range of nucleophils.

It was recently shown that the Kenner safety-catch linker is well suited for the high yielding chemoselective acylation of amino groups in 4-(3-aminopropyl)morpholine, morpholine, benzylamine, piperidine, cyclohexyl-amine, *tert*-butylamine, aniline, leucine methylester, 7-amino-4-methyl-cumarine, and for the synthesis of protected head-to-tail cyclic peptides[16,20,21]. Link et al. first demonstrated the N-selective acylation properties of the Kenner linker acylating multifunctional amino-deoxy-sugar moieties of nucleoside analogs in the presence of primary and secondary

hydroxyl groups[15]. No protecting group operations of primary and secondary hydroxyl groups were needed.

In addition, the chemoselective acylation with activated carboxylic acid equivalents, attached to the Kenner safety-catch linker (**3**) has shown high potential for the discrimination between two primary amino functions in multifunctional templates[13]. Derived from our findings, Gelb et al. demonstrated that the reaction of activated N-acylsulfonamides with amino groups displaying different chemical properties could be fine-tuned by variation of the reaction temperature. At room temperature, only amino functions connected to a primary carbon atom react with the immobilized and activated polymer-bound N-acylsulfonamide. When increasing the temperature up to 55 degrees centigrade, primary amino groups bound to a secondary carbon atom undergo complete reaction, concurrently.

This adjustable chemoselectivity is impressive because it is markedly superior to the results hitherto reported on enzymatically-catalyzed transformations of similar diamino-dideoxy nucleosides to the corresponding monoamides. The first report on enzymatic N-selective acylation of 3′,5′-diamino-3′,5′-dideoxypyrimidine nucleosides using N-selective acylation mediated by *Candida antarctica* lipase B, *Pseudomonas cepacia* lipase (PSL) or immobilized PSL was published by Lavandera et al.[22]. The reaction produced in most of the cases reported mixtures of possible monoamides and the diamide.

In general, promising reagents or reaction schemes carried out in solution are transferred to solid-phase or polymer-assisted protocols. In consideration to the N-selectivity of N-acylsulfonamides, the development was vice versa. Kondo et al. confirmed the N-selective acylation properties of N-acylated sulfonamides in solution acylating primary and secondary alkylamines and *N*-methylbenzylamine with *N*-acyl-*N*-mesylanilines in THF[23]. Further promising N-selective acylation reagents in solution overcoming competing O-acylation of neighboring hydroxyl functions were reported recently[24,25]. Bogdan et al. demonstrated the N-selective acylation of aliphatic primary or secondary amines with 3-acyl-1,3-diaryltriazenes in the presence of aliphatic or aromatic hydroxyl, of thiol and of aromatic amino groups. Kim et al. reported on the chemoselective amide formation of amino alcohols with acid chlorides in the presence of MgO in THF/H_2O. Both approaches furnished N-acylated products in good to excellent yield and purity.

1.2.1.2 Applications of PASP Protocols

The underlying rational of the polymer-assisted approach outlined above is the application of polymer-bound reagents/building blocks for the additional introduction of a diversity fragment to the structure of the target compound within the cleavage step leading to the appropriate N-acylated final compound. Following the same approach, Kryatova et al. established a polymer-assisted protocol for the synthesis of oligonucleotides containing a 2´-acylamido-2´-deoxyuridine residue in their 3´-terminus[26].

Advantages of the PASP methodology described are also applied for other reaction purposes: (A) After activation of the sulfonamide linker, intramolecular attack of a nucleophil upon the linkage functionality can liberate the target compounds from the polymer support facilitating the synthesis of cyclic compounds[20]. (B) In contrast to the use of polymer-bound building blocks establishing final compounds, polymer-bound reagents can also be used as simple reagents within a synthesis sequence; e.g. for the synthesis of 2-deoxyglycosides four different polymer-bound reagents and activators, respectively, for glycal activation, glycosidation, de-iodination, and O-desilylation were employed[27]. (C) Finally, polymer-bound reagents can be used as scavenger reagents. Unreacted starting materials or excess reagents can be removed by treatment with polymer-bound reagents and subsequent filtration of the resin beads[28]. For establishing benzopyran libraries and synthesizing dipeptide *p*-nitroanilides and dipeptide diphenyl phosphonates, polymer-bound reagents were employed as scavengers and as reagents within a synthesis pathway[29,30]. Weidner et al. reported on the principles of complementary molecular reactivity/molecular recognition (CMR/R) within a PASP setting[31]. CMR/R is used as a solution-phase purification strategy employing resins with functionalities complementary to those of reagents in solution and formed byproducts requiring resin sequestration. The same resin is used for sequestration of excess reagents and formed byproduct at the same time. Again the formed polymer adduct is removed from the reaction mixture by simple filtration yielding the pure product.

All strategies mentioned afford products/intermediates in good to excellent yield and/or purity without tedious workup and product isolation using excess polymer-bound reagents to drive reactions to completion followed by a simple filtration step to isolate products/intermediates.

1.2.2 Convergent Polymer-Assisted Solution-Phase (cPASP) Approach for the Synthesis of Adenosine Derivatives

On the contrary to PASP chemistry, where only unchanged diversity fragments are transferred to the target amine, diversity of the immobilized building block is achieved by on-bead modification of the attached residues based on solid-phase organic synthesis (SPOS) principles. The full potential of the acylating species of type **3** can be exploited, when modifications of the carboxylic acid prior to activation are envisioned. The option to synthesize diverse carboxylic acid equivalents directly on the linker, that ensures good acylating properties after cyanomethylation, is thus the most striking advantage of this concept. The additional steps needed (immobilization of the Kenner safety-catch linker/carboxylic acid equivalents and activation prior to cleavage) therefore pay off since the degree of diversity obtainable increases significantly.
For this convergent assembly of ´solid-phase´ modified and solution-phase transferred building blocks we suggested the term convergent polymer-assisted solution-phase (cPASP) amidation[32]. This protocol combines considerable advantages over strategies (SPOS and PASP principles) to access amide libraries by making use of catch-and-release linkers reported so far.
A similar convergent protocol was applied synthesizing peptide vinyl sulfone and peptide epoxyketon proteasome inhibitors[33]. The Kenner safety-catch concept was utilized for the on-bead construction of the building block followed by its transfer to the amino function of the target molecule in solution.

1.2.3 Solid-Phase Organic Synthesis (SPOS)

Solid-phase organic synthesis is employed in a broad variety of applications. From its roots in Solid-Phase Peptide Synthesis (SPPS)[34] SPOS to date is expanding to synthesize virtually all kinds of small organic molecules (such as polyamines[35], heterocyclic compounds like imidazoles[36], prolines[37], isoxazoles and isoxazolines[38], carbohydrates[39], and glycopeptides[39]). Since excess reagents that are necessary to drive the reactions to completion can be used and immobilized products can be purified by simple filtration, SPOS represents a key tool in combinatorial chemistry aimed at the synthesis of large compound libraries[40,41].
The underlying principle of SPOS is that the product always stays attached to the resin throughout the synthesis. Although a wide variety of compounds

can be created, all solid-phase syntheses share a common approach. Initially, the starting material is reversibly anchored via an appropriate linker to the polymer support prior to initiation of the synthesis sequence. On-bead modifications of the attached building block using typical SPOS modifications (such as amide bond forming reactions, condensation reactions, heterocycle forming reactions etc.) yield stepwise the product still attached to the polymer support. At last, cleavage leads to bond breakage liberating the product into solution.
Again, in a solid-phase setting linkers are used to attach building blocks or intermediates onto the solid support and to release them into solution along cleavage. Thus, the linker has to be stable during the course of reaction and at the same time highly reactive during cleavage being sensitive to certain reaction conditions (orthogonality principle). A careful choice of the linker is crucial considering appropriate reaction conditions during cleavage compatible with the final compound and assay. Due to the covalent linkage of the building block to the polymer support, each compound in a library obtained by solid-phase protocols generally displays the same structural feature. Depending on the linker used, final compounds will all be amines, phenols, acids etc.
The main difference of cPASP synthesis compared to SPOS consists of the transformation of the unreactive polymer-bound building block into a reactive intermediate, enabling the introduction of an additional diversity fragment during cleavage. In both approaches, final compounds are obtained after cleavage in solution. However, the cleavage reagent that is necessary to release the final compound during the SPOS sequence has to be removed.

1.3 Biological Targets

1.3.1 The *Plasmodium falciparum* Pathogen

The life cycle of the *P. falciparum* parasite depends on two hosts (the human and the anopheles mosquito host) and the alteration of generation. When entering the human host in form of sporozoites, the parasite initially undergoes asexual exoerythrocytic replication in the liver. Inside of hepatocytes, asexual growth of sporozoites leads to polycaryotic schizonts generating up to 30,000 merozoites, which can invade red blood cells on release from the liver. Merozoites initiate the asexual erythrocytic cycle that is responsible for the clinical symptoms of malaria. Within the erythrocytes,

schizonts are generated followed by bulk disintegration of erythrocytes (going along with fever) and renewed attack of erythrocytes. After several cycles a small portion of these asexual parasites undergo gametocytogenesis. After changing the host, the sexual replication of the parasite including gametogenesis, fertilization, and meiosis takes place in the anopheles mosquito. Finally, sporozoites are generated within the oocyst, transferred to the saliva, and transmitted to the human host[42,43].

The life cycle of *P. falciparum* can be interrupted at several stages, which considerably differ regarding their biochemical and metabolic activities. Whereas sporozoites, merozoites, and gametocytes barely display metabolism, schizonts exhibit a high metabolic activity digesting cell components of hepatocytes and erythrocytes. Thus, chemotherapy of existing drugs mainly focuses on the inhibition of schizonts. For example, quinolines (e.g. chloroquine, amodiaquine) and related arylalcohols (e.g. halofantrine, lumefantrine) hamper the parasite growth during the asexual erythrocytic replication, inhibiting a haem-polymerase located in the lysosomal food vacuole. Antifolates (e.g. primethamine, proguanil) acting in the cytosol of the parasite inhibit the dihydrofolic acid, whereas atovaquone/proguanil hamper the cyt *c* reductase in the mitochondrion of the parasite. Common antibiotics (such as tetracyclines and clindamycines) inhibit the protein biosynthesis. These drugs hinder the parasite growth and are used increasingly in combination with other antimalarials. On the contrary, artemisins (e.g. artemether, arteether) act against gametocytes, the sexual stages of the parasite. Primaquine exhibits activity against extraerythrocytic forms and gametocytes[44].

Due to rapidly spreading resistance against existing drugs, it is crucial to develop new drugs attacking novel targets in the metabolism of the malaria pathogen. Thereby, the efficacy and specificity of anti-infective drugs rely on their ability to interfere with aspects of the metabolism that differ significantly from the human host. New metabolic targets include: (A) Unexploited targets in the food vacuole including plasmepsin aspartic protease and falcipain cysteine protease associated to haemoglobin degradation; (B) plastid DNA replication and transcription, polyamine biosynthesis and the non-mevalonate isoprenyl biosynthesis located in the apicoplast of the parasite; (C) glycolysis (e.g. lactate dehydrogenase) and the nucleotide biosynthesis situated in the cytosol; (D) inhibition of transport mechanisms at the parasite plasma membrane[44].

Polyamines are important for cell differentiation and cell growth. Since parasitic protozoa obtain polyamines either by de novo synthesis (*P. falciparum*) or by accumulating them across their plasma membranes (e.g. *Leishmania donovani*, *Leishmania mexicana*), inhibition of specific enzymes of the polyamine pathway or of transporter proteins involved in the uptake of polyamines into parasites represent promising targets for their chemotherapy[45,46].

In *P. falciparum*, the 1-deoxy-D-xylulose-5-phospate/2-*C*-methyl-D-erythritol-4-phosphate (DOXP/MEP) pathway has been discovered as an alternative mevalonate-independent pathway for the biosynthesis of isoprenoides and thus has been suggested as a new target for antimalarial therapy[47]. Since *P. falciparum* is incapable of *de novo* purine synthesis, preformed purines are transported from the host into the parasite via a nucleoside transporter from *P. falciparum* (PfNT1). Inhibition of PfNT1 with pyrimidine nucleosides and analogs seems to be promising within the asexual stages of the *P. falciparum* life cycle[48]. *P. falciparum* erythrocyte membrane proteins (PfEMP) are responsible for the adhesion of infected erythrocytes to endothelial cells guaranteeing the multiplication of the parasite. Using antibodies to prevent the PfEMP interaction with endothelial tissue is a promising strategy[49]. The phospholipid metabolism represents an excellent target for the chemotherapy of malarial infection, essential for the parasite and at the same time absent from normal mature human erythrocytes[50].

Since enzymes that utilize adenosyl-containing substrates allow for rational design of ligands starting from the adenosine scaffold, *S*-adenosylmethionine decarboxylase (an adenosyl-containing enzyme within the polyamine pathway) and the DOXP reductoisomerase (with NADPH as adenosyl-containing coenzyme within the DOXP/MEP pathway) seemed to be promising metabolic targets (see below) for 5′,N^6- and 3′,N^6-disubstituted adenosines.

1.3.1.1 S-Adenosylmethionine Decarboxylase (AdoMetDC)

The polyamines spermidine (1,8-diamino-4-azaoctane), spermine (1,12-diamino-4,9-diazadodecane) as well as the precursor putrescine (1,4-diaminobutan) are essential for cell differentiation and cell proliferation[51]. Within the biosynthesis of polyamines consisting of the decarboxylation of ornithine and subsequent attachment of aminopropyl moieties, ornithine decarboxylase (ODC) and AdoMetDC represent the key enzymes (scheme 2). Whereas ODC is directly involved in the polyamine pathway AdoMetDC

decarboxylates *S*-adenosylmethionine (AdoMet) furnishing decarboxylated AdoMet (dc-AdoMet), that provides the aminopropyl group.

Scheme 2. Polyamine pathway.

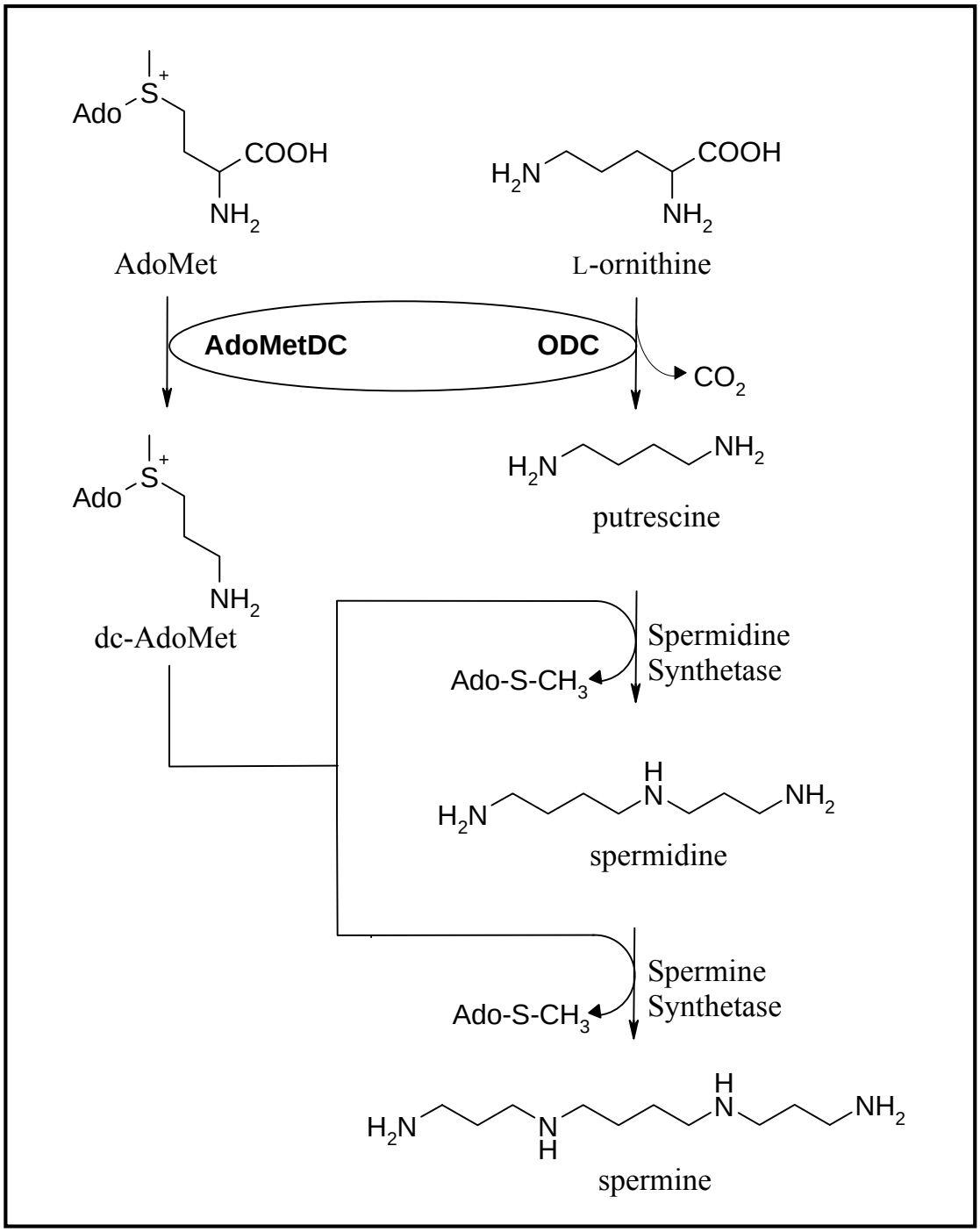

In some parasitic organisms, additional enzymes that are not present in the host cell can be found. In all organisms investigated so far ODC and AdoMetDC are regulated individually with both enzymes displaying low stability. On the contrary, a unique rather stable bifunctional ODC/

AdoMetDC was found in *P. falciparum*[51] providing a possible target in the metabolism of *P. falciparum* for the design of new antimalarial drugs. This outcome is of special interest since human erythrocytes contain only traces of polyamines and lack active biosynthetic enzymes[52].
Previous reports revealed that inhibiting the polyamine biosynthesis as well as utilizing polyamine analogs leads to antiparasitic and antitumor activity[53,54]. First promising inhibition studies of 5´-amino-modified adenosines as structural analogs of dc-AdoMet as well as inhibitors against AdoMetDC have been performed by Kolb et al.[55]. Thus, the inhibition of AdoMetDC as a potential metabolic target of the *P. falciparum* parasite by 5´,N^6-disubstituted adenosines seemed promising and was investigated within this project.

1.3.1.2 1-Deoxy-D-Xylulose-5-Phosphate (DOXP) Reductoisomerase

In plants, the isoprenoid biosynthesis depending on the condensation of different numbers of isopentenyl diphosphate (IPP) units is generally derived from the mevalonate pathway[56]. Recently, the DOXP/MEP pathway was described as an alternative mevalonate-independent pathway for synthesizing IPP units and can be found in algae, higher plants, most bacteria, and *P. falciparum*[47].
Within the DOXP pathway (scheme 3) pyruvate and glyceraldehyde-3-phosphate are converted stepwise to IPP. Thereby, the DOXP reductoisomerase is a key enzyme in the DOXP/MEP pathway, converting DOXP into MEP[57,58]. Since the inhibition of DOXP reductoisomerase displays a substantial antimalarial activity[47,59] and since the DOXP/MEP pathway is present in the malaria parasite *P. falciparum*, but is not in humans, enzymes of the DOXP/MEP pathway can be potential clean targets for new antimalarial and antibacterial drug discovery.

DOXP reductoisomerase is composed of three domains arranged to form an overall V-shaped molecule. Due to its V-like shape DOXP reductoisomerase consists of a deep and wide cleft corresponding to the substrate binding and catalytic site (figure 3). DOXP reductoisomerase only uses NADPH as cofactor. In addition, the enzyme needs a divalent cation (such as Mn^{2+}, Mg^{2+}, or Co^{2+})[47,60,61].

Scheme 3. Schematic diagram of the early steps of the DOXP isoprenoid biosynthetic pathway[56]. DOXP is initially formed from pyruvate and glyceraldehyde-3-phosphate (GAP) catalyzed by DOXP synthase, the second key enzyme of this pathway. Subsequently, DOXP reductoisomerase mediates a C-C skeletal rearrangement followed by reduction using NADPH as hydrogen donor with MEP as product. Finally, IPP is formed by a series of dehydration and reduction steps that are not yet fully understood.

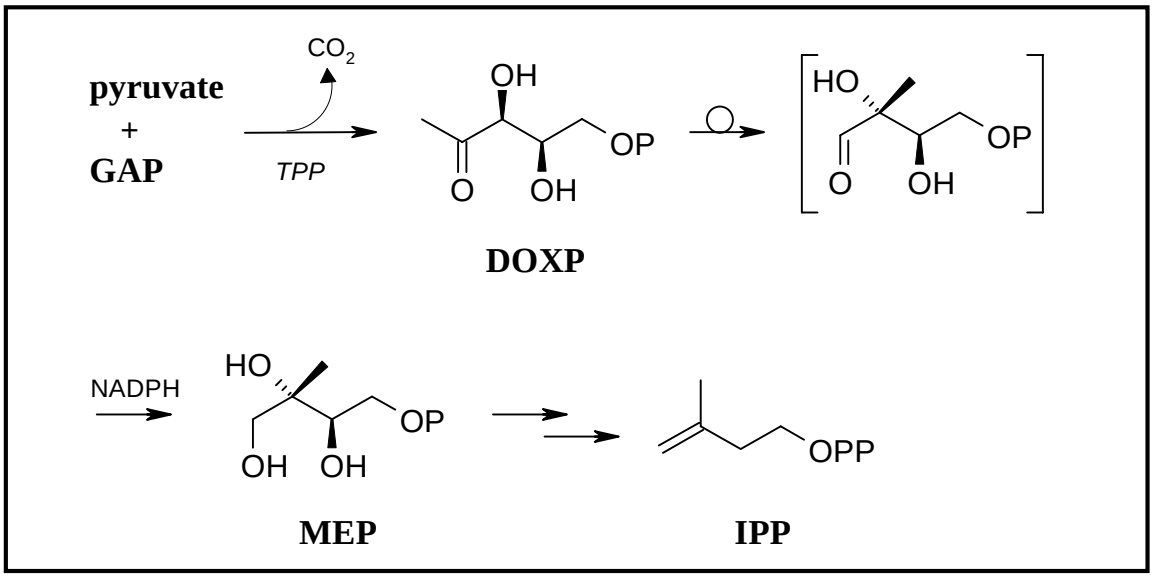

Figure 3. NADPH modeled into the presumed active site of DOXP reductoisomerase.

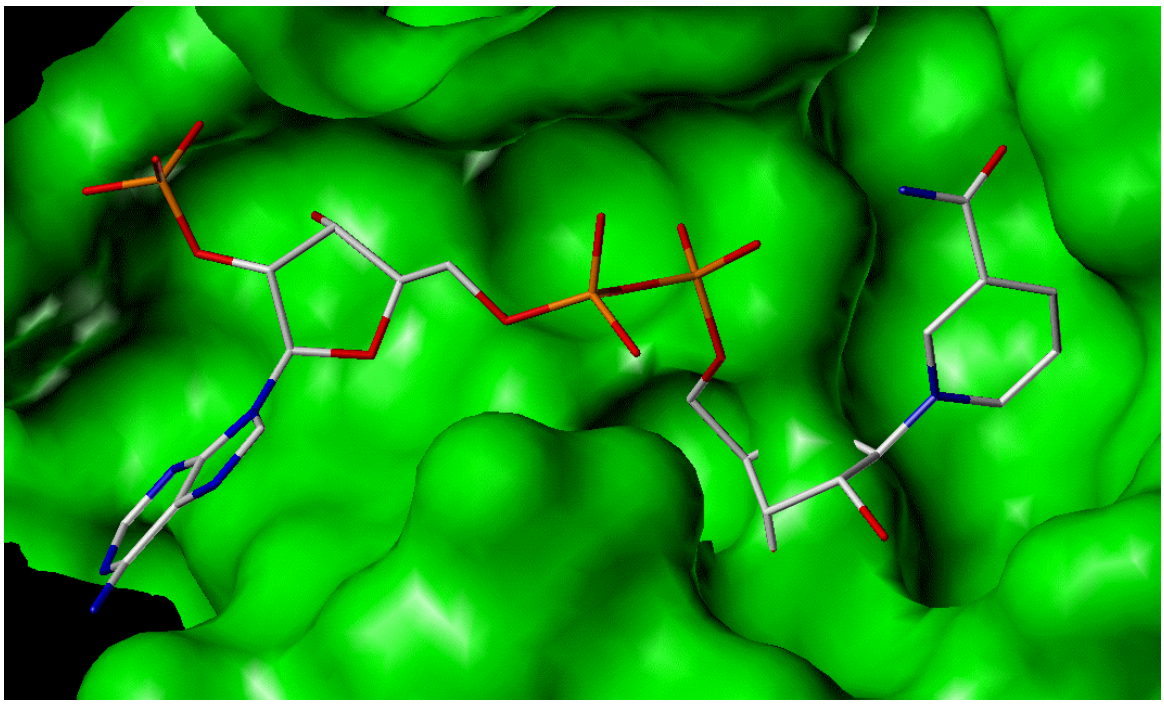

With respect to the model and due to the fact that DOXP reductoisomerase only uses NADPH as cofactor, modifications in the 5´-position of the ribose ring of the adenosine group seem to be a promising strategy to identify inhibitors of the DOXP-reductoisomerase.

1.3.2 Non-Antimalarial Biological Targets

Although the primary interest of this work was focused on the investigation of the antimalarial activity of 5´,N^6- and 3´,N^6-disubstituted adenosines, further promising biological targets were taken into consideration.
Since 2´-monosubstituted and 2´,N^6-disubstituted adenosines displayed inhibitory activity against the GAPDH of *T. cruzi*,[8-14] selected 5´,N^6-disubstituted adenosines were investigated for their antitrypanosomal activity.
A further collaboration with the University of Leuven, Belgium was established investigating the effect of N^6-monosubstituted and 5´,N^6-disubstituted adenosine analogs against the HIV-1(III_B) and HIV-2(ROD) as well as towards unspecific cytotoxicity.
All known adenosine receptor agonists to date are derivatives of the nucleoside adenosine. Only the 5´-position of the ribose moiety and the 2- and N^6-positions of the purine may be modified to increase the affinity to specific receptor subtypes without destroying agonistic activity[2,6]. Thereby, N^6-substituted and/or 5´-*N*-ethyl-carboxamido-substituted adenosines were found to be most potent at the A_3 receptor[4]. Thus, 5´,N^6-disubstituted adenosine derivatives prepared within this project seemed to be promising to exhibit adenosine receptor affinity. In collaboration with the University of Bonn selected adenosine analogs are investigated regarding their affinity against the A_3 A_{2A}, A_{2B}, and A_3 adenosine receptors.

1.4 References

(1) Snow, R. W.; Craig, M.; Deichmann, U.; Marsh, K. *Bull. of the World Health Organ.* **1999**, *77*, 624-640.
(2) Müller, C. E.; Scior, T. *Pharm. Acta Helv.* **1993**, *68*, 77-111.
(3) Klotz, K. N. Naunyn-Schmiedeberg´s Arch. Pharmacol. **2000**, 362, 382-391.
(4) Baraldi, P. G.; Cacciari, B.; Romagnoli, R.; Merighi, S.; Varani, K.; Borea, P. A.; Spalluto, G. *Med. Res. Rev.* **2000**, *20*, 103-128.

(5) Olah, M. E.; Stiles, G. L. *Annu. Rev. Pharmacol. Toxicol.* **1995**, *35*, 581-606.
(6) Poulsen, S.-A.; Quinn, R. J. *Bioorg. Med. Chem.* **1998**, *6*, 619-641.
(7) Golisade, A.; Wiesner, J.; Herforth, C.; Jomaa, H.; Link, A. *Bioorg. Med. Chem.* **2002**, *10*, 769-777.
(8) Golisade, A.; Bressi, J. C.; Van Calenbergh, S.; Gelb, M. H.; Link, A. *J. Comb. Chem.* **2000**, *2*, 537-544.
(9) Van Calenbergh, S.; Van Den Eeckhout, E.; Herdewijn, P. *Helv. Chim. Acta* **1994**, *77*, 631-644.
(10) Van Calenbergh, S.; Verlinde, C.; Soenens, J.; De Bruyn, A.; Callens, M.; Blaton, N. M.; Peeters, O. M.; Rozenski, J.; Hol, W. G.; Herdewijn, P. *J. Med. Chem.* **1995**, *38*, 3838-3849.
(11) Aronov, A. M.; Verlinde, C.; Hol, W. G. J.; Gelb, M. H. *J. Med. Chem.* **1998**, *41*, 4790-4799.
(12) Aronov, A. M.; Suresh, S.; Buckner, F. S.; Van Voorhis, W. C.; Verlinde, C. L. M. J.; Opperdoes, F. R.; Hol, W. G. J.; Gelb, M. H. *Proc. Natl. Acad. Sci. USA* **1999**, *96*, 4273-4278.
(13) Bressi, J. C.; Verlinde, C. L.; Aronov, A. M.; Shaw, M. L.; Shin, S. S.; Nguyen, L. N.; Suresh, S.; Buckner, F. S.; Van Voorhis, W. C.; Kuntz, I. D.; Hol, W. G.; Gelb, M. H. *J. Med. Chem.* **2001**, *44*, 2080-2093.
(14) Golisade, A.; Herforth, C.; Quirijnen, L.; Maes, L.; Link, A. *Bioorg. Med. Chem.* **2002**, *10*, 159-165.
(15) Link, A.; Van Calenbergh, S.; Herdewijn, P. *Tetrahedron Lett.* **1998**, *39*, 5175-5176.
(16) Backes, B. J.; Virgilio, A. A.; Ellman, J. A. *J. Am. Chem. Soc.* **1996**, *118*, 3055-3056.
(17) Shen, D.-M.; Shu, M.; Chapman, K. T. *Org. Lett.* **2000**, *2*, 2789-2792.
(18) Kenner, G. W.; McDermott, J. R.; Sheppard, R. C. *J. Chem. Soc., Chem. Commun.* **1971**, 636-637.
(19) Backes, B. J.; Ellman, J. A. *J. Am. Chem. Soc.* **1994**, *116*, 11171-11172.
(20) Backes, B. J.; Ellman, J. A. *J. Org. Chem.* **1999**, *64*, 2322-2330.
(21) Yang, L.; Morriello, G. *Tetrahedron Lett.* **1999**, *40*, 8197-8200.
(22) Lavandera, I.; Fernández, S.; Ferrero, M.; Gotor, V. *J. Org. Chem.* **2001**, *66*, 4079-4082.
(23) Kondo, K.; Sekimoto, E.; Miki, K.; Murakami, Y. *J. Chem. Soc. Perkin Trans. 1* **1998**, 2973-2974.

(24) Bogdan, S.; Cernigoj, U.; Kocevar, M.; Polanc, S. *Tetrahedron Lett.* **2001**, *42*, 6659-6662.
(25) Kim, D.-H.; Rho, H.-S.; You, J. W.; Lee, J. C. *Tetrahedron Lett.* **2002**, *43*, 277-279.
(26) Kryatova, O. P.; Connors, W. H.; Bleczinski, C. F.; Mokhir, A. A.; Richert, C. *Org. Lett.* **2001**, *3*, 987-990.
(27) Kirschning, A.; Jesberger, M.; Schonberger, A. *Org. Lett.* **2001**, *3*, 3623-3626.
(28) Hardcastle, I. R.; Barber, A. M.; Marriott, J. H.; Jarman, M. *Tetrahedron Lett.* **2001**, *42*, 1363-1365.
(29) Nicolaou, K. C.; Pfefferkorn, J. A.; Barluenga, S.; Mitchell, H. J.; Roecker, A. J.; Cao, G.-Q. *J. Am. Chem. Soc.* **2000**, *122*, 9968-9976.
(30) Senten, K.; Van der Veken, P.; Bal, G.; Haemers, A.; Augustyns, K. *Tetrahedron Lett.* **2001**, *42*, 9135-9138.
(31) Weidner, J. J.; Parlow, J. J.; Flynn, D. L. *Tetrahedron Lett.* **1999**, *40*, 239-242.
(32) Golisade, A.; Van Calenbergh, S.; Link, A. *Tetrahedron* **2000**, *56*, 3167-3172.
(33) Overkleeft, H. S.; Bos, P. R.; Hekking, B. G.; Gordon, E. J.; Ploegh, H. L.; Kessler, B. M. *Tetrahedron Lett.* **2000**, *41*, 6005-6009.
(34) Merrifield, R. B. In *Peptides: Synthesis, Structures, and Applications*; Gutte, B., Ed.; Academic Press, Inc.: San Diego, 1995.
(35) Nefzi, A.; Ostresh, J. M.; Houghton, R. A. *Tetrahedron* **1999**, *55*, 335-344.
(36) Acharya, A. N.; Ostresh, J. M.; Houghten, R. A. *J. Comb. Chem.* **2002**, *4*, 214-222.
(37) Karoyan, P.; Triolo, A.; Nannicini, R.; Giannotti, D.; Altamura, M.; Chassaing, G.; Perrotta, E. *Tetrahedron Lett.* **1999**, *40*, 71-74.
(38) Kantorowski, E. J.; Kurth, M. J. *J. Org. Chem.* **1997**, *62*, 6797-6803.
(39) Macmillan, D.; Daines, A. M.; Bayrhuber, M.; Flitsch, S. L. *Org. Lett.* **2002**, *4*, 1467-1470.
(40) Gordon, E. M.; Barrett, R. W.; Dower, W. J.; Fodor, S. P.; Gallop, M. A. *J. Med. Chem.* **1994**, *37*, 1385-1401.
(41) Ellman, J. A. *Acc. Chem. Res.* **1996**, *29*, 132-143.
(42) Lang-Unnasch, N.; Murphy, A. D. *Annu. Rev. Microbiol.* **1998**, *52*, 561-590.
(43) Miller, L. H.; Baruch, D. I.; Marsh, K.; Doumbo, O. K. *Nature* **2002**, *415*, 673-679.
(44) Ridley, R. G. *Nature* **2002**, *415*, 686-693.

(45) Krause, T.; Lüersen, K.; Wrenger, C.; Gilberger, T. W.; Müller, S.; Walter, R. D. *Biochem. J.* **2000**, *352*, 287-292.
(46) Casero, R. A., Jr.; Woster, P. M. *J. Med. Chem.* **2001**, *44*, 1-26.
(47) Jomaa, H.; Wiesner, J.; Sanderbrand, S.; Altincicek, B.; Weidemeyer, C.; Hintz, M.; Turbachova, I.; Eberl, M.; Zeidler, J.; Lichtenthaler, H. K.; Soldati, D.; Beck, E. *Science* **1999**, *285*, 1573-1576.
(48) Carter, N. S.; Ben Mamoun, C.; Liu, W.; Silva, E. O.; Landfear, S. M.; Goldberg, D. E.; Ullman, B. *J. Biol. Chem.* **2000**, *275*, 10683-10691.
(49) Khattab, A.; Kun, J.; Deloron, P.; Kremsner, P. G.; Klinkert, M. Q. *J. Infect. Dis.* **2001**, *183*, 1165-1169.
(50) Ancelin, M. L.; Calas, M.; Bompart, J.; Cordina, G.; Martin, D.; Ben Bari, M.; Jei, T.; Druilhe, P.; Vial, H. J. *Blood* **1998**, *91*, 1426-1437.
(51) Müller, S.; Da'dara, A.; Lüersen, K.; Wrenger, C.; Das Gupta, R.; Madhubala, R.; Walter, R. D. *J. Biol. Chem.* **2000**, *275*, 8097-8102.
(52) Assaraf, Y. G.; Golenser, J.; Spira, D. T.; Bachrach, U. *Biochem. J.* **1984**, *222*, 815-819.
(53) Marton, L. J.; Pegg, A. E. *Annu. Rev. Pharmacol. Toxicol.* **1995**, *35*, 55-91.
(54) Porter, C. W.; Sufin, J. R. *Anticancer Res.* **1986**, *6*, 525-542.
(55) Kolb, M.; Danzin, C.; Barth, J.; Claverie, N. *J. Med. Chem.* **1982**, *25*, 550-556.
(56) Schwender, J.; Müller, C.; Zeidler, J.; Lichtenthaler, H. K. *FEBS Lett.* **1999**, *455*, 140-144.
(57) Radykewicz, T.; Rohdich, F.; Wungsintaweekul, J.; Herz, S.; Kis, K.; Eisenreich, W.; Bacher, A.; Zenk, M. H.; Arigoni, D. *FEBS Lett.* **2000**, *465*, 157-160.
(58) Jomaa, H.; Feurle, J.; Luhs, K.; Kunzmann, V.; Tony, H. P.; Herderich, M.; Wilhelm, M. *FEMS Immunol. Med. Microbiol.* **1999**, *25*, 371-378.
(59) Reichenberg, A.; Wiesner, J.; Weidemeyer, C.; Dreiseidler, E.; Sanderbrand, S.; Altincicek, B.; Beck, E.; Schlitzer, M.; Jomaa, H. *Bioorg. Med. Chem. Lett.* **2001**, *11*, 833-835.
(60) Kuzuyama, T.; Takahashi, S.; Takagi, M.; Seto, H. *J. Biol. Chem.* **2000**, *275*, 19928-19932.
(61) Reuter, K.; Sanderbrand, S.; Jomaa, H.; Wiesner, J.; Steinbrecher, I.; Beck, E.; Hintz, M.; Klebe, G.; Stubbs, M. T. *J. Biol. Chem.* **2002**, *277*, 5378-5384.

2 Antimalarial Activity of 5´,N^6-Disubstituted Adenosine Derivatives

2.1 Introduction

Regarding supposed interactions with diverse adenosine binding motifs and the unique importance of the purine transport systems to parasite survival, the biological evaluation of substituted adenosine derivatives as possible antimalarial agents was considered rewarding. In the following, the synthesis and biological evaluation of novel 5´,N^6-disubstituted adenosine derivatives is outlined. Novel adenosines with unusual substitution pattern were obtained applying efficient PASP and cPASP approaches, leading to two series of 5´,N^6-disubstituted derivatives in parallel that would have been difficult to synthesize by standard techniques. The scope and the limitations of the methodology used are discussed.

2.2 Synthesis of 5´-Amido-N^6-Arylalkyl-5´-Deoxyadenosines

The construction of desired 5´-amido-N^6-arylalkyl-5´-deoxyadenosines was divided into two independent parts. Nucleoside templates were obtained by conventional synthesis in solution, whereas the 5´-amido-substituents were constructed on a polymer support in up to five subsequent steps without purification, other than washing of resin beads with appropriate solvents. For the final (convergent) connection, the polymer-supported carboxylic acid equivalents were transformed into acylating reagents by activating the safety-catch linker used[1,2]. Chemoselective acylation of the unprotected nucleoside templates with the reactive polymer-bound species obtained yielded the 5´-amido-N^6-arylalkyl-5´-deoxyadenosines **14**-**49**, and **52**, intended for biological evaluation.

The synthesis of 5´-deoxy-N^6-(1-naphthylmethyl)-5´-phthalimidoadenosine (**9**) and 5´-amino-5´-deoxy-N^6-(1-naphthylmethyl)adenosine (**2**) has most recently been described by Bressi et al. (scheme 4, path A)[3]. For the preparation of novel derivates **9** and **10** we followed a different path (scheme 4, path B).

Amination of commercially available 6-chloropurine-9-riboside (**5**) by aminolysis of the attached chlorine substituent at C6 with an excess of the

appropriate primary amine yielded N^6-(4-phenylbenzyl)adenosine (**7**). Conversion with di-*tert*-butylazodicarboxylate and triphenylphosphine applying standard Mitsunobu condensation conditions[4] resulted in the formation of 5′-deoxy-N^6-(4-phenylbenzyl)-5′-(phthalimido)adenosine **9**. Subsequent hydrazine-mediated cleavage of the phthalimide group in **9** as described for **8** by Bressi et al. was the final step of the synthesis sequence in solution and led to the required 5′-amino-N^6-(arylalkyl)-5′-deoxyadeno-sine scaffolds **2** and **10** in sufficient amounts for further derivatizations.

Within the second step of the synthetic pathway, a PASP as well as a cPASP protocol was employed for the N-selective acylation of 5′-amino-5′-deoxyadenosine templates, leading to desired 5′-amido-derivatives of type I (**14**-**46**, and **52**) and of type II (**47**-**49**) (scheme 5, R groups see figure 4).

Utilizing the PASP protocol, commercially available carboxylic acids were attached to the Kenner safety-catch linker connected to aminomethylated polystyrene via in situ anhydride formation with *N*,*N*-diisopropylcarbo-diimide (DIC) in THF. Acylation of the Kenner safety-catch linker thus provided the appropriate polymer-bound N-acylsulfonamide **4**. In the following, the sulfonamide linker was activated with bromoacetonitrile in NMP for nucleophilic cleavage. The obtained highly reactive N-cyanomethyl analog **13** was cleaved under mild reaction conditions, chemoselectively transferring the carboxylic acid residue to the amino function of the nucleoside scaffold **2** or **10**. Along this synthetic pathway, a series of novel adenosine derivatives of type I (**14**-**46**, and **52**) and of type II (**47**-**49**) was obtained.

Scheme 4. Synthetic sequence leading to 5′-amino-5′-deoxy-N^6-(1-naphthylmethyl)adenosine (**2**) and 5′-amino-5′-deoxy-N^6-(4-phenylbenzyl)adenosine (**10**).

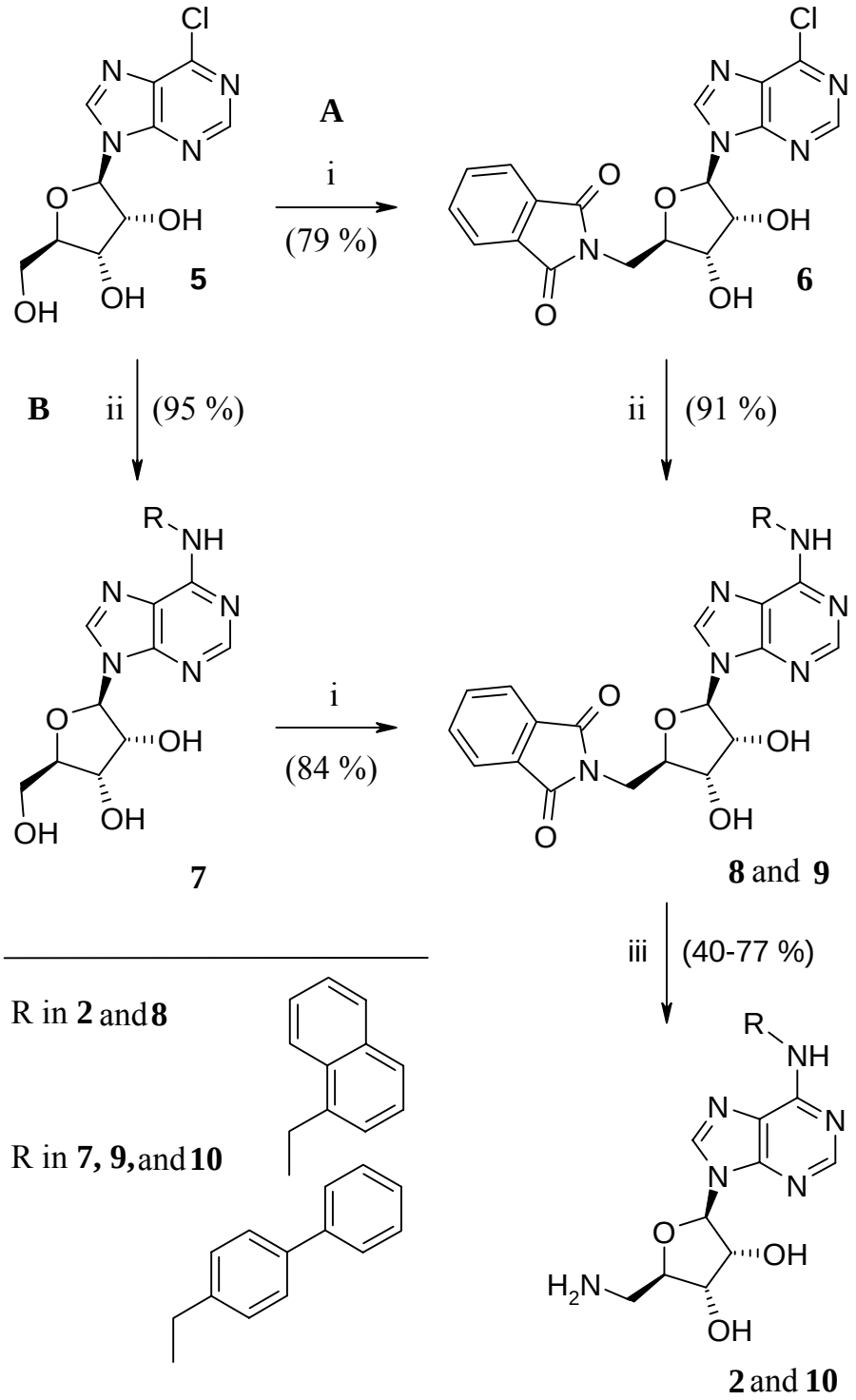

(i) $P(Ph)_3$, di-*tert*-butylazodicarboxylate, phthalimide, dry THF, 48 h; (ii) arylmethylamine derivative, EtOH or 1-propanol, 50 °C, 72 h; (iii) hydrazine hydrate, EtOH, reflux, 1h.

Scheme 5. Synthetic approach leading to 5′-amido-N^6-(arylalkyl)-5′-deoxy-adenosines of type I (**14-46**, and **52**) and of type II (**47-49**) from templates **2** and **10**, respectively.

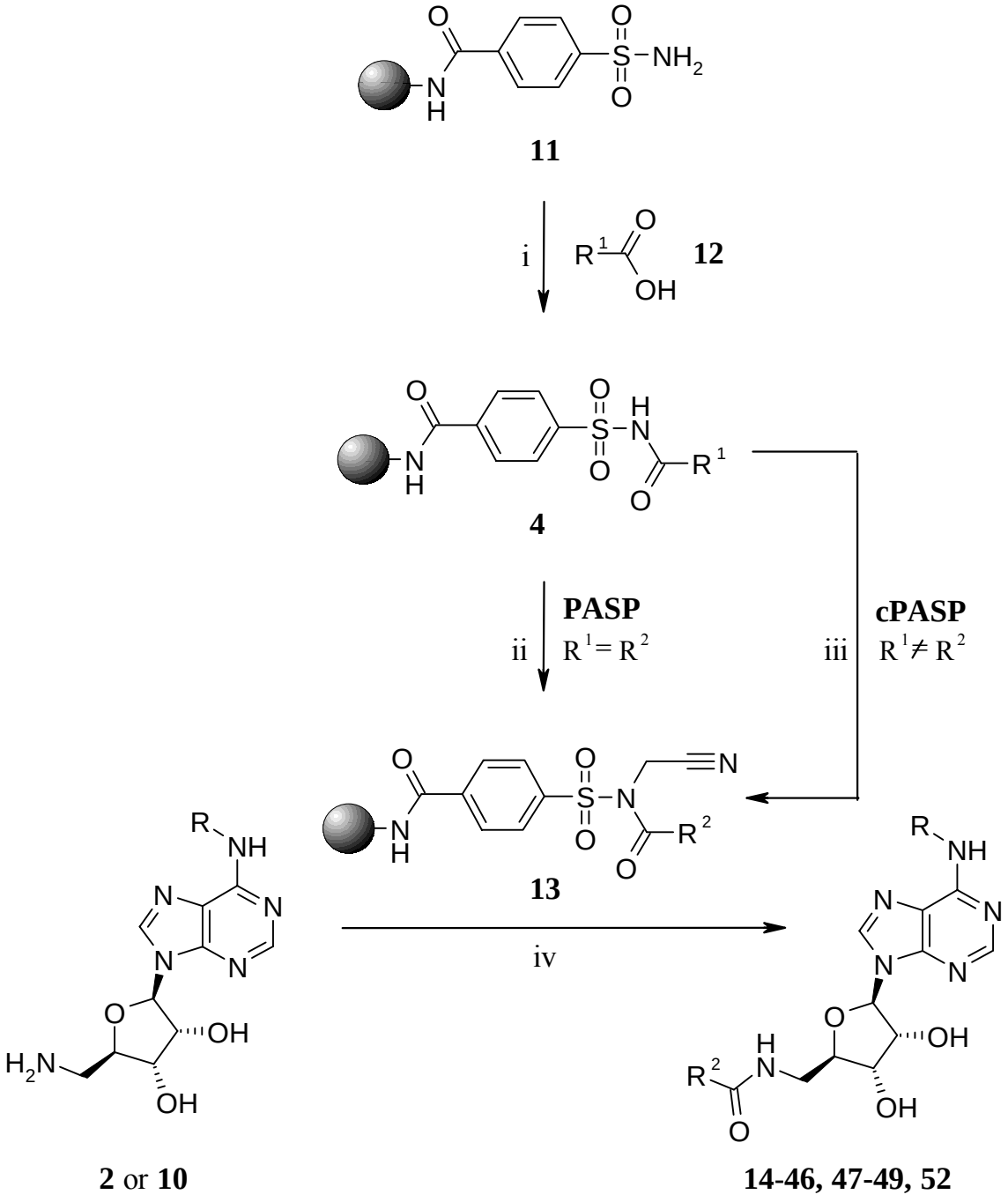

(i) 1. DIC, THF; 2. DIPEA, DMAP, THF; (ii) bromoacetonitrile, NMP, ambient temperature, 12 h; (iii) 1. diverse chemical modifications, e.g. nucleophilic substitution with various amines; 2. bromoacetonitrile, NMP, room temperature, 12-48 h; (iv) THF, 55 °C, 8-24 h.

Following the cPASP approach, the full potential of the acylating species of type **13** was exploited via on-bead modification of carboxylic acid equivalents prior to activation. Thereby, on-bead modification of 4-fluoro-3-nitrobenzoic acid opened the way to sterically demanding 4-aminobenzoic acid derivatives (scheme 6). This route has been shown to be an efficient instrument to achieve diverse carboxylic acid equivalents on conventional linkers in solid-phase synthesis by many groups[5-11].

Scheme 6. CPASP sequence including on-bead modification of a polymer-bound building block and subsequent chemoselective transfer to the amino group of the nucleoside scaffold **2**.

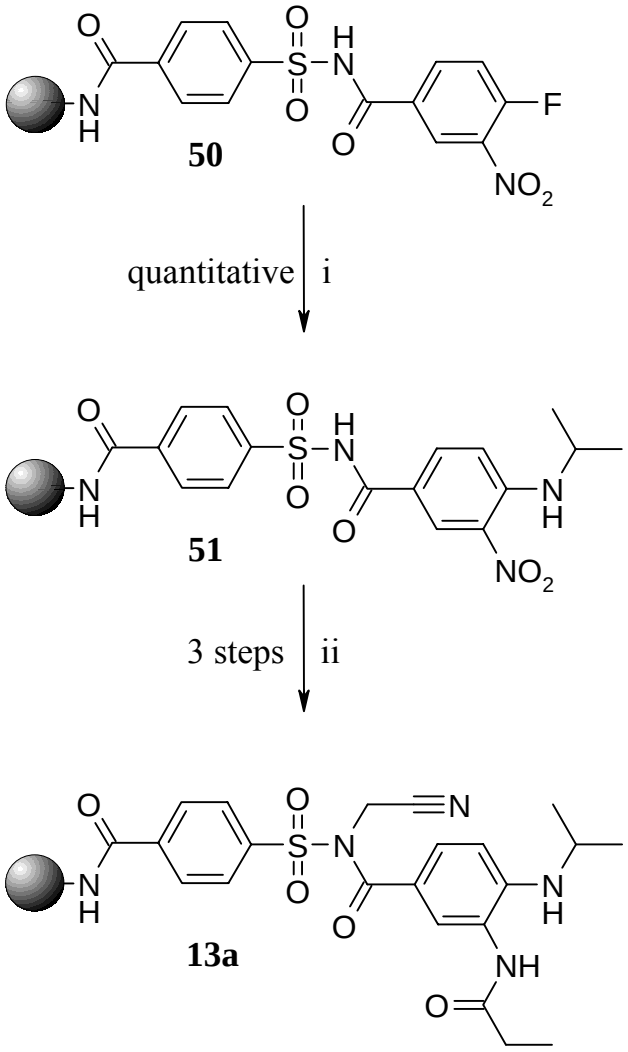

13a

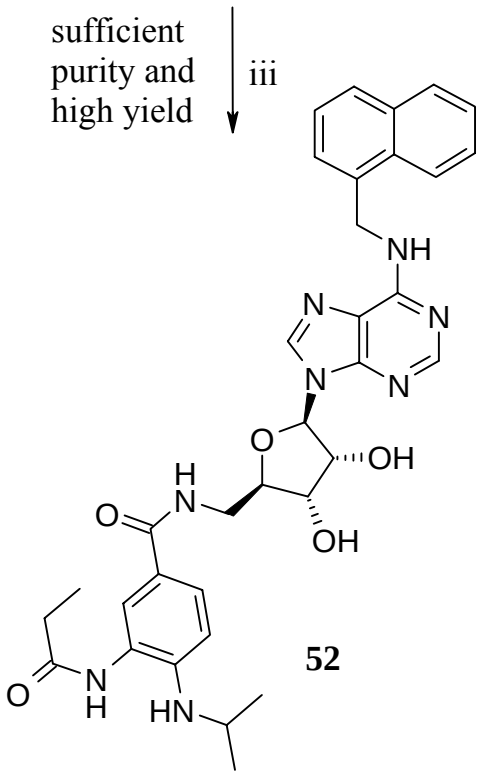

52

(i) 2-Aminopropane, DMF, 24 h; (ii) 1. $SnCl_2$, DMF, 48 h; 2. propionic anhydride, DIPEA, DMAP, THF, 24 h; 3. bromoacetonitrile, NMP, 48 h; (iii) THF, 55 °C, 24 h.

4-Fluoro-3-nitrobenzoic acid was initially attached to the sulfamoyl linker (not shown) via in situ anhydride formation yielding intermediate **50**. Subsequent treatment with excess amine converted **50** to the corresponding nitroaniline analog **51** by nucleophilic aromatic substitution. Reduction of the nitro group in **51** proceeded under established conditions with excess tin-II-chloride in DMF[12]. The following acylation with propionic anhydride and final alkylation with bromoacetonitrile lead to the activated building block **13a** ready for the chemoselective transfer to the amino function of the scaffold **2**. Since alkylation with bromoacetonitrile as activation step for aromatic building blocks often display sub optimal results, prolonged reaction times (48 hours) for the activation protocol were employed[13]. In a similar fashion, a series of analogs of **13a** was effectively prepared using different primary and secondary amines and different carboxylic acids for the amination of 4-fluoro-3-nitrobenzoic acid and the acylation of the aniline nitrogen atoms formed upon reduction (R groups in structures **27**-**46**, **49** and **52** see figure 4).

Figure 4. Structures of adenosine derivatives of type I (**14-46**, and **52**) and of type II (**47-49**).

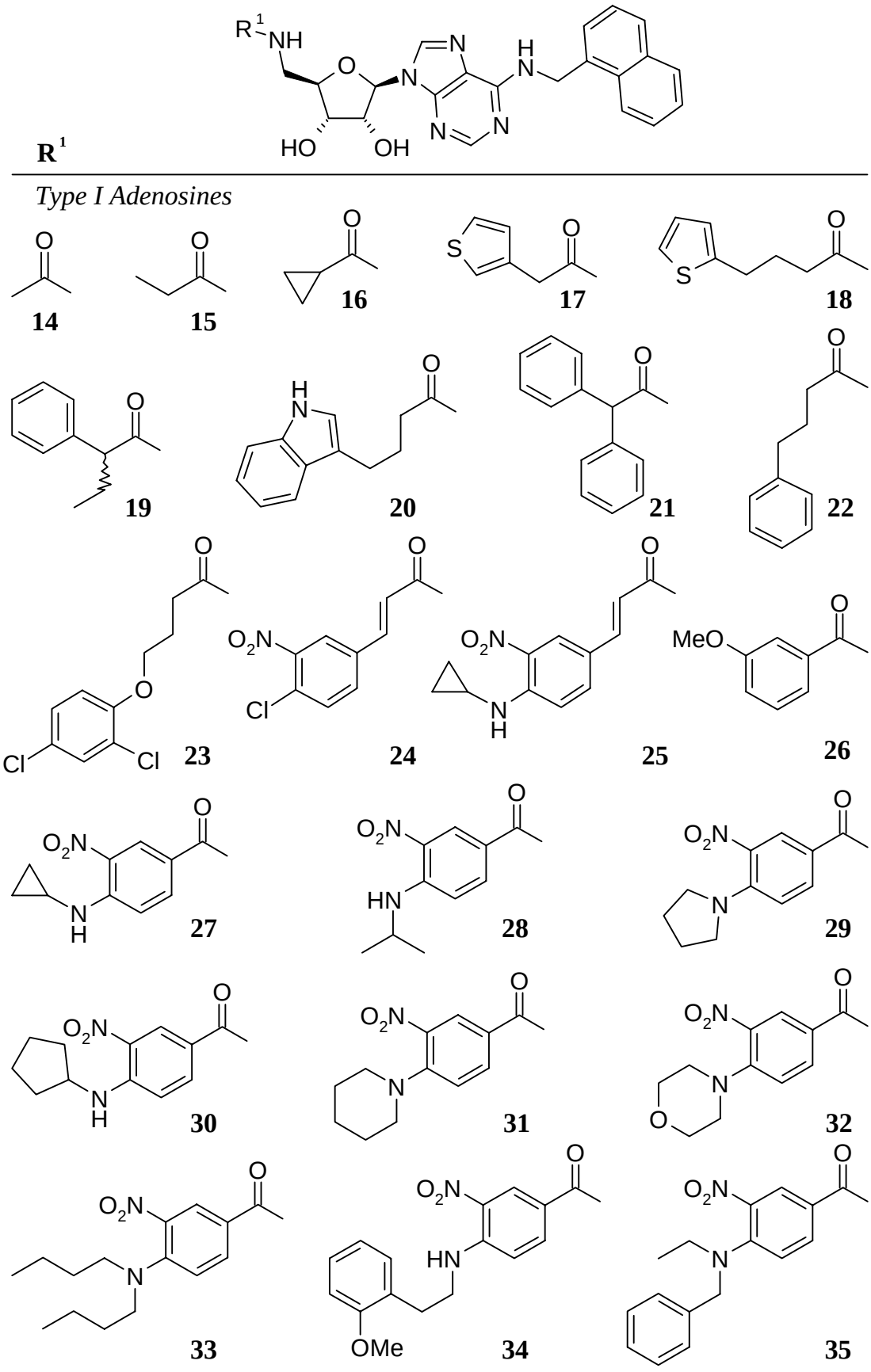

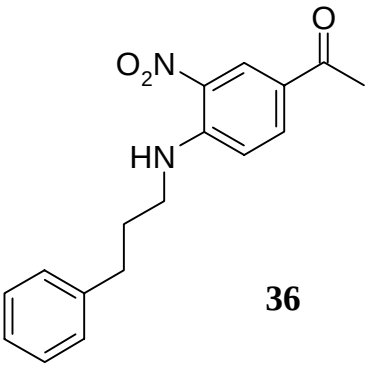

36

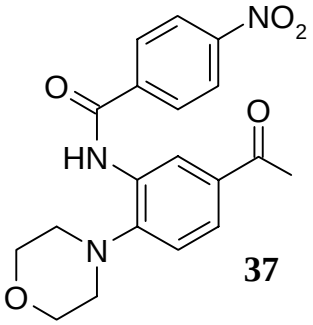

37

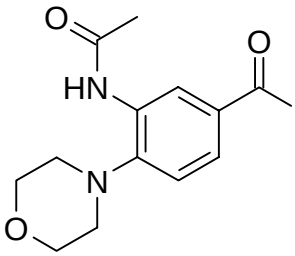

38

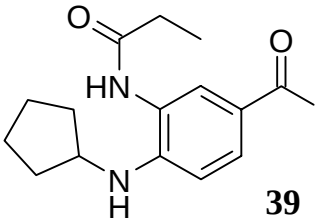

39

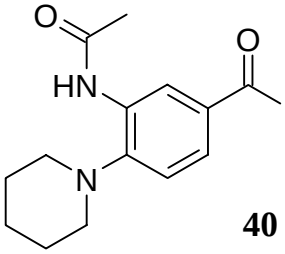

40

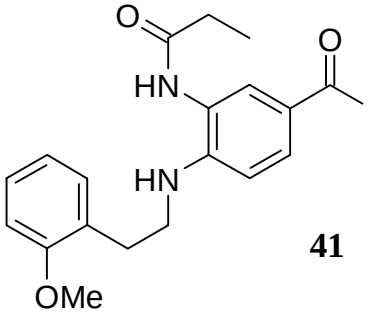

41

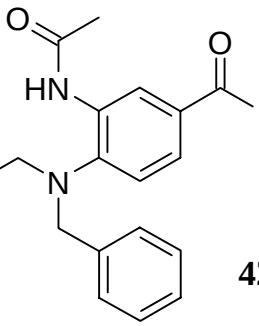

42

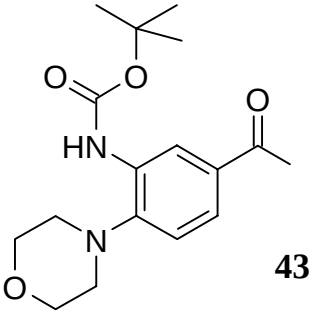

43

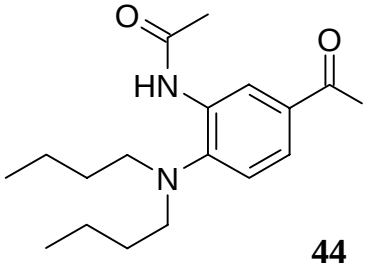

44

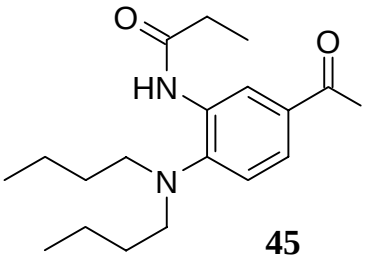

45

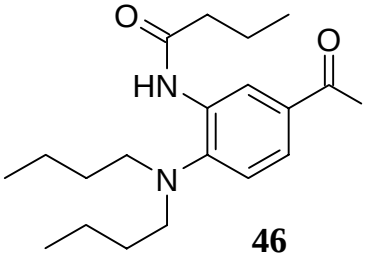

46

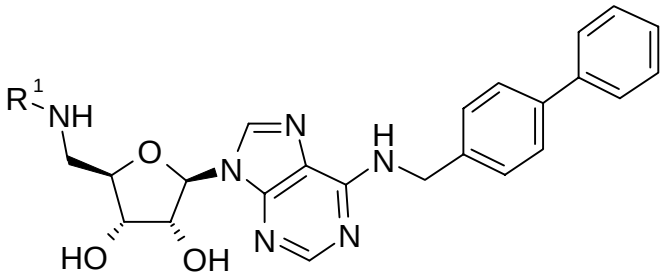

R[1]

Type II Adenosines

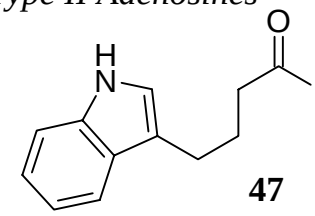

47

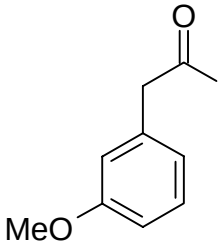

48

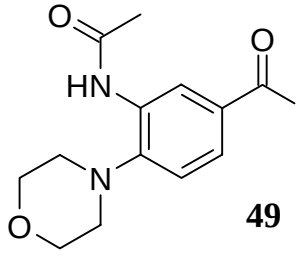

49

In general, the target compounds could be obtained in good yield and purity. However, only the simpler constructs like **14**-**24**, **26** and **47** resulting from a short modification sequence could be obtained in excellent yield and as a result in high purity. These compounds could have been used for biological evaluation without resort to chromatographic purification.

Derivatives obtained from a multi-step on-bead modification sequence in most cases did not meet the commonly accepted purity criterion of 80% purity prior to LC-purification (see table 1). In these cases almost complete conversion of the starting material **2** or **10** could be deduced from TLC analysis, but due to incomplete formation of **50**, in the cases of **37**, **40**-**43,** and **49**, mixtures of two differently substituted 5′-amino-N^6-(arylalkyl)-5′-deoxyadenosines were obtained. This shared impurity resulted from the unintended formation of a second acylating species (e.g. **13a** with R^1= CH_3 or C_2H_5). This second acylating species was obtained, when acylating residual sulfamoyl groups of the Kenner linker (that were not acylated by 4-fluoro-3-nitrobenzoic acid) during amidation of the aniline nitrogen in polymer-bound intermediates like **51**.

Another source for by-product formation is the incomplete acylation of the aniline nitrogen formed upon reduction of the aromatic nitro group in compounds **37**-**46**, **49** and **52**. As can be deduced from the results of the subset **44**-**46**, the increase of the size of the amide substituent adjacent to the secondary aniline nitrogen is unfavorable for a smooth conversion, when the other aniline nitrogen is substituted with space filling residues, as well. The attempted synthesis of resin **54** failed because the homologue isovaleric acid residue could not be sufficiently introduced into resin **53** (scheme 7).

Scheme 7. Incomplete acylation of resin **54** due to sterical hindrance.

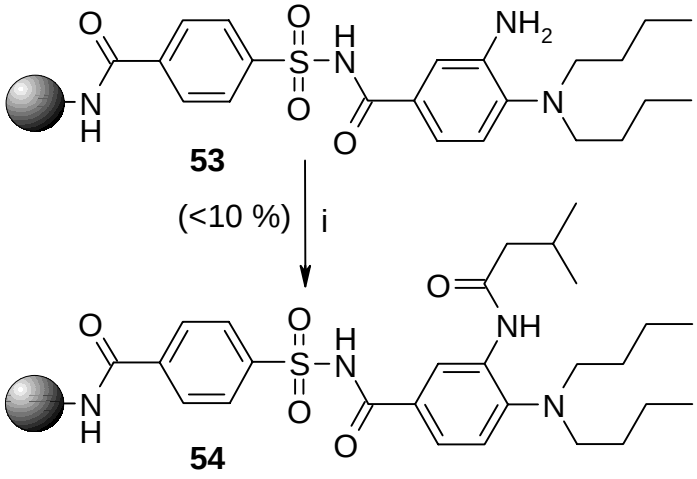

(i) Isovaleric acid anhydride, DIPEA, DMAP, THF, ambient temperature, 24 h.

An attempt to use 4-chloro-3-nitro-*trans*-cinnamic acid attached to the Kenner safety-catch linker (**55**) for an analogous reaction was unsuccessful (scheme 8).

Scheme 8. Failure of analogous cPASP sequence employing 4-chloro-3-nitro-*trans*-cinnamic acid instead of 3-fluoro-4-nitrobenzoic acid.

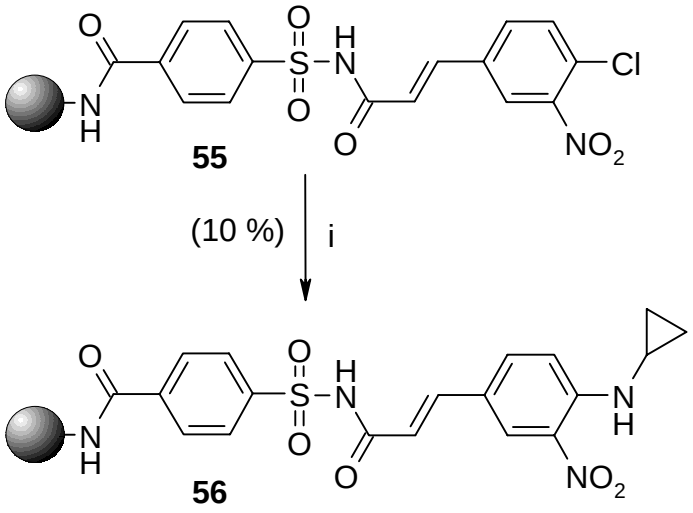

(i) Cyclopropylamine, DMF, 24h.

Treatment with primary aliphatic amines like cyclopropylamine, subsequent activation of the linker and transfer to scaffold **2** did not produce the desired target compounds in sufficient purity.
Regardless of these shortcomings, there is to date no superior preparation protocol for the synthesis of these complex derivatives of this class of compounds.

Table 1. Yield and indication of sufficient purity of adenosine derivatives of type I (**14**-**46**, and **52**) and type II (**47**-**49**) originated from polymer-assisted synthesis.

Compound	Protocol	Sufficient Purity (>80%) [A]	Conversion Rate [%] [B]	Yield [%] [B]
5´-Amido-5´-deoxy-N^6-(1-naphthylmethyl)adenosine derivatives				
14	PASP	prior to MPLC	97	96
15	PASP	prior to MPLC	93	88
16	PASP	prior to MPLC	>99	97
17	PASP	prior to MPLC	>99	86
18	PASP	prior to MPLC [C]	>99	99
19	PASP	prior to MPLC	>99	92
20	PASP	prior to MPLC	>99	97
21	PASP	prior to MPLC	99	92
22	PASP	prior to MPLC [C]	98	97
23	PASP	prior to MPLC	97	91
24	PASP	prior to MPLC	95	95
25	cPASP	not obtained [D]	---	<10
26	PASP	prior to MPLC	---	95
27	cPASP	prior to MPLC	98	87
28	cPASP	after MPLC	98	67
29	cPASP	after MPLC	---	79
30	cPASP	after MPLC	74	66
31	cPASP	after MPLC	>99	78
32	cPASP	after MPLC	99	84
33	cPASP	after MPLC	94	64
34	cPASP	prior to MPLC	98	92
35	cPASP	prior to MPLC	99	91
36	cPASP	prior to MPLC	>99	84

Compound	Protocol	Sufficient Purity (>80%) [A]	Conversion Rate [%] [B]	Yield [%] [B]
37	cPASP	after MPLC	96	65
38	cPASP	prior to MPLC	95	81
39	cPASP	after MPLC	94	71
40	cPASP	prior to MPLC	99	54
41	cPASP	after MPLC	91	58
42	cPASP	after MPLC	98	59
43	cPASP	after MPLC	95	47
44	cPASP	after MPLC	98	72
45	cPASP	after MPLC	90	52
46	PASP	after MPLC	93	51
52	cPASP	prior to MPLC	95	81
5´-Amido-5´-deoxy-N^6-(4-phenylbenzyl)adenosine derivatives				
47	PASP	prior to MPLC	88	82
48	cPASP	after MPLC	98	65
49	PASP	after MPLC	98	71

[A] Purity criterion for libraries (80/80 Standard)[14]: Spectroscopic analysis is required for a random sampling of all new libraries. In most cases 5% (at least 20 members) of a library have to be sampled for purity and identity. The 80% purity criterion is met, when 80% of sampled library members will prove to be the expected compound, present in at least 80% purity. [B] All compounds were purified by a single semi-preparative medium pressure LC (MPLC) run under standard conditions that were not optimized for each individual compound. Product containing fractions were collected and evaporated, the yield of pure compounds obtained is reported above. Purity and conversion rate of compounds were estimated using the 100% method, UV-detection at 254 nm. [C] Samples **18**, **22** and **36** were not purified by MPLC. Purity and conversion rate were obtained by a single HPLC run under standard conditions. [D] Sample **25** could not be purified sufficiently by a single MPLC run.

2.3 Biological Evaluation of 5´,N^6-Disubstituted Adenosines

Compounds **2**, **6**, **8-10**, **14-34**, **36-38**, **40-44**, **46-49**, and **52** were evaluated for their inhibitory activity against intraerythrocytic forms of *P. falciparum* using a semi-automated microdilution assay as described[15-17]. The growth of the parasites was monitored through the incorporation of tritium-labeled hypoxanthine.

For DOXP reductoisomerase inhibition studies compounds **2**, **6**, **8-10**, **14-34**, **36-38**, **40-44**, **46-49**, and **52** were analyzed. The conversion of DOXP to MEP by the recombinant enzyme was determined in an assay based on NADPH dependency of the reaction[18]. Results of both investigations are summarized below (table 2).

Table 2. Antimalarial activity of adenosine derivatives **2**, **6**, **8-10**, **14-34**, **36-38**, **40-44**, **46-49**, and **52**.

Compound	***P. falciparum*** **IC_{50} [µM]** [A]	**DOXP Reductoisomerase Inhibition [%]** [B]
2	12	0
6	42	42
8	11	0
9	4.3	0
10	2.1	41
5´-Amido-5´-deoxy-N^6-(1-naphthylmethyl)adenosine derivatives		
14	23	0
15	15	0
16	11	0
17	11	0
18	7.0	0
19	6.2	0
20	8.5	45
21	6.2	50
22	4.1	0

Compound	*P. falciparum* IC_{50} [µM] [A]	DOXP Reductoisomerase Inhibition [%] [B]
23	10	0
24	5.3	52
25	4.8 [C]	33
26	11	0
27	26 [D]	0
28	4.1	0
29	15 [D]	0
30	4.8	47
31	14 [D]	0
32	13 [D]	0
33	4.2	70
34	1.3	58
37	2.8	27
38	5.0	0
40	4.2	24
41	2.7	0
42	3.3	65
43	3.1	0
44	3.7	59
46	3.2	53
52	3.2	0
5´-Amido-5´-deoxy-N^6-(4-phenylbenzyl)adenosine derivatives		
47	3.7	48
48	14	0
49	3.2	0

[A] The *P. falciparum* strain Dd2 (Indochina) used in this study is resistant to most commonly used antimalarial drugs. When the resistance pattern was checked, the Dd2

strain was found to be highly resistant against chloroquine (IC_{50} = 170 nM), pyrimethamine (IC_{50} = 2500 nM), and cycloguanil (IC_{50} = 2200 nM); and moderately resistant against quinine (IC_{50} = 380 nM) and mefloquine (IC_{50} = 57 nM). It was sensitive to halofantrine (IC_{50} = 18 nM), lumefantrine (IC_{50} = 30 nM), artemisinin (IC_{50} = 18 nM), and atovaquone (IC_{50} = 1 nM). [B] DOXP reductoisomerase inhibition studies were performed under standard assay conditions at compound concentrations of 30 μM. [C] Mixture of compounds **15** and **16**. [D] *P. falciparum* strain 236. Results obtained at Tibotec, Mechelen, Belgium.

Compounds **2**, **9**, **20**, **23**, **40**, and **42** displaying antimalarial activity versus the plasmodial Dd2 strain in the low micromolar range were tested against AdoMetDC of *P. falciparum*. The enzyme activity was assayed by measuring the production of $^{14}CO_2$ from *S*-adenosyl-L-[carboxy-^{14}C]-methionine following conditions previously reported[19]. The inhibition of AdoMetDC by **2**, **9**, **20**, **23**, **40**, and **42** was determined under standard assay conditions varying concentrations of the appropriate inhibitors with a maximum concentration of 100 μM used. None of the compounds inhibited the enzymatic decarboxylation reaction.

Type I adenosines **2**, **6**, **8**, **9**, **14**, **16**, **20**, **23**, **26**, **27**, **29**, **31**, **32**, **38**, **40**, and **42** were tested for in vitro activity upon *T. b. brucei* and *T. cruzi* as described by Hirumi et al.[20]. None of the 16 compounds exhibited activity against *T. cruzi*. Only compounds **20**, **23**, **31**, and **32** showed a moderate inhibitory effect on *T. b. brucei* with IC_{50} values of 17, 17, 16, and 17 μM, respectively.

Adenosine derivatives of type I (**21**, **23**, **26**, **34**, and **39**) and of type II (**47**) were analyzed with regards to their antiviral activity against HIV-1(III_B) and HIV-2(ROD) as well as to their cytotoxicity in an MT-4/MTT based assay[21,22]. All derivatives did not exhibit antiviral activity. Compounds displayed no to minor cytotoxicity against human T-lymphocytes (tested at compound concentrations of 150 μg/ml), with CC_{50} values being ≥ 87.7 μg/ml for compounds **23**, **26**, **34**, and **39** and CC_{50} values of 16 and 14 μg/ml for compounds **21** and **47**, respectively.

To investigate whether N^6-naphthylmethyl substituted adenosine derivatives exhibit adenosine receptor affinity, **2** was selected and tested at all known adenosine receptor subtypes. **2** was investigated in radioligand binding assays at rat brain (A_1 against 3H-CCPA, rat cortex membrane; A_{2A} against 3H-MSX-2, rat striatum membrane) and radioligand binding assays at human recombinant adenosine receptors (A_{2B} against 3H-PSB-298, HEK cell

membrane; A_3 against 3H-PSB-11, CHO cell membrane)[23]. Derivative **2** showed only minor affinity to the A_1 (20% inhibition of radioligand binding at 10 µM; no inhibition at 1 µM) and the A_{2B} subtypes (16% inhibition of radioligand binding at 10 µM) corresponding to K_i values > 10 µM. No inhibition of A_{2A} and A_3 adenosine receptors was observed at concentrations ranging from 25 to 1 µM.

2.4 Analytical Characteristics of 5´,N^6-Disubstituted Adenosines

2.4.1 Electrospray Ionization (ESI)/ Mass Spectrometry (MS) Analysis of Selected 5´,N^6-Disubstituted Adenosines

Mass spectrometry has become one of the most broadly used tools in the analytical chemistry for the investigation of organic molecules with biological functions[24,25]. Major advantages of the ESI/MS technique consist of the lack of fragmentation and the predominance of multiply charged pseudomolecular ions, allowing for the accurate mass determination of macromolecules and biomolecules. However, no information about the molecular structure is obtained. In contrast, ESI connected to tandem mass spectrometry (MS/MS) allows for protein sequencing and peptide mapping providing information with regards to the molecular structure and composition.

Within the course of this work, high-resolution MS data were obtained to establish the accurate molecular weight of all prepared adenosine derivatives. Additionally, MS^n data of selected adenosine derivatives were acquired to obtain fragmentation patterns characterizing modified adenosines that share common structural features.

High-resolution MS and MS^n data were obtained on a Finnigan MAT 95 XL TRAP instrument. Within the Finnigan MAT 95 XL TRAP mass spectrometer a magnetic sector followed by an ion trap based MS system is combined with the ESI technique. While the magnetic sector MS offers the preparation of high-resolution data, the ion trap MS can be operated in the MS/MS mode establishing MS^n data. Thereby, collisional induced decomposition (CID) of pseudomolecular ions (precursor ions, parent compounds) leads to characteristic product ions (daughter fragments) that can be fragmented again.

A range of adenosine derivatives was analyzed by ESI/MS/MS to obtain structure-specific fragment ion information. Adenosines were divided by their structural features into the following classes: (A) N^6-Monosubstituted sugar modified nucleoside scaffolds (e.g. **2**, figure 5); (B) 5´,N^6-di-substituted adenosines established via PASP synthesis, displaying a simple, not modified carboxylic diversity fragment in the 5´-position (e.g. **23**, figure 6); (C) 5´,N^6-disubstituted adenosines established via cPASP synthesis, displaying a nitro-aniline-benzoic acid diversity fragment in the 5´-position (e.g. **32**, figure 8); (D) 5´,N^6-disubstituted adenosines established via cPASP synthesis, displaying an amido-aniline-benzoic acid diversity fragment in the 5´-position (e.g. **38**, figure 9).

2.4.2 Fragmentation Patterns of N^6-Monosubstituted and 5´,N^6-Disubstituted Adenosines

MS^n studies of N^6-monosubstituted and 5´,N^6-disubstituted adenosine derivatives revealed a typical fragmentation pattern of the compounds synthesized. On the basis of obtained product ions, two main fragmentation pathways are demonstrated in scheme 9. Postulated (and potential) formulas of main fragments found in all MS spectra as well as postulated charge sites are illustrated along the fragmentation sequence of **38**.
When fragmenting N^6-monosubstituted or 5´,N^6-disubstituted adenosines, the first fragmentation generally occurs between the N^9-atom of the purine moiety and the anomeric carbon of the sugar moiety. Depending on the location of the charged site in the molecule, pathway A or B is followed. If the charge remains at the purine moiety (pathway A), main fragments of the molecular composition of $C_{16}H_{14}N_5$ (MW 276), $C_{11}H_9$ (MW 141), and C_9H_7 (MW 115) are observed in all derivatives. When charging occurs at the sugar moiety (pathway B), fragmentation generally takes place in the same regions of the molecules, providing characteristic common fragments that were classified by their structural features (oxonium-, amidium-, and acylium-ions). Due to the introduced diversity in the 5´-position, the molecular composition of the sugar moiety differs in each compound synthesized, leading to different molecular compositions and molecular weights of the obtained fragments. In the case of **38**, the following molecular compositions and molecular weights for the oxonium ($C_{18}H_{24}N_3O_6$, MW 378), amidium ($C_{13}H_{18}N_3O_3$, MW 264), and acylium fragments ($C_{13}H_{15}N_2O_3$, MW 247) were observed.

Compound **2** (figure 5) simply fragmented along pathway A. After initial fragmentation, the charge remained within the purine moiety, displaying typical daughter ions 141 and 115.
Figure 6 and 7 demonstrate fragmentation patterns of the ^{35}Cl and ^{37}Cl isotope of **23**. When fragmenting the parent compound (637 and 639, respectively), main daughter ion 276 was found in both spectra. Besides 276, small amounts of 362 and 344 (figure 6) and of 364 and 346 (figure 7) were found, illustrating the difference in molecular weight of fragments including a ^{35}Cl or ^{37}Cl atom. In figure 6, product ion 276 was chosen for further fragmentation showing typical fragments 141and 115 (not shown) according to pathway A. Figure 7 shows the fragmentation of 364 ($C_{15}H_{18}Cl_2NO_5$, oxonium), obtaining typical fragments along pathway B: 346 ($C_{15}H_{16}Cl_2NO_4$, oxonium with additional fragmentation of one molecule of water), 250 ($C_{10}H_{12}Cl_2NO_2$, amidium), and 233 ($C_{10}H_9Cl_2O_2$, acylium).
Compound **32** (figure 8) mainly fragmented according to pathway A. Only a small amount of daughter ion 366 ($C_{16}H_{20}N_3O_7$, oxonium) of pathway B was observed.
In contrast to compounds **2**, **23**, and **32**, compound **38** (figure 9) exclusively fragmented along pathway B. When fragmenting main daughter ion 378 ($C_{18}H_{24}N_3O_6$, oxonium), five product ions were observed. Besides main daughter ions 360 ($C_{18}H_{22}N_3O_5$, oxonium along additional elimination of one molecule of water) and 247 ($C_{13}H_{15}N_2O_3$, acylium), fragments 318, 276, and 264 ($C_{13}H_{18}N_3O_3$, amidium) were obtained. Differences of 18 (378→360), 42 (360→318), and 17 (264→247) typically correspond to losses of water, acetate, and ammonia moieties, respectively. Of special interest was the fragment 276. Since 276 was formed when fragmenting product ion 378, and not when fragmenting precursor ion 653, fragment 276 is part of the fragmentation sequence of pathway B. Thus, the molecular weight of 276 can theoretically be assigned to two different molecular compositions ($C_{14}H_{18}N_3O_3$ or $C_{16}H_{14}N_5$) and therefore to various scaffolds.
In figures 5 to 9, fragmentation arrows F_1 and F_2 illustrate the predominant fragmentation sites in the molecule yielding main fragments along pathway A and/or B.

Analyzed type II adenosine derivatives (not shown) display similar fragmentation patterns compared to type I adenosines described above.

Scheme 9. Likely fragmentation patterns of 5′,N^6-disubstituted adenosine derivatives illustrated along compound **38**.

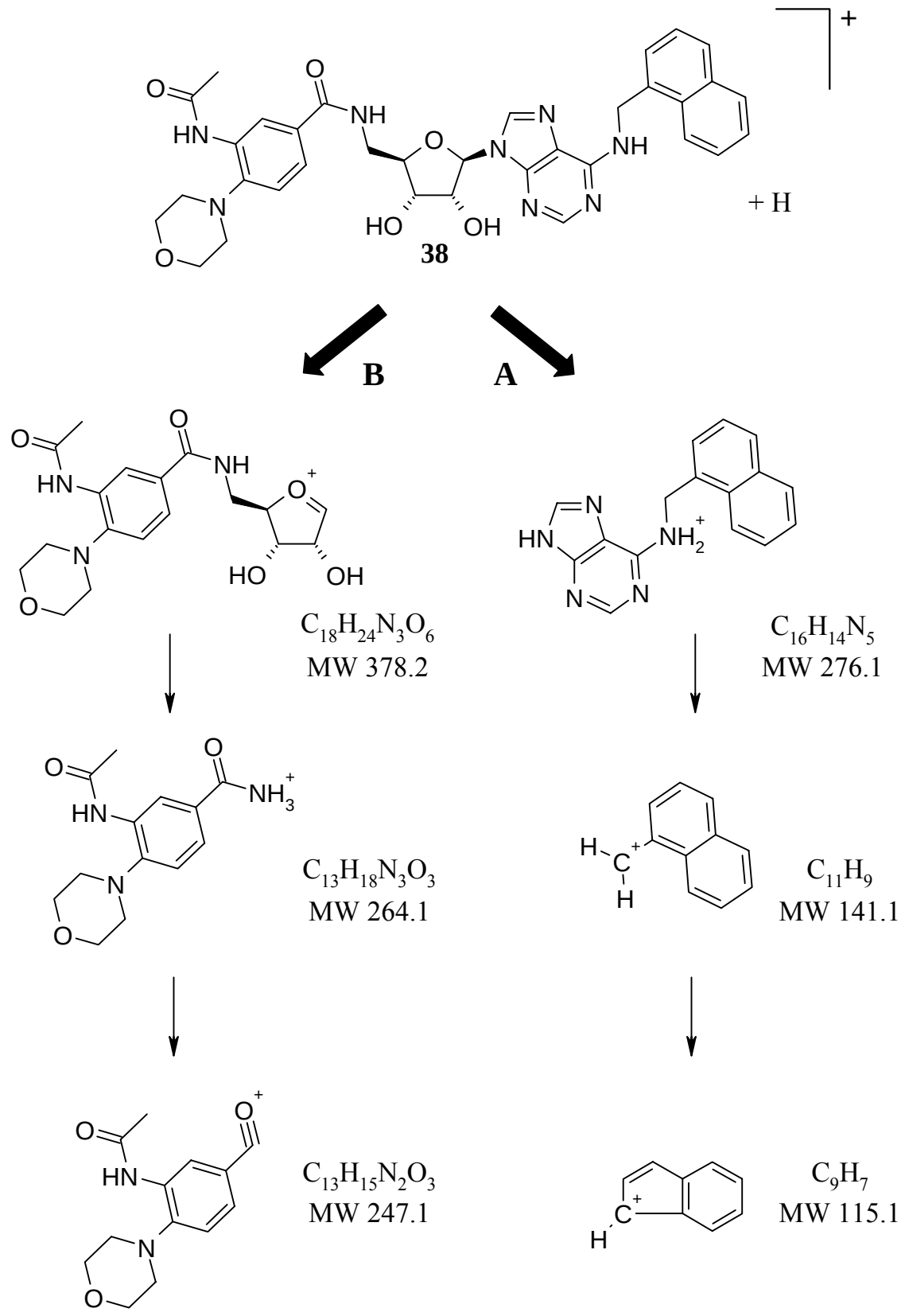

Figure 5. Fragmentation pattern of **2** (MW 406.45; $[M+H]^+$ 407.1832).

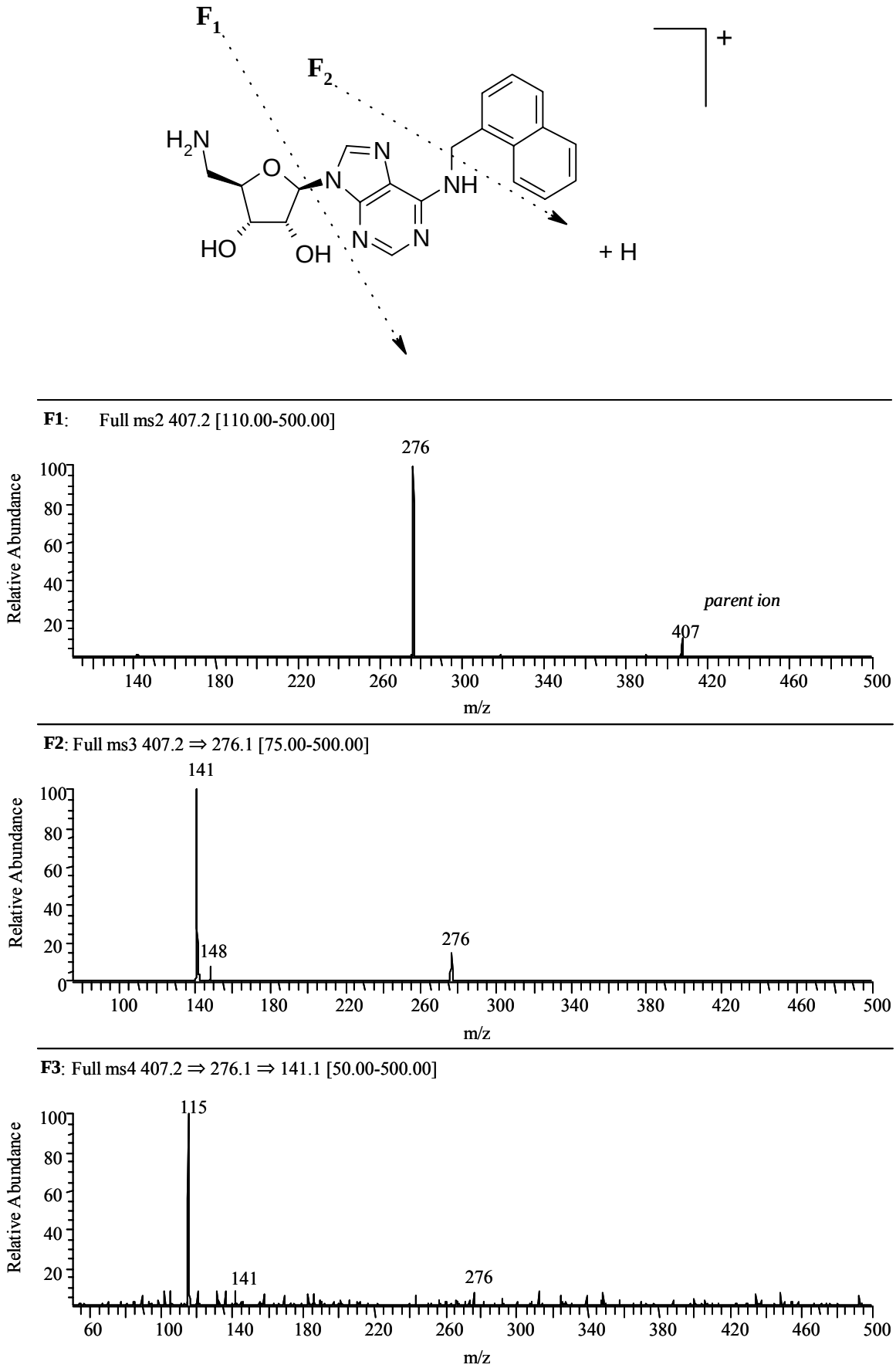

Figure 6. Fragmentation pattern of **23**; ^{35}Cl isotope (MW 637.53; $[M+H]^+$ 637.1734).

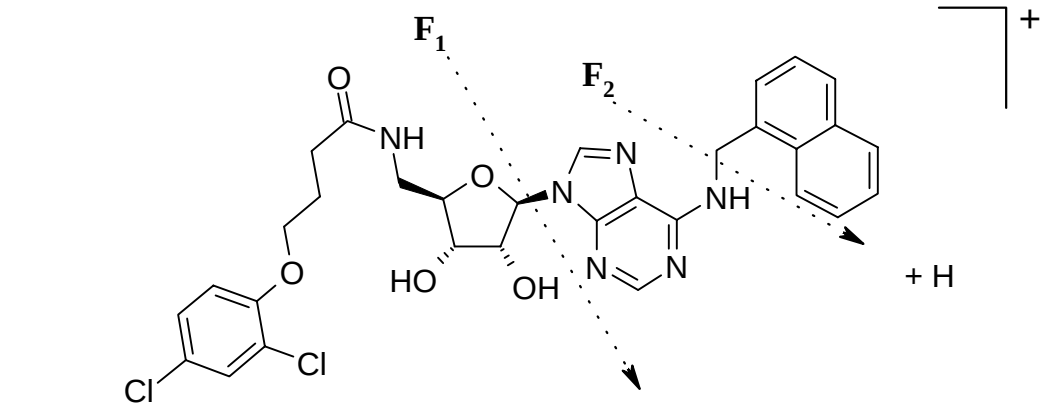

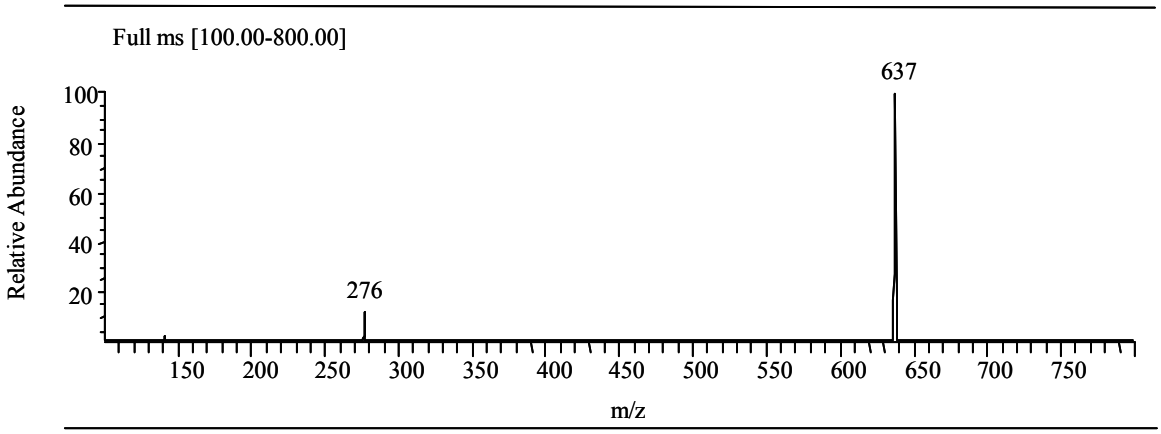

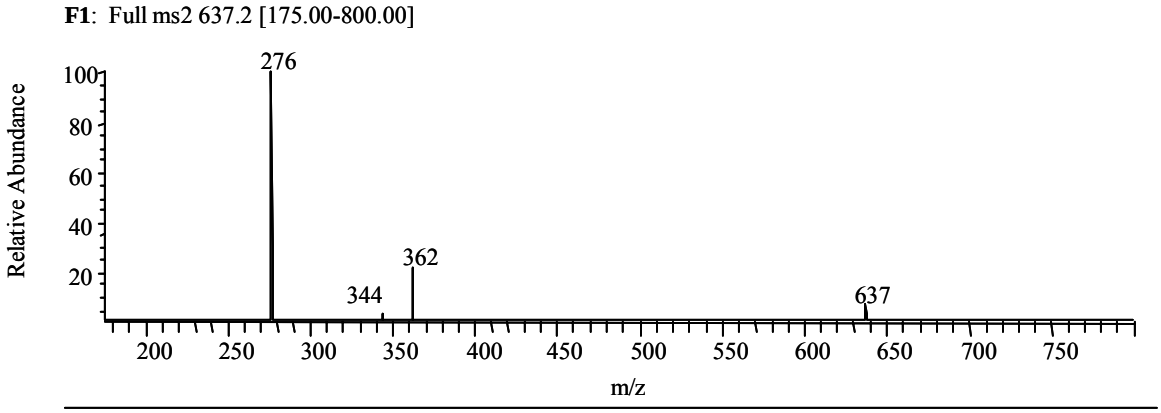

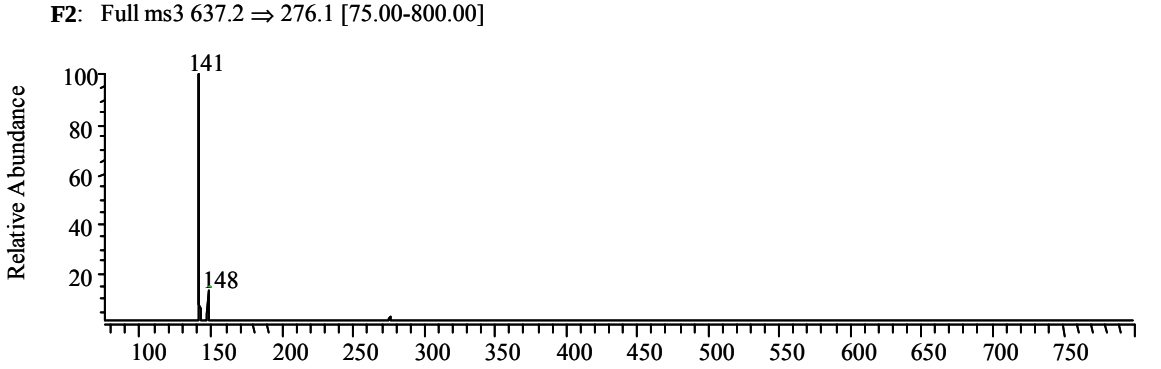

Figure 7. Fragmentation pattern of **23**; ^{37}Cl isotope (MW 639.08; $[M+H]^+$ 639.1788).

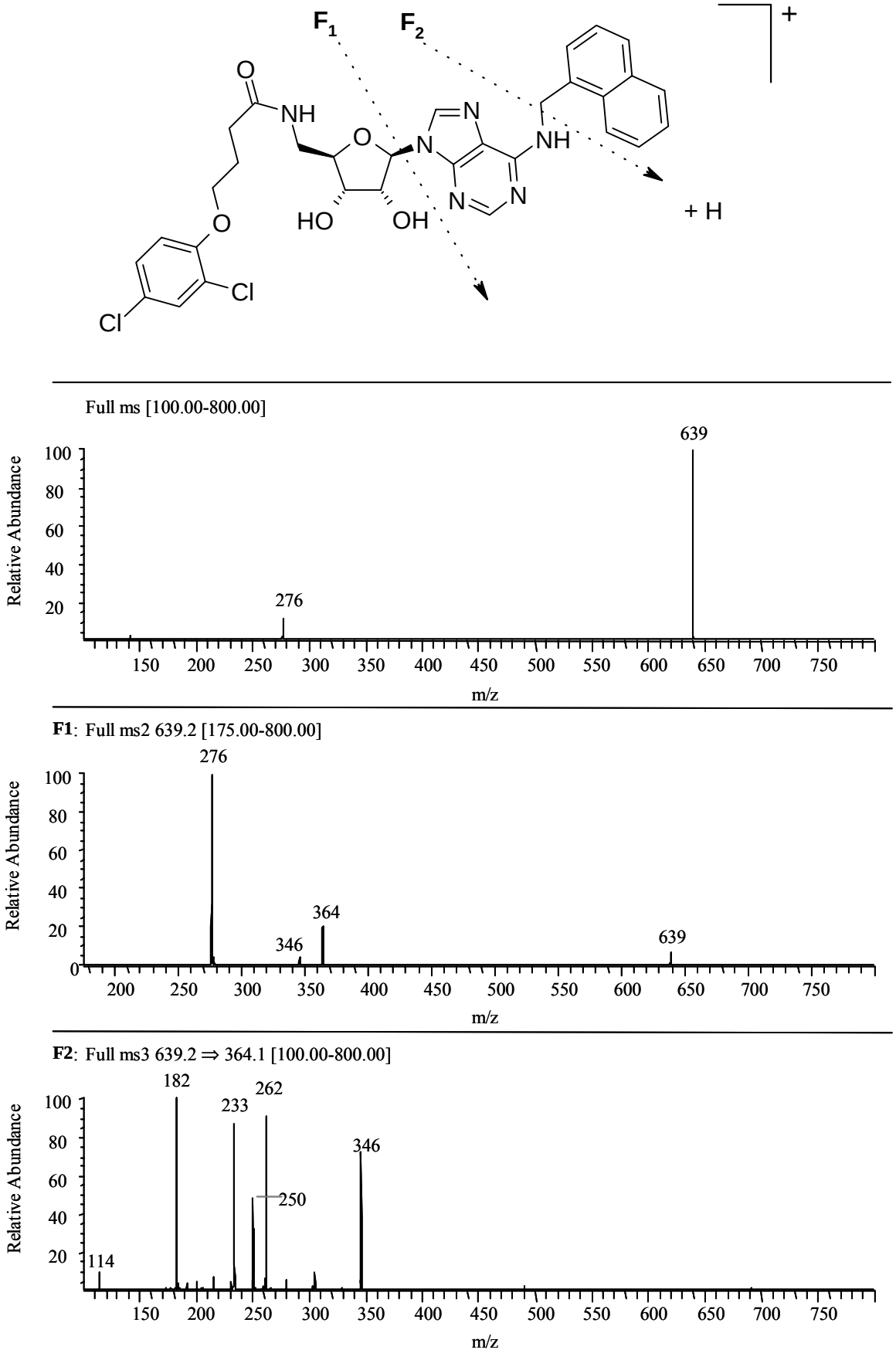

Figure 8. Fragmentation pattern of **32** (MW 640.66; $[M+H]^+$ 641.2473).

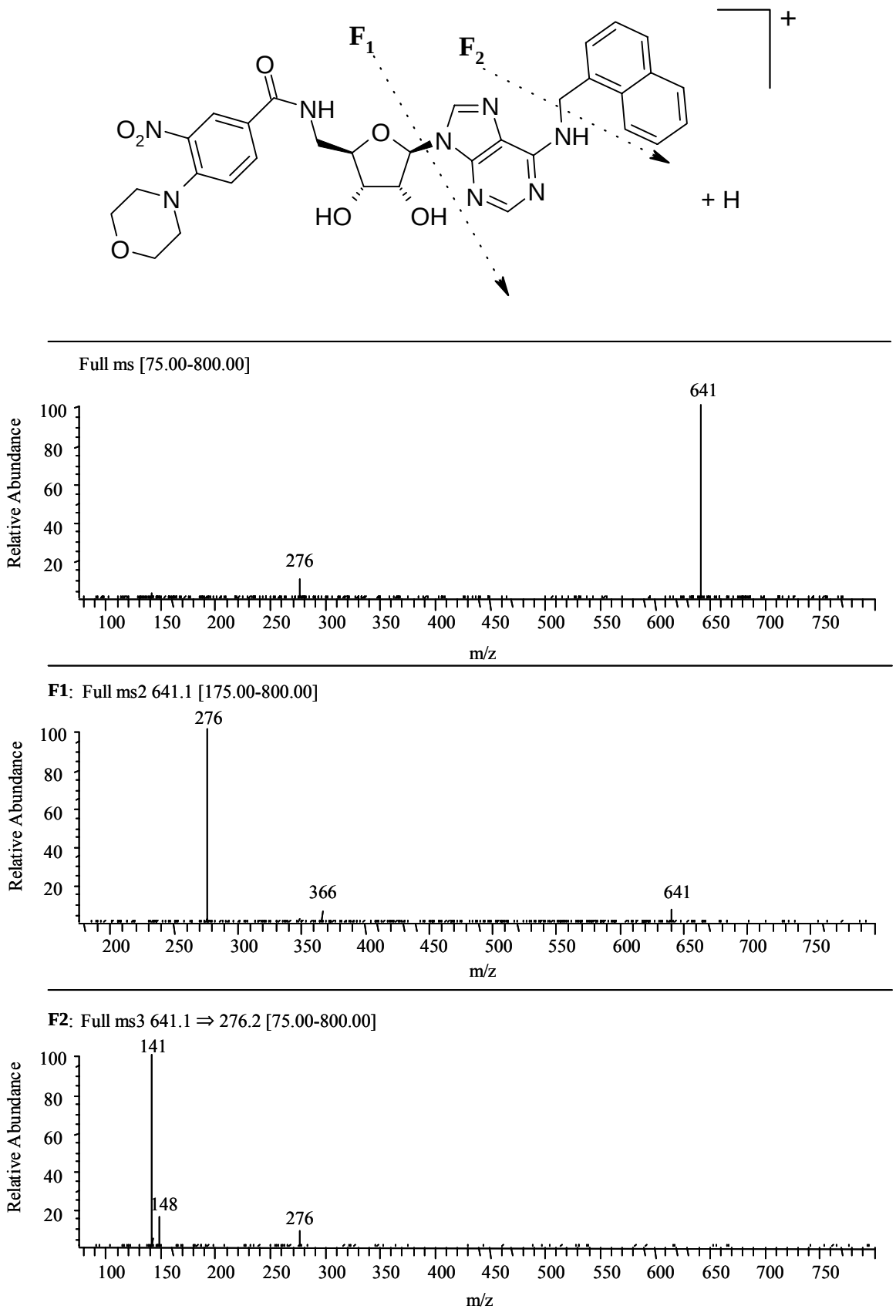

Figure 9. Fragmentation pattern of **38** (MW 652.72; $[M+H]^+$ 653.2837).

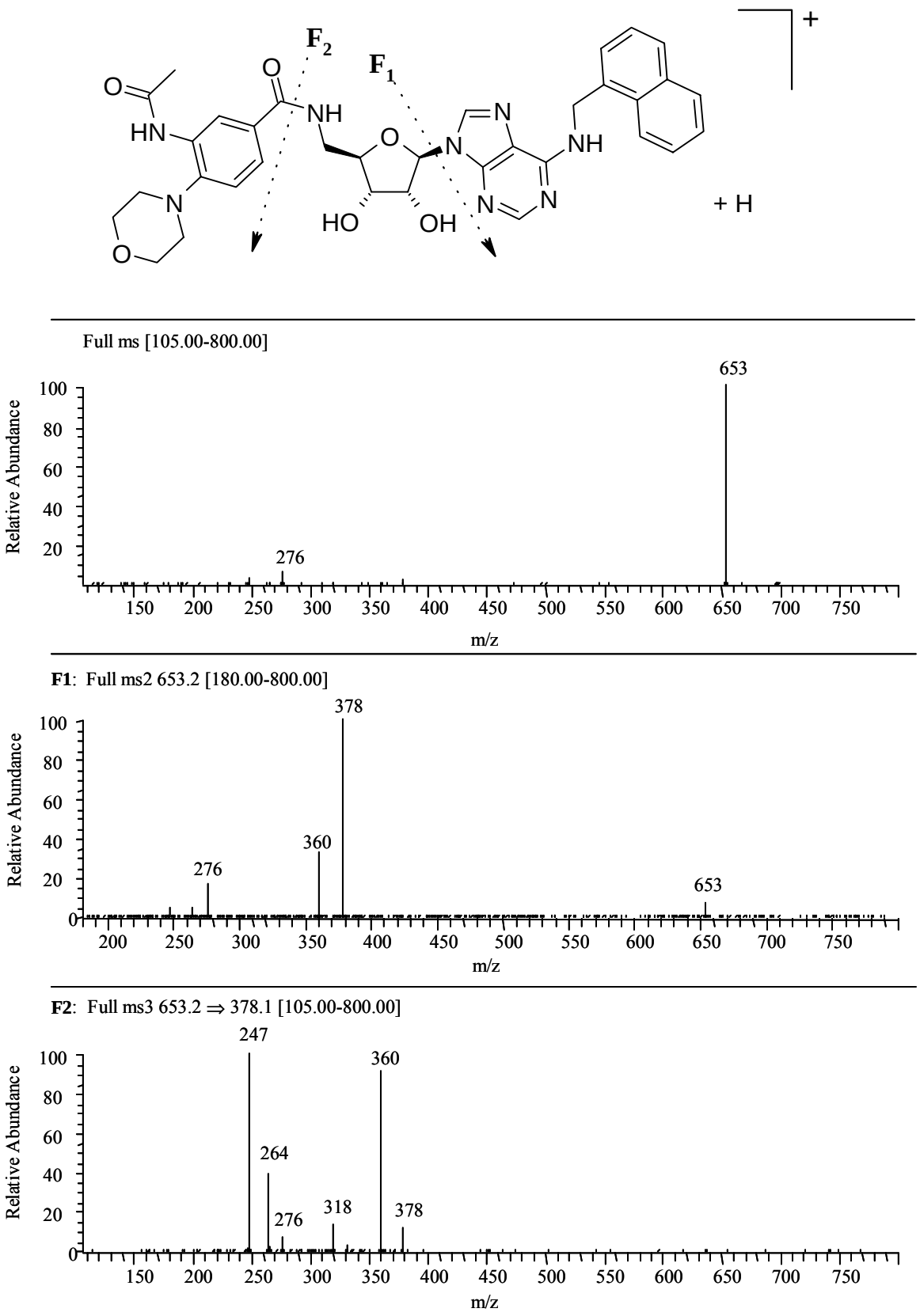

2.5 Discussion

Only two promising benzylic amines were selected for the synthesis of 36 novel and one known (**21**) 5′,N^6-disubstituted adenosine derivatives. Using PASP and cPASP synthesis protocols, diversity fragments were introduced solely into the 5′-position of templates **2** and **10** leading to amido-deoxy-nucleosides of type I (**14-46**, and **52**) and type II (**47-49)** in fair to excellent yield.

The reason for the selection of the 1-naphthyl and the biphenyl ring as fix substituents in the N^6-position of the adenosine scaffold lies in the high probability of favorable lipophilic interactions with hydrophobic binding domains in biological systems, as it has been discussed by Hajduk et al., recently[26].

The second substituent, to be introduced into the 5′-postion of the modified adenosine scaffolds **2** and **10**, was chosen from a broad range of carboxylic acid residues. Because only preliminary data concerning a possible binding orientation for the adenosine core was available, a considerable degree of diversity was regarded necessary.

The scope of the cPASP reaction applied for this purpose is considerable, but limitations were observed. When too large substituents on the aromatic ring adjacent the safety-catch linker were combined, the yield and the purity obtained are below the otherwise high standard obtained when using the PASP protocol. The products had to be purified by LC prior to biological evaluation. Generally speaking, the purity of the target compounds decreases with the extent of the SPOS modification sequence. Further optimization of the individual transformation steps is necessary and should enable to avoid a time consuming chromatographic purification in the future. The formation of the side-products **14** and **15**, respectively, in the cases of acylated aniline derivatives **37**, **40-43**, and **49** is reduced, when no DMAP is added as acylation catalyst during the introduction of the acetyl or propionyl group in **38**, **39**, **44-45**, and **52**. In the presence of DMAP, acetic or propionic anhydride acylates residual sulfamoyl groups of the linker that were not acylated by 4-fluoro-3-nitrobenzoic acid. Therefore, after cyanomethylation, they form a second acylating species (e.g. **13** with R^1= CH_3 or C_2H_5) and the by-products **14** and **15**, respectively, are formed along the desired products and have to be removed by LC. A general solution to this problem is to ensure complete acylation of 4-fluoro-3-nitrobenzoic acid by repeating the immobilization step. In the case of expensive carboxylic acids this might be undesirable. Alternatively, a capping step with bulky sterically hindered

acids is possible. The straightforward way already mentioned above is to avoid the strong acylation catalyst DMAP for further acylation steps. When a less powerful catalyst like 1-hydroxybenzotriazole (HOBt) was applied instead of DMAP in the cases of **38**, **39**, **44**, **45**, and **52**, practically no acylation of residual sulfamoyl groups of the linker is observed and consequently no by-products **14** and **15** were formed.
Comparing the purity obtained of N^6-naphthylmethyl and N^6-biphenyl-methyladenosine analogs, the use of N^6-biphenylmethyladenosine as a rule lead to a decrease of product purity of the derivatives obtained. Partly, this might be attributed to possible alteration of the polymer-bound building blocks during storage, but the small set of biphenyl derivatives **47**-**49** prepared so far does not allow drawing a conclusion. However, for the most part we were unable to detect a difference in the conversion rate between differently related amino-deoxyadenosine derivatives in the final amidation step.

Despite of considerable structural diversity, most of the 5′,N^6-disubstituted adenosine derivatives displayed moderate but significant antimalarial activity against the Dd2 strain of *P. falciparum*. Obviously a small amide residue like in compound **14** is inferior to the parent amino compound or in the same range of activity in the cases of slightly larger residues as seen in derivatives **15** and **16**. Large, lipophilic aniline derived residues like in compounds **34**, **41**, **42**, and **46** lead to increased activity in the low micro molar range (1.3 to 3.3 µM).
While the higher initial activity of scaffold **9** suggested a possible increase in activity by replacing the naphthyl ring for a biphenyl group, this hope was not fulfilled in the in vitro experiments. Compounds **47** and **49** exhibited activity that is comparable to the activity of the compounds from the naphthyl series, but not superior to the parent compound **9**, which displayed an IC_{50} value of 2.1 µM.
Inhibition of the DOXP reductoisomerase by 5′,N^6-disubstituted adenosines of type I and II was observed in 12 out of 33 cases. Generally, lower IC_{50} values were correlated to the incidence of DOXP reductoisomerase inhibition. Compound **33** exhibited the best inhibitory effect on DOXP reductoisomerase (70%), whereas compound **34** showed the best activity on the *P. falciparum* strain Dd2 (IC_{50} = 1.3 µM). Thus, an involvement of 5′,N^6-disubstituted adenosines in the DOXP/MEP pathway inhibiting the DOXP reductoisomerase seems to be likely in some cases and might represent a potential target for the chemotherapy of *P. falciparum*. On the contrary,

inhibition studies of 5′,N^6-disubstituted adenosines against plasmodial AdoMetDC showed no inhibitory effect excluding the polyamine pathway as a potential target for the treatment of malaria caused by *P. falciparum*.
Since most of the structural highly diverse adenosine derivatives displayed comparable antimalarial activity evaluation of the cytotoxicity of the compounds prepared was regarded necessary. Thus, five adenosine derivatives of series I and one out of series II were selected to investigate whether the observed antimalarial effect is related to unspecific cell-mediated cytotoxicity. All of the six derivatives tested displayed an inhibitory effect on in vitro plasmodial development and are devoid of cytotoxicity towards human cells.

None of the 16 5′,N^6-disubstituted adenosine derivatives tested for their antitrypanosomal effect displayed an inhibitory effect against *T. cruzi*. Four out of 16 tested 5′,N^6-modified adenosines revealed moderate inhibition of *T. b. brucei*. While 2′,N^6-disubstituted and the 2′-monosubstituted adenosines have been reported to exhibit selective antitrypanosomal activity[3,27-32], 5′,N^6-disubstitution is predominantly correlated along inhibitory activity against *P. falciparum*. Consequently, substitution in the 5′- and 2′-position, respectively, appears to be crucial for the selectivity of adenosine derivatives towards their effect on either plasmodial or trypanosomal parasites.

With respect to the different modification patterns of 5′,N^6-disubstituted adenosine analogs as well as to the results of the DOXP reductoisomerase inhibition studies, it can be concluded that not a single molecular target is recognized, as we suggested earlier[33]. Potential targets further include a variety of nucleotide dependent enzymes, the parasite′s nucleoside uptake machinery as well as unrelated cell functions.
To further explore the potential of N^6-substituted adenosine derivatives as antimalarial agents, selected N^6-substituted adenosine derivatives can be immobilized on biosensor chip surfaces via a biotin label incorporated in the 5′-position of the 5′-amino-5′-deoxy derivatives (see chapter 4). This approach seems feasible, because the in vitro data derived from this study suggest, that the biological activity is highly robust to alterations in this area of the molecule. The intended ligand fishing from different fractions from plasmodial proteins might become a valuable tool for the further understanding of the capability of non-toxic nucleoside derivatives to inhibit

parasitic protozoa in humans[34]. A suitable method for the biotin labeling will be discussed in chapter 4. Preliminary results have been published recently[35].

2.6 Experimental Section

The structures of all compounds were assigned by ^{1}H NMR spectroscopy. NMR spectra were recorded on a Bruker AMX 400 spectrometer using tetramethylsilane as internal standard. ^{1}H NMR data are reported based on separated spin-spin signals and protons that were not covered by H_2O- or DMSO-signals, unless otherwise noted. Identity and purity of compounds prepared on a larger (g) scale was ascertained by combustion analysis; test samples prepared in mg quantities were evaluated by high-resolution MS. The purity of the latter compounds was deduced from ^{1}H NMR data as well as evaluated from chromatographic purification profiles. Elemental compositions were calculated on the basis of microanalysis results obtained on a Heraeus CHN-O rapid instrument. MPLC simultaneous purity analyses/ purifications were performed using a Büchi 681 pump (flow rate 10 mL/min, methanol/water gradients) and an UV-detector (254 nm) with Merck 310-25 Lobar-LiChroprep®-RP-18 columns. High-resolution MS data were obtained on a Finnigan MAT 95 XL (ESI, methanol/water (1/1, v/v) infusion at 2 µL/min with polypropylene glycol as reference) or on a Micromass VG 70-250 S (FAB, *m*-nitrobenzylic alcohol as matrix with polyethylene glycol as reference) instrument; MS^n data on a Finnigan MAT 95 XL TRAP (ESI, methanol/water (1/1, v/v) infusion at 2 µL/min). Preparative column chromatography was performed on silica gel 100-200 active, 60 Å, from ICN or Dowex® OH^- (1×2-200) using glass columns (4.5×15 cm). TLC reaction control was performed on Macherey-Nagel Polygram® Sil G/UV_{254} pre-coated microplates, spots were visualized under UV-illumination at 254 nm.

1-(6-Chloropurin-9-yl)-ß-D-1,5-dideoxy-(5-phthalimido)ribofuranose (**6**)

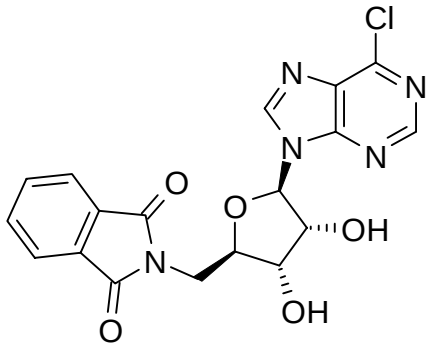

To 1-(6-chloro-purin-9-yl)-ß-D-1-deoxyribofuranose (**5**) (6.0 g, 21 mmol), phthalimide (7.70 g, 52 mmol, 2.5 equivalents), and Ph_3P (13.72 g, 52 mmol, 2.5 equivalents) freshly dried THF (150 mL) was added and the resulting suspension was cooled to -20 °C. Then, di-*tert*-butyldiazocarboxylate (12.0 g, 52 mmol, 2.5 equivalents) was added and the mixture was stirred first for 30 min at -20 °C and then at room temperature for 24 h. The dark yellow suspension initially formed turned into a light yellow solution after 5 min. After 24 h, the solution was evaporated in vacuo and the resulting brownish sticky residue was crystallized from CH_2Cl_2/MeOH (95:5) to give **6** with ^{1}H NMR analytical data comparable to those reported and additional ^{13}C NMR data and combustion analysis[3].

Yield 79%

Purity Combustion analysis
calcd [%] C=52.00, H=3.39, Cl=8.53, N=16.84
found [%] C=51.93, H=3.51, Cl=8.74, N=16.44

^{1}H NMR (400 MHz, DMSO-d_6) = δ (ppm) 8.97 (s, 1H, 8H), 8.61 (s, 1H, 2H), 7.85 (s, 4H, phthalimido), 6.03 (d, 1H, 1´H, *J*=5.1 Hz), 5.66 (d, 1H, 3´OH, *J*=5.6 Hz), 5.45 (d, 1H, 2´OH, *J*=5.6 Hz), 4.85-4.81 (m, 1H, 2´H), 4.33-4.30 (m, 1H, 3´H), 4.23-4.19 (m, 1H, 4´H), 4.02-3.91 (m, 2H, 5´CH_2)

^{13}C NMR (101 MHz, DMSO-d_6) = δ (ppm) 167.72, 151.46, 151.36, 149.21, 146.35, 134.41, 131.38, 131.39, 123.00, 88.41, 81.75, 72.74, 71.32, 39.63

HRFAB-MS $C_{18}H_{14}ClN_5O_5$
MW 415.80
$[M+H]^+$ calcd 416.0762
$[M+H]^+$ found 416.0749

Activity Dd2 strain of *P. falciparum*: IC_{50} = 42 µM
DOXP reductoisomerase: 42%

N^6-(4-Phenylbenzyl)adenosine (**7**)

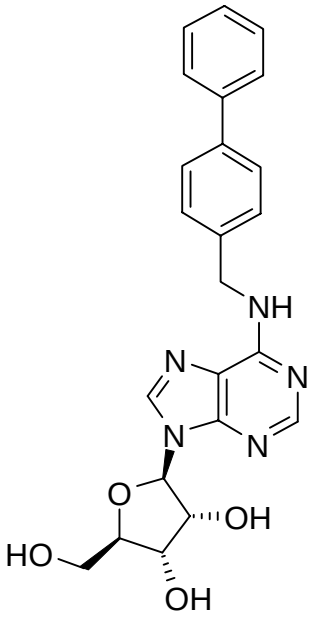

To a solution of 1-(6-chloro-purin-9-yl)-ß-D-1-deoxyribofuranose (**5**) in 1-propanol was added 1.1 equivalent of 4-phenylbenzylamine and one equivalent of DIPEA. The reaction mixture was stirred at 60 °C. The reaction was monitored by TLC and terminated when the starting material had disappeared (12-24 h). The resulting white solid was crystallized from MeOH. ^{1}H NMR data are as reported[33].

HRFAB-MS $C_{23}H_{23}N_5O_4$
MW 433.47
$[M+H]^+$ calcd 434.1829
$[M+H]^+$ found 434.1848

5′-Deoxy-N^6-(1-naphthylmethyl)-5′-phthalimidoadenosine (**8**)

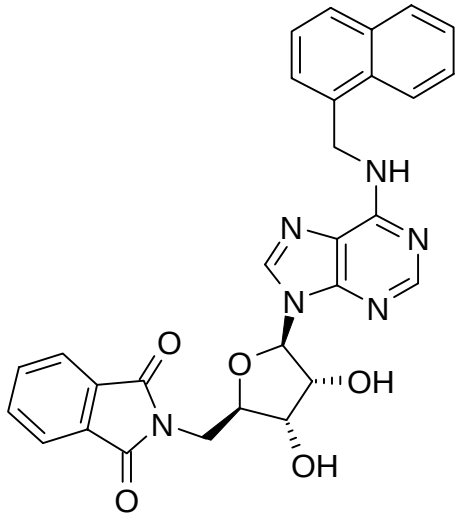

To a suspension of 1-naphthylmethylamine (1.0 g, 6.38 mol, 1.1 equivalent) in absolute EtOH **6** (2.41 g, 5.8 mol) was added and the reaction mixture was stirred at 50 °C for 30 min. DIPEA (0.374 g, 2.9 mmol, 0.5 equivalent) was added and the reaction mixture further agitated at 50 °C for 24 h. As the conversion of **6** to **8** was incomplete another equivalent of 1-naphthyl-methylamine (0.91 g, 5.8 mmol) and of DIPEA (0.75 g, 5.8 mmol) were added to the reaction mixture and again stirred for 48 h at 50 °C. The mixture was evaporated in vacuo. The resulting material was crystallized from MeOH and a white solid was obtained.

Yield 91%

Purity Combustion analysis ($C_{29}H_{24}N_6O_5 \times ½\ H_2O$)
calcd [%] C=63.83, H=4.58, N=15.40
found [%] C=63.83, H=4.42, N=15.19

^{1}H NMR (400 MHz, DMSO-d_6) = δ (ppm) 8.42 (bs, 2H, N^6H overlapping 8H), 8.24 (d, 1H, naphthyl, *J*=7.6 Hz), 8.01 (s, 1H, 2H), 7.96-7.94 (m, 1H, naphthyl), 7.87-7.81 (m, 5H, 1H naphthyl overlapping 4H phthalimido), 7.59-7.53 (m, 2H, naphthyl), 7.45-7.41 (m, 2H, naphthyl), 5.90 (d, 1H, 1′H, *J*=5.6 Hz), 5.53 (d, 1H, 3′OH, *J*=6.1 Hz), 5.34 (d, 1H, 2′OH, *J*=5.08 Hz), 5.17 (bs, 2H, CH_2, naphthylmethyl), 4.81-4.80 (m, 1H, 2′H), 4.28-4.27 (m, 1H, 3′H), 4.17-4.13 (m, 1H, 4′H), 4.01-3.96 (m, 1H, 5′CH_2), 3.89-3.84 (m, 1H, 5′CH_2)

^{13}C NMR (101 MHz, DMSO-d_6) = δ (ppm) 168.21, 152.79, 134.81, 133.62, 131.88, 131.18, 128.87, 127.50, 126.49, 126.08, 125.80, 124.88, 123.72, 123.45, 88.16, 81.75, 72.94, 71.85, 41.35, 40.18

HRESI-MS $C_{29}H_{24}N_6O_5$
MW 536.55
$[M+H]^+$ calcd 537.1886
$[M+H]^+$ found 537.1890

Activity Dd2 strain of *P. falciparum*: IC_{50} = 11 µM
DOXP reductoisomerase: 0%

5´-Deoxy-N^6-(4-phenylbenzyl)-5´-phthalimidoadenosine (**9**)

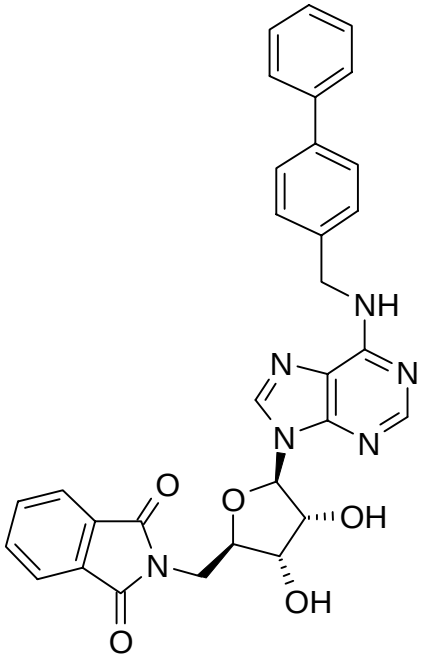

To **7** (0.78 g, 1.8 mmol), phthalimide (0.589 g, 4 mmol), and Ph_3P (1.048 g, 4 mmol) freshly dried THF (14 mL) was added and the resulting suspension was cooled down to -20 °C. Di-*tert*-butyldiazocarboxylate (0.92 g, 4 mmol) was added and the mixture was stirred first for 30 min at -20 °C and then at room temperature resulting in a dark yellow suspension, which turned into a light yellow solution after 5 min. After 12 h the conversion of **7** to **9** was completed. The solution was evaporated in vacuo and the resulting solid residue was crystallized from MeOH to give pure **9** as a white, amorphous solid.

Yield 84%

Purity Combustion analysis ($C_{31}H_{26}N_6O_5 \times ½\ H_2O$)
calcd [%] C=65.14, H=4.76, N=14.70
found [%] C=65.46, H=4.67, N=14.80

^{1}H NMR (400 MHz, DMSO-d_6) = δ (ppm) 8.45 (bs, 1H, N^6H), 8.41 (s, 1H, 8H), 8.01 (bs, 1H, 2H), 7.87-7.81 (m, 4H, phthalimido), 7.64-7.58 (m, 4H, biphenyl), 7.46-7.41 (m, 4H, biphenyl), 7.35-7.32 (m, 1H, biphenyl), 5.89 (d, 1H, 1´H, *J*=5.3 Hz), 5.53 (d, 1H, 3´OH, *J*=5.9 Hz), 5.34 (d, 1H, 2´OH, *J*=5.1 Hz), 4.81-4.77 (m, 1H, 2´H), 4.73 (bs, 2H, CH_2, biphenylmethyl), 4.29-4.26 (m, 1H, 3´H), 4.17-4.12 (m, 1H, 4´H), 4.01-3.96 (m, 1H, 5´CH_2), 3.89-3.84 (m, 1H, 5´CH_2)

^{13}C NMR (101 MHz, DMSO-d_6) = δ (ppm) 167.75, 152.32, 139.95, 139.25, 138.52, 134.36, 131.45, 128.78, 127.65, 127.14, 126.47, 123.0, 87.78, 81.26, 72.53, 71.42

HRESI-MS $C_{31}H_{26}N_6O_5$
MW 562.59
$[M+H]^+$ calcd 563.2043
$[M+H]^+$ found 563.2028

Activity Dd2 strain of *P. falciparum*: IC_{50} = 4.3 µM
DOXP reductoisomerase: 0%

5´-Amino-5´-deoxy-N^6-(1-naphthylmethyl)adenosine (**2**)

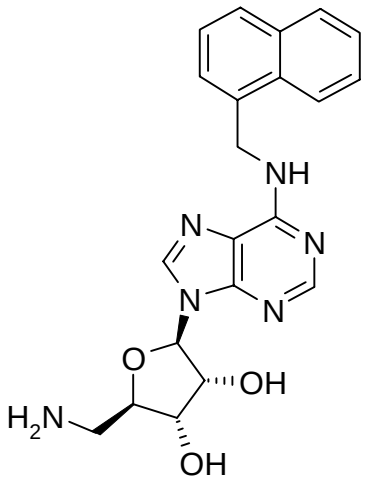

A suspension of **8** (1 g, 1.86 mmol) and hydrazine hydrate (0.153 g, 3 mmol) in EtOH (150 mL) was stirred for 30 min at 50 °C and successively refluxed for 1 h, with the precipitate being dissolved completely after 5 min of refluxing. After cooling to room temperature, one half of the solvent of the reaction mixture was evaporated in vacuo. The resulting precipitate, phthalazide, was separated from the reaction mixture, which subsequently was further evaporated leading to a brownish highly viscous liquid. The product was purified over Dowex® OH^- (1×2-200) with MeOH/H_2O gradients as eluent and gave ^{1}H NMR analytical data comparable to those reported and additional ^{13}C NMR data and combustion analysis[3].

Yield 77%

Purity Combustion analysis ($C_{21}H_{22}N_6O_3 \times ½\ H_2O$)
calcd [%] C=60.65, H=5.54, N=20.22
found [%] C=60.33, H=5.45, N=19.98

^{1}H NMR (400 MHz, DMSO-d_6) = δ (ppm) 8.46 (bs, 1H, N^6H), 8.43 (bs, 1H, 8H), 8.25-8.23 (m, 1H, naphthyl), 8.22 (s, 1H, 2H), 7.96-7.94 (m, 1H, naphthyl), 7.82 (d, 1H, naphthyl, *J*=8.1 Hz), 7.59-7.52 (m, 2H, naphthyl), 7.46-7.40 (m, 2H, naphthyl), 5.89 (d, 1H, 1´H, *J*=6.3 Hz), 5.43 (bs, 1H, 3´OH), 5.19 (bs, 3H, 2´OH overlapping CH_2 naphthylmethyl), 4.71 (bs, 1H, 2´H), 4.17-4.15 (m, 1H, 3´H), 3.89-3.86 (m, 1H, 4´H), 2.85-2.81 (m, 1H, 5´CH_2), 2.77-2.72 (m, 1H, 5´CH_2), 2.32-1.43 (bs, 2H, NH_2)

^{13}C NMR (101 MHz, DMSO-d_6) = δ (ppm) 152.42, 140.07, 133.16, 130.71, 128.40, 127.03, 126.44, 126.02, 125.61, 125.32, 123.26, 87.34, 86.14, 72.90, 70.70, 43.70, 40.89

HRESI-MS $C_{21}H_{22}N_6O_3$
MW 406.45
$[2M+H]^+$ calcd 813.3585
$[2M+H]^+$ found 813.3587

Activity Dd2 strain of *P. falciparum*: IC_{50} = 12 µM
DOXP reductoisomerase: 0%

5´-Amino-5´-deoxy-N^6-(4-phenylbenzyl)adenosine (**10**)

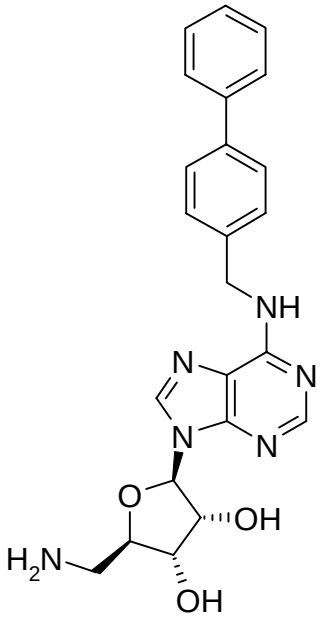

A suspension of **9** (1 g, 1.8 mmol) and hydrazine hydrate (0.180 g, 3.6 mmol) in EtOH/THF 1:1 (150 mL) was stirred for 30 min at 50 °C, successively refluxed for 4 h, and then stirred at room temperature over the weekend. As the conversion was incomplete hydrazine hydrate (0.18 g, 3 mmol) was added again, stirred at 50 °C and subsequently refluxed for 6 h. One half of the solvent of the reaction mixture was evaporated in vacuo. The resulting precipitate, phthalazide, was separated from the reaction mixture, which subsequently was further evaporated leading to a brownish highly viscous liquid. The product was purified over Dowex® OH^- (1×2-200) with MeOH/H_2O gradients as eluent and yielded a white crystalline solid.

Yield 40%

Purity Combustion analysis
calcd [%] C=63.88, H=5.59, N=19.43
found [%] C=63.63, H=5.63, N=19.04

^{1}H NMR (400 MHz, DMSO-d_6) = δ (ppm) 8.44 (bs, 1H, N^6H), 8.41 (s, 1H, 8H), 8.22 (s, 1H, 2H), 7.63-7.58 (m, 4H, biphenyl), 7.46-7.42 (m, 4H, biphenyl), 7.35-7.31 (m, 1H, biphenyl), 5.86 (d, 1H, 1´H, *J*=6.1 Hz), 5.39 (d, 1H, 3´OH, *J*=5.9 Hz), 5.10 (bs, 1H, 2´OH), 4.75 (bs, 2H, CH_2, biphenylmethyl), 4.71-4.69 (m, 1H, 2´H), 4.15-4.12 (m, 1H, 3´H), 3.88-3.85 (m, 1H, 4´H),

2.85-2.80 (m, 1H, 5′CH_2), 2.76-2.72 (m, 1H, 5′CH_2), 1.69-1.41 (bs, 2H, NH_2)

^{13}C NMR (101 MHz, DMSO-d_6) = δ (ppm) 152.40, 140.05, 139.95, 139.25, 138.47, 128.77, 127.60, 127.14, 126.44, 87.36, 86.15, 72.91, 70.69, 43.10

HRESI-MS	$C_{23}H_{24}N_6O_3$	$[M+H]^+$ calcd 433.1989
	MW 432.49	$[M+H]^+$ found 433.1968

Activity Dd2 strain of *P. falciparum*: IC_{50} = 2.1 μM
DOXP reductoisomerase: 41%

General procedure A for the synthesis of simple polymer-supported acids: To a flask containing 2.0 g of dry 4-sulfamoylbenzoylaminomethyl polystyrene with an initial loading level of 1.24 mmol/g as determined by elemental analysis (prepared from very highly loaded aminomethylated polystyrene, purchased from Novabiochem, Switzerland, batch number A20540) was added 20 mL of THF. The resin was allowed to swell at room temperature for 2 h. In another flask, 10 mmol of the appropriate acid was dissolved in 10-20 mL dry THF and preactivated via in situ anhydride formation by adding 780 μL (5 mmol) *N*,*N*-diisopropylcarbodiimide (DIC). **CAUTION**: DIC may lead to severe allergic reactions; strictly avoid skin contact. After addition of 580 μL DIPEA (3.4 mmol) and 15 mg (0.12 mmol) 4-(dimethylamino)pyridine (DMAP) as catalyst to the swollen resin, the coupling mixture was added. The resulting reaction mixture was agitated at room temperature for 24 h. The resin beads were filtered off and washed exhaustively with DMF (three times 5 mL), CH_2Cl_2 (three times 5 mL), and MeOH (three times 5 mL). After careful drying, the increase in weight was determined.

General procedure B for the synthesis of on-bead modified polymer-supported acids: THF (500 mL) was added to a flask containing 52.0 g of dry 4-sulfamoylbenzoyl-aminomethyl polystyrene with an initial loading level of 1.24 mmol/g, as determined by elemental analysis (prepared from very highly loaded aminomethylated polystyrene, purchased from Novabiochem, Switzerland, batch number A20540). The resin was allowed to swell at room temperature for 2 h. In another flask, 44.4 g (240 mmol) of 4-fluoro-3-nitrobenzoic acid was dissolved in 500 mL dry THF and

preactivated via in situ anhydride formation by adding 18.6 mL (120 mmol) DIC overnight. After the addition of 15 mL DIPEA (88 mmol) and 500 mg (4.1 mmol) DMAP as catalyst to the swollen resin, the coupling mixture was added. The resulting reaction mixture was agitated at room temperature for 48 h. The resin beads were filtered off and washed with DMF (three times), CH_2Cl_2 (three times), and MeOH (three times), resulting in 53.48 g resin after careful drying in vacuo. This weight increase of 11.48 g corresponds to a practically quantitative conversion of 4-sulfamoyl-benzamidomethyl polystyrene to [(4-fluoro-3-nitrobenzoyl)-4-sulfamoyl]-benzamidomethyl polystyrene **50**, resulting in a loading level of 1.00 mmol/g. For the derivatization of **50** to the appropriate resins to subsequently give final compounds **27**-**36**, 2.0 g of **50** (2.0 mmol) was treated with 20 mmol of the appropriate amine in 25 mL DMF overnight and subsequently washed with DMF (three times 5 mL) and MeOH (three times 5 mL). The color of the resin beads changed from white to a dark orange.
To 2.0 g of the appropriate nitroanilin-resins thus obtained, each, 40 mL of a 2 M tin-II-chloride solution in DMF was added. The resin suspensions were agitated for 48 h at room temperature and subsequently washed with DMF (three times 5 mL) and MeOH (three times 5 mL). The color of the resin beads changed from orange to yellow. The resulting dianiline-resins were agitated with 40 mL THF, DIPEA (0.580 mL, 3.4 mmol), DMAP (0.02 g, 0.15 mmol) as catalyst, and the appropriate anhydride (5 mmol) for 24 h leading to target compounds **37**, **40**-**43**, and **49**. The resin beads were filtered off and washed with DMF (three times 5 mL), CH_2Cl_2 (three times 5 mL), and MeOH (three times 5 mL). To reduce unwanted by-product formation caused by acylation of uncapped sulfamoyl linker groups, these experiments were repeated replacing DMAP by HOBt (0.80 g, 5.9 mmol) as catalyst for the acylation of the dianiline-resins resulting in final compounds **38**, **39**, **44**, **45**, and **52**.

General procedure C for the activation of polymer-supported acids of type 4 and 13: The sulfonamide linker of the appropriate resins (400 mg, approximately 0.4 mmol) was activated for cleavage by alkylation with 640 µL (9 mmol) bromoacetonitrile (**CAUTION**: Alkylating agent, strictly avoid skin contact), and 340 µL (2 mmol) DIPEA in 4 mL 1-methylpyrrolidone (NMP) for 12 to 48 h. The dark brown slurry was washed with dry DMSO (five times 5 mL) and THF (three times 10 mL) leading to white, yellow, and orange resin particles, respectively.

General procedure D for the synthesis of compounds 14-46, 47-49, and 52: The activated polymer-supported acids resulting from the alkylation of appropriate resins described above were transferred to the amino group of 10 µmol of the appropriate amino template **2** (dissolved in 1 mL THF) and **10** (dissolved in 1 mL NMP) by shaking at 55 degrees centigrade in 4 mL THF. The reaction was monitored by TLC and terminated when the starting material was quenched (12-48 h). Polymer beads and particulates were removed by filtration; the beads where extracted with dry THF (three times 5 mL) and MeOH (three times 5 mL). Combined fractions were collected and evaporated to furnish final compounds. Final compounds were analyzed by MPLC, NMR, and MS. **14-24**, **26**, **37-48**, and **42** were obtained as white, amorphous solids; **25-36** as yellow, amorphous solids.

5´-Acetamido-5´-deoxy-N^6-(1-naphthylmethyl)adenosine (**14**)

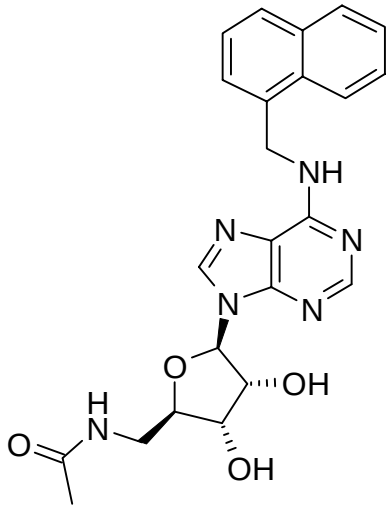

Yield 96%

^{1}H NMR (400 MHz, DMSO-d_6) = δ (ppm) 8.51 (bs, 1H, N^6H), 8.39 (bs, 1H, 8H), 8.25-8.23 (m, 3H, naphthyl overlapping NH amide overlapping 2H), 7.96-7.94 (m, 1H, naphthyl), 7.83-7.81 (m, 1H, naphthyl), 7.59-7.52 (m, 2H, naphthyl), 7.44-7.41 (m, 2H, naphthyl), 5.88 (d, 1H, 1´H, *J*=6.1 Hz), 5.47 (d, 1H, 3´OH, *J*=6.1 Hz), 5.27 (d, 1H, 2´OH, *J*=5.1 Hz), 5.19 (bs, 2H, CH_2, naphthylmethyl), 4.71-4.70 (m, 1H, 2´H), 4.06-4.03 (m, 1H, 3´H), 3.96-3.93 (m, 1H, 4´H), 1.85 (s, 3H, CH_3, acetamido)

HRESI-MS $C_{23}H_{24}N_6O_4$ $[M+Na]^+$ calcd 471.1757
MW 448.49 $[M+Na]^+$ found 471.1764

Activity Dd2 strain of *P. falciparum*: IC_{50} = 23 µM
DOXP reductoisomerase: 0%

5′-Deoxy-N^6-(1-naphthylmethyl)-5′-propanamidoadenosine (**15**)

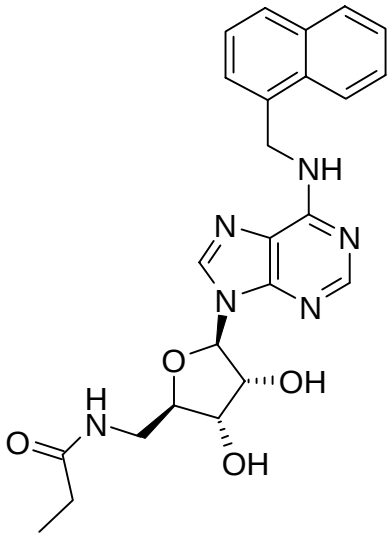

Yield 88%

^{1}H NMR (400 MHz, DMSO-d_6) = δ (ppm) 8.48 (bs, 1H, N^6H), 8.37 (bs, 1H, 8H), 8.24-8.23 (m, 2H, 2H overlapping naphthyl), 8.11 (t, 1H, NH, amide, *J*=5.5 Hz), 7.96-7.94 (m, 1H, naphthyl), 7.83-7.80 (m, 1H, naphthyl), 7.59-7.52 (m, 2H, naphthyl), 7.47-7.41 (m, 2H, naphthyl), 5.87 (d, 1H, 1′H, *J*=6.4 Hz), 5.44 (d, 1H, 3′OH, *J*=5.9 Hz), 5.24 (d, 1H, 2′OH, *J*=4.3 Hz), 5.19 (bs, 2H, CH_2, naphthylmethyl), 4.71-4.67 (m, 1H, 2′H), 4.06-4.03 (m, 1H, 3′H), 3.97-3.94 (m, 1H, 4′H), 3.41-3.36 (m, 2H, 5′CH_2), 2.15-2.09 (m, 2H, CH_2, propanamido), 0.99 (t, 3H, CH_3, propanamido, *J*=7.6)

HRESI-MS $C_{24}H_{26}N_6O_4$
MW 462.51
$[M+Na]^+$ calcd 485.1913
$[M+Na]^+$ found 485.1913

Activity Dd2 strain of *P. falciparum*: IC_{50} = 15 μM
DOXP reductoisomerase: 0%

5′-Cyclopropanamido-5′-deoxy-N^6-(1-naphthylmethyl)adenosine (**16**)

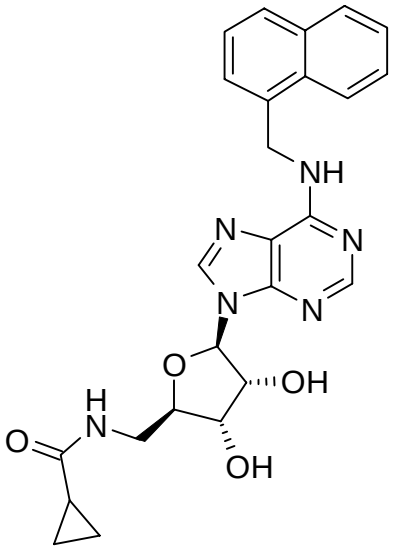

Yield 97%

^{1}H NMR (400 MHz, DMSO-d_6) = δ (ppm) 8.51 (s, 1H, N^6H) 8.44 (t, 1H, NH, amide, *J*=5.2 Hz), 8.39 (bs, 1H, 8H), 8.25-8.23 (m, 2H, 2H overlapping naphthyl), 7.96-7.94 (m, 1H, naphthyl), 7.83-7.81 (m, 1H, naphthyl), 7.59-7.53 (m, 2H, naphthyl), 7.44-7.41 (m, 2H, naphthyl), 5.89 (d, 1H, 1′H, *J*=6.6 Hz), 5.49 (d, 1H, 3′OH, *J*=6.6 Hz), 5.29 (d, 1H, 2′OH, *J*=5.1 Hz), 5.18 (bs, 2H, CH_2, naphthylmethyl), 4.72-4.71 (m, 1H, 2′H), 4.06-4.04 (m, 1H, 3′H), 3.96-3.94 (m, 1H, 4′H), 1.62-1.56 (m, 1H, cyclopropyl), 0.67-0.63 (m, 4H, CH_2, cyclopropyl)

HRFAB-MS $C_{25}H_{26}N_6O_4$
MW 474.52
$[M+H]^+$ calcd 475.2095
$[M+H]^+$ found 475.2112

Activity Dd2 strain of *P. falciparum*: IC_{50} = 11 μM
DOXP reductoisomerase: 0%

5′-Deoxy-N^6-(1-naphthylmethyl)-5′-[(3-thienyl)acetamido]adenosine (**17**)

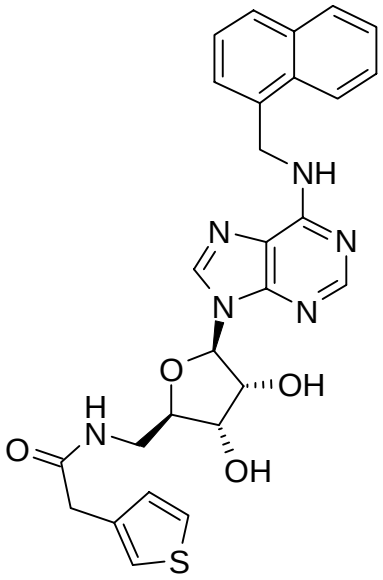

Yield 86%

^{1}H NMR (400 MHz, DMSO-d_6) = δ (ppm) 8.46 (bs, 1H, N^6H), 8.36 (bs, 1H, 8H), 8.31 (t, 1H, NH, amide, *J*=5.7 Hz), 8.25-8.24 (m, 2H, naphthyl overlapping 2H), 7.96-7.94 (m, 1H, naphthyl), 7.82-7.80 (m, 1H, naphthyl), 7.59-7.52 (m, 2H, naphthyl), 7.47-7.40 (m, 3H, 2H naphthyl overlapping 1H thienyl), 7.21-7.20 (m, 1H, thienyl), 7.00-6.99 (m, 1H, thienyl), 5.88 (d, 1H, 1′H, *J*=6.1 Hz), 5.44 (bs, 1H, 3′OH), 5.25 (bs, 1H, 2′OH), 5.18 (bs, 2H, CH_2, naphthylmethyl), 4.71-4.67 (m, 1H, 2′H), 4.08-4.05 (m, 1H, 3′H), 3.98-3.94 (m, 1H, 4′H), 3.47 (s, 2H, CH_2, 3-thienylacetamido)

HRESI-MS $C_{27}H_{26}N_6O_4S$
MW 530.61
$[M+H]^+$ calcd 531.1815
$[M+H]^+$ found 531.1824

Activity Dd2 strain of *P. falciparum*: IC_{50} = 11 μM
DOXP reductoisomerase: 0%

5′-Deoxy-N^6-(1-naphthylmethyl)-5′-[4-(2-thienyl)butanamido]adenosine (**18**)

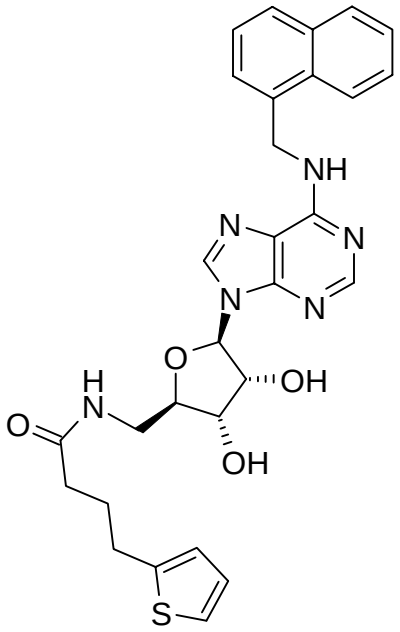

Yield 99%

^{1}H NMR (400 MHz, DMSO-d6) = δ (ppm) 8.47 (bs, 1H, N^6H), 8.37 (s, 1H, 8H), 8.26-8.22 (m, 3H, naphthyl overlapping 2H overlapping NH amide), 7.96-7.94 (m, 1H, naphthyl), 7.83-7.81 (m, 1H, naphthyl), 7.59-7.52 (m, 2H, naphthyl), 7.48-7.41 (m, 2H, naphthyl), 7.27 (d, 1H, thienyl, *J*=5.1 Hz), 6.90-6.88 (m, 1H, thienyl), 6.82-6.81 (m, 1H, thienyl), 5.88 (d, 1H, 1′H, *J*=6.4 Hz), 5.44 (bs, 1H, 3′OH), 5.29 (bs, 1H, 2′OH), 5.20 (bs, 2H, CH_2, naphthylmethyl), 4.71-4.69 (m, 1H, 2′H), 4.07-4.05 (m, 1H, 3′H), 4.00-3.98 (m, 1H, 4′H), 3.49-3.43 (m, 1H, 5′CH_2), 2.77 (t, 2H, CH_2, butyryl, *J*=7.6 Hz), 2.19 (t, 2H, CH_2, butyryl, *J*=7.4 Hz), 1.87-1.80 (m, 2H, CH_2, butyryl)

HRESI-MS $C_{29}H_{30}N_6O_4S$
MW 558.66
$[M+H]^+$ calcd 559.2127
$[M+H]^+$ found 559.2121

Activity Dd2 strain of *P. falciparum*: IC_{50} = 7.0 μM
DOXP reductoisomerase: 0%

5′-Deoxy-N^6-(1-naphthylmethyl)-5′-[(*R*/*S*)(2-phenylbutanamido)]adenosine (**19**) (Mixture of two diastereomers)

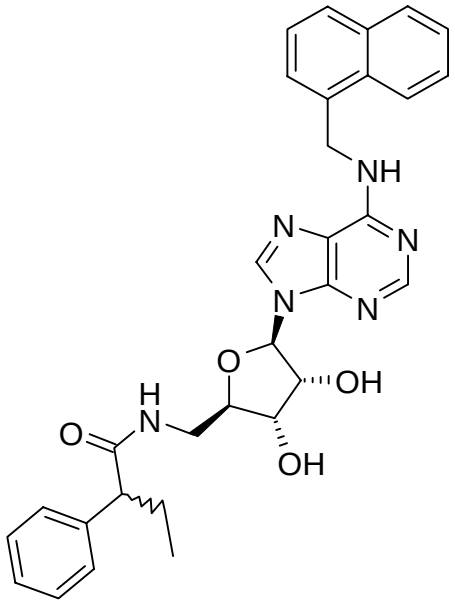

Yield 92%

^{1}H NMR (400 MHz, DMSO-d_6) = δ (ppm) 8.48 (bs, 1H, N^6H), 8.36-8.30 (m, 2H, NH amide overlapping 8H), 8.26-8.24 (m, 2H, naphthyl overlapping 2H), 7.96-7.94 (m, 1H, naphthyl), 7.83-7.81 (m, 1H, naphthyl), 7.59-7.52 (m, 2H, naphthyl), 7.47-7.41 (m, 2H, naphthyl), 7.32 (m, 5H, phenyl), 5.85 (t, 1H, 1′H, *J*=5.6 Hz), 5.45 (bs, 1H, 3′OH), 5.19 (bs, 3H, 2′OH overlapping CH_2 naphthylmethyl), 4.71-4.68 (m, 0.5 H, 2′H), 4.57-4.54 (m, 0.5H, 2′H), 4.06-4.04 (m, 0.5H, 3′H), 3.95-3.92 (m, 1.5 H, 4′H overlapping 3′H), 1.97-1.89 (m, 1H, CH_2, butyryl), 1.64-1.55 (m, 1H, CH_2, butyryl), 0.81-0.77 (m, 3H, CH_3, butyryl)

HRESI-MS $C_{31}H_{32}N_6O_4$
MW 552.64
$[M+H]^+$ calcd 553.2564
$[M+H]^+$ found 553.2579

Activity Dd2 strain of *P. falciparum*: IC_{50} = 6.2 μM
DOXP reductoisomerase: 0%

5′-Deoxy-5′-[4-(3-indolyl)butanamido]-N^6-(1-naphthylmethyl)adenosine (**20**)

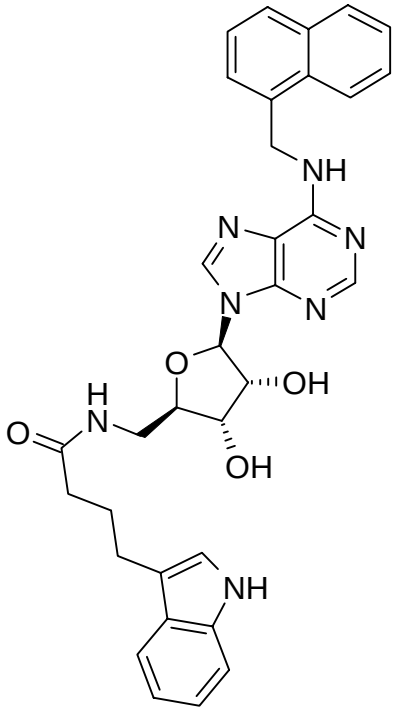

Yield 97%

^{1}H NMR (400 MHz, DMSO-d_6) = δ (ppm) 10.73 (s, 1H, NH, indolyl), 8.50 (bs, 1H, N^6H), 8.39 (bs, 1H, 8H), 8.25-8.23 (m, 1H, naphthyl), 8.21 (s, 1H, 2H), 8.20-8.18 (m, 1H, NH, amide), 7.96-7.94 (m, 1H, naphthyl), 7.83-7.81 (m, 1H, naphthyl), 7.59-7.52 (m, 2H, naphthyl), 7.49-7.40 (m, 3H, 1H indolyl overlapping 2H naphthyl), 7.32 (d, 1H, indolyl, *J*=8.1 Hz), 7.08 (m, 1H, indolyl), 7.05-7.01 (m, 1H, indolyl), 6.95-6.91 (m, 1H, indolyl), 5.87 (d, 1H, 1′H, *J*=6.6 Hz), 5.46 (d, 1H, 3′OH, *J*=6.6 Hz), 5.27 (d, 1H, 2′OH, *J*=4.6 Hz) 5.19 (bs, 2H, CH_2, naphthylmethyl), 4.73-4.68 (m, 1H, 2′H), 4.07-4.04 (m, 1H, 3′H), 3.99-3.95 (m, 1H, 4′H), 2.65 (t, 2H, CH_2, butyryl, *J*=7.6 Hz), 2.20 (t, 2H, CH_2, butyryl, *J*=7.5 Hz), 1.90-1.83 (m, 2H, CH_2, butyryl)

HRESI-MS $C_{33}H_{33}N_7O_4$
MW 591.68
$[M+H]^+$ calcd 592.2673
$[M+H]^+$ found 592.2666

Activity Dd2 strain of *P. falciparum*: IC_{50} = 8.5 μM
DOXP reductoisomerase: 45%

5′-Deoxy-5′-diphenylacetamido-N^6-(1-naphthylmethyl)adenosine (**21**)

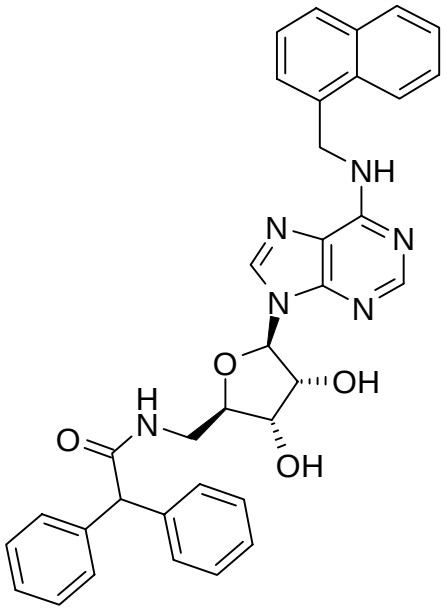

Analytical data as reported, with the following deviations[3].

Yield 92%

^{1}H NMR (400 MHz, DMSO-d_6) = δ (ppm) 8.54 (t, 1H, NH, amide, *J*=5.6 Hz), 8.46 (bs, 1H, N^6H), 8.33 (bs, 1H, 8H), 8.25-8.22 (m, 2H, naphthyl overlapping 2H), 7.96-7.94 (m, 1H, naphthyl), 7.83-7.80 (m, 1H, naphthyl), 7.59-7.52 (m, 2H, naphthyl), 7.47-7.40 (m, 2H, naphthyl), 7.29-7.25 (m, 8H, phenyl), 7.23-7.16 (m, 2H, phenyl), 5.87 (d, 1H, 1′H, *J*=6.1 Hz), 5.43 (bs, 1H, 3′OH), 5.27 (bs, 1H, 2′OH), 5.19 (bs, 2H, CH_2, naphthylmethyl), 4.98 (s, 1H, CH, diphenylmethyl), 4.65 (bs, 1H, 2′H), 4.06-4.03 (m, 1H, 3′H), 3.98-3.94 (m, 1H, 4′H), 3.53-3.36 (m, 2H, 5′CH_2)

HRESI-MS $C_{35}H_{32}N_6O_4$
MW 600.68
$[M+H]^+$ calcd 601.2564
$[M+H]^+$ found 601.2562

Activity Dd2 strain of *P. falciparum*: IC_{50} = 6.2 μM
DOXP reductoisomerase: 50%

5′-Deoxy-N^6-(1-naphthylmethyl)-5′-(4-phenylbutanamido)adenosine (**22**)

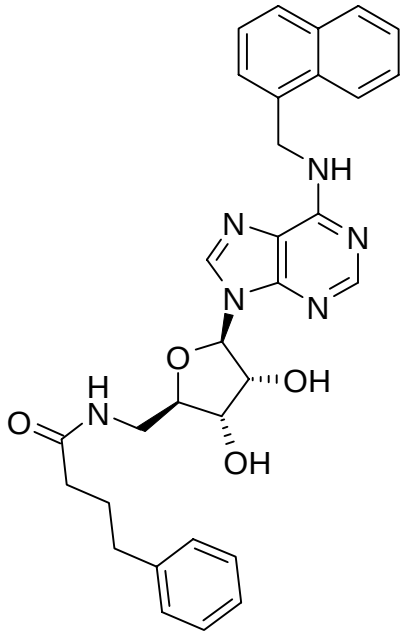

Yield 97%

^{1}H NMR (400 MHz, DMSO-d_6) = δ (ppm) 8.47 (bs, 1H, N^6H), 8.37 (s, 1H, 8H), 8.26 (d, 1H, naphthyl, *J*=7.9 Hz), 8.19-8.17 (m, 2H, 2H overlapping NH amide), 7.96-7.94 (m, 1H, naphthyl), 7.83-7.81 (m, 1H, naphthyl), 7.58-7.52 (m, 2H, naphthyl), 7.47-7.41 (m, 2H, naphthyl), 7.25-7.22 (m, 2H, phenyl), 7.16-7.11 (m, 3H, phenyl), 5.88 (d, 1H, 1′H, *J*=6.4 Hz), 5.45 (d, 1H, 3′OH, *J*=6.1 Hz), 5.25 (d, 1H, 2′OH, *J*=4.6 Hz), 5.19 (bs, 2H, CH_2 naphthylmethyl), 4.72-4.68 (m, 1H, 2′H), 4.07-4.04 (m, 1H, 3′H), 3.99-3.96 (m, 1H, 4′H), 3.49-3.43 (m, 1H, 5′CH_2), 3.39-3.36 (m, 1H, 5′CH_2), 2.54 (t, 2H, CH_2, butyryl, *J*=7.7 Hz), 2.14 (t, 2H, CH_2, butyryl, *J*=7.5 Hz), 1.83-1.76 (m, 2H, CH_2, butyryl)

HRESI-MS $C_{31}H_{32}N_6O_4$
MW 552.64
$[M+H]^+$ calcd 553.2563
$[M+H]^+$ found 553.2564

Activity Dd2 strain of *P. falciparum*: IC_{50} = 4.1 μM
DOXP reductoisomerase: 0%

5′-[4-(2,4-Dichlorophenoxy)butanamido]-5′-deoxy-N^6-(1-naphthylmethyl)-adenosine (**23**)

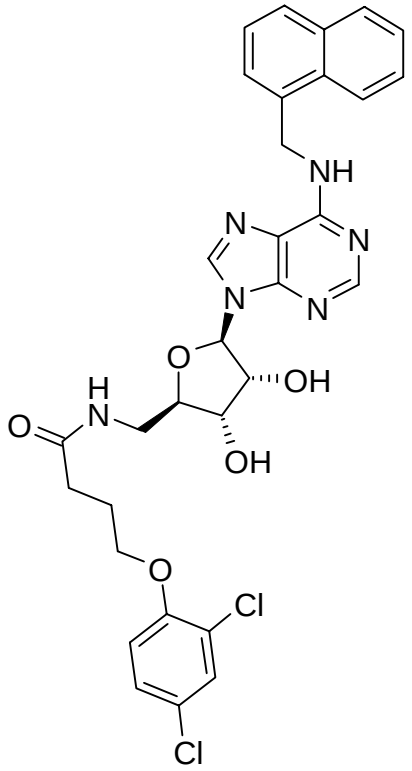

Yield 91%

^{1}H NMR (400 MHz, DMSO-d_6) = δ (ppm) 8.49 (bs, 1H, N^6H), 8.35 (bs, 1H, 8H), 8.26 (s, 1H, 2H), 8.24 -8.22 (m, 1H, naphthyl), 7.83-7.80 (m, 1H, naphthyl), 7.59-7.52 (m, 2H, naphthyl), 7.51 (d, 1H, aromatic, *J*=2.5 Hz), 7.46-7.40 (m, 2H, naphthyl), 7.38-7.35 (m, 2H, aromatic), 7.13 (d, 1H, naphthyl, *J*=8.9 Hz), 5.90 (d, 1H, 1′H, *J*=6.1 Hz), 5.45 (d, 1H, 3′OH, *J*=6.4 Hz), 5.26 (d, 1H, 2′OH, *J*=4.8 Hz), 5.18 (bs, 2H, CH_2, naphthylmethyl), 4.80-4.75 (m, 1H, 2′H), 4.17-4.15 (m, 1H, 3′H), 3.89-3.86 (m, 1H, 4′H), 2.35-2.32 (m, 2H, CH_2, butyryl), 2.00-1.92 (m, 2H, CH_2, butyryl)

HRESI-MS $C_{31}H_{30}Cl_2N_6O_5$
MW 637.53
$[M+Na]^+$ calcd 659.1552
$[M+Na]^+$ found 659.1540

Activity Dd2 strain of *P. falciparum*: IC_{50} = 10 μM
DOXP reductoisomerase: 0%

5′-{*trans*-3-[(4-Chloro-3-nitro)phenyl]prop-2-enamido}-5′-deoxy-N^6-(1-naphthylmethyl)adenosine (**24**)

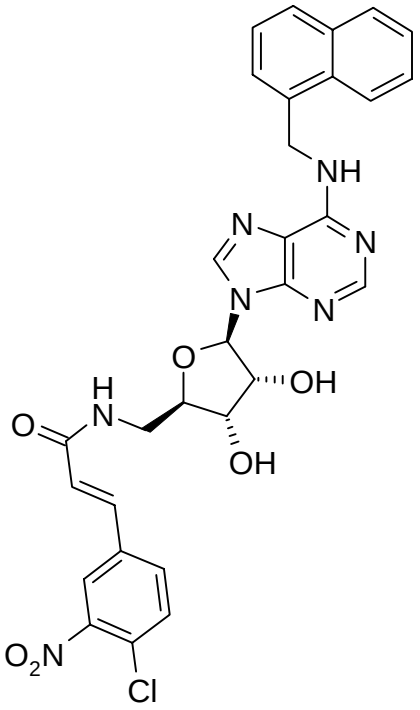

Yield 95%

^{1}H NMR (400 MHz, DMSO-d_6) = δ (ppm) 8.47-8.40 (m, 3H, NH amide overlapping N^6H overlapping 8H), 8.27-8.23 (m, 3H, naphthyl overlapping 2H overlapping cinnamoyl), 7.96-7.94 (m, 1H, naphthyl), 7.89-7.86 (m, 1H, cinnamoyl), 7.83-7.78 (m, 2H, naphthyl overlapping cinnamoyl), 7.59-7.41 (m, 5H, 4 H naphthyl overlapping 1H cinnamoyl), 6.83 (d, 1H, cinnamoyl, *J*=16.0 Hz), 5.91 (d, 1H, 1′H, *J*=6.1 Hz), 5.48 (d, 1H, 3′OH, *J*=6.1 Hz), 5.30 (d, 1H, 2′OH, *J*=4.83 Hz), 5.19 (bs, 2H, CH_2, naphthylmethyl), 4.74-4.72 (m, 1H, 2′H), 4.15-4.11 (m, 1H, 3′H), 4.04-4.00 (m, 1H, 4′H)

HRESI-MS $C_{30}H_{26}ClN_7O_6$
MW 616.04
$[M+H]^+$ calcd 617.1712
$[M+H]^+$ found 617.1711

Activity Dd2 strain of *P. falciparum*: IC_{50} = 5.3 μM
DOXP reductoisomerase: 52%

5′-Deoxy-N^6-(1-naphthylmethyl)-5′-{*trans*-3-[(3-nitro-4-propylamino)-phenyl]prop-2-enamido}adenosine (**25**) (Mixture of compounds **24** and **25)**

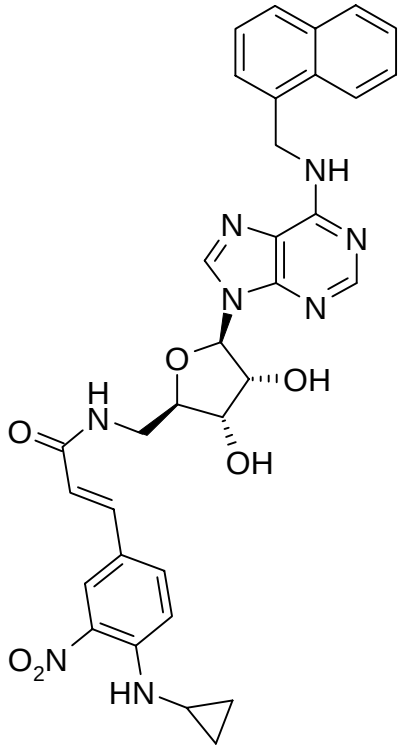

Yield <10%

^{1}H NMR (400 MHz, DMSO-d_6) = δ (ppm) 8.46 (t, 1H, NH, amide, *J*=6.1, 5.9 Hz), 8.40 (bs, 2H, N^6H overlapping 8H), 8.27-8.23 (m, 3H, naphthyl overlapping 2H overlapping cinnamoyl), 7.96-7.94 (m, 1H, naphthyl), 7.89-7.86 (m, 1H, cinnamoyl), 7.83-7.78 (m, 2H, naphthyl overlapping cinnamoyl), 7.59-7.40 (m, 5H, 4 H naphthyl 1H cinnamoyl), 6.83 (d, 1H, cinnamoyl, *J*=15.8 Hz**)**, 5.91 (d, 1H, 1′H, *J*=6.1 Hz), 5.47 (d, 1H, 3′OH, *J*=6.1 Hz), 5.29 (d, 1H, 2′OH, *J*=4.8 Hz), 5.19 (bs, 2H, CH_2, naphthylmethyl), 4.75-4.71 (m, 1H, 2′H), 4.15-4.12 (m, 1H, 3′H), 4.04-4.00 (m, 1H, 4′H), 3.62-3.51 (m, 2H, 5′H), 0.89-0.86 (m, 0.2H, CH_2, cyclopropyl), 0.65 (m, 0.2H, CH_2, cyclopropyl)

HRESI-MS $C_{33}H_{32}N_8O_6$
MW 636.67
$[M+Na]^+$ calcd 659.2342
$[M+Na]^+$ found 659.2326

Activity Dd2 strain of *P. falciparum*: IC_{50} = 4.8 μM
DOXP reductoisomerase: 33%

5′-Deoxy-5′-(3-methoxybenzamido)-N^6-(1-naphthylmethyl)adenosine (**26**)

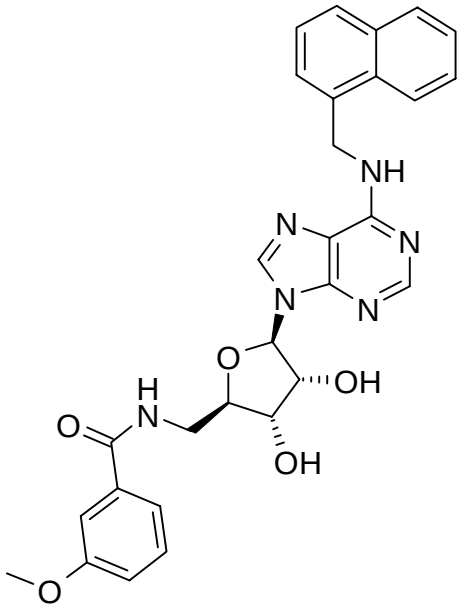

Yield 95%

^{1}H NMR (400 MHz DMSO-d_6) = δ (ppm) 8.70 (t, 1H, NH, amide, *J*=5.6 Hz), 8.48 (bs, 1H, N^6H), 8.40 (bs, 1H, 8H), 8.24 (m, 1H, naphthyl), 8.14 (s, 1H, 2H), 7.96-7.94 (m, 1H, naphthyl), 7.83-7.81 (m, 1H, naphthyl), 7.59-7.53 (m, 2H, naphthyl), 7.44-7.35 (m, 5H, 3H benzoyl overlapping 2H naphthyl), 7.10-7.07 (m, 1H, benzoyl), 5.90 (d, 1H, 1′H, *J*=6.6 Hz), 5.50 (d, 1H, 3′OH, *J*=6.1 Hz), 5.31 (d, 1H, 2′OH, *J*=4.6 Hz), 5.18 (bs, 2H, CH_2, naphthylmethyl), 4.79-4.78 (m, 1H, 2′H), 4.19-4.17 (m, 1H, 3′H), 4.11-4.07 (m, 1H, 4′H), 3.78 (s, 3H, CH_3, methoxy)

HRESI-MS $C_{29}H_{28}N_6O_5$
MW 540.58
$[M+H]^+$ calcd 541.2200
$[M+H]^+$ found 541.2185

Activity Dd2 strain of *P. falciparum*: IC_{50} = 11 μM
DOXP reductoisomerase: 0%

5′-(4-Cyclopropylamino-3-nitrobenzamido)-5′-deoxy-N^6-(1-naphthylmethyl)adenosine (**27**)

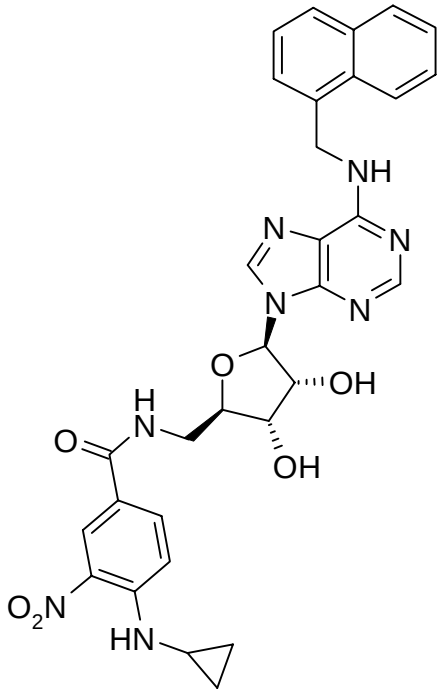

Yield 87%

^{1}H NMR (400 MHz, DMSO-d_6) = δ (ppm) 8.75 (t, 1H, NH, amide, *J*=5.6 Hz), 8.65 (d, 1H, aromatic, *J*=2.0 Hz), 8.46 (bs, 1H, N^6H), 8.41 (bs, 1H, 8H), 8.25 (bs, 1H, NH), 8.22 (m, 1H, naphthyl), 8.18 (s, 1H, 2H), 8.08-8.05 (m, 1H, aromatic), 7.96-7.94 (m, 1H, naphthyl), 7.83-7.80 (m, 1H, naphthyl), 7.59-7.52 (m, 2H, naphthyl), 7.44-7.39 (m, 3H, 2H naphthyl overlapping 1H aromatic), 5.90 (d, 1H, 1′H, *J*=6.1 Hz), 5.51 (d, 1H, 3′OH, *J*=5.6 Hz), 5.32 (d, 1H, 2′OH, *J*=4.6 Hz), 5.17 (bs, 2H, CH_2, naphthylmethyl), 4.79-4.77 (m, 1H, 2′H), 4.21-4.19 (m, 1H, 3′H), 4.09-4.06 (m, 1H, 4′H), 1.94-1.86 (m, 1H, cyclopropyl), 0.91-0.86 (m, 2H, CH_2, cyclopropyl), 0.68-0.64 (m, 2H, CH_2, cyclopropyl)

HRFAB-MS $C_{31}H_{30}N_8O_6$
MW 610.63
$[M+H]^+$ calcd 611.2367
$[M+H]^+$ found 611.2379

Activity Dd2 strain of *P. falciparum*: IC_{50} = 26 μM
DOXP reductoisomerase: 0%

5′-Deoxy-5′-[4-(1-methylethyl)amino-3-nitrobenzamido]-N^6-(1-naphthylmethyl)adenosine (**28**)

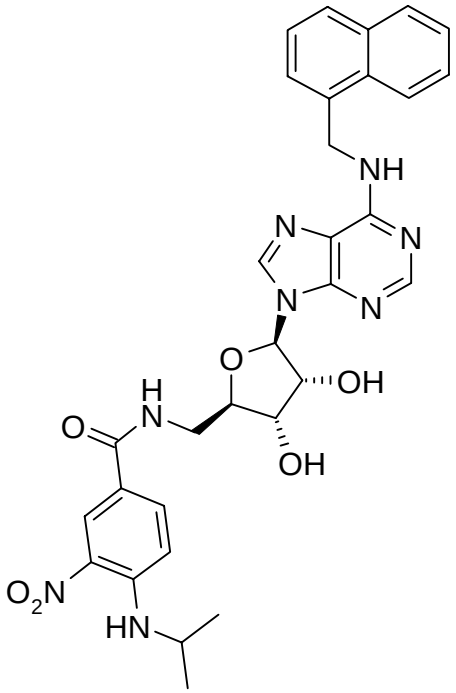

Yield 67%

^{1}H NMR (400 MHz, DMSO-d_6) = δ (ppm) 8.70 (t, 1H, NH, amide, *J*=5.9 Hz), 8.66 (d, 1H, aromatic, *J*=2.29 Hz), 8.43 (bs, 1H, N^6H), 8.39 (bs, 1H, 8H), 8.24 (d, 1H, naphthyl, *J*=8.0 Hz), 8.18 (s, 1H, 2H), 8.08 (d, 1H, NH, 2-propylamino, *J*=7.6 Hz), 8.01-7.99 (m, 1H, aromatic), 7.96-7.94 (m, 1H, naphthyl), 7.83-7.80 (m, 1H, naphthyl), 7.59-7.52 (m, 2H, naphthyl), 7.46-7.40 (m, 2H, naphthyl), 7.15 (d, 1H, aromatic, *J*=9.4 Hz), 5.90 (d, 1H, 1′H, *J*=6.1 Hz), 5.45 (d, 1H, 3′OH, *J*=6.35 Hz), 5.26 (d, 1H, 2′OH, *J*=4.8 Hz), 5.18 (bs, 2H, CH_2, naphthylmethyl), 4.80-4.75 (m, 1H, 2′H), 4.21-4.18 (m, 1H, 3′H), 4.09-4.05 (m, 1H, 4′H), 3.84-3.74 (m, 1H, CH, 2-propyl-amino), 1.27 (d, 6H, CH_3, 2-propylamino, *J*=6.4 Hz)

HRESI-MS $C_{31}H_{32}N_8O_6$
MW 612.65
$[M+H]^+$ calcd 613.2523
$[M+H]^+$ found 613.2533

Activity Dd2 strain of *P. falciparum*: IC_{50} = 4.1 μM
DOXP reductoisomerase: 0%

5′-Deoxy-N^6-(1-naphthylmethyl)-5′-[3-nitro-4-(pyrrolid-1-yl)benzamido]-adenosine (**29**)

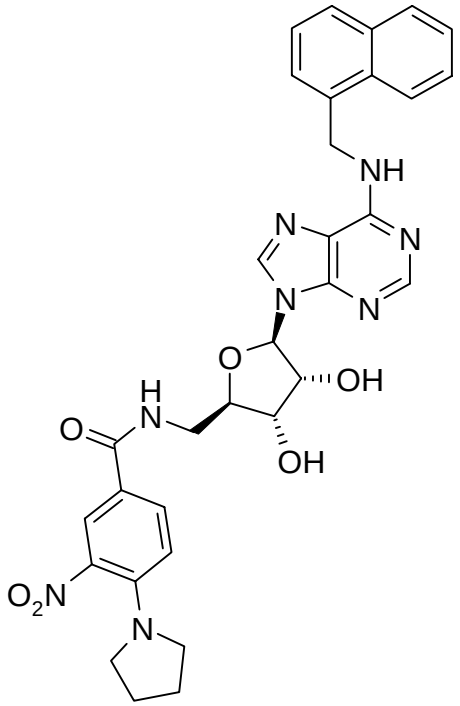

Yield 79%

^{1}H NMR (400 MHz, DMSO-d_6) = δ (ppm) 8.62 (t, 1H, NH, amide, J=5.7 Hz), 8.43 (bs, 1H, N^6H), 8.39 (bs, 1H, 8H), 8.29 (d, 1H, aromatic, J=2.3 Hz), 8.24-8.21 (m, 1H, naphthyl), 8.19 (s, 1H, 2H), 7.96-7.92 (m, 2H, naphthyl overlapping aromatic), 7.83-7.80 (m, 1H, naphthyl), 7.59-7.52 (m, 2H, naphthyl), 7.46-7.40 (m, 2H, naphthyl), 7.08 (d, 1H, aromatic, J=8.9 Hz), 5.90 (d, 1H, 1′H, J=6.1 Hz), 5.45 (d, 1H, 3′OH, J=6.4 Hz), 5.26 (d, 1H, 2′H, J=4.8 Hz), 5.19 (bs, 2H, CH_2, naphthylmethyl), 4.78-4.75 (m, 1H, 2′H), 4.20-4.17 (m, 1H, 3′H), 4.10-4.05 (m, 1H, 4′H), 3.20-3.16 (m, 4H, CH_2, pyrrolidyl), 1.93-1.90 (m, 4H, CH_2, pyrrolidyl)

HRESI-MS $C_{32}H_{32}N_8O_6$
MW 624.66
$[M+Na]^+$ calcd 647.2342
$[M+Na]^+$ found 647.2345

Activity Dd2 strain of *P. falciparum*: IC_{50} = 15 μM
DOXP reductoisomerase: 0%

5′-(4-Cyclopentylamino-3-nitrobenzamido)-5′-deoxy-N^6-(1-naphthyl-methyl)adenosine (**30**)

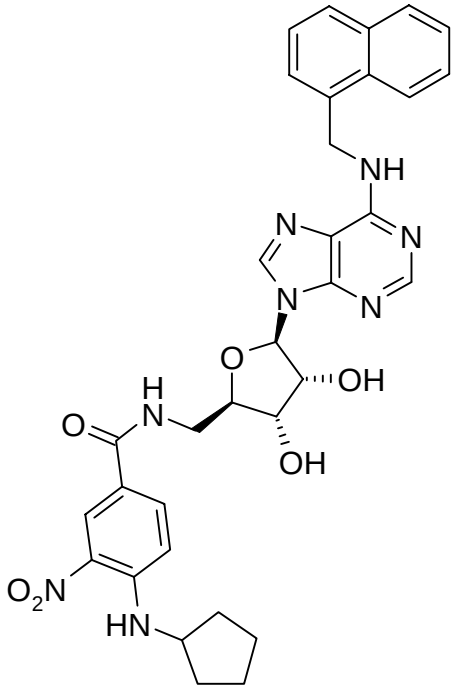

Yield 66%

^{1}H NMR (400 MHz, DMSO-d_6) = δ (ppm) 8.70 (t, 1H, NH, amide, *J*=5.9 Hz), 8.66 (d, 1H, aromatic, *J*=2.0 Hz), 8.42 (bs, 1H, N^6H), 8.39 (bs, 1H, 8H), 8.24 (d, 1H, naphthyl, *J*=8.1 Hz), 8.18 (s, 1H, 2H), 8.17-8.15 (m, 1H, NH, cyclopentylamino), 8.02-7.99 (m, 1H, aromatic), 7.96-7.94 (m, 1H, naphthyl), 7.83-7.80 (m, 1H, naphthyl), 7.59-7.52 (m, 2H, naphthyl), 7.46-7.40 (m, 2H, naphthyl), 7.16 (d, 1H, aromatic, *J*=9.4 Hz), 5.90 (d, 1H, 1′H, *J*=6.1 Hz), 5.46 (d, 1H, 3′OH, *J*=6.1 Hz), 5.26 (d, 1H, 2′OH, *J*=4.8 Hz), 5.18 (bs, 2H, CH_2, naphthyl-methyl), 4.80-4.76 (m, 1H, 2′H), 4.22-4.18 (m, 1H, 3′H), 4.07-4.05 (m, 1H, 4′H), 3.84-3.74 (m, 1H, CH, cyclopentylamino), 2.11-2.04 (m, 2H, CH_2, cyclopentyl-amino), 1.77-1.51 (m, 6H, CH_2, cyclopentylamino)

HRESI-MS $C_{33}H_{34}N_8O_6$
MW 638.69
$[M+H]^+$ calcd 639.2680
$[M+H]^+$ found 639.2699

Activity Dd2 strain of *P. falciparum*: IC_{50} = 4.8 μM
DOXP reductoisomerase: 47%

5′-Deoxy-N^6-(1-naphthylmethyl)-5′-[3-nitro-4-(piperid-1-yl)benzamido]-adenosine (**31**)

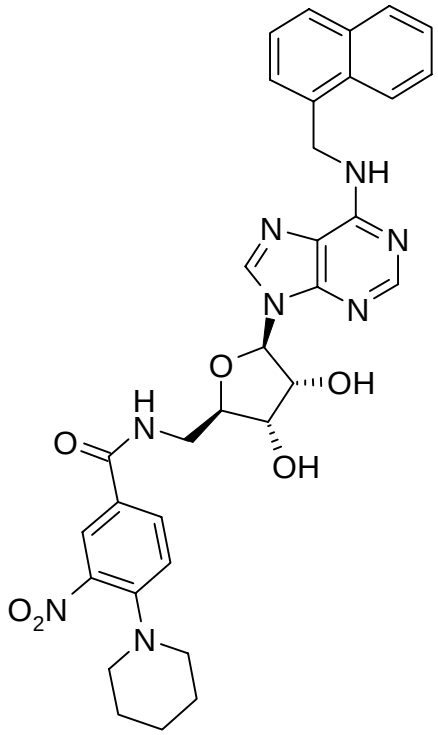

Yield 78%

^{1}H NMR (400 MHz, DMSO-d_6) = δ (ppm) 8.73 (t, 1H, NH, amide, *J*=6.6 Hz), 8.47 (bs, 1H, N^6H), 8.40 (bs, 1H, 8H), 8.30 (d, 1H, aromatic, *J*=2.0 Hz), 8.24-8.22 (m, 1H, naphthyl), 8.17 (s, 1H, 2H), 8.00-7.99 (m, 1H, aromatic), 7.96-7.94 (m, 1H, naphthyl), 7.83-7.80 (m, 1H, naphthyl), 7.59-7.52 (m, 2H, naphthyl), 7.45-7.40 (m, 2H, naphthyl), 7.29 (d, 1H, aromatic, *J*=9.2 Hz), 5.90 (d, 1H, 1′H, *J*=6.1 Hz), 5.50 (d, 1H, 3′OH, *J*=6.6 Hz), 5.32 (d, 1H, 2′OH, *J*=4.6 Hz), 5.18 (bs, 2H, CH_2, naphthyl-methyl), 4.79-4.75 (m, 1H, 2′H), 4.21-4.17 (m, 1H, 3′H), 4.08-4.04 (m, 1H, 4′H), 3.05-3.04 (m, 4H, CH_2, piperidyl), 1.64-1.51 (m, 6H, CH_2, piperidyl)

HRESI-MS $C_{33}H_{34}N_8O_6$
MW 638.69
$[M+H]^+$ calcd 639.2679
$[M+H]^+$ found 639.2687

Activity Dd2 strain of *P. falciparum*: IC_{50} = 14 μM
DOXP reductoisomerase: 0%

5′-Deoxy-5′-[4-(morphol-4-yl)-3-nitrobenzamido]-N^6-(1-naphthylmethyl)-adenosine (**32**)

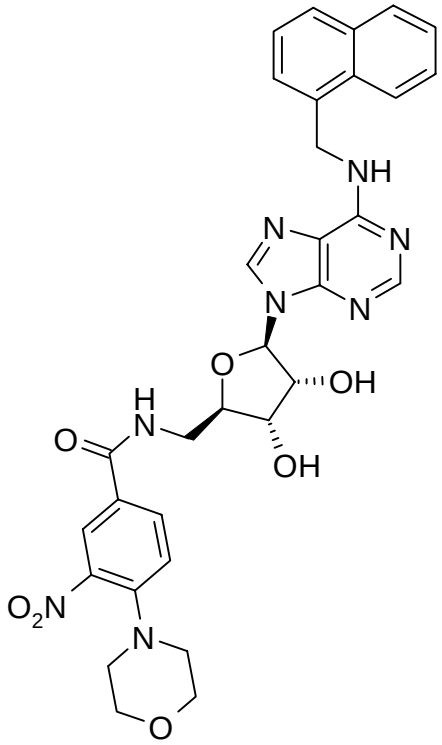

Yield 84%

^{1}H NMR (400 MHz, DMSO-d_6) = δ (ppm) 8.78 (t, 1H, NH, amide, *J*= 5.5 Hz), 8.47 (bs, 1H, N^6H), 8.40 (bs, 1H, 8H), 8.33 (d, 1H, aromatic, *J*=2.1 Hz), 8.24-8.22 (m, 1H, naphthyl), 8.17 (s, 1H, 2H), 8.05-8.03 (m, 1H, aromatic), 7.96-7.94 (m, 1H, naphthyl), 7.83-7.81 (m, 1H, naphthyl), 7.59-7.53 (m, 2H, naphthyl), 7.44-7.40 (m, 2H, naphthyl), 7.34 (d, 1H, aromatic, *J*=8.6 Hz), 5.90 (d, 1H, 1′H, *J*=6.1 Hz), 5.51 (bs, 1H, 3′OH), 5.32 (bs, 1H, 2′OH), 5.18 (bs, 2H, CH_2, naphthylmethyl), 4.80-4.76 (m, 1H, 2′H), 4.19 (bs, 1H, 3′H), 4.08-4.05 (m, 1H, 4′H), 3.68 (t, 4H, CH_2, morpholyl, *J*=4.5 Hz), 3.07 (t, 4H, CH_2, morpholyl, *J*=4.6)

HRESI-MS $C_{32}H_{32}N_8O_7$
MW 640.66
$[M+Na]^+$ calcd 663.2292
$[M+Na]^+$ found 663.2293

Activity Dd2 strain of *P. falciparum*: IC_{50} = 13 μM
DOXP reductoisomerase: 0%

5′-(4-Dibutylamino-3-nitrobenzamido)-5′-deoxy-N^6-(1-naphthylmethyl)-adenosine (**33**)

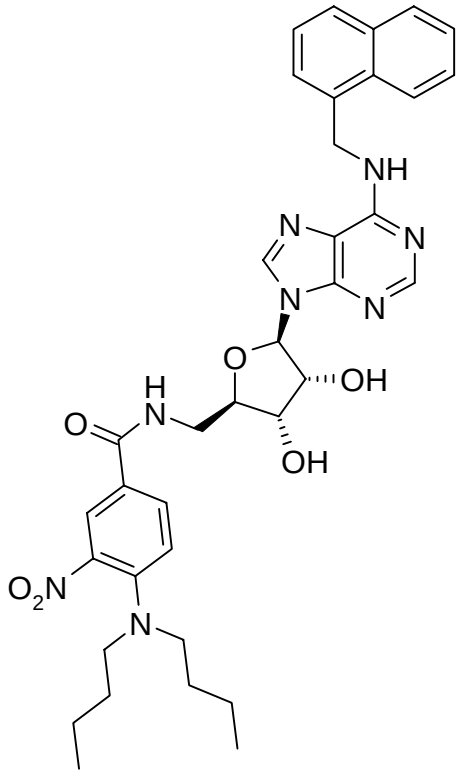

Yield 64%

^{1}H NMR (400 MHz, DMSO-d_6) = δ (ppm) 8.67 (t, 1H, NH, amide, *J*=5.9 Hz), 8.42-8.39 (m, 2H, N^6H overlapping 8H), 8.24-8.22 (m, 2H, naphthyl overlapping aromatic), 8.16 (s, 1H, 2H), 7.96-7.91 (m, 2H, naphthyl overlapping aromatic), 7.82-7.80 (m, 1H, naphthyl), 7.59-7.52 (m, 2H, naphthyl), 7.46-7.40 (m, 2H, naphthyl), 7.31 (d, 1H, aromatic, *J*=9.2 Hz), 5.90 (d, 1H, 1′H, *J*=6.1 Hz), 5.45 (d, 1H, 3′OH, *J*=6.1 Hz), 5.26 (d, 1H, 2′OH, *J*=4.8 Hz), 5.18 (bs, 2H, CH_2, naphthylmethyl), 4.79-4.75 (m, 1H, 2′H), 4.20-4.17 (m, 1H, 3′H), 4.08-4.04 (m, 1H, 4′H), 3.18-3.13 (m, 4H, CH_2, dibutylamino), 1.48-1.40 (m, 4H, CH_2, dibutylamino), 1.25-1.18 (m, 4H, CH_2, dibutylamino), 0.81 (t, 6H, CH_3, dibutylamino, *J*=7.3 Hz)

HRESI-MS $C_{36}H_{42}N_8O_6$
MW 682.79
$[M+H]^+$ calcd 683.3305
$[M+H]^+$ found 683.3294

Activity Dd2 strain of *P. falciparum*: IC_{50} = 4.2 μM
DOXP reductoisomerase: 70%

5′-Deoxy-5′-{4-[2-(2-methoxyphenyl)ethylamino]-3-nitrobenzamido}-N^6-(1-naphthylmethyl)adenosine (**34**)

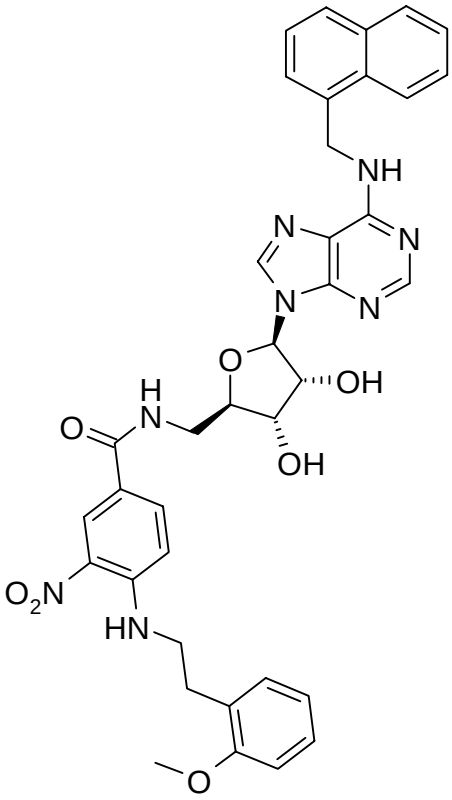

Yield 92%

^{1}H NMR (400 MHz, DMSO-d_6) = δ (ppm) 8.69 (t, 1H, NH, amide, *J*=5.6 Hz), 8.65 (d, 1H, aromatic, *J*=2.03 Hz), 8.43-8.39 (m, 3H, N^6H overlapping 8H overlapping NH), 8.24 (d, 1H, naphthyl, *J*=7.9 Hz), 8.18 (s, 1H, 2H), 8.04-8.01 (m, 1H, aromatic), 7.96-7.94 (m, 1H, naphthyl), 7.82-7.80 (m, 1H, naphthyl), 7.59-7.52 (m, 2H, naphthyl), 7.46-7.40 (m, 2H, naphthyl), 7.24-7.20 (m, 2H, aromatic), 7.17 (d, 1H, aromatic, *J*=9.2 Hz), 6.98 (d, 1H, aromatic, *J*=8.1 Hz), 6.89 (t, 1H, aromatic, *J*=7.3 Hz), 5.90 (d, 1H, 1′H, *J*=6.1 Hz), 5.45 (d, 1H, 3′OH, *J*=6.1 Hz), 5.27 (d, 1H, 2′OH, *J*=4.8 Hz), 5.18 (bs, 2H, CH_2, naphthylmethyl), 4.78-4.76 (m, 1H, 2′H), 4.20-4.18 (m, 1H, 3′H), 4.09-4.06 (m, 1H, 4′H), 3.81 (s, 3H, CH_3, methoxy), 2.93 (t, 2H, CH_2, ethylamino, *J*=7.0 Hz)

HRESI-MS $C_{37}H_{36}N_8O_7$ $[M+H]^+$ calcd 705.2785
MW 704.75 $[M+H]^+$ found 705.2797

Activity Dd2 strain of *P. falciparum*: IC_{50} = 1.3 μM
DOXP reductoisomerase: 58%

5′-[4-(*N*-Benzyl-*N*-ethyl)amino-3-nitrobenzamido]-5′-deoxy-N^6-(1-naphthylmethyl)adenosine (**35**)

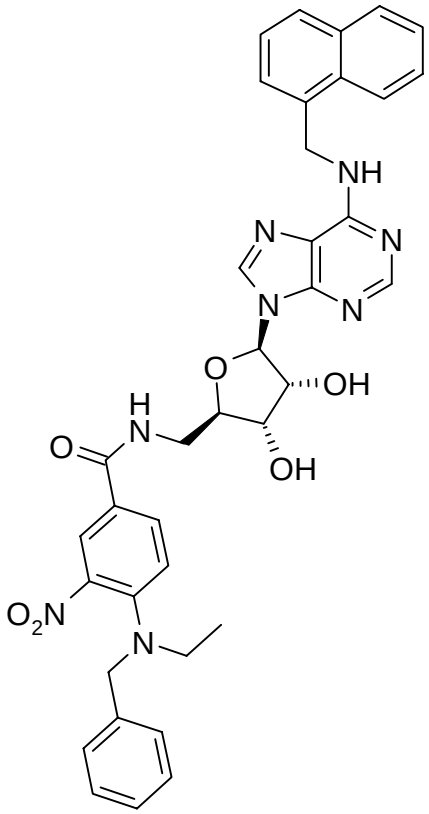

Yield 91%

^{1}H NMR (400 MHz, DMSO-d_6) = δ (ppm) 8.71 (t, 1H, NH, amide, *J*=6.1 Hz), 8.46 (bs, 1H, N^6H), 8.40 (bs, 1H, 8H), 8.25-8.23 (m, 2H, naphthyl overlapping 2H), 8.15 (s, 1H, aromatic), 7.96-7.94 (m, 1H, naphthyl), 7.92-7.89 (m, 1H, aromatic), 7.83-7.81 (m, 1H, naphthyl), 7.59-7.52 (m, 2H, naphthyl), 7.44-7.40 (m, 2H, naphthyl), 7.32-7.26 (m, 4H, aromatic), 7.23-7.19 (m, 1H, aromatic), 5.89 (d, 1H, 1′H, *J*=6.1 Hz), 5.48 (d, 1H, 3′OH, *J*=6.1 Hz), 5.29 (d, 1H, 2′OH, *J*=4.6 Hz), 5.18 (bs, 2H, CH_2, naphthylmethyl), 4.79-4.76 (m, 1H, 2′H), 4.44 (s, 2H, CH_2, benzyl), 4.18-4.16 (m, 1H, 3′H), 4.06-4.03 (m, 1H, 4′H), 1.06 (t, 3H, CH_3, *J*=7.1 Hz)

HRESI-MS $C_{37}H_{36}N_8O_6$
MW 668.75
$[M+Na]^+$ calcd 711.2655
$[M+Na]^+$ found 711.2662

5′-Deoxy-N^6-(1-naphthylmethyl)-5′-[4-(3-phenylpropanamino)-3-nitro-benzamido]adenosine (**36**)

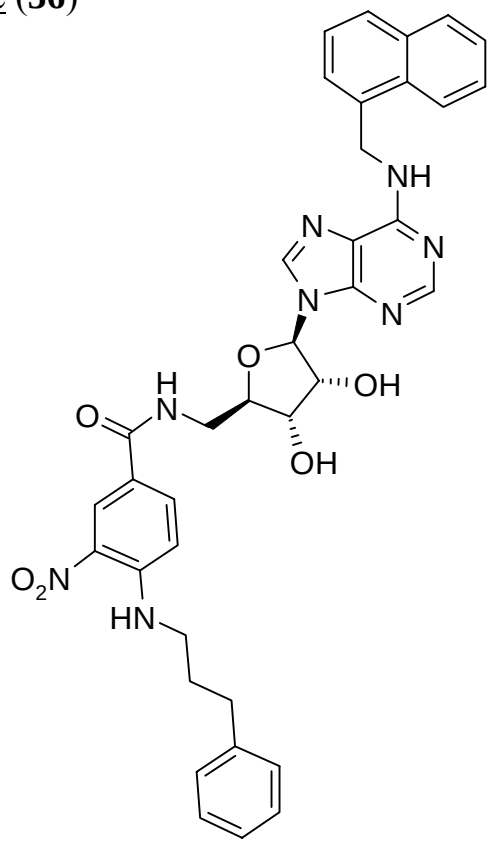

Yield 84%

^{1}H NMR (400 MHz, DMSO-d_6) = δ (ppm) 8.69 (t, 1H, NH, amide, *J*=5.6 Hz), 8.65 (d, 1H, 4-amino-3-nitrobenzyl, *J*=1.8 Hz), 8.44-8.39 (m, 3H, N^6H overlapping NH amide overlapping 8H), 8.24-8.22 (m, 1H, naphthyl), 8.18 (s, 1H, 2H), 7.99-7.93 (m, 2H, naphthyl overlapping 4-amino-3-nitrobenzyl), 7.82-7.80 (m, 1H, naphthyl), 7.59-7.52 (m, 2H, naphthyl), 7.44-7.40 (m, 2H, naphthyl), 7.29-7.15 (m, 5H, phenyl), 7.06 (d, 1H, 4-amino-3-nitrobenzyl, *J*=9.2 Hz), 5.90 (d, 1H, 1′H, *J*=5.9 Hz), 5.46 (d, 1H, 3′OH, *J*=5.9 Hz), 5.26 (d, 1H, 2′OH, *J*=4.6 Hz), 5.18 (bs, 2H, CH_2 naphthylmethyl), 4.79-4.77 (m, 1H, 2′H), 4.21-4.20 (m, 1H, 3′H), 4.09-4.07 (m, 1H, 4′H), 3.44-3.39 (m, 2H, CH_2, propyl), 2.69-2.66 (m, 2H, CH_2, propyl)

HRESI-MS $C_{37}H_{36}N_8O_6$
MW 688.75
$[M+H]^+$ calcd 689.2836
$[M+H]^+$ found 689.2840

5′-Deoxy-5′-[4-(morphol-4-yl)-3-(4-nitrobenzamido)benzamido]-N^6-(1-naphthylmethyl)adenosine (**37**)

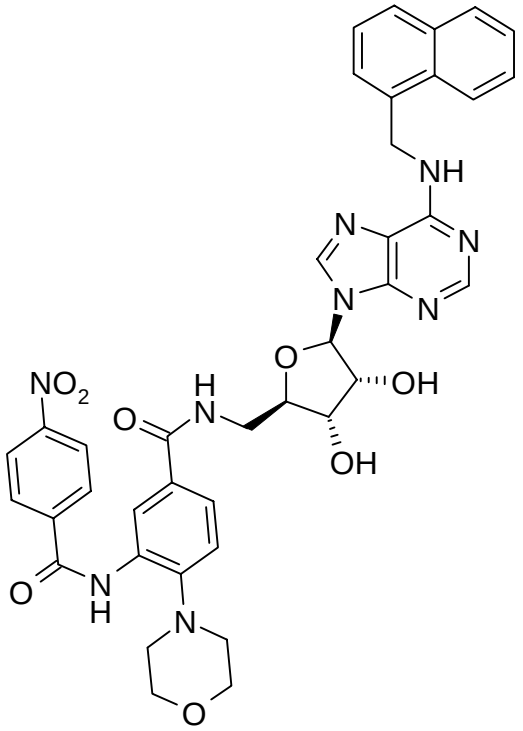

Yield 65%

^{1}H NMR (400 MHz, DMSO-d_6) = δ (ppm) 9.97 (s, 1H, NH, amide), 8.62 (bs, 1H, NH, amide), 8.40-8.38 (m, 4H, N^6H overlapping 8H overlapping 2H aromatic), 8.31 (m, 1H, naphthyl), 8.21-8.17 (m, 4H, 2H overlapping 3H aromatic), 7.96-7.93 (m, 1H, naphthyl), 7.82-7.80 (m, 1H, naphthyl), 7.76-7.70 (m, 1H, aromatic), 7.57-7.53 (m, 2H, naphthyl), 7.45-7.41 (m, 2H, naphthyl), 7.27-7.23 (m, 1H, aromatic), 5.90 (d, 1H, 1′H, *J*=6.1 Hz), 5.44 (bs, 1H, 3′OH), 5.29 (bs, 1H, 2′OH), 5.17 (bs, 2H, CH_2, naphthylmethyl), 4.79-4.77 (m, 1H, 2′H), 4.20-4.18 (m, 1H, 3′H), 4.11-4.07 (m, 1H, 4′H), 3.74-3.72 (m, 4H, CH_2, morpholyl), 2.95-2.92 (m, 4H, CH_2, morpholyl)

HRESI-MS $C_{39}H_{37}N_9O_8$
MW 759.79
$[M+H]^+$ calcd 760.2843
$[M+H]^+$ found 760.2845

Activity Dd2 strain of *P. falciparum*: IC_{50} = 2.8 μM
DOXP reductoisomerase: 27%

5′-[3-Acetamido-4-(morphol-4-yl)benzamido]-5′-deoxy-N^6-(1-naphthyl-methyl)adenosine (**38**)

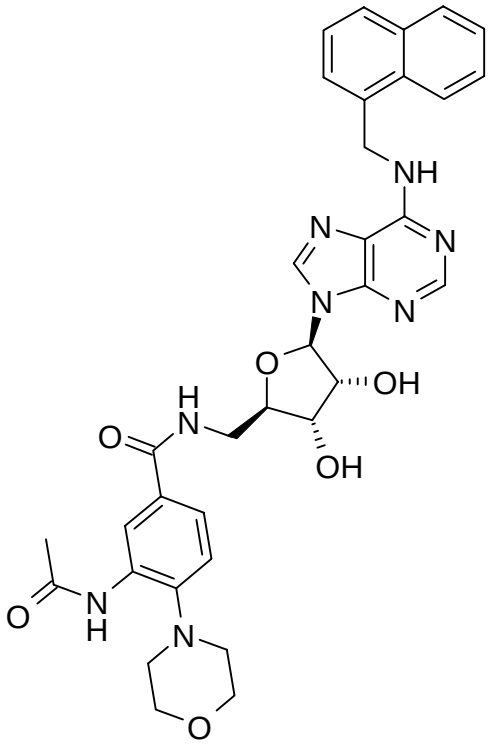

Yield 81%

^{1}H NMR (400 MHz, DMSO-d_6) = δ (ppm) 9.01 (s, 1H, NH, amide), 8.57 (t, 1H, NH, amide, *J*=5.7 Hz), 8.47 (bs, 1H, N^6H), 8.41 (bs, 1H, 8H), 8.25-8.22 (m, 2H, aromatic overlapping naphthyl), 8.16 (s, 1H, 2H), 7.96-7.94 (m, 1H, naphthyl), 7.83-7.81 (m, 1H, naphthyl), 7.61-7.53 (m, 3H, 1H aromatic overlapping 2H naphthyl), 7.44-7.40 (m, 2H, naphthyl), 7.14 (d, 1H, aromatic, *J*=8.1 Hz), 5.89 (d, 1H, 1′H, *J*=6.6 Hz), 5.46 (d, 1H, 3′OH, *J*=6.1 Hz), 5.29 (d, 1H, 2′OH, *J*=4.6 Hz), 5.19 (bs, 2H, CH_2, naphthylmethyl), 4.78-4.77 (m, 1H, 2′H), 4.17-4.16 (m, 1H, 3′H), 4.10-4.08 (m, 1H, 4′H), 3.78 (t, 4H, CH_2, morpholyl, *J*=4.1 Hz), 2.85 (t, 4H, CH_2, morpholyl, *J*=4.1 Hz), 2,10 (s, 3H, CH_3, acetamido)

HRESI-MS $C_{34}H_{36}N_8O_6$
MW 652.72
$[M+Na]^+$ calcd 675.2655
$[M+Na]^+$ found 675.2670

Activity Dd2 strain of *P. falciparum*: IC_{50} = 5.0 μM
DOXP reductoisomerase: 0%

5′-[(4-Cyclopentylamino-3-propanamido)benzamido]-5′-deoxy-N^6-(1-naphthylmethyl)adenosine (**39**)

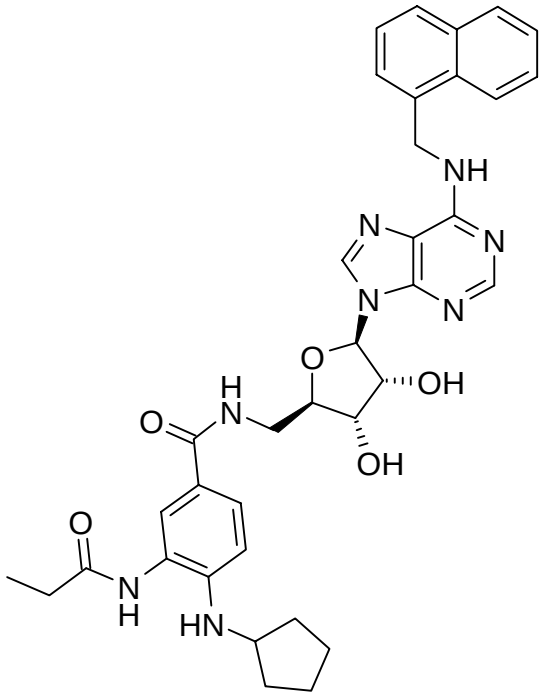

Yield 71%

^{1}H NMR (400 MHz, DMSO-d_6) = δ (ppm) 9.10 (s, 1H, NH, amide), 8.44 (bs, 1H, N^6H), 8.38 (bs, 1H, 8H), 8.30 (t, 1H, NH, amide, *J*=5.8 Hz), 8.24 (d, 1H, naphthyl, *J*=7.6 Hz), 8.20 (s, 1H, 2H), 7.96-7.94 (m, 1H, naphthyl), 7.83-7.80 (m, 1H, naphthyl), 7.70 (d, 1H, aromatic, *J*=1.5 Hz), 7.61-7.52 (m, 3H, 2H naphthyl overlapping 1H aromatic), 7.46-7.41 (m, 2H, naphthyl), 6.67 (d, 1H, aromatic, *J*=8.9 Hz), 5.88 (d, 1H, 1′H, *J*=6.6 Hz), 5.42 (d, 1H, 3′OH, *J*=6.4 Hz), 5.25 (d, 1H, 2′OH, *J*=4.6 Hz), 5.19 (bs, 2H, CH_2, naphthylmethyl), 5.10 (d, 1H, NH, amine, *J*=6.4 Hz), 4.78-4.74 (m, 1H, 2′H), 4.16-4.14 (m, 1H, 3′H), 4.08-4.05 (m, 1H, 4′H), 3.82-3.75 (m, 1H, CH, cyclopentylamino), 2.36-2.30 (m, 2H, CH_2, propanamido), 2.01-1.93 (m, 2H, CH_2, cyclopentylamino), 1.70-1.63 (m, 2H, CH_2, cyclopentylamino), 1.60-1.52 (m, 2H, CH_2, cyclopentylamino), 1.47-1.39 (m, 2H, CH_2, cyclopentylamino), 1.09-1.06 (m, 3H, CH_3, propanamido)

HRESI-MS $C_{36}H_{40}N_8O_5$
MW 664.77
$[M+Na]^+$ calcd 687.3019
$[M+Na]^+$ found 687.3040

5′-[3-Acetamido-4-(piperid-1-yl)benzamido]-5′-deoxy-N^6-(1-naphthyl-methyl)adenosine (**40**)

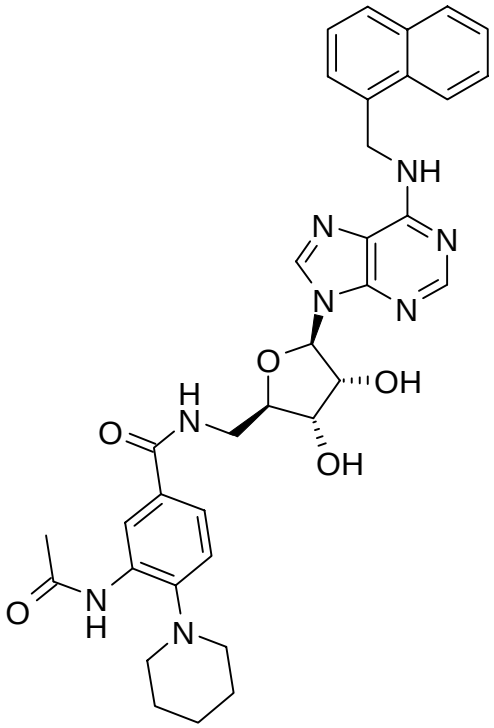

Yield 54%

^{1}H NMR (400 MHz, DMSO-d_6) = δ (ppm) 8.86 (s, 1H, NH, amide), 8.54 (t, 1H, NH, amide, *J*=5.8 Hz), 8.47 (bs, 1H, N^6H), 8.40 (bs, 1H, 8H), 8.24-8.22 (m, 2H, aromatic overlapping naphthyl), 8.15 (s, 1H, 2H), 7.96-7.94 (m, 1H, naphthyl), 7.83-7.81 (m, 1H, naphthyl), 7.59-7.53 (m, 3H, 2H naphthyl overlapping 1H aromatic), 7.44-7.41 (m, 2H, naphthyl), 7.10 (d, 1H, aromatic, *J*=8.6 Hz), 5.89 (d, 1H, 1′H, *J*=6.1 Hz), 5.45 (d, 1H, 3′OH, *J*=6.1 Hz), 5.28 (d, 1H, 2′OH, *J*=4.6 Hz), 5.19 (bs, 2H, CH_2, naphthylmethyl), 4.78-4.75 (m, 1H, 2′H), 4.17-4.15 (m, 1H, 3′H), 4.09-4.06 (m, 1H, 4′H), 2.79 (t, 4H, CH_2, piperidyl, *J*=4.8 Hz), 2.10 (s, 3H, CH_3, acetamido), 1.69-1.68 (m, 4H, CH_2, piperidyl), 1.56-1.51 (m, 2H, CH_2, piperidyl)

HRFAB-MS $C_{35}H_{38}N_8O_5$
MW 650.74
$[M+H]^+$ calcd 651.3043
$[M+H]^+$ found 651.3062

Activity Dd2 strain of *P. falciparum*: IC_{50} = 4.2 μM
DOXP reductoisomerase: 24%

5′-Deoxy-5′-{4-[2-(2-methoxyphenyl)ethylamino]-3-propanamido-benzamido}-N^6-(1-naphthylmethyl)adenosine (**41**)

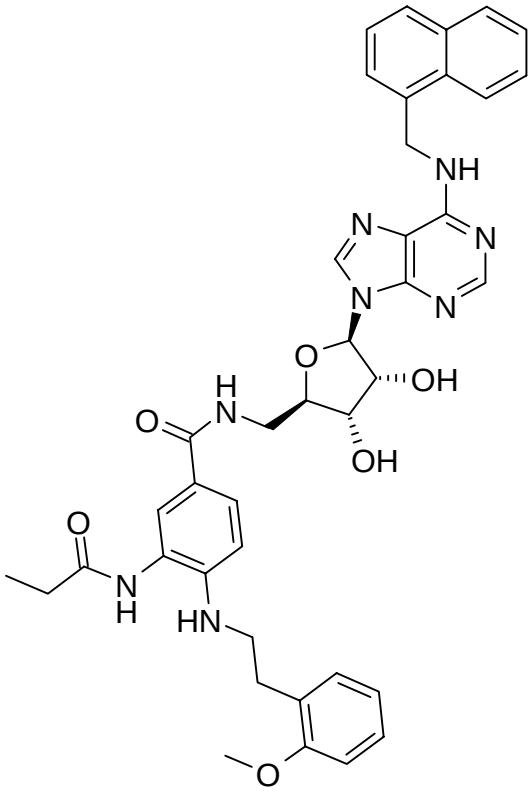

Yield 58%

^{1}H NMR (400 MHz, DMSO-d_6) = δ (ppm) 9.03 (s, 1H, NH, amide), 8.45 (bs, 1H, N^6H), 8.39 (bs, 1H, 8H), 8.31 (t, 1H, NH, amide, *J*=5.9 Hz), 8.24-.8.22 (m, 2H, naphthyl overlapping 2H), 7.96-7.94 (m, 1H, naphthyl), 7.82-7.80 (m, 1H, naphthyl), 7.67-7.64 (m, 2H, aromatic), 7.59-7.52 (m, 2H, naphthyl), 7.46-7.37 (m, 2H, naphthyl), 7.23-7.18 (m, 2H, aromatic), 6.97-6.86 (m, 2H, aromatic), 6.75 (d, 1H, aromatic, *J*=8.7 Hz), 5.88 (d, 1H, 1′H, *J*=6.6 Hz), 5.48-5.46 (m, 1H, NH, amine), 5.42 (d, 1H, 3′OH, *J*=6.4 Hz), 5.25 (d, 1H, 2′OH, *J*=4.6 Hz), 5.19 (bs, 2H, CH_2, naphthylmethyl), 4.81-4.74 (m, 1H, 2′H), 4.16-4.13 (m, 1H, 3′H), 4.11-4.06 (m, 1H, 4′H), 3.80 (s, 3H, CH_3, methoxy), 2.83 (t, 2H, CH_2, ethylamino, *J*=7.4 Hz), 2.36-2.27 (m, 2H, CH_2, propanamido), 1.10-1.02 (m, 3H, CH_3, propanamido)

HRESI-MS $C_{40}H_{42}N_8O_6$ $[M+Na]^+$ calcd 753.3125
MW 730.83 $[M+Na]^+$ found 753.3132

Activity Dd2 strain of *P. falciparum*: IC_{50} = 2.7 μM
DOXP reductoisomerase: 0%

5′-[3-Acetamido-4-(*N*-benzyl-*N*-ethylamino)benzamido]-5′-deoxy-N^6-(1-naphthylmethyl)adenosine (**42**)

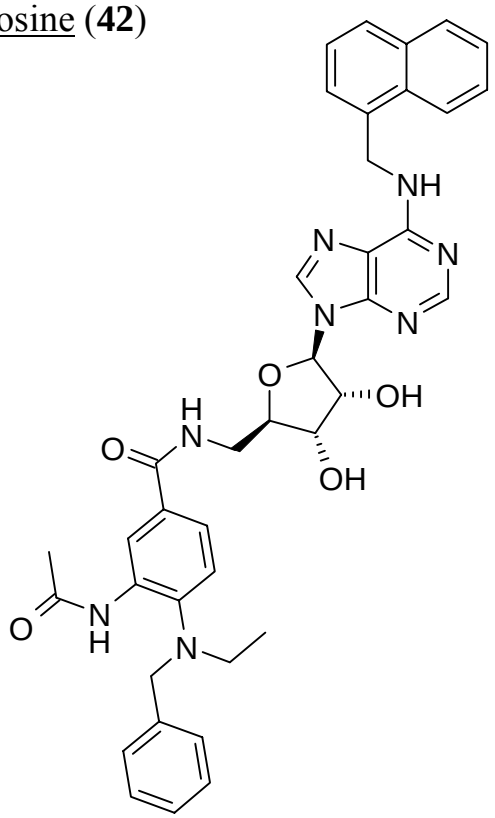

Yield 59%

^{1}H NMR (400 MHz, DMSO-d_6) = δ (ppm) 9.02 (s, 1H, NH, amide), 8.53 (t, 1H, NH, amide, *J*=5.9 Hz), 8.47 (bs, 1H, N^6H), 8.40 (bs, 1H, 8H), 8.24-8.22 (m, 2H, aromatic overlapping naphthyl), 8.13 (s, 1H, 2H), 7.96-7.94 (m, 1H, naphthyl), 7.83-7.80 (m, 1H, naphthyl), 7.59-7.40 (m, 5H, 4H naphthyl overlapping 1H aromatic), 7.33-7.31 (d, 2H, aromatic, *J*=7.12 Hz), 7.27-7.12 (m, 4H, aromatic), 5.88 (d, 1H, 1′H, *J*=6.6 Hz), 5.45 (d, 1H, 3′OH, *J*=6.6 Hz), 5.29 (d, 1H, 2′OH, *J*=4.6 Hz), 5.19 (bs, 2H, CH_2, naphthylmethyl), 4.78-4.77 (m, 1H, 2′H), 4.16-4.13 (m, 3H, 3′H overlapping CH_2, benzylamino), 4.08-4.05 (m, 1H, 4′H), 3.03-2.97 (m, 2H, CH_2, ethylamino), 2.05 (s, 3H, CH_3, acetamido), 1.00-0.93 (m, 3H, CH_3, ethylamine)

HRESI-MS $C_{39}H_{40}N_8O_5$
MW 700.80
$[M+H]^+$ calcd 701.3200
$[M+H]^+$ found 701.3196

Activity Dd2 strain of *P. falciparum*: IC_{50} = 3.3 μM
DOXP reductoisomerase: 65%

5′-[3-*tert*-Butyloxycarbonylamido-4-(morphol-4-yl)benzamido]-5′-deoxy-N^6-(1-naphthylmethyl)adenosine (**43**)

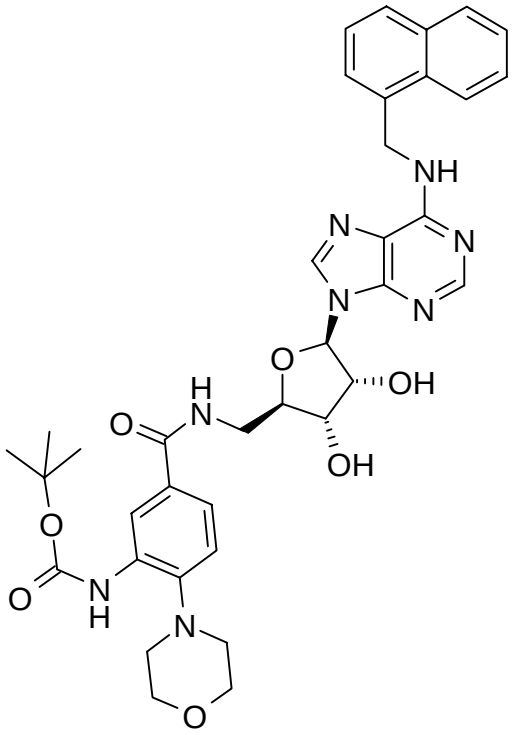

Yield 47%

^{1}H NMR (400 MHz, DMSO-d_6) = δ (ppm) 8.56 (t, 1H, NH, amide, *J*=5.9 Hz), 8.44 (bs, 1H, N^6H), 8.39 (bs, 1H, 8H), 8.24 (d, 1H, naphthyl, *J*=8.7 Hz), 8.18 (d, 1H, aromatic, *J*=2.0 Hz), 8.16 (s, 1H, 2H), 7.97 (s, 1H, NH, amide), 7.96-7.94 (m, 1H, naphthyl), 7.82-7.80 (m, 1H, naphthyl), 7.59-7.52 (m, 3H, 2H naphthyl overlapping 1H aromatic), 7.46-7.40 (m, 2H, naphthyl), 7.19 (d, 1H, aromatic, *J*=8.1 Hz), 5.89 (d, 1H, 1′H, *J*=6.4 Hz), 5.44 (d, 1H, 3′OH, *J*=5.6 Hz), 5.27 (d, 1H, 2′OH, *J*=4.3 Hz), 5.18 (bs, 2H, CH_2, naphthylmethyl), 4.77 (bs, 1H, 2′H), 4.18-4.15 (m, 1H, 3′H), 4.10-4.07 (m, 1H, 4′H), 3.74 (t, 4H, CH_2, morpholyl, *J*=4.5 Hz), 2.83 (t, 4H, CH_2, morpholyl, *J*=4.6 Hz), 1.45 (s, 9H, CH_3, BOC)

HRESI-MS $C_{37}H_{42}N_8O_7$
MW 710.80
$[M+H]^+$ calcd 711.3255
$[M+H]^+$ found 711.3252

Activity Dd2 strain of *P. falciparum*: IC_{50} = 3.1 μM
DOXP reductoisomerase: 0%

5′-[(3-Acetamido-4-dibut-1-ylamino)benzamido]-5′-deoxy-N^6-(1-naphthylmethyl)adenosine (**44**)

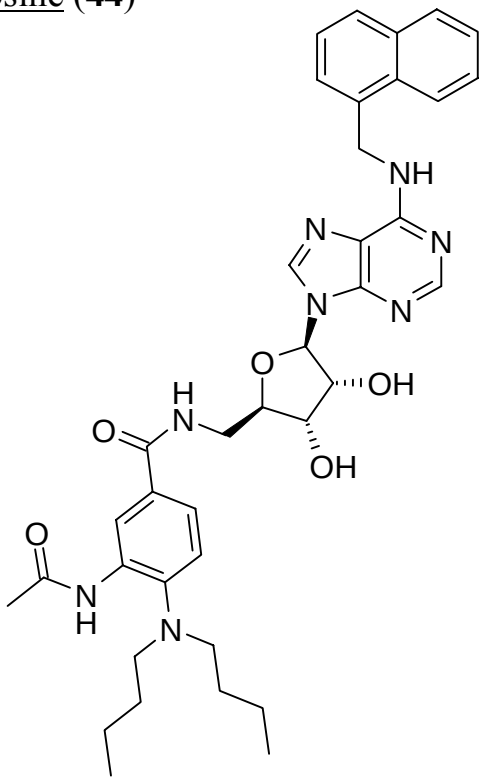

Yield 72%

^{1}H NMR (400 MHz, DMSO-d_6) = δ (ppm) 8.91 (bs, 1H, NH, amide), 8.54 (t, 1H, NH, amide, *J*=5.6 Hz), 8.45-8.36 (m, 3H, N^6H overlapping 8H overlapping aromatic), 8.24 (d, 1H, naphthyl, *J*=7.9 Hz), 8.11 (s, 1H, 2H), 7.96-7.94 (m, 1H, naphthyl), 7.82-7.80 (m, 1H, naphthyl), 7.59-7.52 (m, 3H, 2H naphthyl overlapping 1H aromatic), 7.44-7.40 (m, 2H, naphthyl), 7.21 (d, 1H, aromatic, *J*=8.4 Hz), 5.89 (d, 1H, 1′H, *J*=6.4 Hz), 5.44 (d, 1H, 3′OH, *J*=6.4 Hz), 5.27 (d, 1H, 2′OH, *J*=4.8 Hz), 5.18 (bs, 2H, CH_2, naphthylmethyl), 4.80-4.74 (m, 1H, 2′H), 4.20-4.17 (m, 1H, 3′H), 4.11-4.07 (m, 1H, 4′H), 2.90 (t, 4H, CH_2, dibut-1-ylamino, *J*=7.3 Hz), 2.09 (s, 3H, CH_3, acetamido), 1.37-1.29 (m, 4H, CH_2, dibut-1-ylamino), 1.25-1.20 (m, 4H, CH_2, dibut-1-ylamino), 0.81 (t, 6H, CH_3, dibut-1-ylamino, *J*=7.2 Hz)

HRESI-MS $C_{38}H_{46}N_8O_5$ $[M+Na]^+$ calcd 717.3489
MW 694.84 $[M+Na]^+$ found 717.3491

Activity Dd2 strain of *P. falciparum*: IC_{50} = 3.7 μM
DOXP reductoisomerase: 59%

5′-[(4-Dibut-1-ylamino-3-propanamido)benzamido]-5′-deoxy-N^6-(1-naphthylmethyl)adenosine (**45**)

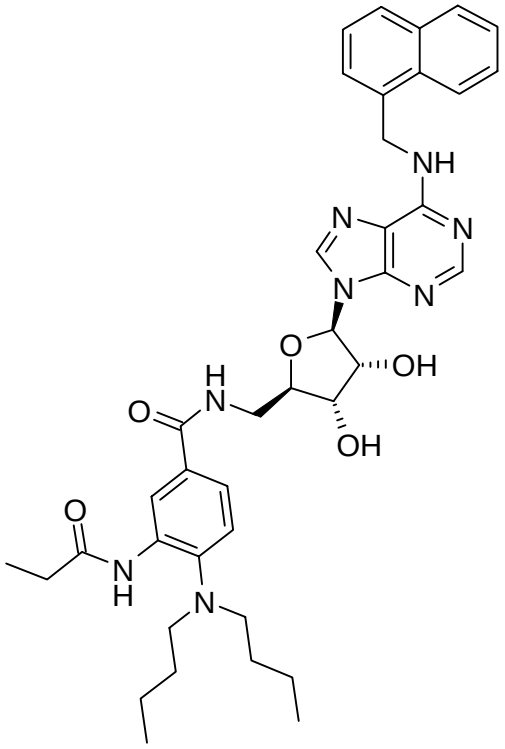

Yield 52%

^{1}H NMR (400 MHz, DMSO-d_6) = δ (ppm) 8.86 (s, 1H, NH, amide), 8.56 (t, 1H, NH, amide, *J*=5.6 Hz), 8.43-8.40 (m, 3H, N^6H overlapping 8H overlapping aromatic), 8.24 (d, 1H, naphthyl, *J*=7.9 Hz), 8.11 (s, 1H, 2H), 7.96-7.94 (m, 1H, naphthyl), 7.82-7.80 (m, 1H, naphthyl), 7.59-7.51 (m, 3H, 2H naphthyl overlapping 1H aromatic), 7.46-7.40 (m, 2H, naphthyl), 7.23 (d, 1H, aromatic, *J*=8.4 Hz), 5.89 (d, 1H, 1′H, *J*=6.4 Hz), 5.44 (d, 1H, 3′OH, *J*=6.4 Hz), 5.27 (d, 1H, 2′OH, *J*=4.6 Hz), 5.18 (bs, 2H, CH_2, naphthylmethyl), 4.80-4.77 (m, 1H, 2′H), 4.18-4.16 (m, 1H, 3′H), 4.10-4.08 (m, 1H, 4′H), 2.89 (t, 4H, CH_2, dibut-1-ylamino, *J*=7.8 Hz), 2.41-2.35 (m, 2H, CH_2, propan-amido), 1.36-1.28 (m, 4H, CH_2, dibut-1-ylamino), 1.25-1.19 (m, 4H, CH_2, dibut-1-ylamino), 1.09 (t, 3H, CH_3, propan-amido, *J*=7.5 Hz), 0.81 (t, 6H, CH_3, dibut-1-ylamino, *J*=7.3 Hz)

HRESI-MS $C_{39}H_{48}N_8O_5$
MW 708.87
$[M+Na]^+$ calcd 731.3645
$[M+Na]^+$ found 731.3645

5′-[(4-Dibut-1-ylamino-3-butanamido)benzamido]-5′-deoxy-N^6-(1-naphthylmethyl)adenosine (**46**)

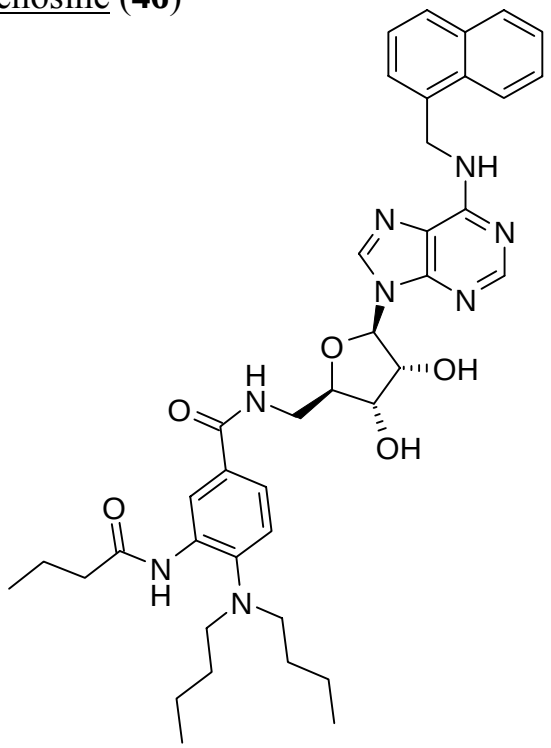

Yield 51%

^{1}H NMR (400 MHz, DMSO-d_6) = δ (ppm) 8.87 (s, 1H, NH, amide), 8.56 (t, 1H, NH, amide, *J*=5.7 Hz), 8.44-8.37 (m, 3H, N^6H overlapping 8H overlapping aromatic), 8.23 (d, 1H, naphthyl, *J*=7.9 Hz), 8.11 (s, 1H, 2H), 7.96-7.94 (m, 1H, naphthyl), 7.82-7.80 (m, 1H, naphthyl), 7.59-7.51 (m, 3H, 2H naphthyl overlapping 1H aromatic), 7.46-7.40 (m, 2H, naphthyl), 7.24 (d, 1H, aromatic, *J*=8.39 Hz), 5.89 (d, 1H, 1′H, *J*=6.6 Hz), 5.44 (d, 1H, 3′OH, *J*=6.1 Hz), 5.28 (d, 1H, 2′OH, *J*=4.3 Hz), 5.18 (bs, 2H, CH_2, naphthylmethyl), 4.79-4.74 (m, 1H, 2′H), 4.17 (m, 1H, 3′H), 4.11-4.08 (m, 1H, 4′H), 2.89 (t, 4H, CH_2, dibut-1-ylamino, *J*=7.2 Hz), 2.35 (t, 2H, CH_2, butyryl, *J*=7.3 Hz), 1.64-1.59 (m, 2H, butyryl), 1.35-1.28 (m, 4H, CH_2, dibut-1-ylamino), 1.24-1.17 (m, 4H, CH_2, dibut-1-ylamino), 0.92 (t, 3H, CH_3, butyryl, *J*=7.4 Hz), 0.80 (t, 6H, CH_3, dibut-1-ylamino, *J*=7.3 Hz)

HRESI-MS $C_{40}H_{50}N_8O_5$ $[M+H]^+$ calcd 723.3983
MW 722.90 $[M+H]^+$ found 723.3960

Activity Dd2 strain of *P. falciparum*: IC_{50} = 3.2 μM
DOXP reductoisomerase: 53%

5′-Deoxy-5′-[4-(3-indolyl)butanamido]-N^6-(4-phenylbenzyl)adenosine (**47**)

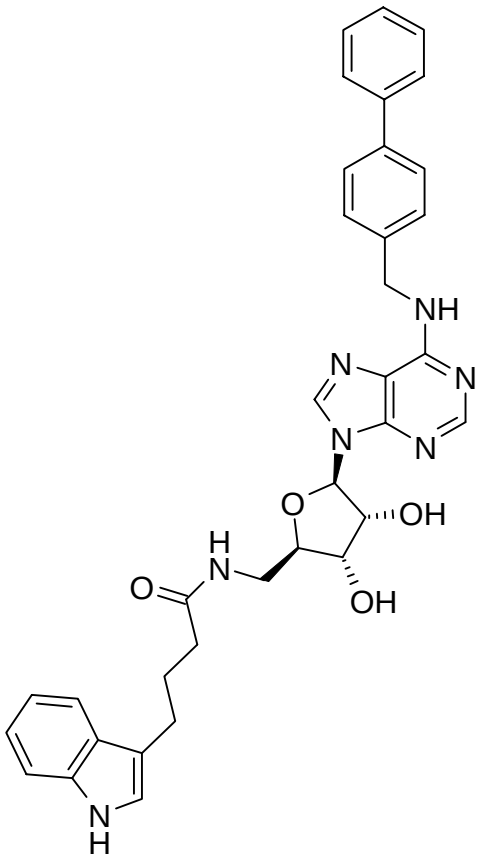

Yield 82%

^{1}H NMR (400 MHz, DMSO-d_6) = δ (ppm) 10.71 (bs, 1H, NH, indolyl), 8.48 (bs, 1H, N^6H), 8.38 (s, 1H, 8H), 8.22 (s, 1H, 2H), 8.18 (t, 1H, NH, amide, *J*=5.6 Hz), 7.62-7.57 (m, 4H, biphenyl), 7.49-7.42 (m, 5H, 4H biphenyl overlapping 1H indolyl), 7.35-7.30 (m, 2H, biphenyl overlapping indolyl), 7.08 (d, 1H, indolyl, *J*=2.3 Hz), 7.05-7.01 (m, 1H, indolyl), 6.95-6.91 (m, 1H, indolyl), 5.88 (d, 1H, 1′H, *J*=6.4 Hz), 5.44 (d, 1H, 3′OH, *J*=6.4 Hz), 5.25 (d, 1H, 2′OH, *J*=4.6 Hz), 4.76 (bs, 2H, CH_2, biphenylmethyl), 4.73-4.69 (m, 1H, 2′H), 4.08-4.05 (m, 1H, 3′H), 3.99-3.96 (m, 1H, 4′H), 2.66 (t, 2H, CH_2, butyryl, *J*=7.5 Hz), 2.21 (t, 2H, CH_2, butyryl, *J*=7.4 Hz), 1.89 (t, 2H, CH_2, butyryl, *J*=7.62 Hz)

HRESI-MS $C_{35}H_{35}N_7O_4$ $[M+H]^+$ calcd 618.2830
MW 617.71 $[M+H]^+$ found 618.2815

Activity Dd2 strain of *P. falciparum*: IC_{50} = 3.7 μM
DOXP reductoisomerase: 48%

5′-Deoxy-5′-(3-methoxyphenylacetamido)-N^6-(4-phenylbenzyl)adenosine (**48**)

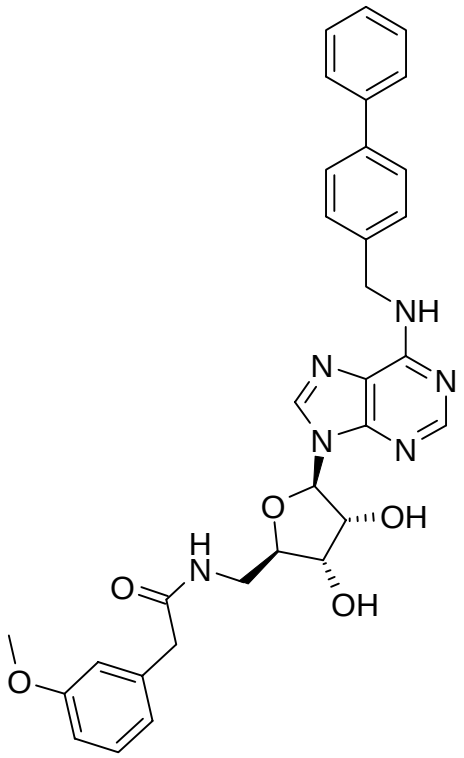

Yield 65%

^{1}H NMR (400 MHz, DMSO-d_6) = δ (ppm) 8.48 (bs, 1H, N^6H), 8.36 (s, 1H, 8H), 8.35-8.32 (m, 1H, NH, amide), 8.25 (s, 1H, 2H), 7.63-7.58 (m, 4H, biphenyl), 7.46-7.42 (m, 4H, biphenyl), 7.35-7.32 (m, 1H, biphenyl), 7.17 (t, 1H, aromatic, *J*=7.7 Hz), 6.81-6.78 (m, 3H, aromatic), 5.88 (d, 1H, 1′H, *J*=6.1 Hz), 5.45 (d, 1H, 3′OH, *J*=6.1 Hz), 5.26 (d, 1H, 2′OH, *J*=4.6 Hz), 4.76 (bs, 2H, CH_2, biphenylmethyl), 4.71-4.65 (m, 1H, 2′H), 4.10-4.05 (m, 1H, 3′H), 3.97-3.96 (m, 1H, 4′H), 3.82-3.76 (m, 2H, 5′CH_2), 3.69 (s, 3H, CH_3, methoxy)

HRESI-MS $C_{32}H_{32}N_6O_5$
MW 580.65
$[M+H]^+$ calcd 581.2513
$[M+H]^+$ found 581.2524

Activity Dd2 strain of *P. falciparum*: IC_{50} = 14 μM
DOXP reductoisomerase: 0%

5′-[3-Acetamido-4-(morphol-4-yl)benzamido]-5′-deoxy-N^6-(4-phenyl-benzyl)adenosine (**49**)

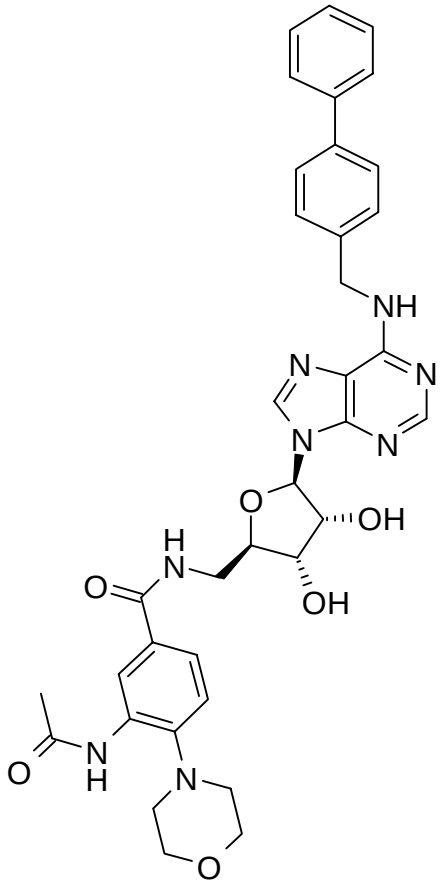

Yield 71%

^{1}H NMR (400 MHz, DMSO-d_6) = δ (ppm) 8.99 (s, 1H, NH, amide), 8.55 (t, 1H, NH, amide, *J*=5.8 Hz), 8.46 (bs, 1H, N^6H), 8.39 (s, 1H, 8H), 8.25 (bs, 1H, aromatic), 8.17 (s, 1H, 2H), 7.63-7.58 (m, 5H, 4H biphenyl overlapping 1H aromatic), 7.46-7.42 (m, 4H, biphenyl), 7.35-7.32 (m, 1H, biphenyl), 7.14 (d, 1H, aromatic, *J*=8.7 Hz), 5.89 (d, 1H, 1′H, *J*=6.4 Hz), 5.44 (d, 1H, 3′OH, *J*=6.1 Hz), 5.27 (d, 1H, 2′OH, *J*=4.8 Hz), 4.79-4.74 (m, 3H, CH_2 biphenylmethyl overlapping 2′H), 4.19-4.16 (m, 1H, 3′H), 4.10-4.07 (m, 1H, 4′H), 3.82-3.74 (m, 4H, CH_2, morpholyl), 2.87-2.85 (m, 4H, CH_2, morpholyl), 2.10 (s, 3H, CH_3, acetamido)

HRESI-MS $C_{36}H_{38}N_8O_6$ $[M+H]^+$ calcd 679.2993
MW 678.75 $[M+H]^+$ found 679.2990

Activity Dd2 strain of *P. falciparum*: IC_{50} = 3.2 μM
DOXP reductoisomerase: 0%

5′-Deoxy-5′-{[4-(1-methylethyl)amino-3-propanamido]benzamido}-N^6-(1-naphthylmethyl)adenosine (**52**)

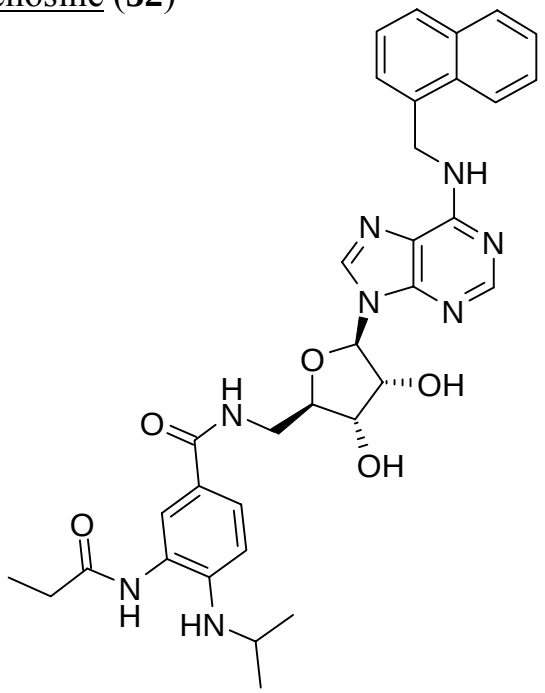

Yield 81%

^{1}H NMR (400 MHz, DMSO-d_6) = δ (ppm) 9.05 (s, 1H, NH, amide), 8.44 (bs, 1H, N^6H), 8.39 (bs, 1H, 8H), 8.30 (t, NH, amide, *J*=5.6 Hz), 8.25 (d, 1H, naphthyl, *J*=7.9 Hz), 8.20 (s, 1H, 2H), 7.96-7.94 (m, 1H, naphthyl), 7.83-7.80 (m, 1H, naphthyl), 7.70 (s, 1H, aromatic), 7.61-7.52 (m, 3H, 2H naphthyl overlapping 1H aromatic), 7.46-7.41 (m, 2H, naphthyl), 6.66 (d, 1H, aromatic, *J*=8.7 Hz), 5.88 (d, 1H, 1′H, *J*=6.4 Hz), 5.42 (d, 1H, 3′OH, *J*=6.4 Hz), 5.25 (d, 1H, 2′OH, *J*=4.6 Hz), 5.19 (bs, 2H, CH_2, naphthylmethyl), 4.95 (d, 1H, NH, 2-propylamino, *J*=7.6 Hz), 4.77-4.74 (m, 1H, 2′H), 4.16-4.14 (m, 1H, 3′H), 4.10-4.05 (m, 1H, 4′H), 3.68-3.61 (m, 1H, CH, 2-propylamino), 2.37-2.31 (m, 2H, CH_2, propanamido), 1.16 (d, 6H, CH_3, 2-propylamino, *J*=6.1 Hz), 1.11-1.04 (m, 3H, CH_3, propanamido)

HRESI-MS $C_{34}H_{38}N_8O_5$
MW 638.73
$[M+H]^+$ calcd 639.3043
$[M+H]^+$ found 639.3040

Activity Dd2 strain of *P. falciparum*: IC_{50} = 3.2 μM
DOXP reductoisomerase: 0%

In vitro measurement of *P. falciparum* growth inhibition[15-17]: The *P. falciparum* strain Dd2 was cultivated by a modification of the method described by Trager and Jensen. The culture medium consisted of RPMI 1640 supplemented with 10% human type 0^+ serum and 25 mM HEPES. Human type 0^+ erythrocytes served as host cells. The cultures were kept at 37 °C in an atmosphere of 5% O_2, 3% CO_2, and 92% N_2. Testing of compounds was carried out in 96-well microtiter plates. The compounds were dissolved in DMSO (10 mM) and prediluted in complete culture medium. Infected erythrocytes (200 µL per well, with 2% haematocrit and 0.4% parasitemia) were incubated in duplicate with a serial dilution of the compounds for 48 h. After the addition of 0.8 µCi [^{3}H]-hypoxanthine in 50 µL medium per well, the plates were further incubated for 24 h. Cells were collected on glass fiber filters with a cell harvester (Micromate 196, Packard) and incorporated radioactivity measured using a β-counter (Matrix 9600, Packard).

In vitro measurement of DOXP reductoisomerase inhibition: The expression and purification of the recombinant DOXP reductoisomerase were carried out as described[18]. Inhibition studies were performed by Jomaa Pharmaka GmbH, Gießen, Germany, as reported[18].

In vitro measurement of AdoMetDC inhibition: The enzyme activity was assayed by measuring the production of $^{14}CO_2$ from *S*-adenosyl-L-[carboxy-^{14}C]methionine following conditions previously reported[19]. In vitro measurement of AdoMetDC was performed by the Bernhard-Nocht-Institut für Tropenmedizin, Hamburg, Germany.

In vitro measurement of *T. b. brucei and T. cruzi* growth inhibition[20]: Blood stream forms of *T. b. brucei* and *T. cruzi* were cultivated in HMI-9 medium. In a 96-well microplate, 10,000 haemoflagellates were incubated at different drug concentrations for four days. Parasitic multiplication was evaluated microscopically. IC_{50} values were determined by measuring growth inhibition at three to five concentrations. Suramin was included as standard agent. In vitro measurement of *T. b. brucei and T. cruzi* growth inhibition was accomplished by Tibotec, Mechelen, Belgium.

In vitro measurement of HIV-1(III_B) and HIV-2(ROD) inhibition: MT-4 and CEM cells were grown and maintained in RPMI 1640 medium

supplemented with 10% heat-inactivated fetal calf serum, 2 mM L-glutamine, 0.1% sodium bicarbonate, and 20 μg of gentamicin per mL[36,37].
The origin of the HIV type 1 (HIV-1) (strain III_B) and HIV-2 (strain ROD) has been described previously. HIV-1(III_B) and HIV-2(ROD) stocks were obtained from the culture supernatants of virus-infected MT-4 cell cultures[38,39].
The inhibitory effects of the test compounds on HIV-1 and HIV-2 replication were monitored by the inhibition of virus-induced cytopathicity and syncytium formation in MT-4 cells and CEM cells as described by Pauwels et al. and Balzarini et al., respectively[21,22]. Virus-induced cytopathicity and cytotoxicity was assessed five days post-infection.
In vitro measurement of HIV-1(III_B) and HIV-2(ROD) inhibition as well as determination of cytotoxicity of selected compounds was performed at the Rega Institute, Katholike Universiteit Leuven, Belgium.

Radioligand binding assays for the investigation of A_1, A_{2A}, A_{2B}, and A_3 adenosine receptor inhibition[23]: Compound **2** was investigated in radioligand binding studies employing [^{3}H]*N*^{6}-cyclohexyladenosine (CHA) and [^{3}H]-2-({[4-(carboxyethyl)phenyl]ethyl}amino)-5′-*N*-(ethylcarboxamido)]adenosine (CGS21680), respectively, as radioligands. Inhibition of binding of CHA to A_1 adenosine receptors of rat cerebral cortical membranes and inhibition of CGS21680 to A_{2A} of rat striatal membranes were assayed as previously described[40,41]. Binding of [125I]*N*^{2}-methyl-3,4-dihydroxy-5-[6-[3-iodobenzyl) amino]- 9*H*-9- purinyl)- 3-tetrahydro-2 -furancarboxamide ([^{125}I]AB-MECA) to human A_3 adenosine receptors stably expressed in CHO cells was determined as reported[42]. Tests were performed two to three times at various concentrations.
In vitro measurement of A_1, A_{2A}, A_{2B}, and A_3 adenosine receptor inhibition was carried out at the Rheinische Friedrich-Wilhelms-Universität Bonn, Bonn, Germany.

2.7 References

(1) Kenner, G. W.; McDermott, J. R.; Sheppard, R. C. *J. Chem. Soc., Chem. Commun.* **1971**, 636-637.
(2) Backes, B. J.; Ellman, J. A. *J. Am. Chem. Soc.* **1994**, *116*, 11171-11172.

(3) Bressi, J. C.; Verlinde, C. L.; Aronov, A. M.; Shaw, M. L.; Shin, S. S.; Nguyen, L. N.; Suresh, S.; Buckner, F. S.; Van Voorhis, W. C.; Kuntz, I. D.; Hol, W. G.; Gelb, M. H. *J. Med. Chem.* **2001**, *44*, 2080-2093.

(4) Mitsunobu, O. *Synthesis Rev.* **1981**, 1-28.

(5) Yeh, C.-M.; Tung, C.-L.; Sun, C.-M. *J. Comb. Chem.* **2000**, *2*, 341-348.

(6) Kilburn, J. P.; Lau, J.; Jones, C. C. F. *Tetrahedron Lett.* **2000**, *41*, 5419-5421.

(7) Lee, J.; Murray, W. V.; Rivero, R. A. *J. Org. Chem.* **1997**, *62*, 3874-3879.

(8) Phillips, G. B.; Wei, G. P. *Tetrahedron Lett.* **1996**, *37*, 4887-4890.

(9) Tumelty, D.; Schwarz, M. K.; Needels, M. C. *Tetrahedron Lett.* **1998**, *39*, 7467-7470.

(10) Dankwardt, S. M.; Newman, S. R.; Krstenansky, J. L. *Tetrahedron Lett.* **1995**, *36*, 4923-4926.

(11) Morales, G. A.; Corbett, J. W.; DeGrado, W. F. *J. Org. Chem.* **1998**, *63*, 1172-1177.

(12) Meyers, H.; Dilley, G.; Durgin, T.; Powers, T.; Winssinger, N. *Mol. Diversity* **1995**, *1*, 13-20.

(13) Backes, B. J.; Virgilio, A. A.; Ellman, J. A. *J. Am. Chem. Soc.* **1996**, *118*, 3055-3056.

(14) http://pubs.acs.org/instruct/jccff.pdf

(15) Ancelin, M. L.; Calas, M.; Bompart, J.; Cordina, G.; Martin, D.; Ben Bari, M.; Jei, T.; Druilhe, P.; Vial, H. J. *Blood* **1998**, *91*, 1426-1437.

(16) Desjardins, R. E.; Canfield, C. J.; Haynes, J. D.; Chulay, J. D. *Antimicrob. Agents Chemother.* **1979**, *16*, 710-718.

(17) Trager, W.; Jensen, J. B. *Science* **1976**, *193*, 673-675.

(18) Jomaa, H.; Wiesner, J.; Sanderbrand, S.; Altincicek, B.; Weidemeyer, C.; Hintz, M.; Turbachova, I.; Eberl, M.; Zeidler, J.; Lichtenthaler, H. K.; Soldati, D.; Beck, E. *Science* **1999**, *285*, 1573-1576.

(19) Rathaur, S.; Wittich, R. M.; Walter, R. D. *Exp. Parasitol.* **1988**, *65*, 277-281.

(20) Hirumi, H.; Hirumi, K. *J. Parasitology* **1989**, *75*, 985-989.

(21) Balzarini, J.; Karlsson, A.; Perez-Perez, M.-J.; Camarasa, M.-J.; De Clercq, E. *Virology* **1993**, *196*, 576-585.

(22) Pauwels, R.; Balzarini, J.; Baba, M.; Snoeck, R.; Schols, D.; Herdewijn, P.; De Clercq, E. *J. Virol. Methods* **1988**, *20*, 309-321.

(23) Müller, C. E.; Thorand, M.; Qurishi, R.; Diekmann, M.; Jacobson, K. A.; Padgett, W. L.; Daly, J. W. *J. Med. Chem.* **2002**, *45*, 3440-3450.
(24) Smith, R. D.; Loo, J. A.; Edmonds, C. G.; Barinaga, C. J.; Udseth, H. R. *Anal. Chem.* **1990**, *62*, 882-899.
(25) Dass, C. *Curr. Org. Chem.* **1999**, *3*, 193-209.
(26) Hajduk, P. J.; Gomtsyan, A.; Didomenico, S.; Cowart, M.; Bayburt, E. K.; Solomon, L.; Severin, J.; Smith, R.; Walter, K.; Holzman, T. F.; Stewart, A.; McGaraughty, S.; Jarvis, M. F.; Kowaluk, E. A.; Fesik, S. W. *J. Med. Chem.* **2000**, *43*, 4781-4786.
(27) Golisade, A.; Van Calenbergh, S.; Link, A. *Tetrahedron* **2000**, *56*, 3167-3172.
(28) Golisade, A.; Bressi, J. C.; Van Calenbergh, S.; Gelb, M. H.; Link, A. *J. Comb. Chem.* **2000**, *2*, 537-544.
(29) Golisade, A.; Herforth, C.; Quirijnen, L.; Maes, L.; Link, A. *Bioorg. Med. Chem.* **2002**, *10*, 159-165.
(30) Aronov, A. M.; Verlinde, C. L. M. J.; Hol, W. G. J.; Gelb, M. H. *J. Med. Chem.* **1998**, *41*, 4790-4799.
(31) Aronov, A. M.; Suresh, S.; Buckner, F. S.; Van Voorhis, W. C.; Verlinde, C. L. M. J.; Opperdoes, F. R.; Hol, W. G. J.; Gelb, M. H. *Proc. Natl. Acad. Sci. USA* **1999**, *96*, 4273-4278.
(32) Van Calenbergh, S.; Verlinde, C. M. L. V.; Soenens, J.; De Bruyn, A.; Callens, M.; Blaton, N. M.; Peeters, O. M.; Rozenski, J.; Hol, W. G.; Herdewijn, P. *J. Med. Chem.* **1995**, *38*, 3838-3849.
(33) Golisade, A.; Wiesner, J.; Herforth, C.; Jomaa, H.; Link, A. *Bioorg. Med. Chem.* **2002**, *10*, 769-777.
(34) Seok, Y. J.; Sondej, M.; Badawi, P.; Lewis, M. S.; Briggs, M. C.; Jaffe, H.; Peterkofsky, A. *J. Biol. Chem.* **1997**, *272*, 26511-26521.
(35) Golisade, A.; Herforth, C.; Wieking, K.; Kunick, C.; Link, A. *Bioorg. Med. Chem. Lett.* **2001**, *11*, 1783-1786.
(36) Foley, G. E. *Cancer* **1965**, *18*, 522-529.
(37) Miyoshi, I.; Kubonishi, I.; Yoshimoto, S.; Akagi, T.; Ohtsuki, Y.; Shiraishi, Y.; Nagata, K.; Hinuma, Y. *Nature* **1981**, *270*, 770.
(38) Popovic, M.; Sarngadharan, M. G.; Read, E.; Gallo, R. C. *Science* **1984**, *224*, 497-500.
(39) Barre-Sinoussi, F.; Chermann, J. C.; Rey, F.; Nugeyre, M. T.; Chamaret, S.; Gruest, J.; Dauguet, C.; Axler-Blin, C.; Vezinet-Brun, F.; Rouzioux, C.; Rozenbaum, W.; Montagnier, L. *Science* **1983**, *220*, 868-871.

(40) Müller, C. E.; Sauer, R.; Geis, U.; Frobenius, W.; Talik, P.; Pawlowski, M. *Arch. Pharm. Pharm. Med. Chem.* **1997**, *330*, 181-189.

(41) Hipp, J. Dissertation. University of Würzburg, Würzburg, Germany, 1997.

(42) Kim, Y.-C.; Ji, X.-D.; Jacobson, K. A. *J. Med. Chem.* **1996**, *39*, 4142-4148.

3 Antimalarial Activity of 3´,N^6-Disubstituted Adenosine Derivatives

3.1 Introduction

By random screening, compound **57** has been identified as a further lead structure exhibiting antimalarial activity against the *P. falciparum* pathogen. In the course of ongoing development establishing structure-activity relationships of adenosine derivatives, 3´,N^6-disubtituted adenosines as potential inhibitors of *P. falciparum* were prepared and investigated. Structural modifications of the lead compound covering the replacement of the 3´-(6-phenylhexanoyl) residue and the 6-amino group by a number of acyl residues and 1-naphthylmethylamine, respectively, were performed.

Figure 10. Lead structure **57** displaying pronounced antimalarial activity against the Dd2 strain of *P. falciparum* (IC_{50} = 3.2 μM).

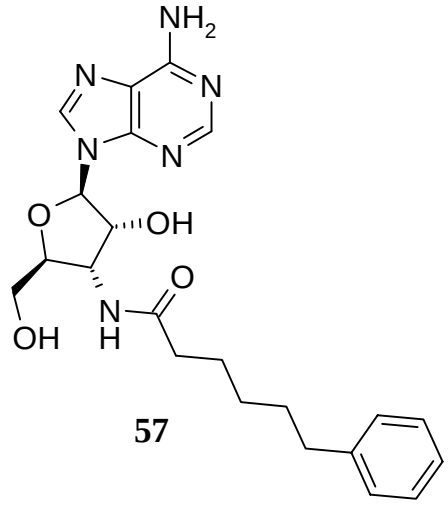

57

Within this chapter, the preparation and biological evaluation of 3´-amido-3´-deoxy-N^6-(1-naphthylmethyl)adenosines is described and discussed. Furthermore, N^6-monosubstituted adenosine derivatives derived from previous studies, displaying moderate antimalarial activity[1] were investigated with regards to DOXP reductoisomerase inhibition. Results are discussed along findings of the biological evaluation of 3´,N^6- and 5´,N^6-disubstituted adenosines.

3.2 Synthesis of 3´-Amido-3´-Deoxy-N^6-(1-Naphthylmethyl)-Adenosines

In chapter 2, the structure-based design of adenosine analogs as selective micromolar inhibitors of *P. falciparum* (5´,N^6-disubstituted adenosines) and trypanosomal GAPDH (2´,N^6-disubstituted and 2´-monosubstituted adenosines) was demonstrated. Following the same approach, a small series of 3´,N^6-disubstituted adenosines was prepared and subsequently tested for antimalarial activity. Again, the synthetic approach of these derivatives required the preparation of a novel nucleoside template, the nucleoside template 3´-amino-3´-deoxy-N^6-(1-naphthylmethyl)adenosine (**63**). In order to access a sequence of 3´-amido-3´-deoxy-N^6-(1-naphthylmethyl)adenosine derivatives, the PASP protocol for the chemoselective acylation of the 3´-amino group of **63** was employed.

The nucleoside template **63** was obtained by conventional synthesis in solution (scheme 10). Initially, 3´-azido-3´-deoxyadenosine (**58**) gently provided from Van Calenbergh and co-workers was simultaneously protected at the 2´- and 5´-position by treatment with acetic anhydride in pyridine, following a protocol reported by Ikehara and Takatsuka[2]. Crystalline **59** was then subjected to chlorination using tetrachloromethane and isoamylnitrite for the exchange of the 6-amino group for a chlorine atom[3-5]. Deprotection with saturated methanolic ammonia solution and subsequent quantitative aminolysis with 1-naphthylmethylamine in 1-propanol yielded compound **62**. The reduction of the azido functionality represented the key step of this synthetic pathway. Generally, Pd-catalyzed hydrogenation is used to afford reduction of this type of modified nucleosides[2]. Nevertheless, considering the possible loss of the N^6-substituent, Pd-catalyzed hydrogenation was not suited for this purpose. Instead, the reagent couple indium/NH_4Cl was selected. Our group demonstrated that indium-mediated reduction of 2´-azido-2´-deoxy-N^6-(1-naphthylmethyl)adenosine led to practical quantitative conversion of the azido functionality without detectable loss of the N^6-substituent[5]. Thus, the reduction of the azido group of **62** employing indium/NH_4Cl in ethanol led to a smooth conversion of **62** to the desired novel template **63**. The course of reaction was monitored by IR (see chapter 3.4.1). Compounds **59**, **62**, and **63** were isolated and characterized by NMR, HPLC and MS.

Scheme 10. Synthetic sequence yielding 3′-amino-3′-deoxy-N^6-(1-naphthylmethyl)adenosine (**63**).

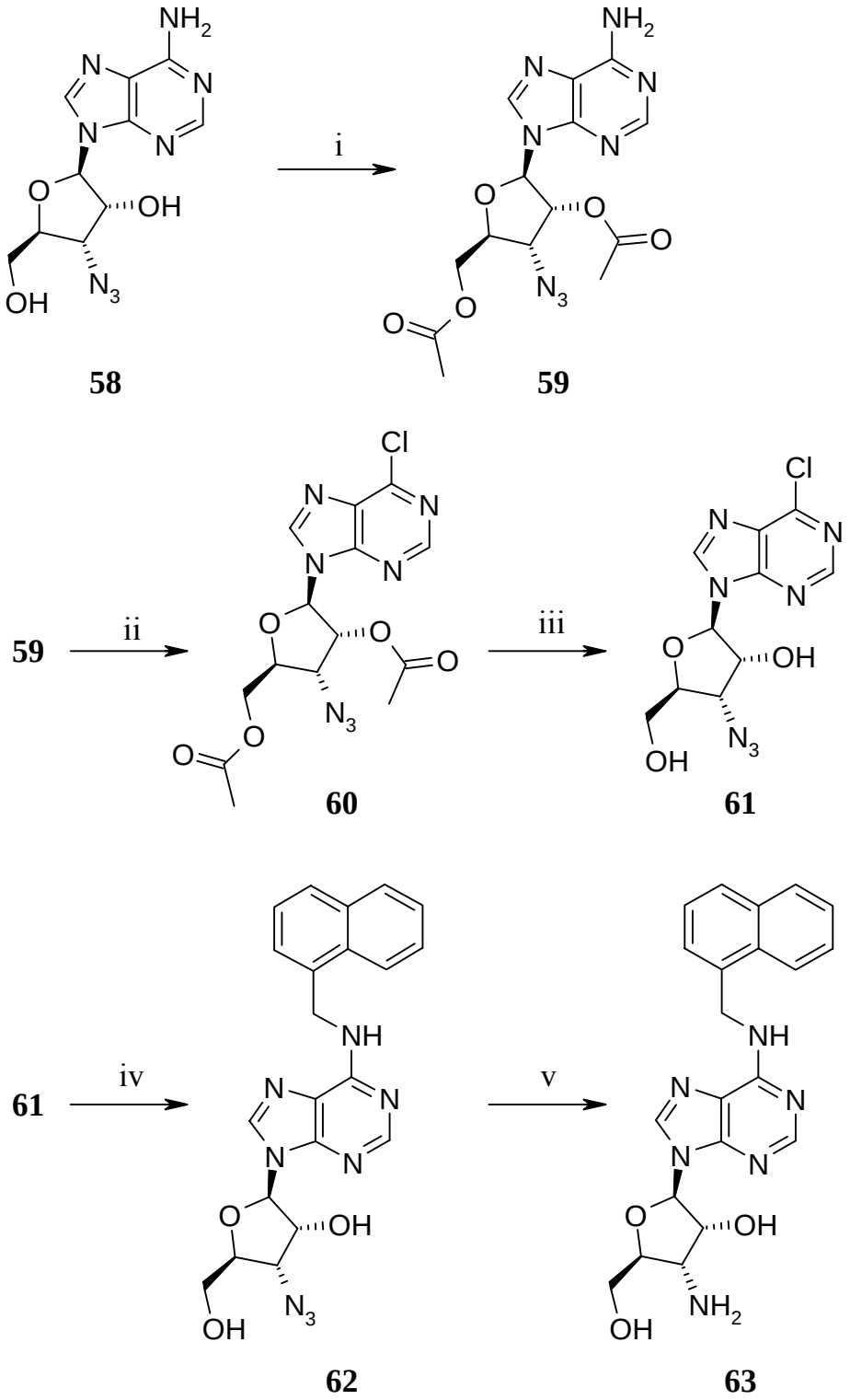

(i) Ac_2O, pyridine abs., ambient temperature, 1 h; (ii) CCl_4, isoamylnitrite, 60 °C, 24 h; (iii) methanolic ammonia (saturated), 0 °C, 1 h; (iv) 1-naphthylmethylamine, 1-propanol, DIPEA, 50 °C, 4 h; (v) indium/NH_4Cl, ethanol, reflux, 4 h.

Diversity fragments were introduced employing the PASP protocol (scheme 11).

Scheme 11. PASP synthesis furnishing 3′-amido-3′-deoxy-N^6-(1-naphthylmethyl)adenosines **65-68**.

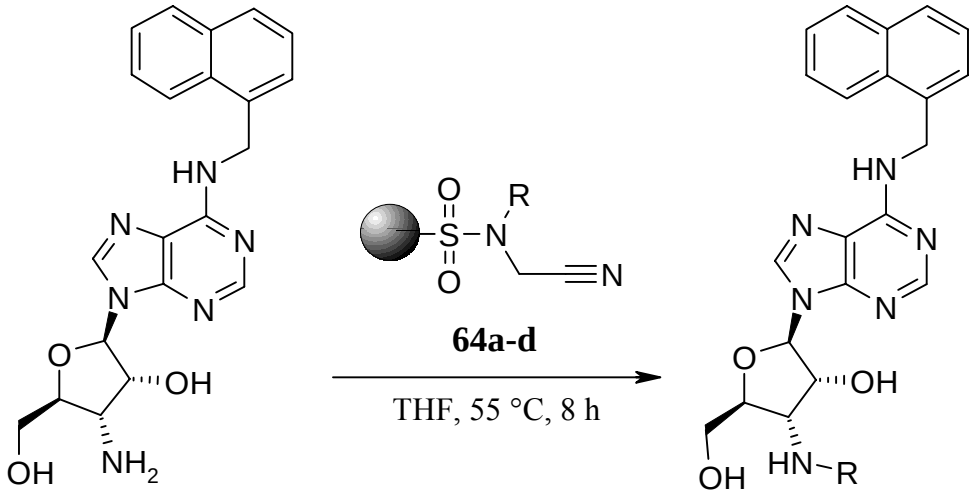

63 **65-68**

R

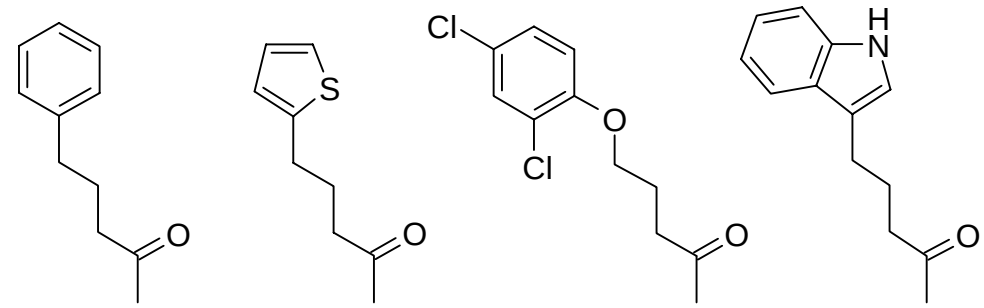

65 **66** **67** **68**

Commercially available carboxylic acid equivalents were attached via in situ anhydride formation to the Kenner safety-catch linker connected to aminomethylated polystyrene. Prior to the chemoselective transfer of the polymer-bound acid to the primary amino group of the nucleoside template **63**, the safety-catch linker had to be activated by N-alkylation to form a good leaving group. Appropriate activated polymer-bound carboxylic acid equivalents **64a-d** were subsequently converted to the corresponding 3′-

amido-3´-deoxy-N^6-(1-naphthylmethyl)adenosines **65-68** when agitating with a solution of the amino nucleoside **63** at slightly elevated temperatures. The reactions were terminated after TLC analysis indicated complete conversion of the amino nucleoside. As PASP synthesis generally leads to simple product isolation because the excess of polymer-bound reagent that is necessary to drive the reaction to completion can be removed by filtration, **65-68** were obtained in excellent to good yield (table 3).

Table 3. Yield and indication of sufficient purity of type III adenosines (**65-68**) originating from polymer-assisted synthesis.

Compound	Sufficient Purity (>80%) [A]	Conversion Rate [%] [A]	Yield [%] [A]
65	prior to MPLC	99	95
66	prior to MPLC	97	96
67	prior to MPLC	>99	95
68	after to MPLC [B]	76 [B]	70 [B]

[A] All compounds were purified by single semi-preparative medium pressure LC (MPLC) runs under standard conditions that were not optimized for each individual compound. Product containing fractions were collected and evaporated. The yield of pure compounds is reported above. Purity and conversion rate of compounds were estimated using the 100% method. Sufficient purity was classified according to the 80/80 Standard (see table 1, chapter 2.2). [B] Due to possible alteration of the polymer-bound building block during storage, purity, conversion rate, and yield are below the expected standard.

3.3 Biological Evaluation of 3´,N^6-Disubstituted Adenosines

Adenosine analogs **62** and **63** and type III adenosines **65-68** were evaluated for their inhibitory activity against intraerythrocytic forms of *P. falciparum* using a semi-automated microdilution assay as described[6-8]. The growth of the parasites was monitored through the incorporation of tritium-labeled hypoxanthine. The results obtained are summarized below (table 4).
For DOXP reductoisomerase inhibition studies compounds **62**, **63**, and **65-68** were analyzed. The conversion of DOXP to MEP by the recombinant enzyme was determined in an assay based on NADPH dependency of the reaction[9]. For results see table 4.

In addition, 26 N^6-monosubstituted adenosines (type IV adenosine derivatives) derived from previous studies were tested for DOXP

reductoisomerase inhibition. Briefly, these 26 type IV adenosine derivatives have either been prepared by simple amination of 6-(chloropurin-9-yl)-β-D-1-deoxyribofuranose in solution or by PASP synthesis of N^6-(2-aminoethyl)-adenosine and N^6-(3,6-dioxa-8-aminooctyl)adenosine, respectively[1]. Since N^6-monosubstituted adenosines displayed moderate antimalarial activity versus the *P. falciparum* pathogen DOXP reductoisomerase inhibition studies were regarded necessary to obtain further information on the structure-activity relationships of mono- or disubstituted adenosine derivatives of type I-IV (figure 11).

Figure 11. Adenosine derivatives of type I-IV.

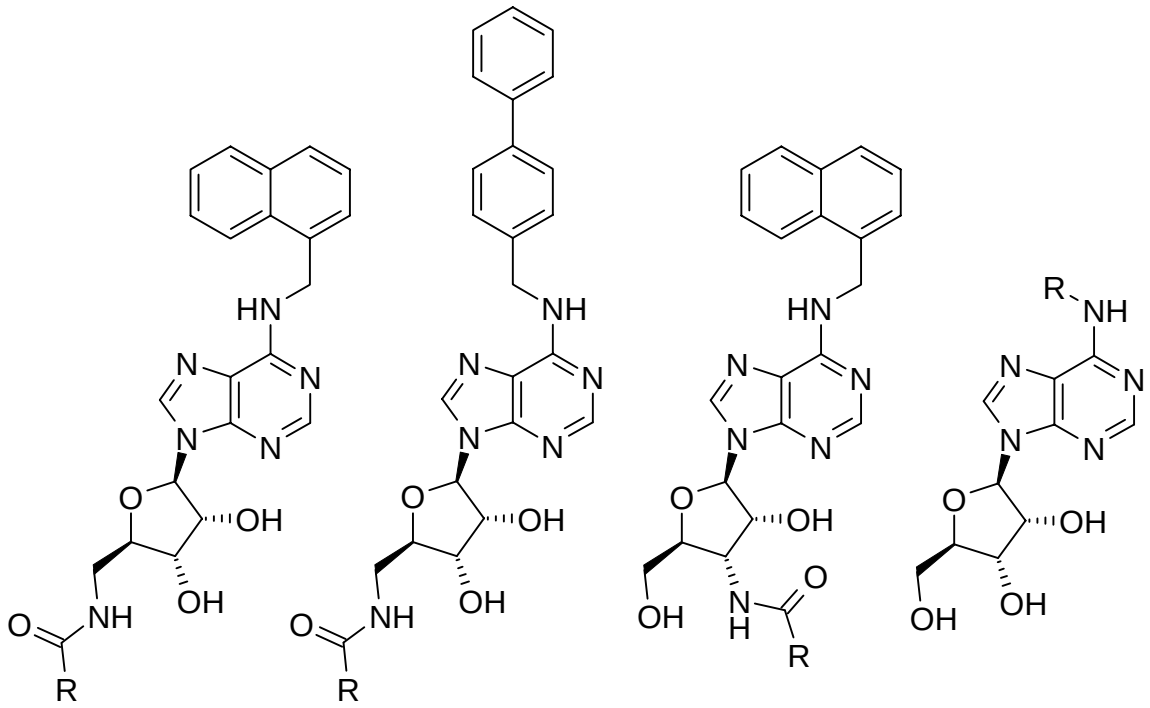

As none of the 26 type IV adenosine derivatives exhibited an inhibitory activity on DOXP reductoisomerase, only outcomes of type III adenosines are listed in table 4.

Table 4. Antimalarial activity of the lead structure **57** and of adenosine derivatives **62**, **63**, and **65-68**.

Compound	R Group in Main Scaffold	IC_{50} [µM] [A]	DOXP Reductoisomerase [%] [B]
57	---	3.2	0
62	---	12	0
63	---	11	0
3´-Amido-3´-deoxy-N^6-(1-naphthylmethyl)adenosine derivatives			
65	4-phenylbutanamido	17	38
66	4-(2-thienyl)butanamido	17	30
67	4-(2,4-dichlorophenyloxy)-butanamido	15	41
68	4-(3-indolyl)butanamido	2.8	75

[A] The *P. falciparum* strain Dd2 (Indochina) used in this study is resistant to most commonly used antimalarial drugs. When the resistance pattern was checked, the Dd2 strain was found to be highly resistant against chloroquine (IC_{50} = 170 nM), pyrimethamine (IC_{50} = 2500 nM), and cycloguanil (IC_{50} = 2200 nM); and moderately resistant against quinine (IC_{50} = 380 nM) and mefloquine (IC_{50} = 57 nM). It was sensitive to halofantrine (IC_{50} = 18 nM), lumefantrine (IC_{50} = 30 nM), artemisinin (IC_{50} = 18 nM), and atovaquone (IC_{50} = 1 nM). [B] DOXP reductoisomerase inhibition studies were performed under standard assay conditions at compound concentrations of 30 µM.

Exemplary, 3´-azido-3´-deoxy-N^6-(1-naphthylmethyl)adenosine (**62**) was investigated regarding to its antiviral activity against HIV-1(III_B) and HIV-2(ROD) as well as to its cytotoxicity in an MT-4/MTT based assay[10,11]. Compound **62** did not show antiviral activity. Further, **62** did not exhibit pronounced cytotoxicity against human T-lymphocytes (tested at compound concentrations of 150 µg/ml) with a CC_{50} value ≥ 87.7 µg/ml.

3.4 Analytical Characteristics of 3´,N^6-Disubstituted Adenosines

3.4.1 IR Analysis of 3´,N^6-Disubstituted Adenosines

Indium-mediated reduction of the azido functionality of 3´-azido-3´-deoxy-N^6-(1-naphthylmethyl)adenosine (**62**) yielding 3´-amino-3´-deoxy-N^6-(1-naphthylmethyl)adenosine (**63**) was monitored by IR (figure 12). In general,

azido groups display characteristic absorption at about 2100 cm^{-1}. The reaction was terminated when the peak at 2104 cm^{-1} completely disappeared.

Figure 12. Indium-mediated reduction of **62** followed by IR.

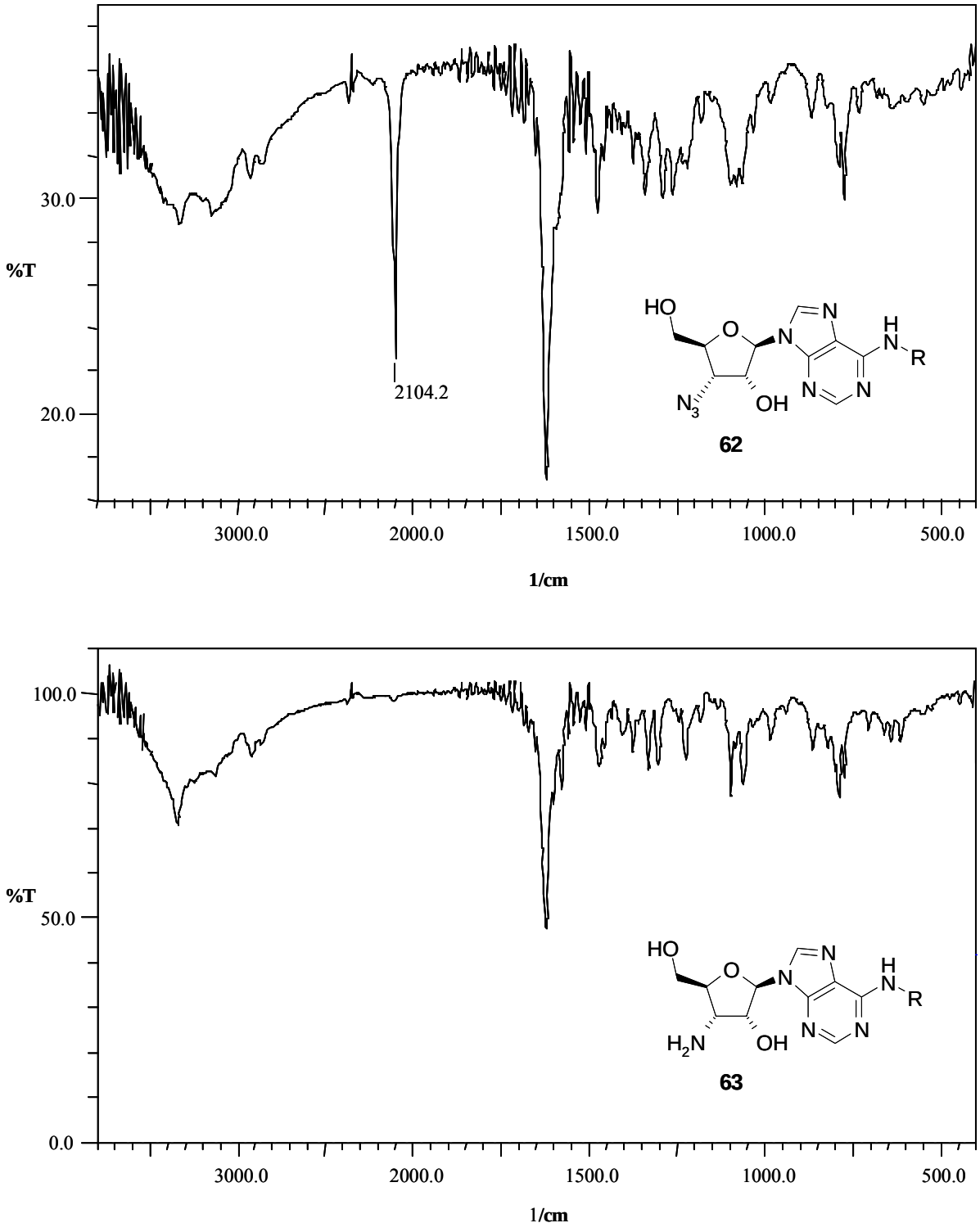

3.4.2 HPLC Analysis of 3′,N^6-Disubstituted Adenosines

In figure 13 an exemplary HPLC run (methanol/water (1/1, v/v), flow rate 1 mL/min) of **65** prior to final MPLC purification is shown. The diagram demonstrates the convenient assessment of modified adenosines in high purity employing the PASP methodology. The 80% purity criterion is met.

Figure 13. HPLC run prior to MPLC purification of **65** (peak quantitation = 92%; peak purity = 100%).

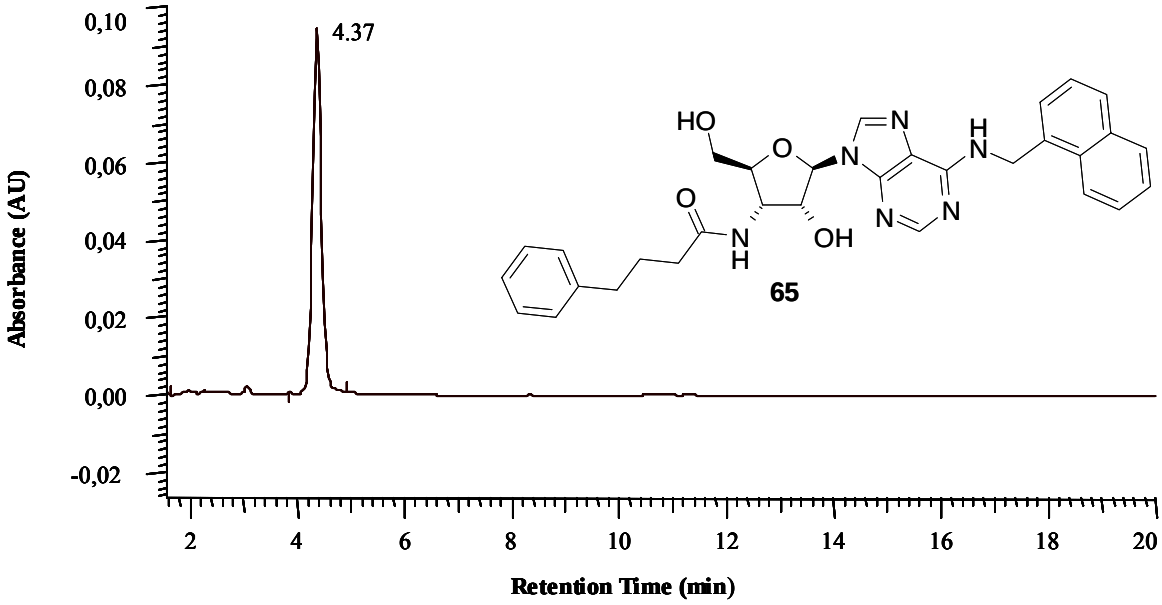

3.4.3 Electrospray Ionization (ESI)/Mass Spectrometry (MS) Analysis of Selected 3′,N^6-Disubstituted Adenosines

The nucleoside template **63** and 3′,N^6-disubstituted adenosine derivatives **65** and **66** were analyzed by ESI/MS^n to obtain structure-specific fragment ion information.

The fragmentation of **63** is shown in figure 14. Expected fragments 276, 141, and 115 along pathway A (see scheme 9, chapter 2.4.2) were obtained.

Figure 15 initially demonstrates the fragmentation of the parent ion 553 of compound **65**, yielding product ions 278 ($C_{15}H_{20}NO_4$, oxonium) and 276. The second spectra shows the fragmentation of 278 along pathway B with main daughter ion 147 ($C_{10}H_{11}O$, acylium) and small amounts of fragment 164 ($C_{10}H_{14}NO$, amidium). When fragmenting product ion 276 (spectra 3) expected fragments 141 and 115 (not shown) according to pathway A were observed.

Figure 14. Fragmentation pattern of **63** (MW 406.45; $[M+H]^+$ 407.1832).

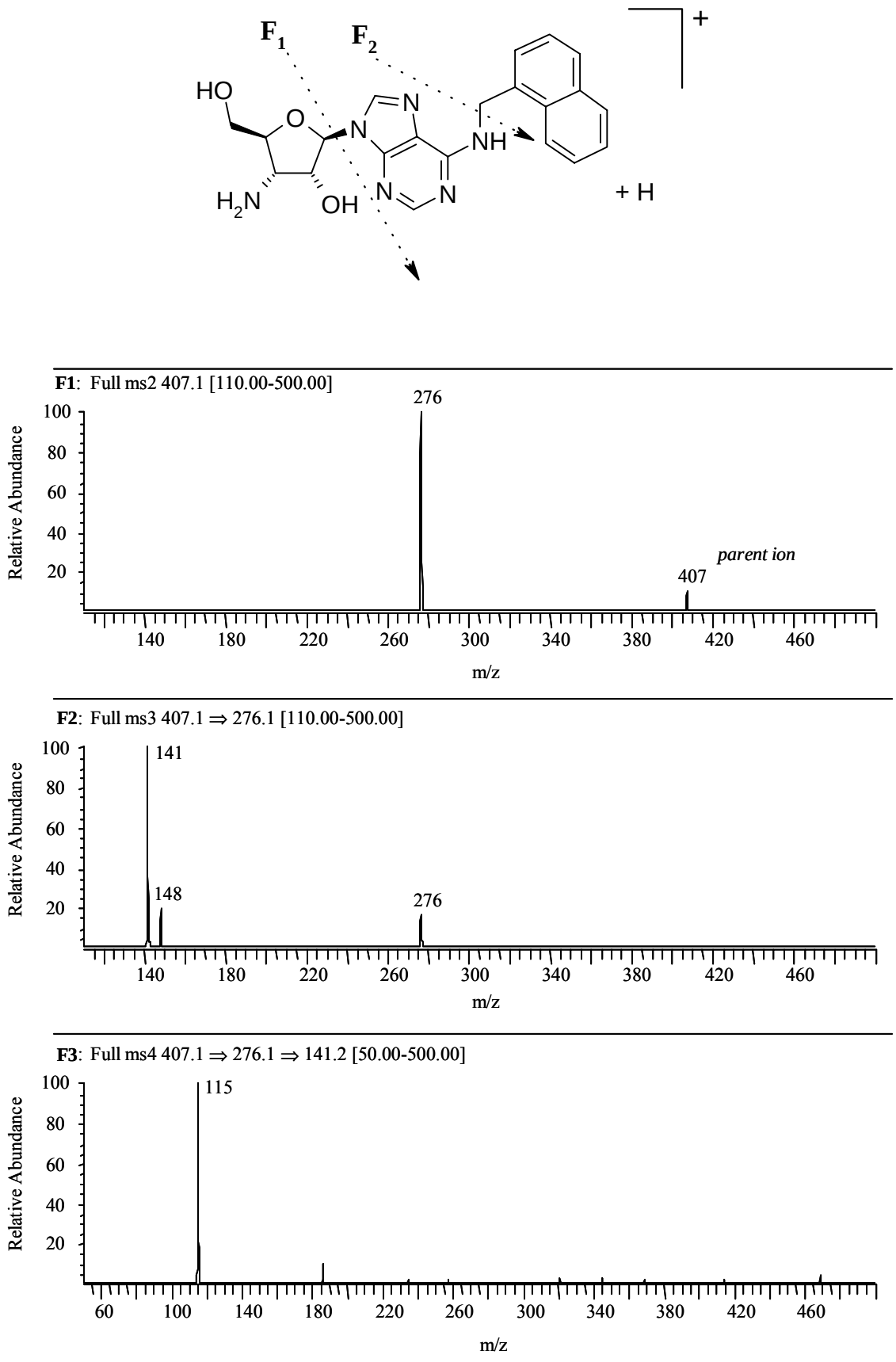

Figure 15. Fragmentation pattern of **65** (MW 552.64; $[M+H]^+$ 553.2564).

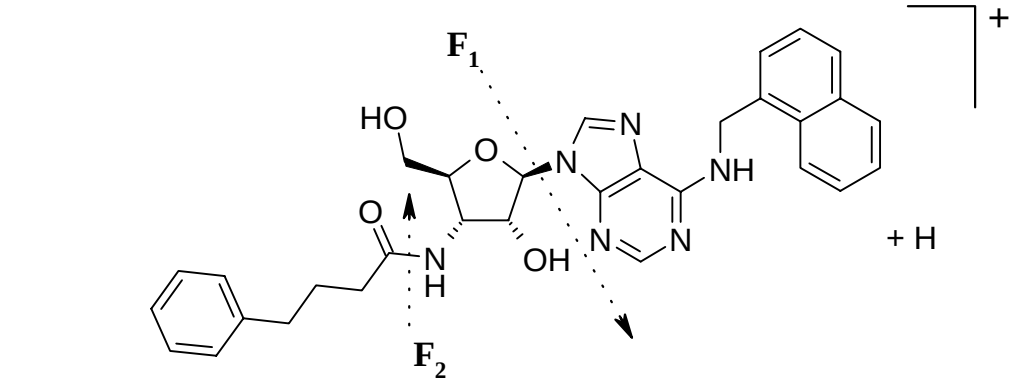

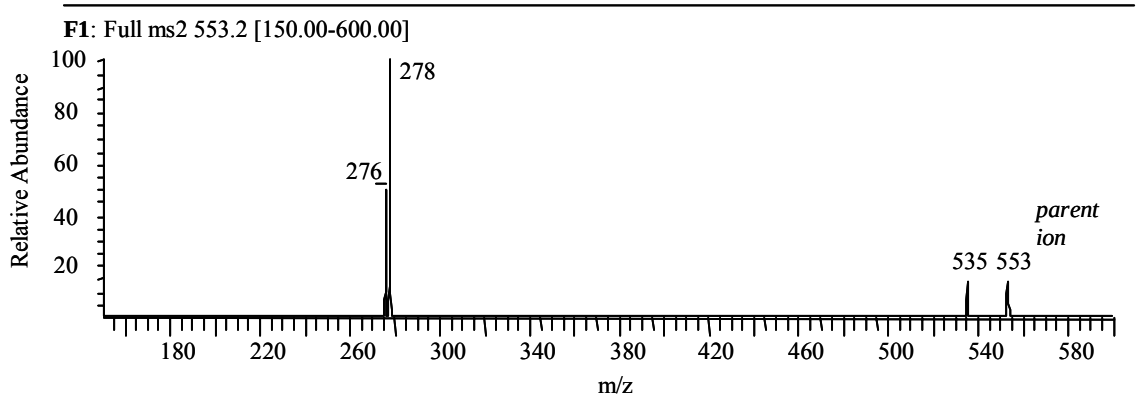

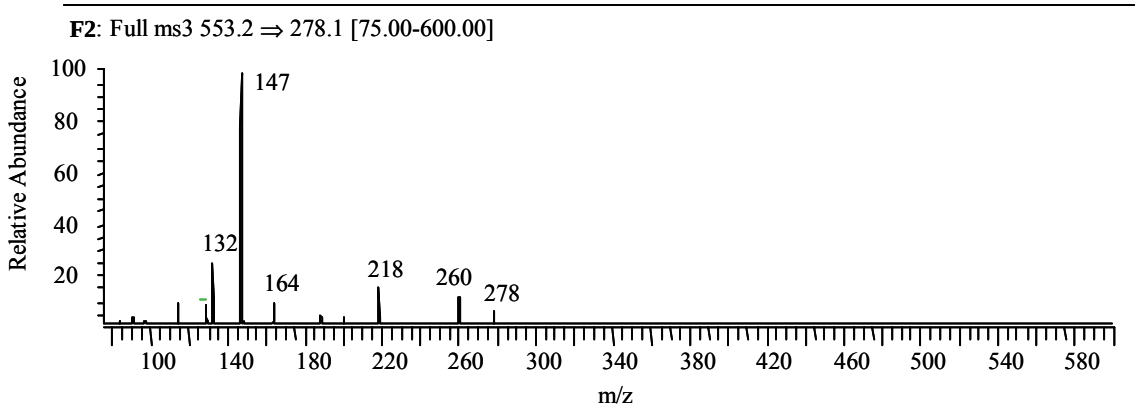

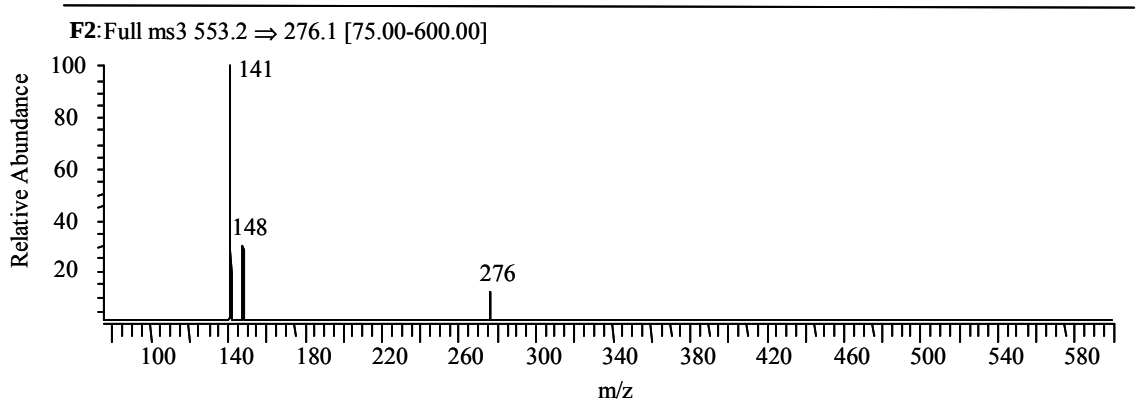

Figure 16. Fragmentation pattern of **66** (MW 558.66; $[M+H]^+$ 559.2128).

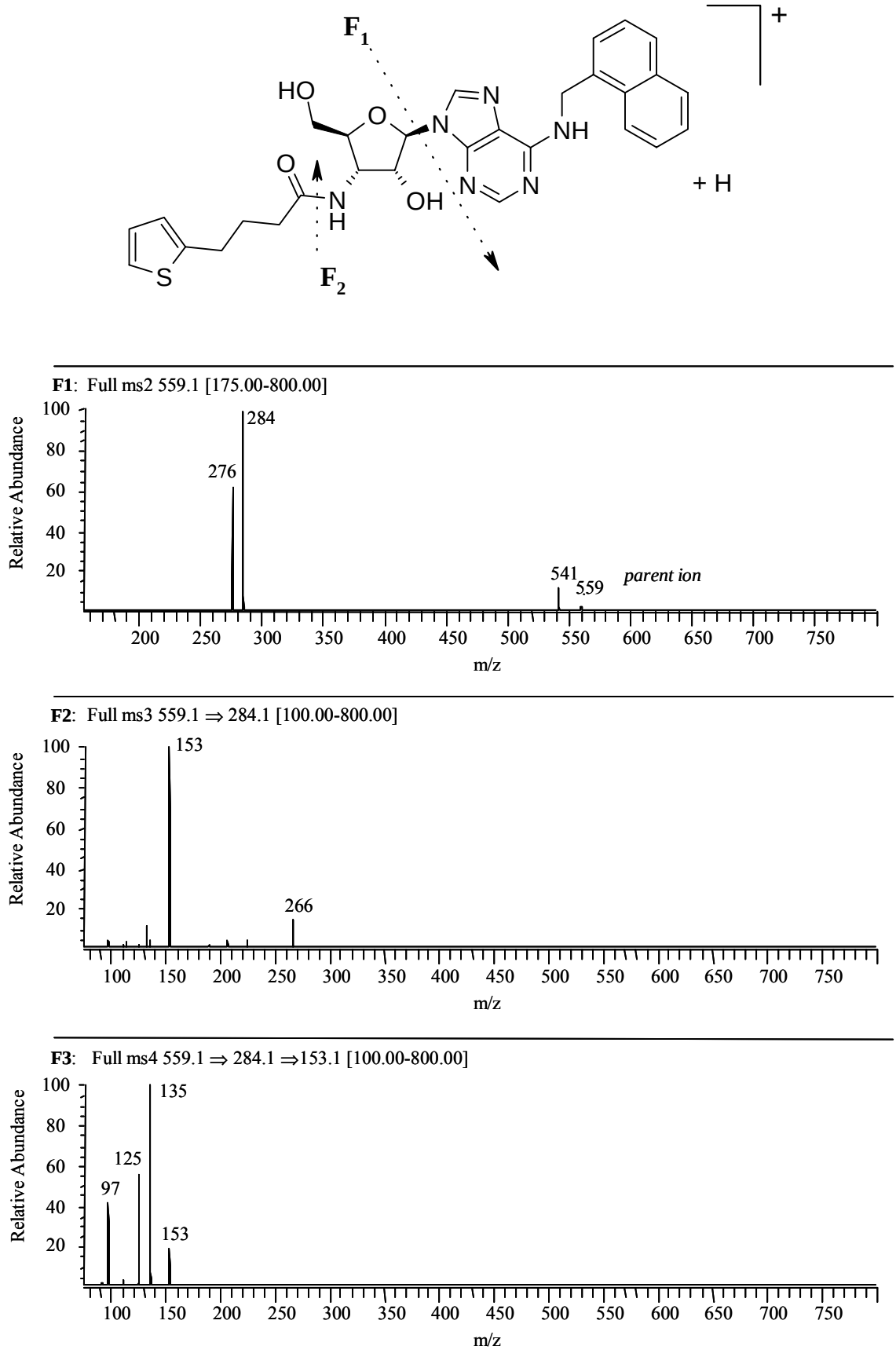

Figure 16 displays the fragmentation sequence of compound **66** along pathway B, providing expected oxonium (284, $C_{13}H_{18}NO_4S$) and acylium ions (153, C_8H_9OS). Again, typical differences of 18, 42, 17, and 28, corresponding to losses of water, acetate, ammonia, and carbon monoxide moieties, respectively, were observed. Daughter ion 276 fragmented as expected (not shown) providing fragments 141 and 115.

Comparing **63** (3′-amino replacement) (figure 14) with **2** (5′-amino replacement) (figure 5, chapter 2.4.2), no difference in the fragmentation patterns were found. Thus, it is impossible to distinguish these nucleoside scaffolds via MS^n analysis. On the contrary, when fragmenting 3′,N^6-disubstituted adenosines **65** and **66** (obtained via PASP synthesis, displaying a simple, non-modified diversity fragment in 3′-position) fragmentation primarily occurred along pathway B, whereas fragmentation of **23** (figure 6 and 7, chapter 2.4.2) mainly occurred along pathway A.
Interestingly, when fragmenting parent ions of 3′,N^6-disubstituted adenosines, additional elimination of one molecule of water was observed (553→535 and 559→541 for compounds **65** and **66**, respectively). This observed elimination during initial fragmentation is only found along 3′,N^6-disubstituted adenosines (not along 5′,N^6-disubstituted adenosines) and can thus be used for differentiating identical 3′,N^6- from 5′,N^6-disubstituted adenosine derivatives.

3.5 Discussion

Employing a PASP protocol developed by our group[12-14], a small series of 3′-amido-3′-deoxy-N^6-(1-naphthylmethyl)adenosines was prepared ready for biological testing. All compounds of this series displayed moderate antimalarial activity against the *P. falciparum* parasite with IC_{50} values in the low micromolar range. Nonetheless, more striking was the outcome that all 3′-amido-3′-deoxy-N^6-(1-naphthylmethyl)adenosines (**65**-**68**) showed an inhibitory effect on the DOXP reductoisomerase whereas the mono-substituted adenosine derivatives (**57**, **62**, and **63**) did not. Exemplarily investigated **62** did not exhibit pronounced cytotoxicity against T-lymphocytes.

Within the series of type III adenosines, promising diversity fragments established from previous structure-based surveys were introduced into the

aminonucleoside template. The observed activity on the Dd2 strain of *P. falciparum* is comparable to the activity of type I and type II adenosine derivatives. In general, the activity of disubstituted adenosine derivatives of type I-III is superior to the observed antimalarial effect along N^6-monosubstituted adenosines of type IV.

Considerable inhibitory activity against the DOXP reductoisomerase was observed with all 3′,N^6-disubstituted adenosines (**65**-**68**). On the contrary, 5′,N^6-disubstituted adenosine derivatives only showed an inhibitory effect in 13 out of 34 cases and N^6-monosubstituted adenosines displayed no inhibitory activity at all. Consequently, disubstitution in 3′- and N^6- or 5′- and N^6-position seems to be crucial for exhibiting activity against the DOXP reductoisomerase.

Compound **68** revealed equal to slightly increased activity against the whole parasite compared to the lead structure **57**. While **68** simultaneously displayed a good inhibitory effect on the DOXP reductoisomerase (75%), **57** had no effect. This outcome confirms the assumption that a disubstitution pattern of adenosines might be favorable for DOXP reductoisomerase inhibition.

DOXP reductoisomerase inhibition through 3′,N^6-disubstituted adenosine analogs tend to be superior compared to the appropriate 5′,N^6-disubstituted derivatives; e.g. **68** (75%) vs. **20** (45%) vs. **47** (48%); and **67** (41%) vs. **23** (0%). In addition, all 3′,N^6-disubstituted adenosines exhibited DOXP reductoisomerase inhibition whereas only 13 out of 34 5′,N^6-disubstituted analogs showed an inhibitory effect. Nevertheless, this observed tendency might be biased when comparing a small with a large series consisting of four and 34 disubstituted adenosine derivatives, respectively. Further investigations are planned to solidify the assumption made.

In summary, the novel series of 3′,N^6-disubstituted adenosines displayed antiplasmodial activity in the low micromolar range as well as DOXP reductoisomerase inhibition. Disubstitution in 3′- and N^6- or 5′- and N^6-position seems to be essential for the inhibitory activity on DOXP reductoisomerase, whereas the 3′,N^6-disubstitution is favorable compared to the 5′,N^6-disubstitution. The results described above again emphasize the suggestion made in chapter 2 that not only a single molecular target is recognized.

3.6 Experimental Section

The structures of all compounds were assigned by NMR spectroscopy. NMR spectra were recorded on a Bruker AMX 400 spectrometer, using tetramethylsilane as internal standard. ^{1}H NMR data are reported based on separated spin-spin signals and protons that were not covered by H_2O- or DMSO-signals, unless otherwise noted. Identity of compounds prepared in mg quantities was evaluated by high-resolution MS; purity was deduced by MPLC/HPLC and from ^{1}H NMR. MPLC purification was performed employing a Büchi 681 pump (flow rate 10 mL, methanol/water gradients) and UV detector (254 nm) with a Merck 310-25 Lobar-LiChroprep™-RP-18 (40-63 µm) column. HPLC was performed on a Merck Hitachi L-7000 series connected to a diode array detector (methanol/water gradients, flow rate 1 mL/min, UV absorption at 240 to 261 nm). High-resolution MS data were obtained on a Finnigan MAT 95 XL instrument (ESI, methanol/water (1/1, v/v) infusion at 2 µL/min with polypropylene glycol as reference), MS^n data on a Finnigan MAT 95 XL TRAP instrument (ESI, methanol/water (1/1, v/v) infusion at 2 µL/min). IR spectra were obtained on a Shimadzu FTIR-8300 instrument. Preparative column chromatography was performed on silica gel 100-200 active, 60 Å, from ICN or Dowex® OH^- (1×2-200) using glass columns (4.5×15 cm). TLC reaction control was performed on Macherey-Nagel Polygram® Sil G/UV_{254} precoated microplates; spots were visualized under UV-illumination at 254 nm.

2′,5′-Di-*O*-acetyl-3′-azido-3′-deoxyadenosine (**59**)

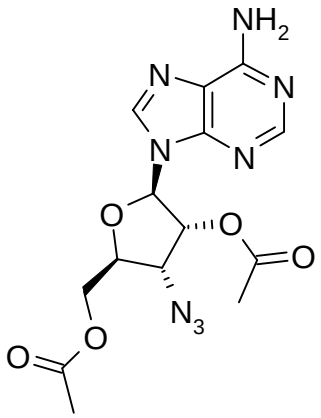

3′-Azido-3′-deoxyadenosine (**58**) (1.0 g, 3.4 mmol) was dissolved in absolute pyridine (12.5 mL). Ac_2O (6.4 mL, 68 mmol) was added and the reaction mixture incubated at room temperature for 1 h. The solvent was evaporated in vacuo. Traces of pyridine were removed by evaporation with toluol three times; traces of Ac_2O by evaporating with H_2O/EtOH (50/50, v/v) two times. The resulting residue was washed with ether yielding **59** as a white and amorphous solid.

Yield 61%

^{1}H NMR (400 MHz, DMSO-d_6) = δ (ppm) 8.32 (s, 1H, 8H), 8.17 (s, 1H, 2H), 7.36 (bs, 2H, NH_2), 6.18 (d, 1H, 1′H, *J*=3.6 Hz), 6.01-5.98 (m, 1H, 3′H), 4.90 (t, 1H, 2′H, *J*=6.5 Hz), 4.40-4.36 (m, 1H, 5′CH_2), 4.30-4.25 (m, 1H, 5′CH_2), 4.21-4.17 (m, 1H, 4′H), 2.14 (s, 3H, CH_3, acetyl), 1.98 (s, 3H, CH_3, acetyl)

^{13}C NMR (101 MHz, DMSO-d_6) = δ (ppm) 169.45, 168.81, 154.80, 151.90, 147.81, 139.05, 85.34, 78.23, 73.48, 61.39, 58.54, 19.37, 19.21

HRESI-MS $C_{14}H_{16}N_8O_5$
MW 376.33
$[M+H]^+$ calcd 377.1322
$[M+H]^+$ found 377.1318

3′-Azido-3′-deoxy-N^6-(1-naphthylmethyl)adenosine (**62**)

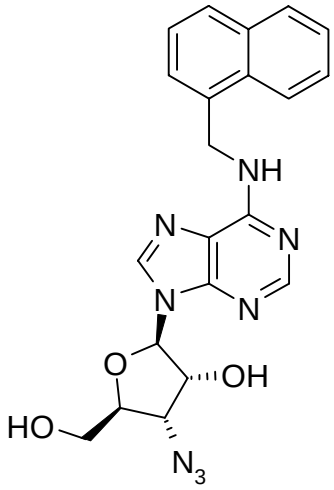

Isoamylnitrite (0.7 g, 6 mmol) was added to a solution of 2′, 5′-di-*O*-acteyl-3′-azido-3′-deoxyadenosine (**59**) (770 mg, 2 mmol) in CCl_4 (12 g, 78 mmol). The reaction mixture was stirred at room temperature for 12 h. As the conversion of **59** to **60** was incomplete, an additional equivalent of isoamylnitrite (230 mg, 2 mmol) was added to the reaction mixture, and again the mixture was stirred at room temperature for 4 h. The solution was evaporated yielding a viscous slurry of **60**. Without further purification, 2′,5′- di- *O*-acetyl- 3′-azido- 1-(6-chloropurin-9-yl)-β-D- 1′,3′-dideoxyribofuranose (**60**) was dissolved in methanolic ammonia (saturated, 0 ºC, 100 mL) and stirred for 1 h. The resulting red solution was then stored for 12 h at 4 ºC and subsequently evaporated in vacuo (20 mbar, 20 ºC) yielding **61**. Finally, 1-naphthylmethylamine (346 mg, 2.2 mmol) was added to a solution of 3-azido-1-(6-chloropurin-9-yl)-β-D-1,3-dideoxyribofuranose (**61**) in 1-propanol (25 mL). After stirring the reaction mixture at 50 ºC for half an hour DIPEA (0.17 mL, 1 mmol) was added. The resulting mixture was stirred at 50 ºC for 4 h and subsequently evaporated in vacuo. Purification by column chromatography with CH_2Cl_2/MeOH gradients as eluent gave **62** as a white solid.

Yield 27% (three-step synthesis starting from **60)**

^{1}H NMR (400 MHz, DMSO-d_6) = δ (ppm) 8.52 (bs, 1H, N^6H), 8.40 (bs, 1H, 8H), 8.24-8.23 (m, 2H, 2H overlapping naphthyl), 7.96-7.94 (m, 1H, naphthyl), 7.83-7.80 (m, 1H, naphthyl), 7.59-7.52 (m, 2H, naphthyl), 7.44-7.41 (m, 2H, naphthyl), 6.22 (d, 1H,

OH, *J*=5.3 Hz), 5.93 (d, 1H, 1´H, *J*=6.1 Hz), 5.54-5.52 (m, 1H, OH), 5.19 (bs, 2H, CH_2, naphthylmethyl), 5.04-5.01 (m, 1H, 2´H), 4.32 (t, 1H, 3´H, *J*=4.1 Hz), 4.00-3.99 (m, 2H, 4´H), 3.71-3.68 (m, 1H, 5´CH_2), 3.61-3.55 (m, 1H, 5´CH_2)

^{13}C NMR (101 MHz, DMSO-d_6) = δ (ppm) 152.35, 139.88, 133.16, 130.70, 128.41, 127.07, 126.03, 125.62, 125.31, 124.48, 123.25, 87.66, 82.77, 73.77, 61.96, 61.44, 40.92, 39.20

HRESI-MS $C_{21}H_{20}N_8O_3$
MW 432.45
$[M+H]^+$ calcd 433.1737
$[M+H]^+$ found 433.1721

Activity Dd2 strain of *P. falciparum*: IC_{50} = 12 µM
DOXP reductoisomerase: 0%

3´-Amino-3´-deoxy-N^6-(1-naphthylmethyl)adenosine (**63**)

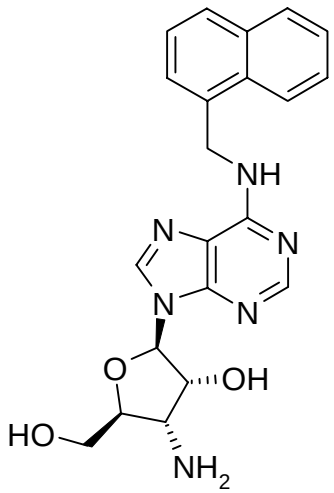

A solution of **62** (225 mg, 0.51 mmol), indium (59 mg, 0.51 mmol) and NH_4Cl (29 mg, 0.56 mmol) in EtOH (10 mL) was refluxed. The reaction was monitored by TLC (EtOAc) and IR. Quantitative conversion was observed after 4 h. Evaporation of the solvent and purification over Dowex® OH^- with MeOH/H_2O gradients yielded **63** as a white, amorphous solid.

Yield 62%

^{1}H NMR (400 MHz, DMSO-d_6) = δ (ppm) 8.42 (bs, 2H, N^6H overlapping 8H), 8.25-8.22 (m, 2H, naphthyl overlapping 2H), 7.96-7.93 (m, 1H, naphthyl), 7.82-7.80 (m, 1H, naphthyl), 7.59-7.52 (m, 2H, naphthyl), 7.47-7.41 (m, 2H, naphthyl), 5.95 (d, 1H, 1´H, *J*=2.8 Hz), 5.77 (bs, 1H, OH), 5.19 (bs, 3H, CH_2 naphthylmethyl overlapping OH), 4.32 (bs, 1H, 2´H), 4.10-4.09 (m, 1H, 3´H), 3.75-3.74 (m, 2H), 3.50-3.48 (m, 1H), 1.64 (bs, 2H, NH_2)

^{13}C NMR (101 MHz, DMSO-d_6) = δ (ppm) 152.30, 139.24, 133.17, 130.72, 128.40, 127.05, 126.03, 125.61, 125.31, 124.57, 123.27, 89.07, 85.50, 74.67, 60.94, 59.17, 57.09, 52.49, 48.49

HRESI-MS $C_{21}H_{22}N_6O_3$ $[M+H]^+$ calcd 407.1832
MW 406.45 $[M+H]^+$ found 407.1841

Activity Dd2 strain of *P. falciparum*: IC_{50} = 11 µM
DOXP reductoisomerase: 0%

For the synthesis and subsequent activation of simple polymer-supported acids, see **general procedure A** and **general procedure C** (chapter 2.6). Final compounds **65-68** were obtained utilizing **general procedure D** (chapter 2.6) with the following deviations (see general procedure D_1).

General procedure D_1 for the synthesis of compounds 65-68: Activated polymer-supported acids **64a-d** were transferred to the amino group of 10 µmol of **63** dissolved in 1 mL NMP, by shaking at 55 °C in 4 mL THF. Polymer beads and particulates were removed by filtration; the beads where extracted exhaustively with dry THF and MeOH and the combined THF fractions were evaporated to furnish the target compounds. To remove residual NMP, water (10-20 mL) was added to appropriate **65-68**, each, and subsequently evaporated in vacuo (20 mbar, 60 ºC). This process was repeated four times. Finally, **65-68** were purified by a single semi-preparative MPLC run under standard conditions. Purity prior to MPLC was estimated using the 100% method, UV detection at 254 nm. All final compounds were obtained as white, amorphous solids.

3′-Deoxy-N^6-(1-naphthylmethyl)-3′-(4-phenylbutanamido)adenosine (**65**)

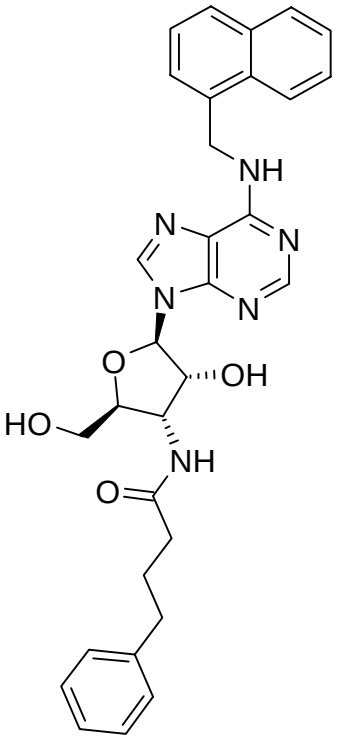

Yield 95%

^{1}H NMR (400 MHz, DMSO-d_6) = δ (ppm) 8.45 (bs, 2H, N^6H overlapping 8H), 8.25-8.23 (m, 2H, naphthyl overlapping 2H), 7.96-7.92 (m, 2H, naphthyl overlapping amide), 7.82-7.80 (m, 1H, naphthyl), 7.59-7.52 (m, 2H, naphthyl), 7.47-7.41 (m, 2H, naphthyl), 7.30-7.26 (m, 2H, phenyl), 7.20-7.17 (m, 3H, phenyl), 5.98-5.95 (m, 2H, 1′H overlapping OH), 5.19-5.17 (m, 3H, CH_2 naphthylmethyl overlapping OH), 4.50-4.48 (m, 2H, 2′H overlapping 3′H), 4.02-3.99 (m, 1H, 4′H), 3.73-3.64 (m, 1H, 5′CH_2), 3.56-3.50 (m, 1H, 5′CH_2), 2.58 (t, 2H, CH_2, butyryl, *J*=7.7 Hz), 2.19 (t, 2H, CH_2, butyryl, *J*=7.2 Hz), 1.84-1.79 (m, 2H, CH_2, butyryl)

HRESI-MS $C_{31}H_{32}N_6O_4$
MW 552.64
$[M+H]^+$ calcd 553.2563
$[M+H]^+$ found 553.2574

Activity Dd2 strain of *P. falciparum*: IC_{50} = 17 μM
DOXP reductoisomerase: 38%

3′-Deoxy-3′-N^6-(1-naphthylmethyl)-4-[(2-thienyl)butanamido]adenosine (**66**)

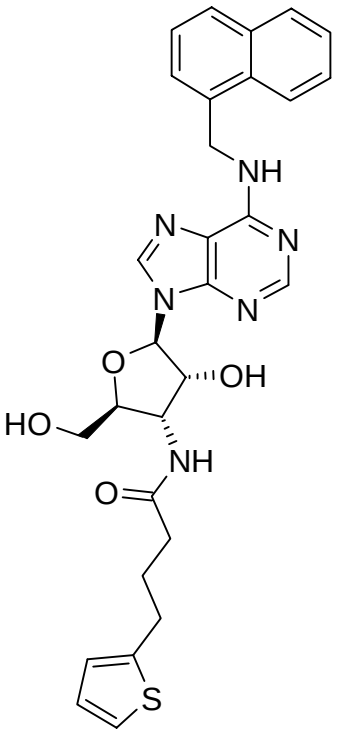

Yield 96%

^{1}H NMR (400 MHz, DMSO-d_6) = δ (ppm) 8.44 (bs, 2H, N^6H overlapping 8H), 8.25-8.23 (m, 2H, naphthyl overlapping 2H), 7.97-7.93 (m, 2H, naphthyl overlapping amide), 7.82-7.80 (m, 1H, naphthyl), 7.59-7.52 (m, 2H, naphthyl), 7.47-7.41 (m, 2H, naphthyl), 7.31-7.30 (m, 1H, thienyl), 6.95-6.93 (m, 1H, thienyl), 6.85-6.84 (m, 1H, thienyl), 5.98-5.97 (m, 2H, 1′H overlapping OH), 5.21-5.17 (m, 3H, CH_2 naphthylmethyl overlapping OH), 4.50-4.47 (m, 2H, 2′H overlapping 3′H), 4.03-3.99 (m, 1H, 4′H), 3.73-3.68 (m, 1H, 5′CH_2), 3.57-3.49 (m, 1H, 5′CH_2), 2.80 (t, 2H, CH_2, butyryl, *J*=7.5 Hz), 2.69 (t, 2H, CH_2, butyryl, *J*=7.5 Hz), 1.88-1.81 (m, 2H, CH_2, butyryl)

HRESI-MS $C_{29}H_{30}N_6O_4S$
MW 558.66
$[M+H]^+$ calcd 559.2127
$[M+H]^+$ found 559.2129

Activity Dd2 strain of *P. falciparum*: IC_{50} = 17 μM
DOXP reductoisomerase: 30%

3′-[4-(2,4-Dichlorophenyloxy)butanamido]-3′-deoxy-N^6-(1-naphthyl-methyl)adenosine (**67**)

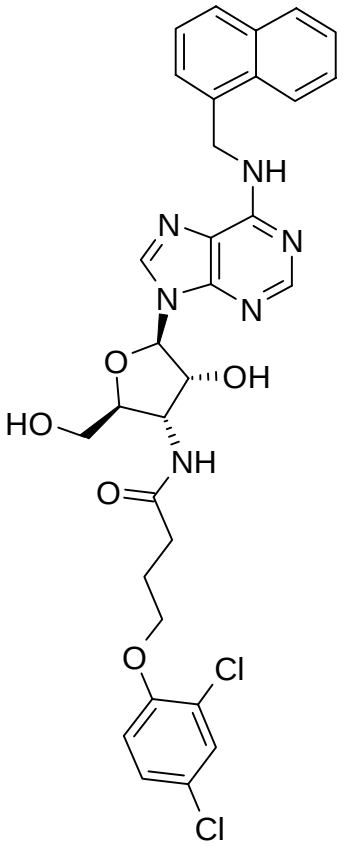

Yield 95%

^{1}H NMR (400 MHz, DMSO-d_6) = δ (ppm) 8.45 (bs, 2H, N^6H overlapping 8H), 8.25-8.23 (m, 2H, naphthyl overlapping 2H), 8.04 (d, 1H, NH, amide, *J*=7.1 Hz), 7.96-7.94 (m, 1H, naphthyl), 7.82-7.80 (m, 1H, naphthyl), 7.59-7.52 (m, 3H, 2H naphthyl overlapping 1H phenyloxy), 7.47-7.41 (m, 2H, naphthyl), 7.37-7.34 (dd, 1H, phenyloxy, *J*=2,5 Hz, 8,9 Hz), 7.17 (d, 1H, phenyloxy, *J*=9.2 Hz), 5.98 (bs, 2H, 1′H overlapping OH), 5.21-5.18 (m, 3H, CH_2 naphthylmethyl overlapping OH), 4.51-4.49 (m, 2H, 2′H overlapping 3′H), 4.08 (t, 2H, CH_2, butyryl, *J*=6.4 Hz), 4.03-4.02 (m, 1H, 4′H), 3.73-3.69 (m, 1H, 5′CH_2), 3.56-3.51 (m, 1H, 5′CH_2), 2.37 (t, 2H, CH_2, butyryl, *J*=7.4 Hz), 2.01-1.94 (m, 2H, CH_2, butyryl)

HRESI-MS $C_{31}H_{30}Cl_2N_6O_5$ $[M+H]^+$ calcd 637.1734
MW 637.53 $[M+H]^+$ found 637.1749

Activity Dd2 strain of *P. falciparum*: IC_{50} = 15 µM
DOXP reductoisomerase: 41%

3′-Deoxy-3′-[4-(3-indolyl)butanamido]-N^6-(1-naphthylmethyl)adenosine (**68**)

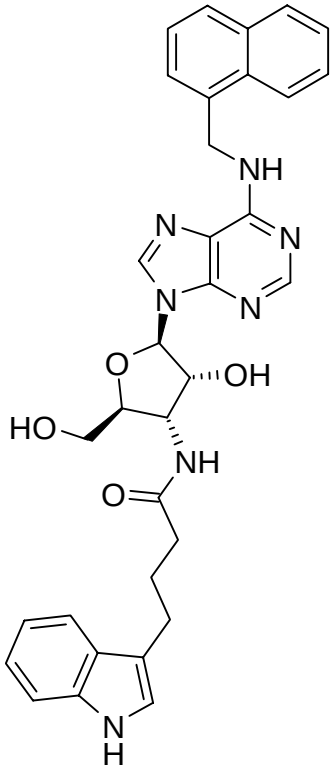

Yield 70%

^{1}H NMR (400 MHz, DMSO-d_6) = δ (ppm) 10.74 (bs, 1H, NH, indolyl), 8.45 (bs, 2H, N^6H overlapping 8H), 8.25-8.23 (m, 2H, naphthyl overlapping 2H), 7.96-7.90 (m, 2H, naphthyl overlapping amide), 7.82-7.80 (m, 1H, naphthyl), 7.59-7.42 (m, 5H, 4H naphthyl overlapping 1H indolyl), 7.33 (d, 1H, indolyl, *J*=7.6 Hz), 7.10 (bs, 1H, indolyl), 7.07-7.03 (m, 1H, indolyl), 6.99-6.94 (m, 1H, indolyl), 5.98-5.94 (m, 2H, 1′H overlapping OH), 5.18 (bs, 3H, CH_2 naphthylmethyl overlapping OH), 4.50 (bs, 2H, 2′H overlapping 3′H), 4.03-4.00 (m, 1H, 4′H), 3.74-3.69 (m, 1H, 5′CH_2), 3.56-3.51 (m, 1H, 5′CH_2), 2.69 (t, 2H, CH_2, butyryl, *J*=7.6 Hz), 2.28-2.22 (m, 2H, CH_2, butyryl), 1.92-1.86 (m, 2H, CH_2, butyryl)

HRESI-MS $C_{33}H_{33}N_7O_4$
MW 591.68
$[M+H]^+$ calcd 592.2672
$[M+H]^+$ found 592.2670

Activity Dd2 strain of *P. falciparum*: IC_{50} = 2.8 μM
DOXP reductoisomerase: 75%

For in vitro measurement of *P. falciparum* growth inhibition, in vitro measurement of DOXP reductoisomerase inhibition, in vitro measurement of HIV-1(III_B) and HIV-(ROD) inhibition and in vitro cytotoxicity measurement of selected disubstituted adenosine derivatives see chapter 2.6.

3.7 References

(1) Golisade, A.; Wiesner, J.; Herforth, C.; Jomaa, H.; Link, A. *Bioorg. Med. Chem.* **2002**, *10*, 769-777.

(2) Ikehara, M.; Takatsuka, Y. *Chem. Pharm. Bull.* **1978**, *26*, 985-988.

(3) Ha, S. B.; Nair, V. *Tetrahedron Lett.* **1996**, *37*, 1567-1570.

(4) Morr, M.; Heeg, E. *Liebigs Ann. Chem.* **1983**, 575-584.

(5) Golisade, A.; Van Calenbergh, S.; Link, A. *Tetrahedron* **2000**, *56*, 3167-3172.

(6) Ancelin, M. L.; Calas, M.; Bompart, J.; Cordina, G.; Martin, D.; Ben Bari, M.; Jei, T.; Druilhe, P.; Vial, H. J. *Blood* **1998**, *91*, 1426-1437.

(7) Desjardins, R. E.; Canfield, C. J.; Haynes, J. D.; Chulay, J. D. *Antimicrob. Agents Chemother.* **1979**, *16*, 710-718.

(8) Trager, W.; Jensen, J. B. *Science* **1976**, *193*, 673-675.

(9) Jomaa, H.; Wiesner, J.; Sanderbrand, S.; Altincicek, B.; Weidemeyer, C.; Hintz, M.; Turbachova, I.; Eberl, M.; Zeidler, J.; Lichtenthaler, H. K.; Soldati, D.; Beck, E. *Science* **1999**, *285*, 1573-1576.

(10) Balzarini, J.; Karlsson, A.; Perez-Perez, M.-J.; Camarasa, M.-J.; De Clercq, E. *Virology* **1993**, *196*, 576-585.

(11) Pauwels, R.; Balzarini, J.; Baba, M.; Snoeck, R.; Schols, D.; Herdewijn, P.; De Clercq, E. *J. Virol. Methods* **1988**, *20*, 309-321.

(12) Herforth, C.; Wiesner, J.; Franke, S.; Golisade, A.; Jomaa, H.; Link, A. *J. Comb. Chem.* **2002**, *4*, 302-314.

(13) Golisade, A.; Bressi, J. C.; Van Calenbergh, S.; Gelb, M. H.; Link, A. *J. Comb. Chem.* **2000**, *2*, 537-544.

(14) Golisade, A.; Herforth, C.; Quirijnen, L.; Maes, L.; Link, A. *Bioorg. Med. Chem.* **2002**, *10*, 159-165.

4 Biotin Labeling of Amino-Modified Adenosine Derivatives by PASP/cPASP Protocols

4.1 Introduction

The avidin-biotin and streptavidin-biotin complex has become a very useful and extremely versatile general mediator in a wide range of bioanalytical applications[1]. Biotin coupled to low- or high-molecular-weight molecules can still be recognized by the glycoproteins avidin and streptavidin, respectively, with dissociation constants of the high affinity complex formed in the pico- to femtomolar range. The bicyclic hexahydro-2-oxo-1*H*-thieno[4,3-*d*]imidazol ring system and the valeric acid side chain of the biotin molecule is essential for the specific recognition by these glycoproteins, whereas modification of the carboxyl group of the valeric acid group can be used for the design of biotinyl derivatives with retained molecular recognition capability.
Recently, the use of the avidin-biotin and streptavidin-biotin complex has been extended to a novel application for drug development using biosensors, based on the principles of SPR[2-5].

4.1.1 General Principle of Surface Plasmon Resonance (SPR) Detection

Biosensors (e.g. Biacore) selectively detect molecules based on an interaction between a sensor chip surface-immobilized receptor and a solution-borne analyte. Interactions are monitored using a non-invasive optical detection principle based on SPR[6-8].
In general, SPR measures changes in the refractive index close to the sensor chip surface. When samples of interest are presented to the biosensor, binding of the target analyte to its immobilized partner occurs. Binding at the chip surface where polarized light is focused causes a change in the refractive index that is monitored via a photoelectrical signal, the SPR wave. Since the SPR response is proportional to the surface concentration of the analyte, a change in the refractive index enables to monitor and quantitate the amount of analyte bound.
For this type of intermolecular interaction studies, various modified dextran covered gold surface chips are commercially available. Streptavidin modified chips bring about a much tighter immobilization than chips that permit attachment of analytes via nickel histidine chelates. Other chip

surface functionalities like carboxylic acid groups are designed for the covalent immobilization of analytes after in situ activation. In addition, amine- or hydrazine-activated surfaces and immobilization via thiol/ disulfide exchange or aldehyde have been reported[9,10]. However, in these cases, multi-functional molecules can only be attached in a statistic distribution resulting from the simultaneous reaction of all possible reactive sites to a varying degree. This might be tolerable in the cases of macro-molecules where a truly statistic distribution of attachment patterns is achieved, but not for the immobilization of small molecules where attachment via unintended functionalities leads to the display of a totally different binding epitope[10].

In contrast, the streptavdin-biotin complexation in which biotin is used to anchor biological ligands determines the mode of immobilization specifically and reproducibly. Thus, biotin labeling of small molecule drug candidates represents a useful tool for the study of molecular interactions, with biological target molecules by SPR ligand-fishing experiments where a reproducible high affinity attachment is required. The display of the putative binding epitope can be predicted and functional groups required for binding events remain unchanged.

For all applications employing biotinylated compounds in SPR-assays, residual biotin originating from the use of excess reagent during covalent attachment to the substrate must be removed efficiently after the biotinylation process to avoid blocking of streptavidin sites on the sensor chip surface. Furthermore, derivatives with long spacer arms (a minimum of six carbon atoms) are recommended to minimize sterical hindrance and facilitate streptavidin binding[11]. To control the exact biotinylation site in multi-functional substrates, regio- and chemoselective labeling is crucial. Although a wide range of biotinylation reagents is available commercially, none of them accomplishes these requirements needed for a biosensor assay[12,13].

In the following, a simple and efficient polymer-assisted method is presented to chemoselectively label multi-functional amines with a custom tailored biotin label, to be utilized for SPR experiments using a Biacore system in particular or for any other bioanalytical application needed.

4.2 Synthesis and Transfer of Polymer-Bound Biotin Labels

The polymer-assisted protocol for the N-selective acylation of amino-modified adenosines demonstrated in chapter 2 and 3 seemed to be ideally

suited for the synthesis of various polymer-bound biotinylation reagents to covalently label multi-functional amines with biotin.
Initially, a polymer-bound, chemoselective biotinylation reagent applying the Kenner safety-catch linker was prepared. Biotin was coupled to the sulfamoyl group of the linker attached to aminomethylated polystyrene, activated with bromoacetonitrile and in the following chemoselectively transferred to the amino function of target compounds **2**, **69**, and **70** providing **72-74** in excellent yield and purity (scheme 12 and table 5)[14].

Scheme 12. PASP synthesis of biotinylated compounds **72-74**.

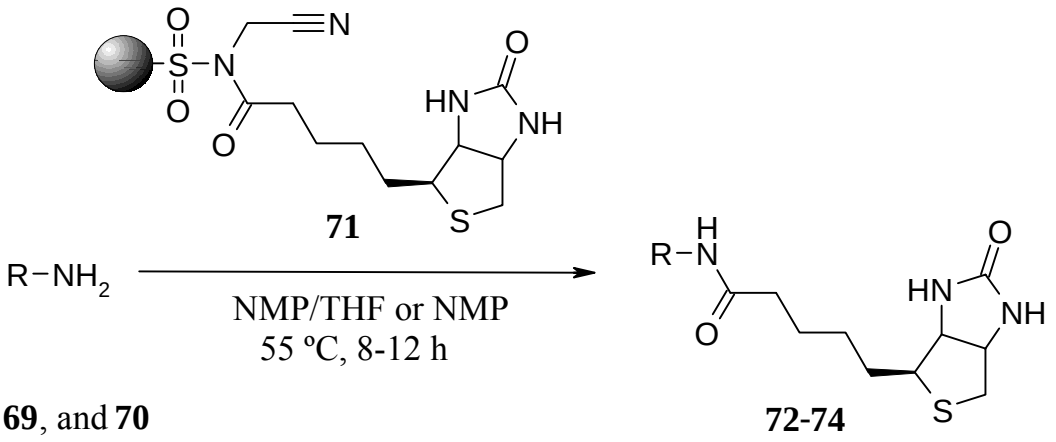

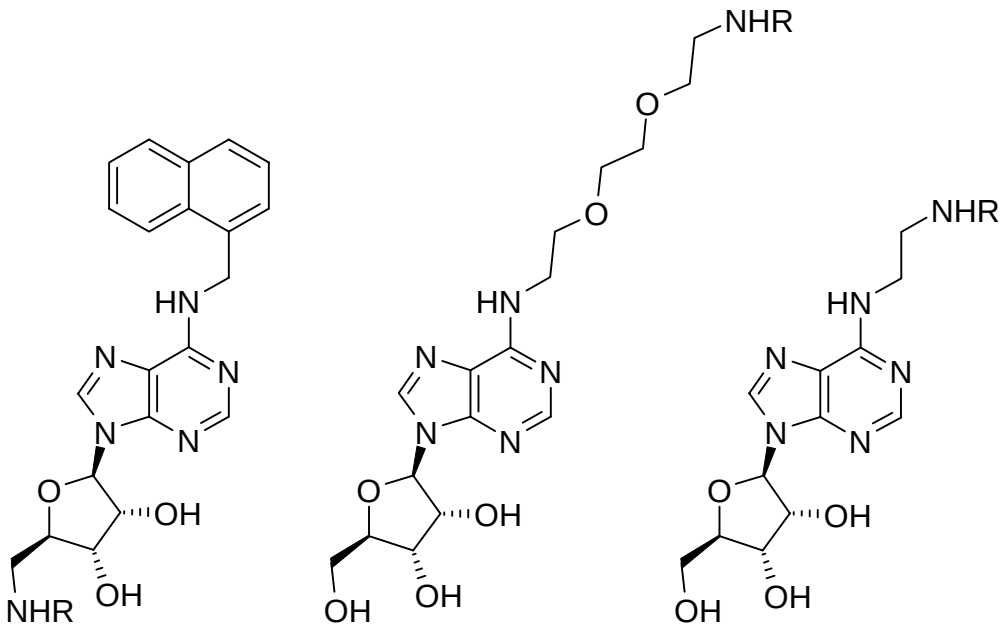

2 (R=H) **69** (R=H) **70** (R=H)
72 (R=biotinyl) **73** (R=biotinyl) **74** (R=biotinyl)

Besides the advantage of chemoselective acylation, the Kenner safety-catch linker is also suited for on-bead modifications of attached building blocks permitting for the incorporation of spacer atoms between the biotin moiety and the compound to be labeled. Thus, various amino acid residues between the biotin and amine moiety of compounds **2**, **69**, and **70** were introduced (scheme 13).

Scheme 13. PASP synthesis of spacer-modified biotinylated compounds **2**, **69**, and **70**.

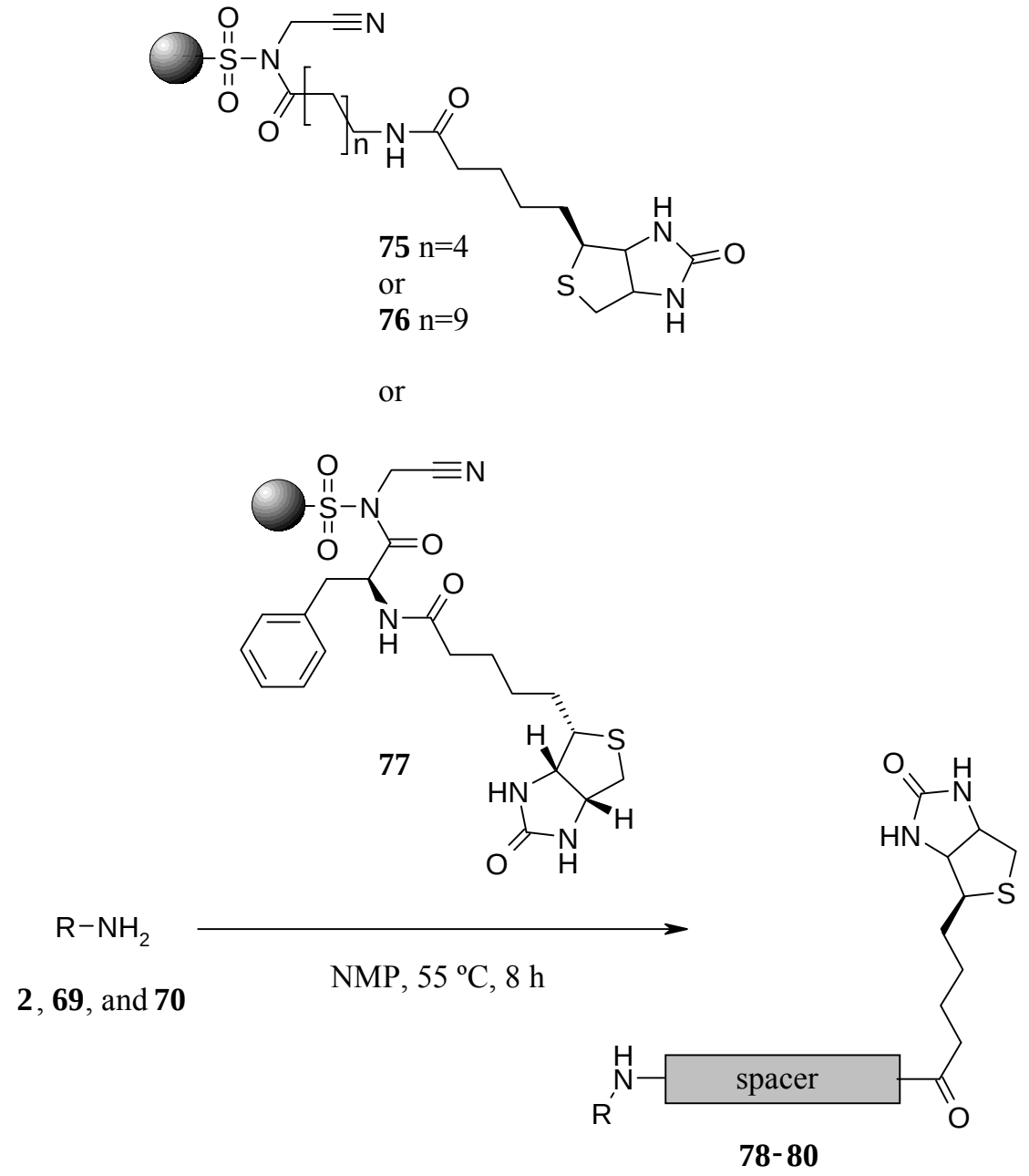

(R see scheme 12; spacer see table 5)

Appropriate Fmoc protected amino acids were immobilized via the Kenner safety-catch linker on aminomethylated polystyrene. After cleavage of the Fmoc protecting group with 20% piperidine in DMF, biotin was attached via in situ anhydride formation to the amino function of the polymer-supported building block yielding the appropriate biotin labels. Finally, the spacer-biotin-loaded sulfonamide linker was alkylated with bromoacetonitrile, leading to activated polymer-bound N-cyanomethyl analogs **75**-**77**, ready for the chemoselective transfer to the primary amino function of the appropriate target template yielding compounds **78**-**80** in good yield and purity (table 5). To establish customized polymer-bound biotinylating reagents, flexible spacers of various lengths were generated via on-bead construction of amide chains, demonstrated in the nine-step synthesis below (scheme 14).

Scheme 14. On-bead construction of spacer-modified biotin conjugate **84**.

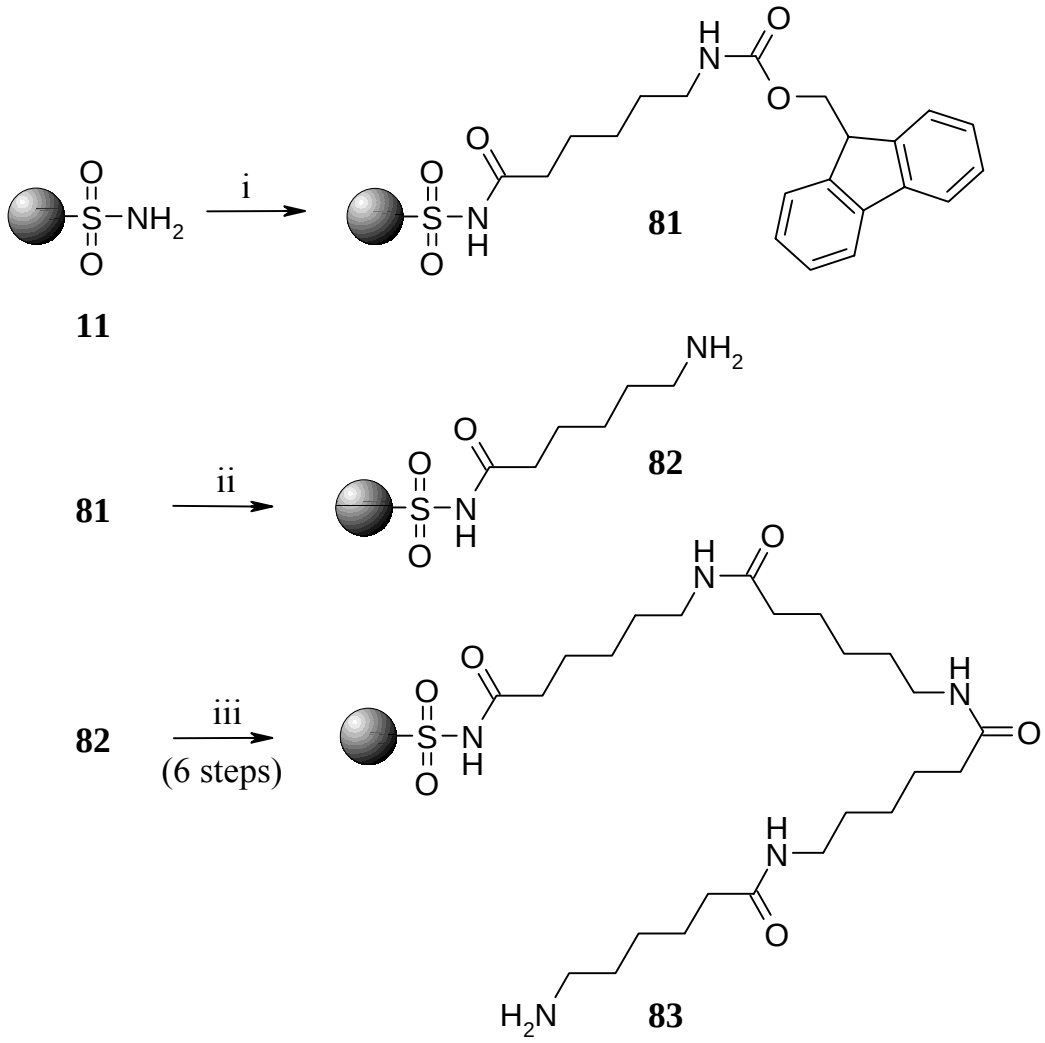

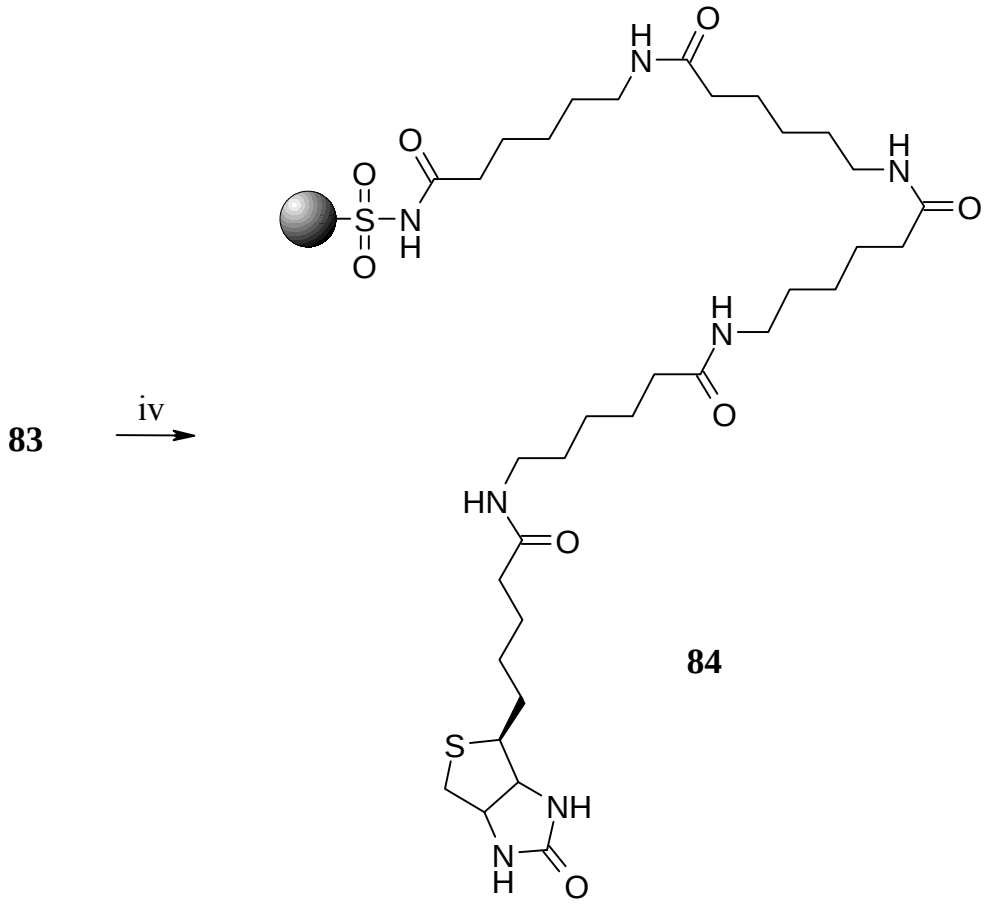

(i) DIC, DMAP, DMF/DCM, ambient temperature, 6h; (ii) 20% piperidine in DMF, ambient temperature, 30 min; (iii) 1. DIC, DMAP, DMF/DCM, ambient temperature, 6h; 2. 20% piperidine in DMF, ambient temperature, 30 min; (iv) DIC, HOBt, DIPEA, DMF, ambient temperature, 24h.

Initially, 6-(Fmoc-amino)caproic acid was immobilized on aminomethylated polystyrene via the Kenner safety-catch linker **11** yielding the polymer-bound N-acylsulfonamide **81**. After cleavage of the Fmoc protecting group with 20% piperidine in DMF, three additional 6-(Fmoc-amino)caproic acid equivalents were attached to the polymer-supported building block and deprotected stepwise, yielding derivative **83**. In the following, biotin was attached to the amino function of **83** via in situ anhydride formation. The spacer-modified polymer-bound biotin label **84** was again activated with bromoacetonitrile. The activated analog was chemoselectively transferred to the primary amino group of the unprotected multi-functional adenosine scaffold **2** when agitating in NMP at 55 degrees centigrade (not shown), leading to **85** in good yield and purity (figure 17).

Figure 17. Custom tailored biotin label introduced into a multi-functional amine.

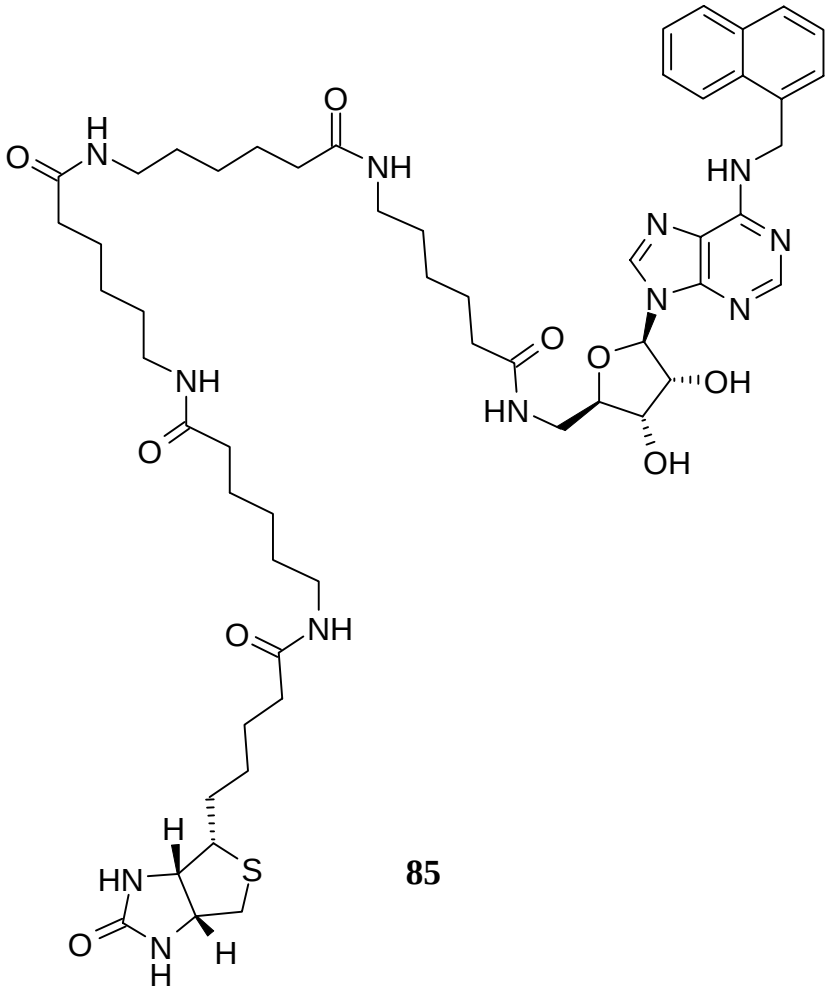

85

According to conditions described above, biotinylated compounds **72**-**74**, **78**-**80**, and **85** were synthesized in excellent to good yield and purity (table 5).

Table 5. Yield and purity of biotinylated compounds **72-74**, spacer-modified biotinylated compounds **78-80**, and **85**, appropriate (spacer)-modified biotinylated derivatives **86-91** resulting from peroxide mediated sulfoxidation, and spacer-modified biotinylated derivatives **95-98** resulting from on-bead modification of 4-fluoro-3-nitrobenzoic acid and peroxide mediated sulfoxidation.

Product	From R-NH_2	Spacer in Construct Substrate-Spacer-Biotinyl/ *S*-Oxobiotinyl	Sufficient Purity (>80%) [A]	Yield [%] [A]
Biotinylated derivatives				
72	**2**	-	prior to MPLC	95
73	**69**	-	prior to MPLC	97
74	**70**	-	prior to MPLC	95
78	**2**	-$CO(CH_2)_5NH$-	after MPLC	79
79	**69**	-$CO(CH_2)_{10}NH$-	after MPLC	79
80	**70**	-L-phenylalanyl-	prior to MPLC	81
85	**2**	-$[CO(CH_2)_5NH]_4$-	prior to MPLC	88
Derivatives from peroxide mediated sulfoxide formation				
86	**2**	-	prior to MPLC	97
87	**2**	-$CO(CH_2)_3NH$-	prior to MPLC	97
88	**2**	-$CO(CH_2)_5NH$-	prior to MPLC	95
89	**69**	-$CO(CH_2)_{10}NH$-	prior to MPLC	80
90	**2**	-$[CO(CH_2)_5NH]_2$-	prior to MPLC	91
91	**70**	-$CO(CH_2)_5NH$-L-phenylalanyl-	after MPLC	71
Derivatives from on-bead modification of 4-fluoro-3-nitrobenzoic acid				
94	$C_6H_5CH_2NH_2$	-$NH(CH_2)_3O[(CH_2)_2O]_2(CH_2)_3NH$-	after MPLC	39
95	$C_6H_5CH_2NH_2$	-$NH(CH_2)_9NH$-	after MPLC	29
96	$C_6H_5CH_2NH_2$	-$NH(CH_2)_8NH$-	after MPLC	43
97	**2**	-$NH(CH_2)_8NH$-	after MPLC	21

[A] All compounds were purified by single semi-preparative medium pressure LC (MPLC) runs under standard conditions (flow rate 10 mL/min, UV detection at 254 nm) that were not optimized for each individual compound. Product containing fractions were collected and evaporated; the yield of pure compound is reported above. Purity of reaction product was estimated using the 100% method. Sufficient purity was classified according to the 80/80 Standard (see table 1, chapter 2.2).

When transferring the activated polymer-supported construct to the amino function of the adenosine scaffold in THF at 55 degrees centigrade, un-intended sulfoxide formation of the biotin moiety occurred, in most of the cases quantitatively (figure 18, table 5, R groups see scheme 12).

Figure 18. Products from peroxide mediated sulfoxide formation.

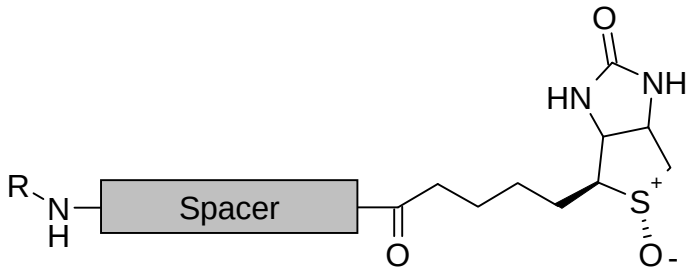

86-91

Since the formation of two sulfoxides is possible, a mixture of two diastereomers was expected. However, NMR analysis revealed that only one isomer was formed. This almost exclusive formation of one sulfoxide isomer was also observed and analyzed by others[15]. Lui et al. found that sulfoxides are easily accessible via peroxide mediated oxidation with the predominance of the α-isomer over the β-isomer.

In order to widen the scope of the reaction reported, phenylalanine was introduced (see entry **80** and **91**, table 5) to obtain a biotinylation reagent along with an UV-quenching group that is of interest for labeling compounds such as amino-sugars. An additional attempt for incorporating a UV-quenching group into the biotin label was the on-bead modification of 4-fluoro-3-nitrobenzoic acid (scheme 15). Initially, 4-fluoro-3-nitrobenzoic acid was attached to the sulfamoyl linker **11** via in situ anhydride formation (not shown) yielding intermediate **50**. Subsequent treatment with excess diamine converted **50** to the corresponding nitroaniline analog **92** by nucleophilic aromatic substitution. Acylation attaching biotin via in situ anhydride formation and final activation with bromoacetonitrile led to the activated cyanomethyl analog **93**. The activated biotin label was finally transferred to the amino group of benzylamine resulting in **94** in moderate to poor yield and purity. Compounds **95-97** were obtained following the same synthetic approach also displaying moderate to poor yield and purity (table 5). As the final step, the transfer of the activated biotin conjugate to the amino function of the target compound was carried out in THF, quantitative sulfoxidation of the biotin moiety was observed.

Scheme 15. On-bead modification of 4-fluoro-3-nitrobenzoic acid.

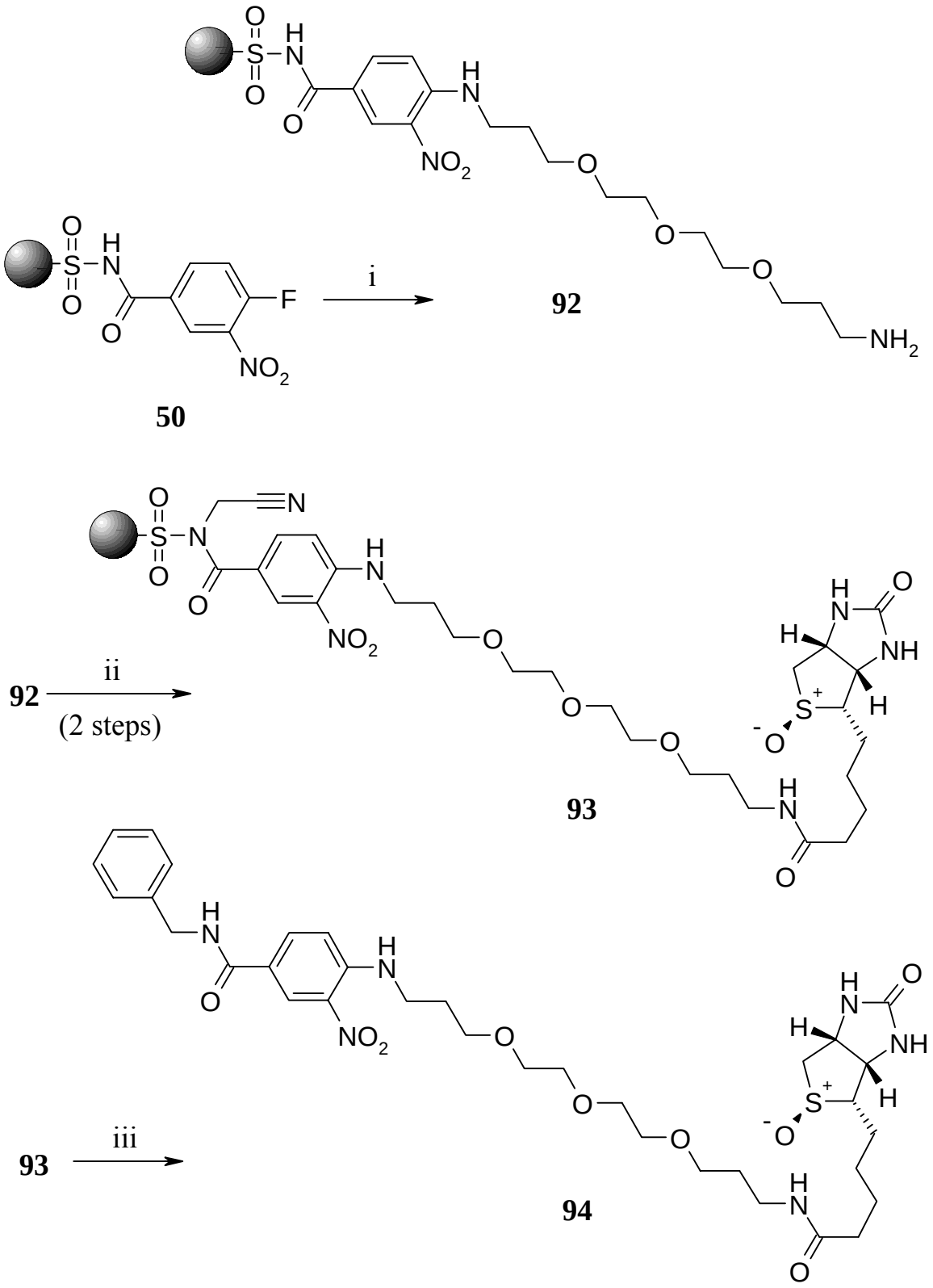

(i) 1,13-diamino-4,7,10-trioxatridecan, DMF, ambient temperature, 2 d; (ii) 1. biotin, DIC, HOBt, DIPEA, DMF, ambient temperature, 2 d; 2. bromoacetonitrile, DIPEA, NMP, ambient temperature, 12 h; (iii) benzylamine, THF, 55 ºC, 8h.

Incomplete conversion of **92** to **93** and subsequent activation with bromo-acetonitrile furnished side-product **98** (figure 19). Side-product formation was observed in all four cases elucidating unsatisfactory yields and purities obtained of compounds **94**-**97**. Isolated side-products **98** and **99** (for scaffold see experimental section) were characterized by NMR and MS.

Figure 19. Side-product formation of spacer-modified biotinylated derivative **94** along on-bead modification of 4-fluoro-3-nitrobenzoic acid.

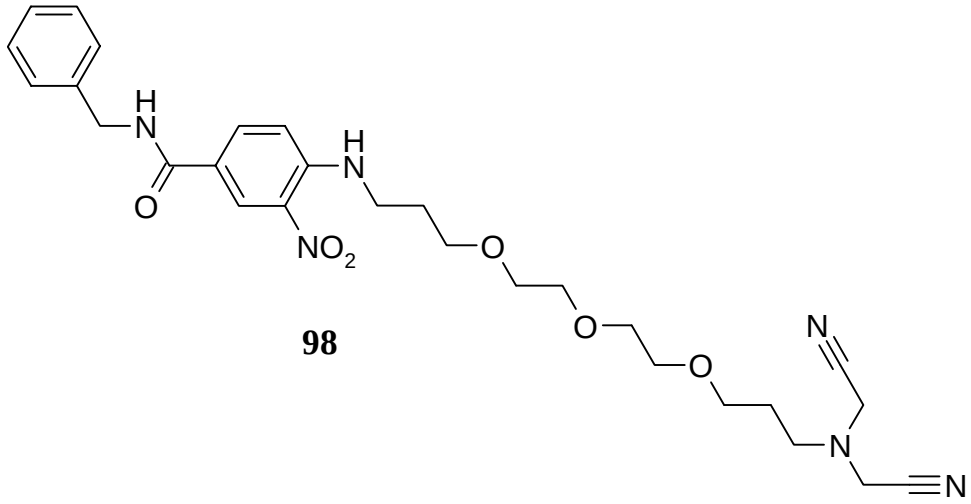

98

4.3 Application of the Polymer-Assisted Biotinylation Protocol to Other Molecules Bearing an Amino Functionality

Recently, our group demonstrated the applicability of the PASP protocol described above for the N-selective biotinylation of the paullone **100** (figure 20) in good yield (87%) and purity (>80% prior to MPLC)[14].

Figure 20. Structure of paullone derivative **100**.

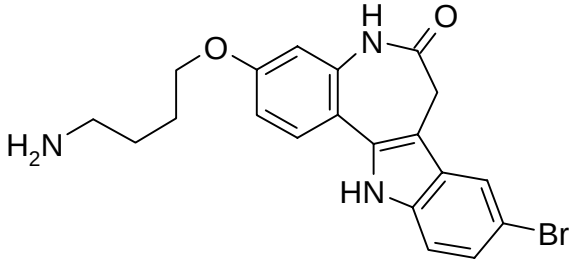

100

In collaboration with the Johann-Wolfgang-Goethe University of Frankfurt, 4-[4-(2-methoxyphenyl)piperazin-1-yl]butylamine was biotinylated yielding **101** ready to be subjected to SPR analysis using a Biacore system. **101** was obtained in good to excellent yield (90%) and purity (>80% prior to MPLC).

Figure 21. Biotin labeled 4-[4-(2-methoxyphenyl)piperazin-1-yl]butylamine.

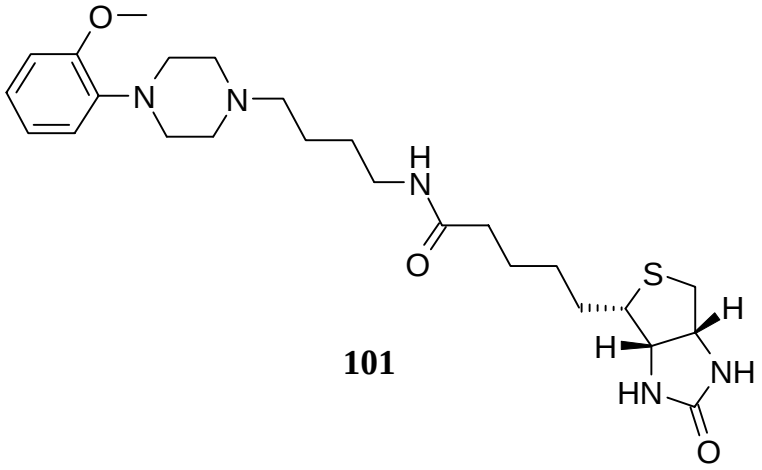

101

4.3.1 Biotin Labeling of Guanosine by cPASP Synthesis

The objective of a joined project with the Philipps-University of Marburg was the chemoselective introduction of a biotin label into the 5′-position of guanosine. Biotinylated guanosine was planned to be subjected in a Biacore assay to perform intermolecular interaction studies. Protein based pre-studies revealed that a spacer of about 18 carbon atoms between the biotin and the guanosine moiety is required for optimal binding of guanosine and its binding partner.

Prior to biotinylation, a guanosine scaffold bearing an amino functionality in 5′-position had to be prepared. Therefore, two different approaches were followed providing 5′-amino-5′-deoxyguanosine (**107**) and 5′-{2-[2-(2-amino-ethoxy)ethoxy]ethylamino}-5′-deoxyguanosine (**108**). Within the synthesis of 5′-amino-5′-deoxyguanosine (scheme 16), initially the 2′- and 3′-hydroxy groups of guanosine (**102**) were protected with 2,2-dimethoxy-propane in anhydrous acetone yielding **103**[16]. In the following, a tosylate group was introduced into the 5′-position. Subsequently the 2′- and 3′-hydroxy groups were deprotected with 50% formic acid providing **105**, as reported by Schattka and Jastorff[17]. Then, the tosylate was replaced by azide. Finally, reduction of the azido functionality of **106** with Pd/H_2 in THF/H_2O (v/v 70/30) led to **107**.

The reaction was monitored by IR and terminated when the absorption peak at 2127 cm^{-1} completely disappeared.

Scheme 16. Synthetic pathway providing 5′-amino-5′-deoxyguanosine (**108**).

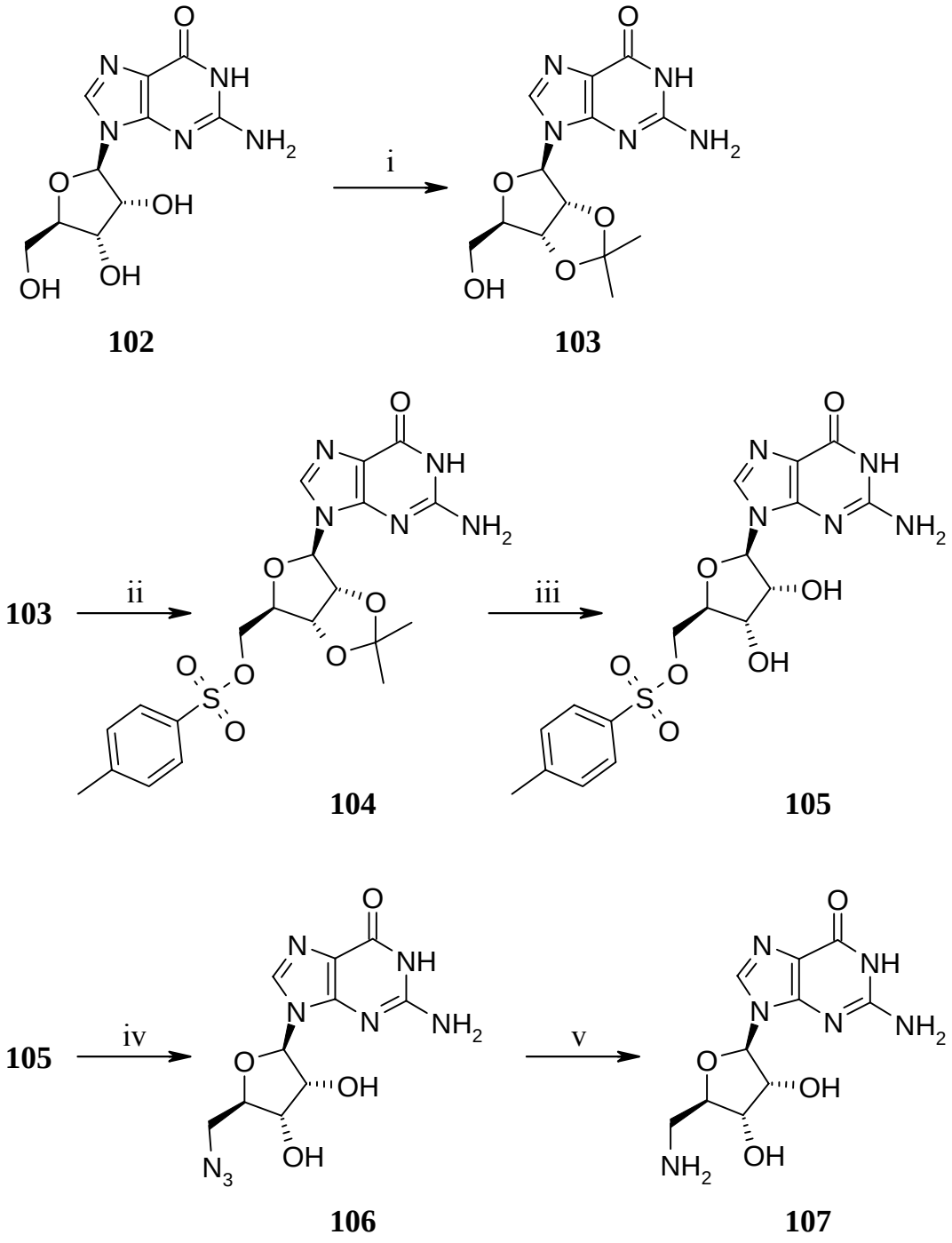

(i) 2,2-Dimethoxypropane, p-toluensulfonic acid monohydrate, anhydrous acetone, ambient temperature, 48 h; (ii) tosylchloride, pyridine, 3 d; (iii) formic acid (50%), ambient temperature, 7 d; (iv) NaN_3, DMF, ambient temperature, 3 d; (v) Pd/H_2, THF/H_2O (v/v, 70/30), ambient temperature, 2 h.

The second approach for the synthesis of 5′-{2-[2-(2-amino-ethoxy)ethoxy]-ethylamino}-5′-deoxyguanosine (**108**) only differed at the final step of the synthetic pathway, replacing the tosylate group of **105** by 2,2′-(ethyldioxy)-bis(ethylamino) yielding **108** (scheme 17). Thus, a spacer of ten atoms was directly incorporated into the guanosine main scaffold that still displayed an amino functionality for the subsequent introduction of a biotin label. Compounds **106** and **108** of these synthetic sequences were isolated and characterized by NMR and MS.

Scheme 17. Synthetic pathway providing 5′-{2-[2-(2-amino-ethoxy)ethoxy]-ethylamino}-5′-deoxyguanosine (**108**).

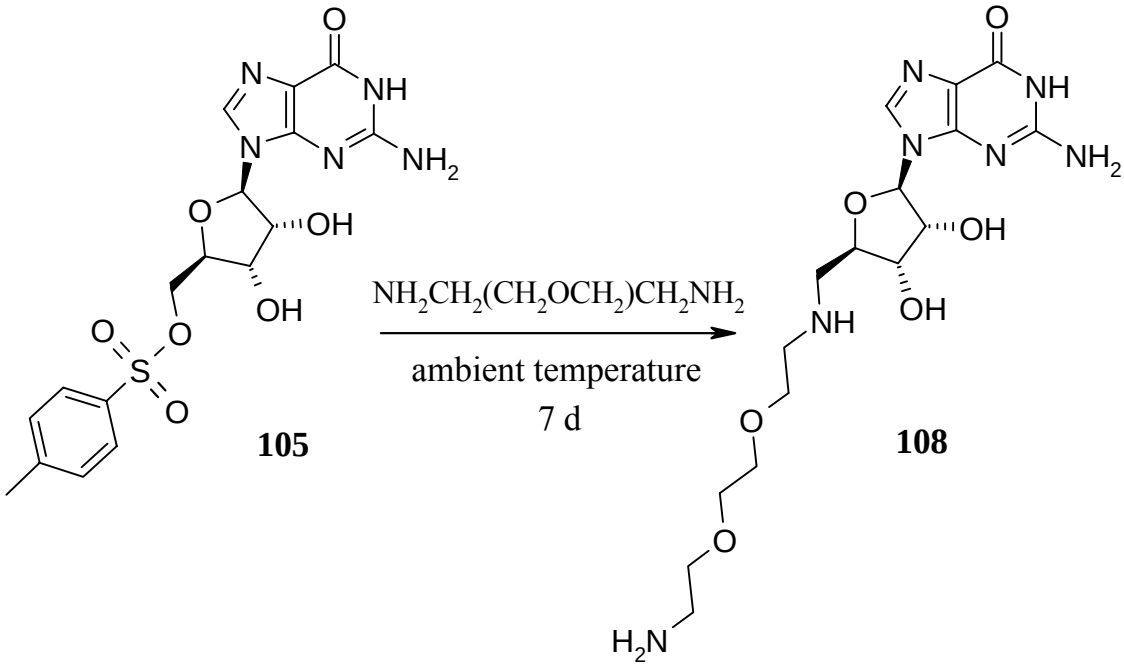

For chemoselectively transferring biotin labels to the primary amino group of guanosine templates **107** and **108** the cPASP protocol described in chapter 4.2 was applied. Initially, **109** (figure 22) was prepared via PASP synthesis to prove the applicability of the polymer-assisted approach for the N-selective acylation of guanosines. **109** was obtained in good to excellent yield and purity.

In the following, cPASP synthesis was used to chemoselectively label 5′-amino-5′-deoxyguanosine (**107**) and 5′-{2-[2-(2-amino-ethoxy)ethoxy]ethyl-amino}-5′-deoxyguanosine (**108**), employing biotin labels as illustrated in scheme 18.

Figure 22. Guanosine derivative **109** obtained by PASP synthesis.

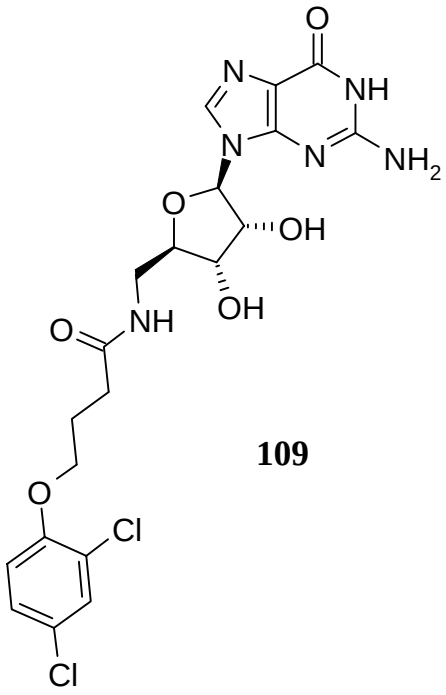

109

Scheme 18. PASP/cPASP synthesis of amino-modified guanosine templates.

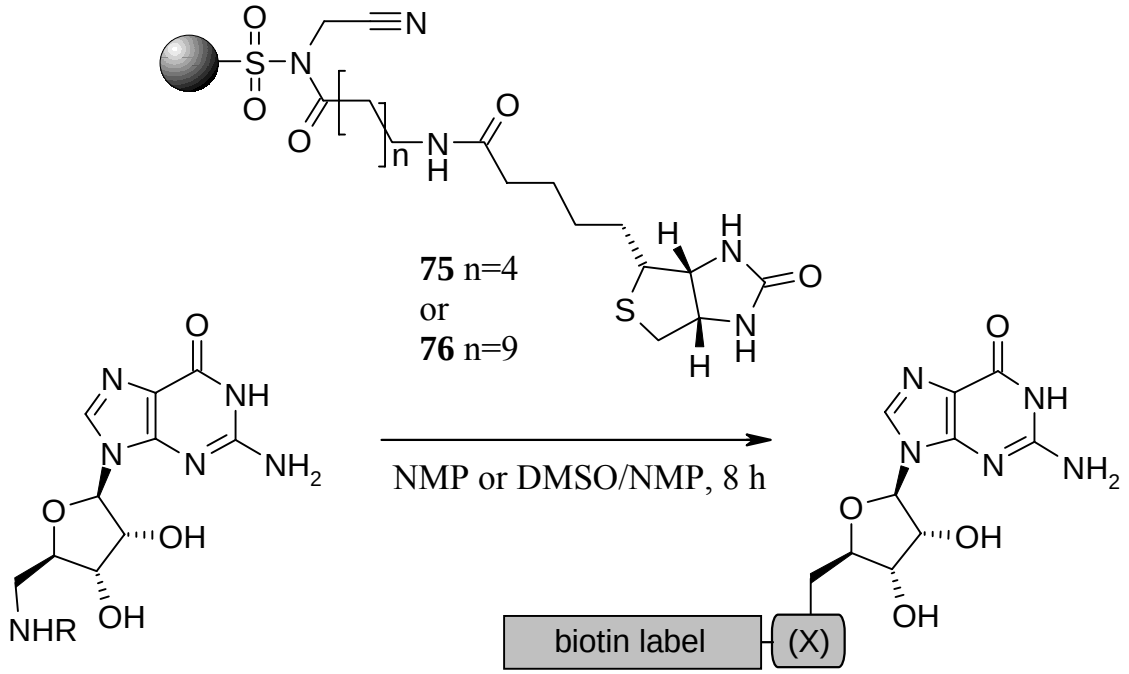

107 or **108**

110 and **111** (X)=NH

112 and **113** (X)=$NH_2CH_2(CH_2OCH_2)CH_2NH$

(biotin label see table 6)

In general, the preparation and purification of biotin labeled guanosine derivatives, including the synthesis in solution as well as the final convergent connection were limited due to very poor solubility of guanosine and guanosine derivatives in organic solvents. Traces of residual tosylate were found in **106**, **107**, **110**, and **111** after silica gel/MPLC purification. When transferring the biotin label to template **108**, **108** was only soluble in a mixture of DMSO/NMP, partly leading to expected sulfoxidation of the biotin moiety (see **112**, **113**). Yield of **110-113** is summarized in table 6.

Table 6. Yield of biotinylated guanosine derivatives **110-113**.

Product	From R-NH_2	Biotin Label	Yield [%][A]
110	**107**	6-biotinylamidohexanoyl-	89 [B]
111	**107**	11-biotinylamido-undecanoyl-	92 [B]
112	**108**	6-biotinylamidohexanoyl-	103 [C]
113	**108**	11-biotinylamido-undecanoyl-	101 [C]

[A] All compounds were purified by single semi-preparative medium pressure LC (MPLC) runs under standard conditions (flow rate 10 mL/min, UV detection at 254 nm) that were not optimized for each individual compound. Product containing fractions were collected and evaporated; the yield of compound is reported above. [B] Yield reported includes traces of tosylate. [C] Mixture of biotin- and biotin sulfoxide labeled guanosine derivatives (approximately 1:1). Since yield calculation is based on the biotinylated compound, values of above 100% were obtained.

4.4 Analytical Characteristics of Biotin Labeled Molecules

4.4.1 ^{1}H NMR Analysis of Selected Biotin Labeled Amino-Nucleosides

Peroxide-mediated biotin sulfoxidation could easily be detected by ^{1}H NMR spectroscopy. In figure 23, sections of ^{1}H NMR spectra displaying characteristic peaks of the biotin and biotin sulfoxide moiety, respectively, are compared. Most obvious is the chemical shift of the NH groups of the carbamide structure (biotin: 6.41 and 6.34 ppm; biotin sulfoxide: 6.79 and 6.69 ppm). Within the ppm range of 2.5 to 3.5, biotin displays a multiplet, a doublet of doublet, and a doublet, whereas the multiplet and doublet of doublet overlap in biotin sulfoxide spectra. The doublet is shifted to lower ppm values, overlapping with the DMSO peak.

Figure 23. Comparison of ^{1}H NMR spectra of biotin and biotin sulfoxide labeled adenosine derivatives.

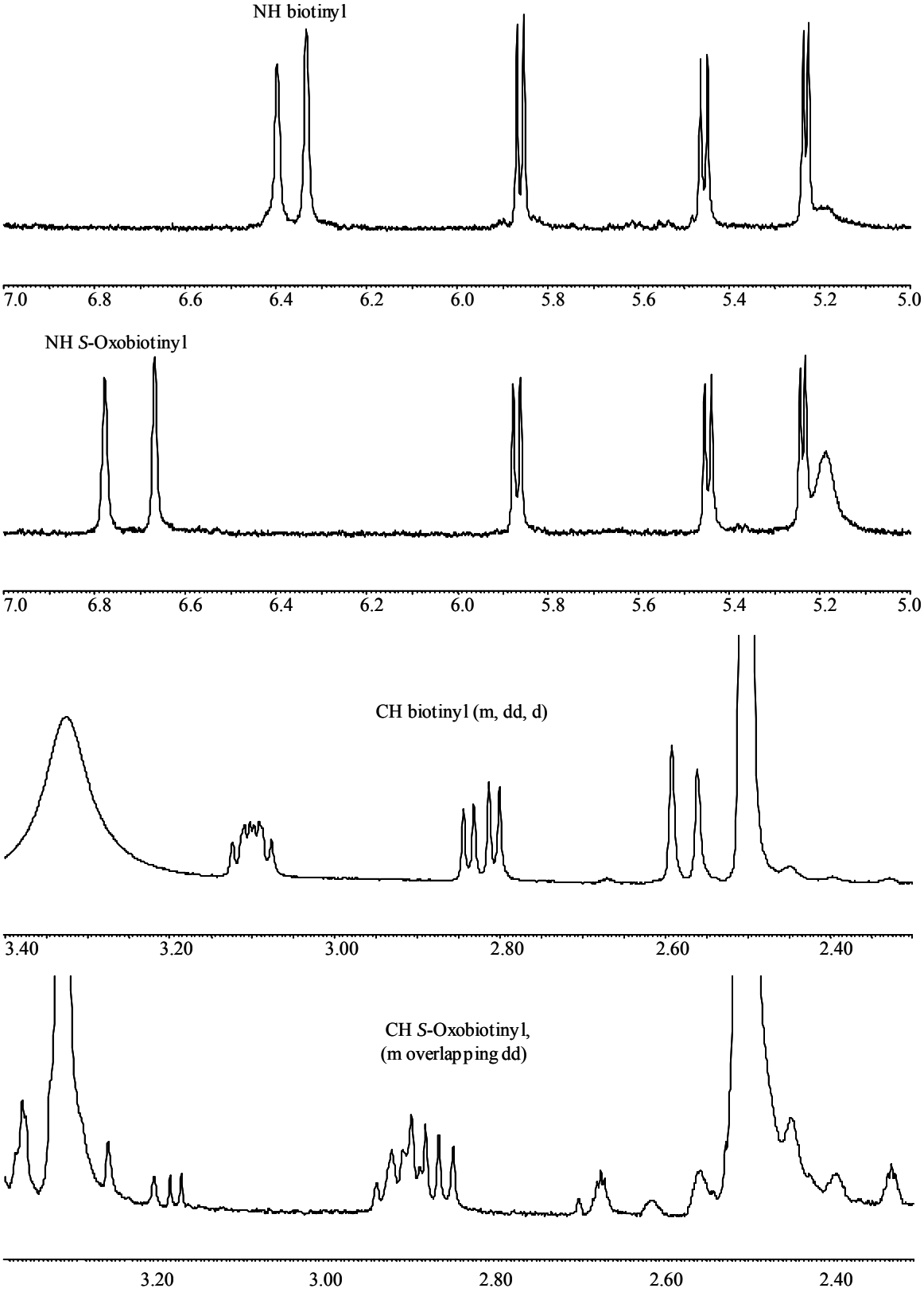

4.4.2 Electrospray Ionization (ESI)/Mass Spectrometry (MS) of Selected Biotin Labeled Amino-Modified Adenosines

The biotin labeled N^6-substituted adenosines **72**, **86**, **78**, and **85** were analyzed by ESI/MS^n to obtain structure-specific fragment ion information.
Concerning the fragmentation patterns of 5′,N^6- and 3′,N^6-disubstituted adenosine derivatives, compounds **71** and **78** were expected to fragment comparable to compound **23** (for figures 6 and 7 as well as scheme 9 see chapter 2.4.2). Surprisingly, fragmentation patterns of **72** and **86** mainly followed pathway B. As expected, the fragmentation sequence of **78** and **85** exclusively followed pathway B, according to **38** (figure 9, chapter 2.4.2).
Figure 24 demonstrates the fragmentation of **72**. Depending on the location of the charge within the molecule, initial fragmentation (F_1) led to daughter ions 358 ($C_{15}H_{24}N_3O_5S$, oxonium) and 276 of pathway B and A, respectively. The following two spectra show the fragmentation of 358 yielding expected fragments 244 ($C_{10}H_{18}N_3O_2S$, amidium) and 227 ($C_{10}H_{15}N_2O_2S$, acylium) and of 276 providing 141 and 115 (not shown).
The biotin sulfoxide analog **86** fragmented along pathway B (figure 25), with expected product ions 374 ($C_{15}H_{24}N_3O_6S$, oxonium), 260 ($C_{10}H_{18}N_3O_3S$, amidium), and 243 ($C_{10}H_{15}N_2O_3S$, acylium). Again, typical differences of 18, 42, 17, and 28 corresponding to losses of water, acetate, ammonia and carbon monoxide groups, respectively, were observed. The product ion 276 fragmented as anticipated (not shown), with fragments 141 and 115.
In **78** (figure 26) the fragmentation predominantly occurred at the amide functionality (see F_1 and F_2), with main fragments 340 ($C_{16}H_{26}N_3O_3S$, acylium) and 227 ($C_{10}H_{15}N_2O_2S$, acylium). Since on-bead construction of amide chains provided products containing two amide functions, two different acylium fragments were observed. Fragment 471 corresponds to the oxonium structure; the amidium fragment was not found. Fragmentation along pathway A did not occur at all.
As ionization was induced by sodium ions instead of protons, a different fragmentation pattern of **85** (figure 27) was observed. Nevertheless, some Na^+ adducts of expected fragments were found: 718 ($C_{34}H_{61}N_7NaO_6S$, amide), 675 ($C_{33}H_{60}N_6NaO_5S$, amide), and 492 ($C_{22}H_{39}N_5NaO_4S$, amide). Thus, fragmentations also occurred at amide groups. Daughter ion 832 ($C_{37}H_{48}N_9O_6S$) resulted from the initial fragmentation between the N^9-atom of the purine moiety and the anomeric carbon of the sugar moiety, as observed before. The charged site is located on the sugar moiety leading to fragments described.

Figure 24. Fragmentation pattern of **72** (MW 632.75; $[M+H]^+$ 633.2608).

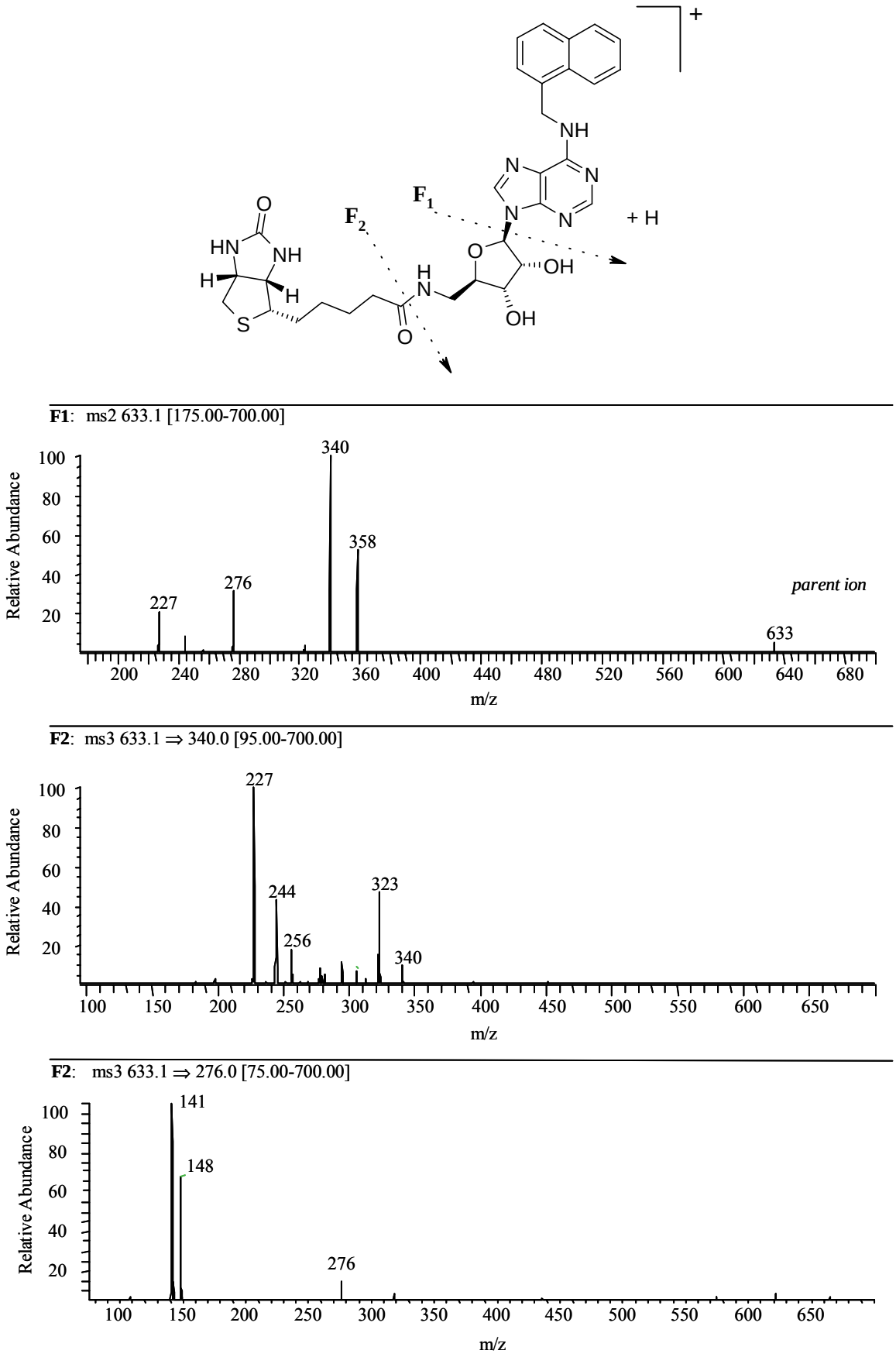

Figure 25. Fragmentation pattern of **86** (MW 648.75; $[M+H]^+$ 649.2558).

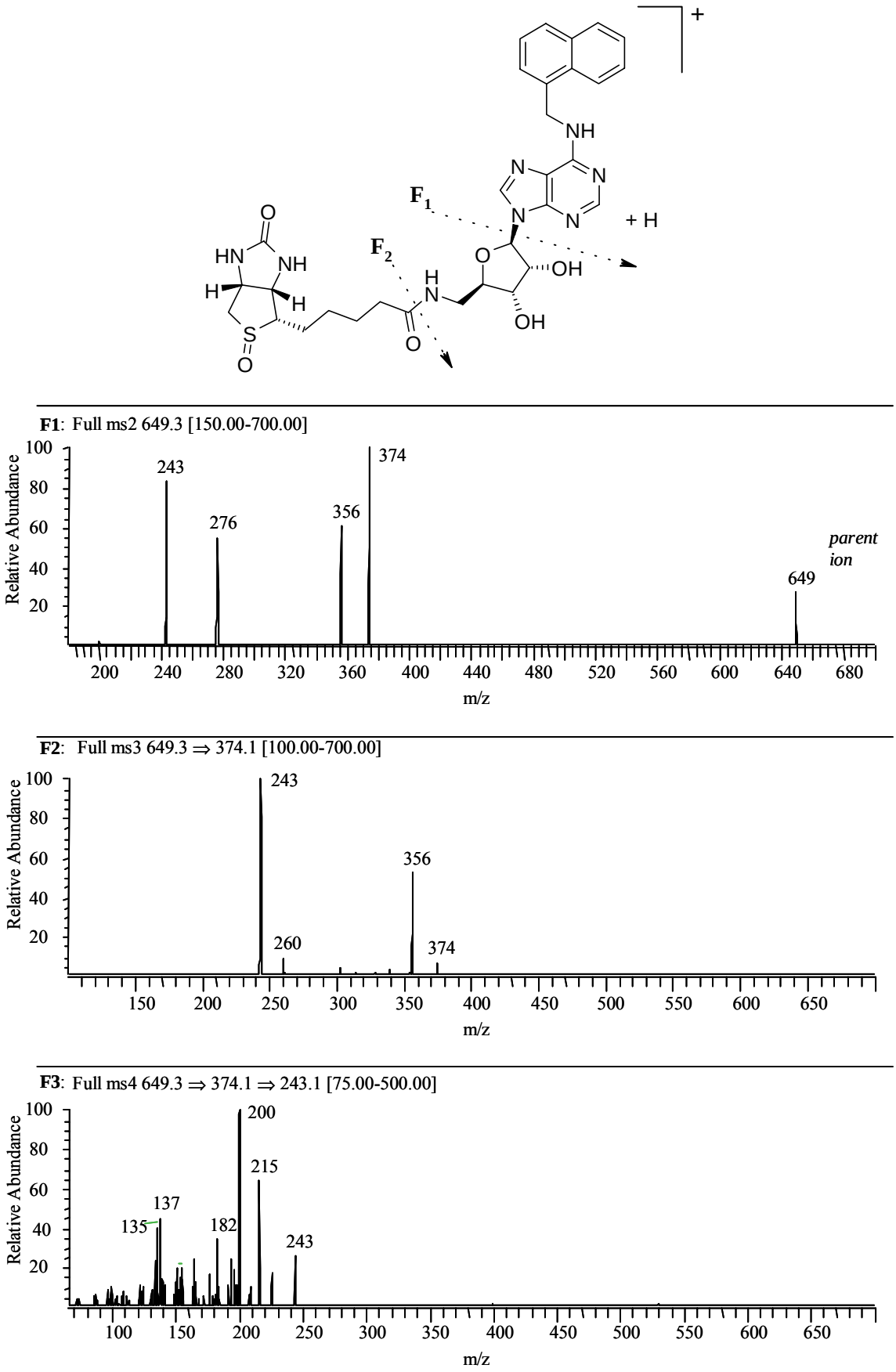

Figure 26. Fragmentation pattern of **78** (MW 745.91; $[M+H]^+$ 746.3449).

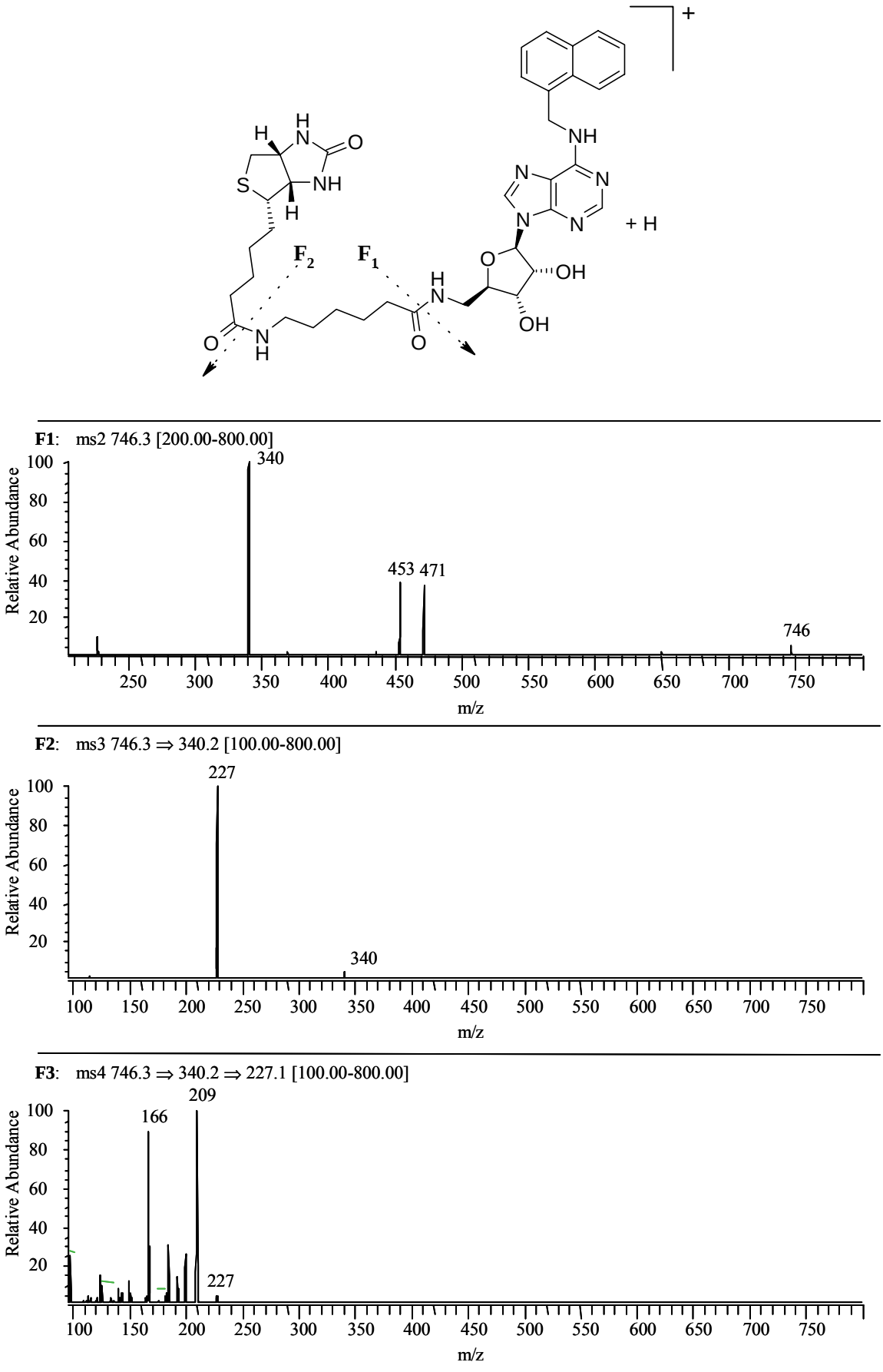

Figure 27. Fragmentation pattern of **85** (MW 1085.39; $[M+Na]^+$ 1107.5789).

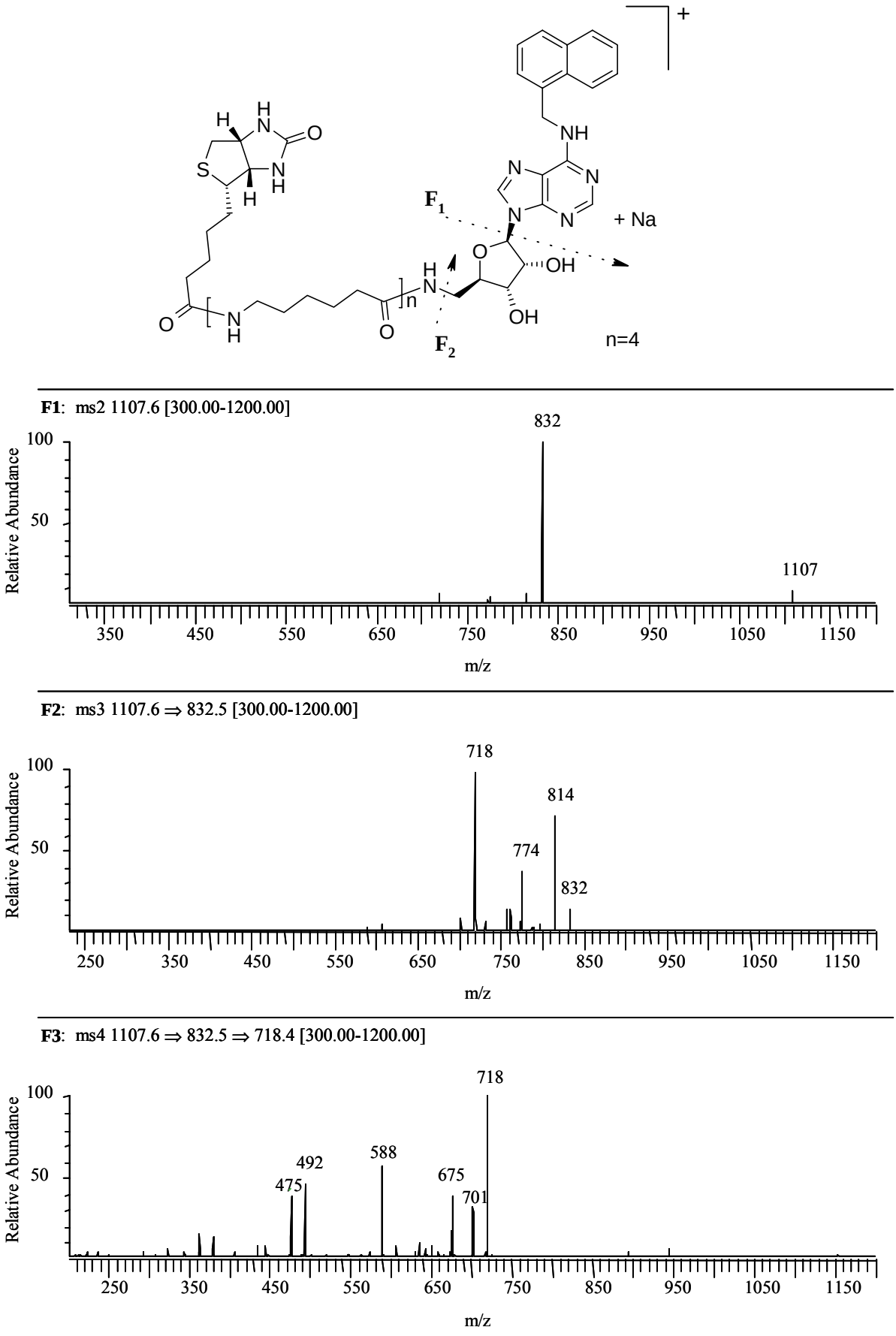

4.5 Discussion

The protocol demonstrated above permits the simple on-bead construction of custom tailored biotin labels using established amide bond forming procedures. PASP synthesis leads to simple product isolation because the excess of polymer-bound reagent that is applied to drive reactions to completion can be removed by simple filtration, allowing for the fast and convenient access of biotinylated compounds in high yield and purity.

When using biotinylated compounds in an SPR assay, chemoselective labeling is crucial to know the exact binding site of the molecule. Control of the labeling site is required due to the fact, that a biotin label might inactivate the compounds binding ability when being incorporated into the wrong region of the molecule. As shown above, N-selective acylation observed with alkylated acylsulfonamides offers the opportunity to incorporate the biotin label into a desired region of the molecule; no protecting group operations are needed.
Besides the necessity of chemoselectivity, additional requirements for the biotinylation process have to be fulfilled. For the reason that excess biotin blocks streptavidin sites on the sensor chip surface, the absence of biotin is of utmost importance for reproducible binding to streptavidin on the sensor chip surface. During PASP synthesis, excess biotin remains coupled to the polymer support and can thus be easily removed by simple filtration, whereas the biotinylated compound stays in solution. Further, the degree of biotinylation should be kept low; one biotin label per molecule is sufficient and optimal. Uncontrolled higher biotinylation degrees per molecule affect the optimal display of the ligand bound to the sensor chip surface and again influence the reproducibility of binding. Derivatives with long spacer arms (a minimum of six carbon atoms) are recommended to minimize sterical hindrance and to facilitate streptavidin binding.
Although a wide range of biotinylation reagents is commercially available (figure 28), none of them accomplishes all of the requirements needed for performing SPR experiments.

Figure 28. Representative selection of commercially available biotinylation reagents.

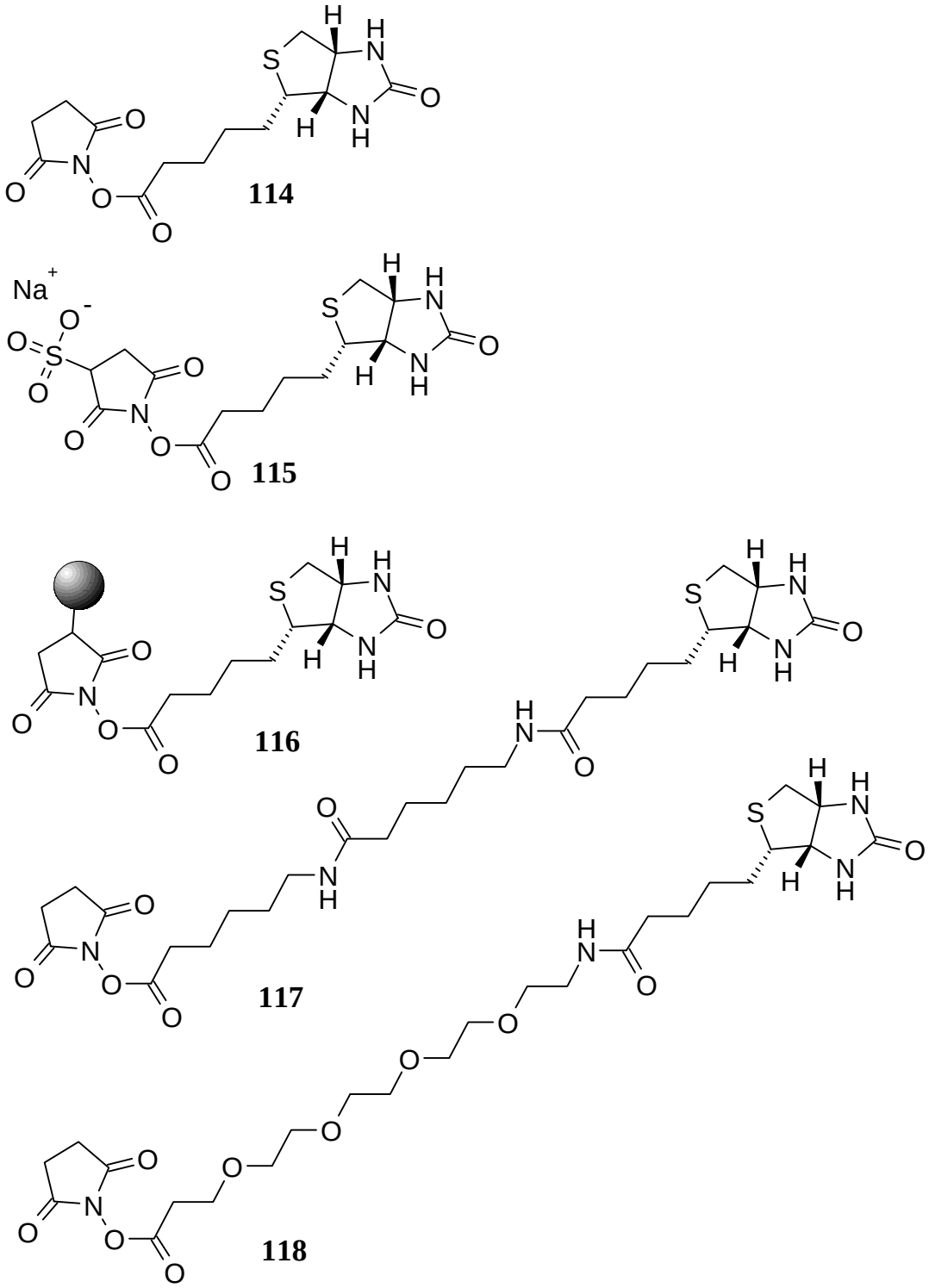

The use of commercially available biotinylation reagents **114-118** will undoubtedly yield quantitative reactions in many cases. However, the need for protecting group operations as well as the separation of the product from

excess reagent in the cases of **114**, **115**, **117**, and **118** (by e.g. HPLC, dialysis or affinity chromatography) are time-consuming; often excess biotin remains in the sample. Reagents **117** and **118** display the advantage of an incorporated flexible spacer. Whereas **117** is well established, **118** represents a novel labeling agent, available from Quantabiodesign. This compound shows improved water-soluble characteristics, which is an interesting feature for lipophilic compounds to be studied. This is especially important when employing the Biacore system for SPR experiments because solubility of the sample in aqueous buffers is required.
Via on-bead construction of amide chains, customized spacers can be obtained by varying the building blocks as shown in table 5. Since polymer-bound acylsulfonamides like the Kenner linker also possess a high orthogonal stability, they again play a key role in the reaction pattern. This property enables it to work under drastic conditions, so that a wide range of on-bead spacer constructions is possible. Therefore, the polymer-assisted solution-phase protocol allows for the incorporation of spacers of variable length and characteristics (such as water solubility, UV-absorbing properties). Thus, labels can be designed according to the demands of each compound to be labeled.

The known, almost exclusive formation of α-sulfoxides[15,18] that we observed when the reaction was performed in THF, can easily be avoided resorting to solvents that are not prone to peroxide formation. However, peroxides preformed in THF that completely oxidize polymer-bound biotin might be useful for the development of biotin sulfoxide labels. Biotin sulfoxide is suited for rendering attached molecules even more water-soluble. Preliminary SPR experiments comparing the immobilization properties of biotin and biotin sulfoxide labels showed, that biotin sulfoxide labeled compounds also bind to the streptavidin surface of the sensor chip sufficiently, but to a lesser extend. These findings will be further investigated by our group.

The applicability of the polymer-assisted biotinylation approach to molecules bearing an amino functionality was demonstrated. While biotin labeling of the paullone derivative **100** and of 4-[4-(2-methoxyphenyl)-piperazin-1-yl]butylamine (**101**) proceeded smoothly in good yield and purity, the biotinylation of guanosine templates **107** and **109** was limited. Thereby, poor solubility of all guanosine derivatives in organic and aqueous solvents was the limiting factor. Whereas the biotinylation of **107** was successful, purification of target compounds was complex with traces of

tosylate remaining in the target samples. Since tosylate does not affect the biotin-streptavidin-complexation, biotinylated guanosine derivatives **110** and **111** still can be applied to SPR experiments employing a Biacore system. A mixture of DMSO/NMP was the only feasible solvent for the biotinylation of **108** leading to expected sulfoxidation of the biotin moiety. A mixture of biotin and biotin sulfoxide of **112** and **113** was obtained; sufficient purification was not accomplished.

In conclusion, a rapid and efficient polymer-assisted approach to biotinylate nucleoside derivatives bearing an amine functionality has been developed. The protocol reported enables the incorporation of spacers of various lengths and chemical characteristics via on-bead construction. Custom tailored spacers are obtained using established amide bond forming procedures. The results obtained suggest that this derivatization technique is a useful addition to existing biotin labeling protocols, in particular for introducing custom tailored spacer-biotin anchors as prerequisite in the analysis of drug candidates using streptavidin chips via SPR methodology.

4.6 Experimental Section

Identity of all compounds was assigned by NMR spectroscopy. ^{1}H NMR spectra were recorded on a Bruker AMX 400 spectrometer at 400 MHz in DMSO-d_6, using tetramethylsilane as internal standard. ^{1}H NMR data are reported based on separated spin-spin signals and protons that were not covered by H_2O- or DMSO-signals, unless otherwise noted. Identity of compounds prepared in mg quantities was evaluated by high-resolution MS; sample purity was calculated from chromatographic purification profiles. Yields are reported as isolated material. MPLC simultaneous purity analyses/purifications were performed using a Büchi 681 pump (flow rate 10 mL/min, methanol/water gradients) and an UV-detector (254 nm) with Merck 310-25 Lobar-LiChroprep®-RP-18 columns. HPLC was performed on a Merck Hitachi L-7000 series connected to a diode array detector (methanol/water gradients, flow rate 1 mL/min, UV absorption at 240 to 261 nm). High-resolution MS data of pure compounds were obtained on a Finnigan MAT 95 XL (ESI, methanol/water (1/1, v/v) infusion at 2 µL/min with polypropylene glycol as reference); MS^n data on a Finnigan MAT 95 XL TRAP (ESI, methanol/water (1/1, v/v) infusion at 2 µL/min). IR spectra were obtained on a Shimadzu FTIR-8300 instrument. Preparative column chromatography was performed on silica gel 100-200 active, 60 Å, from ICN

or Dowex® OH^- (1×2-200) using glass columns (4.5×15 cm). TLC reaction control was performed on Macherey-Nagel Polygram® Sil G/UV_{254} precoated microplates; spots were visualized under UV-illumination at 254 nm.

4.6.1 Biotin Labeling of Adenosine Templates

Introduction of spacer atoms (general procedure E) and attachment of biotin to the polymer-supported building block (general procedure F) were carried out according to procedures reported for other carboxylic acids (see chapter 2.6 and 3.6) with the following deviations.

General procedure E for the on-bead construction of spacer atoms: DMF (10 mL) was added to dry 4-sulfamoylbenzoylaminomethyl polystyrene (2.0 g) with an initial loading level of 1.23 mmol/g. The resin was allowed to swell at room temperature for 30 min. Separately, an appropriate Fmoc-aminocarboxylic acid equivalent (9.8 mmol, 4 equivalent) was dissolved in DMF (5-7.5 mL) and preactivated for 30 min via in situ anhydride formation with DIC (1,5 mL, 9.8 mmol, 4 equivalent). After adding DMAP (7 mg, 0.05 mmol) and CH_2Cl_2 (2 mL), the coupling mixture was subsequently poured onto the swollen resin. The resulting reaction mixture was agitated at room temperature for 6 h. The resin beads were filtered off and washed exhaustively with DMF (three times 5 mL) and MeOH (five times 5 mL). Only when acylating the sulfamoyl linker with Fmoc-protected 11-amino-undecyl acid, resin particles turned slightly pink. To reach quantitative acylation, the coupling reaction was performed in duplicates for all Fmoc-amino acids. After cleavage of the Fmoc protecting group with 20% piperidine in DMF, further building blocks (appropriate Fmoc-amino acids or biotin) were attached to the polymer-supported building block.

General procedure F for attaching biotin to polymer-supported building blocks and to the Kenner safety-catch linker, respectively: Biotin (2.4 g, 10 mmol) was suspended in DMF (30 mL) at 50 °C and preactivated via in situ anhydride formation by adding 780 µL (5 mmol) DIC. After 3 h, first DIPEA (580 µL, 3.4 mmol) and HOBt (1.4 g, 10 mmol) and then the obtained coupling mixture were added to the swollen resin. The resulting reaction mixture was shaken at room temperature for 24 h. The resin beads were filtered off and washed exhaustively with DMF, CH_2Cl_2 and MeOH

(three times 5 mL). To reach quantitative conversion, biotinylation was carried out twice.

For the activation of simple polymer-supported acids and the subsequent synthesis of final compounds **72**, **78-80**, **85**, and **86-91 general procedure C** and **general procedure D** (chapter 2.6) were employed with the following deviations (see general procedure C_1 and D_2).

General procedure C_1 for the activation of polymer-supported acids: The sulfonamide linker was activated (see chapter 2.6). Resin beads were washed with dimethylsulfoxide (five times 5 mL) and NMP (once 5 mL).

General procedure D_2 for the synthesis of compounds 72, 78-80, 85, and 86-91: The polymer-bound, activated building block was transferred to the amino group of 10 μmol of **2**, **69**, and **70**, by adding a solution of **2**, **69**, and **70** in 1 mL NMP to a slurry of 400 mg of the appropriate resin in 4 mL NMP. The reaction mixture was shaken at 55 °C for 10 h yielding **72**, **78-80**, and **85**. Polymer beads and particulates were removed by filtration. The beads where extracted with MeOH. The combined MeOH layers were evaporated to furnish target compounds. To remove residual NMP, water (10-20 mL) was added and subsequently evaporated in vacuo (20 mbar, 60 ºC). This process was repeated four times. Finally, compounds were analyzed by a single semi-preparative MPLC run under standard conditions.
The synthesis of final compounds **73** and **74** was carried out by A. Golisade according to procedures reported[14].
Target compounds **86-91** were obtained as described in general procedures E, F, and C_1 with the deviation of using THF as solvent instead of NMP. The polymer-bound, activated building block was transferred to the amino group of 10 μmol of **2, 69**, and **70** by adding a solution of **2, 69**, and **70** in 0.5 mL NMP to a slurry of 400 mg of the appropriate resin in 4 mL THF and shaking at 55 °C for 10 h.
All compounds were obtained as white, amorphous solids, except **79** and **89**, which furnished a light pink-colored solid. Yield of pure compounds obtained is reported below.

General procedure G for the derivatization of [(4-fluoro-3-nitrobenzoyl)-4-sulfamoyl]benzamidomethyl polystyrene: To give final compounds **94-97**, [(4-fluoro-3-nitrobenzoyl)-4-sulfamoyl]benzamidomethyl polystyrene (2.0 g, 2.0 mmol) was treated with the appropriate amine (20

mmol) in DMF (40 mL) overnight. The resin beads were washed with DMF (three times 5 mL) and MeOH (three times 5 mL). The color of the resin beads changed from white to a dark orange. In the following, biotin was attached to the amino function of the building block via in situ anhydride formation as described in **general procedure F**, using THF as solvent. Finally, the Kenner safety-catch linker was activated and carboxylic acid equivalents transferred to the amino function of the appropriate amine according to **general procedure C** and **general procedure D** (chapter 2.6).

5´-Biotinylamido-5´-deoxy-N^6-(1-naphthylmethyl)adenosine (**72**)

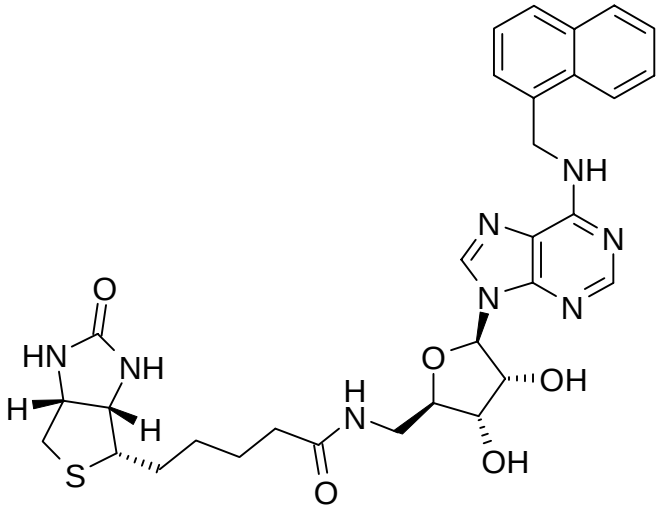

Yield 95%

^{1}H NMR (400 MHz, DMSO-d_6) δ (ppm) = 8.49 (bs, 1H, N^6H), 8.37 (bs, 1H, 8H), 8.25-8.23 (m, 2H, 2H overlapping naphthyl), 8.14 (bs, 1H, NH, amide), 7.96-7.94 (m, 1H, naphthyl), 7.83-7.80 (m, 1H, naphthyl), 7.59-7.52 (m, 2H, naphthyl), 7.47-7.41 (m, 2H, naphthyl), 6.41 (s, 1H, NH, biotinyl), 6.33 (s, 1H, NH, biotinyl), 5.87 (d, 1H, 1´H, *J*=6.1 Hz), 5.45 (d, 1H, 3´OH, *J*=5.8 Hz), 5.24 (d, 1H, 2´OH, *J*=4.8 Hz), 5.19 (bs, 2H, CH_2, naphthylmethyl), 4.69-4.67 (m, 1H, 2´H), 4.30-4.26 (m, 1H, biotinyl), 4.12-4.08 (m, 1H, biotinyl), 4.07-4.03 (m, 1H, 3´H), 3.98-3.94 (m, 1H, 4´H), 3.11-3.04 (m, 1H, biotinyl), 2.80-2.77 (m, 1H, biotinyl), 2.12 (t, 2H, biotinyl, *J*=7.5 Hz), 1.68-1.23 (m, 6H, biotinyl)

HRESI-MS $C_{31}H_{36}N_8O_5S$ $[M+Na]^+$ calcd 655.2427
MW 632.75 $[M+Na]^+$ found 655.242

5′-(6-Biotinylamido-hexanoylamino)-5′-deoxy-N^6-(1-naphthylmethyl)-adenosine (**78**)

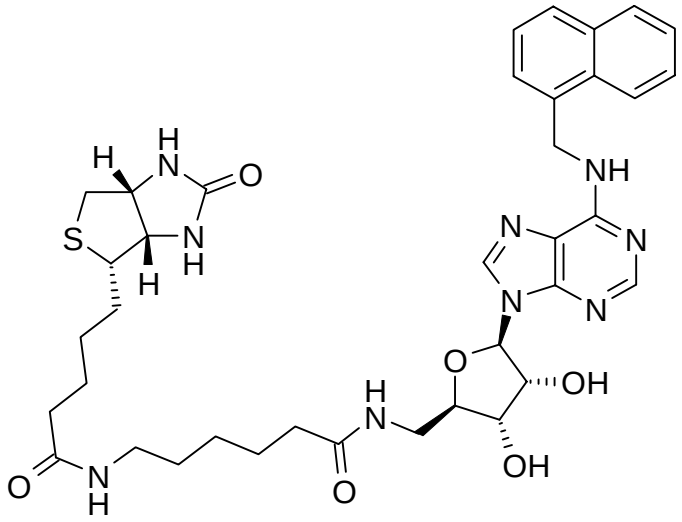

Yield 79%

^{1}H NMR (400 MHz, DMSO-d_6) = δ (ppm) 8.48 (bs, 1H, N^6H), 8.37 (bs, 1H, 8H), 8.25-8.23 (m, 2H, 2H overlapping naphthyl), 8.16-8.15 (m, 1H, NH, amide), 7.96-7.94 (m, 1H, naphthyl), 7.83-7.81 (m, 1H, naphthyl), 7.71 (t, 1H, NH, amide, *J*=5.5 Hz), 7.59-7.52 (m, 2H, naphthyl), 7.47-7.41 (m, 2H, naphthyl), 6.41 (s, 1H, NH, biotinyl), 6.34 (s, 1H, NH, biotinyl), 5.88 (d, 1H, 1′H, *J*=6.4 Hz), 5.48-5.44 (m, 1H, 3′OH), 5.25-5.23 (m, 1H, 2′OH), 5.20 (bs, 2H, CH_2, naphthylmethyl), 4.71-4.70 (m, 1H, 2′H), 4.31-4.28 (m, 1H, biotinyl), 4.13-4.09 (m, 1H, biotinyl), 4.05 (bs, 1H, 3′H), 3.97 (bs, 1H, 4′H), 3.10-3.05 (m, 1H, biotinyl), 3.02-2.97 (m, 2H, CH_2, hexanoyl), 2.83-2.78 (dd, 1H, biotinyl, *J*=5.1Hz, 12.5 Hz), 2.18-2.10 (m, 2H, hexanoyl), 2.02 (t, 2H, biotinyl, *J*=7.4 Hz), 1.53-1.16 (m, 12H, 6H biotinyl overlapping 6H hexanoyl)

HRESI-MS $C_{37}H_{47}N_9O_6S$
MW 745.91
$[M+H]^+$ calcd 768.3268
$[M+H]^+$ found 768.3269

N^6-(2-{2-[2-(11-Biotinylamido-undecanoylamino)ethoxy]ethoxy}ethyl)-adenosine (**79**)

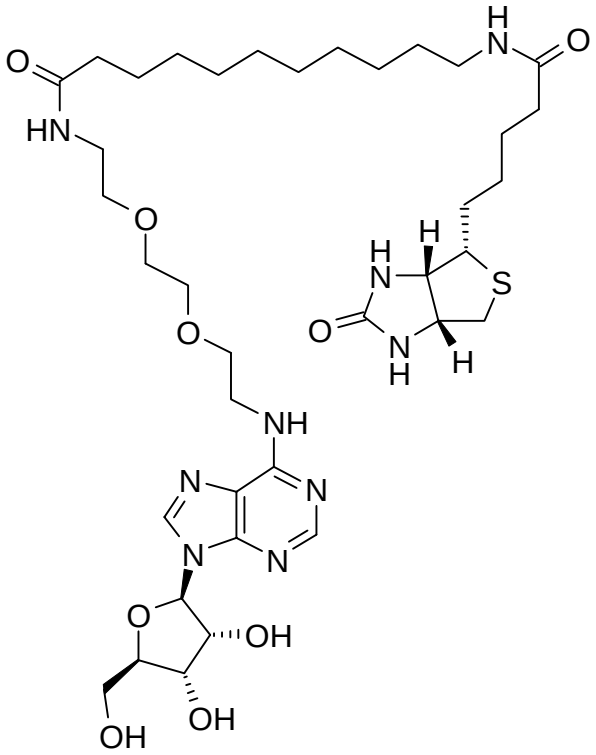

Yield 79%

^{1}H NMR (400 MHz, DMSO-d_6) = δ (ppm) 8.36 (s, 1H, 8H), 8.22 (s, 1H, 2H), 7.82-7.71 (m, 3H, N^6H overlapping amides), 6.41 (s, 1H, NH, biotinyl), 6.35 (s, 1H, NH, biotinyl), 5.89 (d, 1H, 1´H, *J*=6.1 Hz), 5.44 (d, 1H, 3´OH, *J*=6.4 Hz), 5.40-5.38 (m, 1H, 5´OH), 5.19 (d, 1H, 2´OH, *J*=4.6 Hz), 4.62-4.58 (m, 1H, 2´H), 4.32-4.28 (m, 1H, biotinyl), 4.16-4.13 (m, 2H, biotinyl overlapping 3´H), 3.97-3.95 (m, 1H, 4´H), 3.70-3.48 (m, 10H, 5´CH_2 overlapping CH_2, 1,8-diamino-3,6-dioxa-octyl), 3.39-3.36, (m, 2H, CH_2, 1,8-diamino-3,6-dioxa-octyl), 3.11-3.06 (m, 1H, biotinyl), 3.02-2.97 (m, 2H, CH_2, 1,8-diamino-3,6-dioxa-octyl), 2.83-2.79 (dd, 1H, biotinyl, *J*=5.1 Hz, *J*=12.5 Hz), 2.59 (d, 1H, biotinyl, *J*=12.5 Hz), 2.03 (t, 4H, biotinyl overlapping CH_2 undecanoyl, *J*=7.4 Hz), 1.65-1.22 (m, 24H, 6H biotinyl overlapping 18H undecanoyl)

HRESI-MS $C_{37}H_{61}N_9O_9S$
MW 808.02
[M+Na]+ calcd 830.4210
[M+Na]+ found 830.4201

N^6-[2-((2*S*)-Biotinylamido-3-phenylpropionylamino)ethyl]adenosine (**80**)

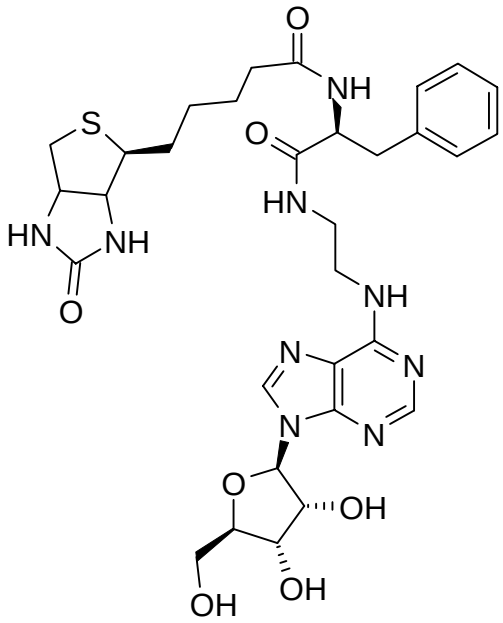

Yield 81%

^{1}H NMR (400 MHz, DMSO-d_6) = δ (ppm) 8.36 (s, 1H, 8H), 8.22 (bs, 1H, 2H), 8.12 (t, 1H, NH, *J*=5.3 Hz), 8.01 (d, 1H, NH, *J*=8.4 Hz), 7.91-7.78 (m, 1H, NH), 7.24-7.10 (m, 5H, phenyl), 6.38 (s, 1H, NH, biotinyl), 6.34 (s, 1H, NH, biotinyl), 5.90 (d, 1H, 1´H, *J*=6.3 Hz), 5.40 (bs, 3H, CH_2 phenyl overlapping OH), 4.60 (t, 1H, 2´H, *J*=5.4 Hz), 4.48-4.42 (m, 1H, phenylalanyl), 4.31-4.28 (m, 1H, biotinyl), 4.16-4.14 (m, 1H, 3´H), 4.11-4.08 (m, 1H, biotinyl), 3.97-3.96 (m, 1H, 4´H), 3.70-3.66 (m, 1H, 5´CH_2), 3.57-3.51 (m, 3H, 5´CH_2 overlapping CH_2, 1,2-diamino-ethyl), 3.05-2.94 (m, 3H, biotinyl overlapping 1,2-diamino-ethyl), 2.83-2.76 (m, 1H, biotinyl), 2.59 (d, 1H, biotinyl, *J*=12.5 Hz), 2.03 (t, 2H, biotinyl, *J*=7.4 Hz), 1.60-1.15 (m, 6H, biotinyl)

HRESI-MS $C_{31}H_{41}N_9O_7S$
MW 683.79
$[M+Na]^+$ calcd 706.2747
$[M+Na]^+$ found 706.2753

5′-(6-{6-[6-(6-Biotinylamido-hexanoylamino)hexanoylamino]hexanoyl amino}hexanoylamino)-5′-deoxy-N^6-(1-naphthylmethyl)adenosine (**85**)

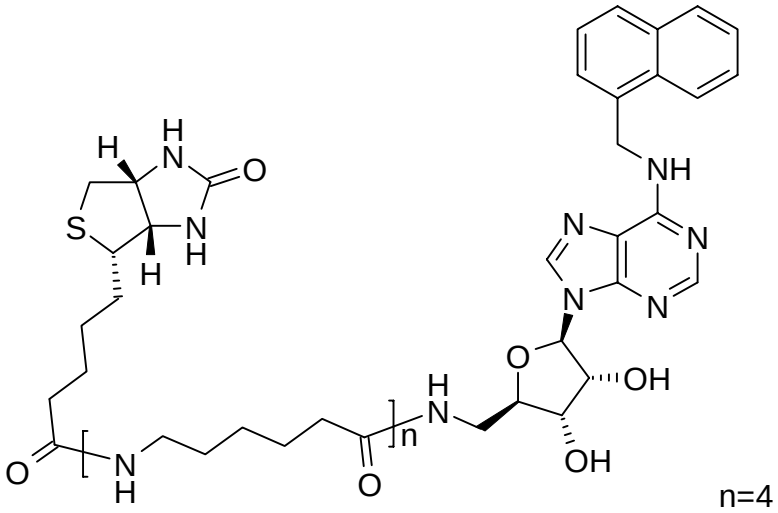

Yield 88%

^{1}H NMR (400 MHz, DMSO-d_6) = δ (ppm) 8.50 (bs, 1H, N^6H), 8.38 (bs, 1H, 8H), 8.24-8.23 (m, 2H, 2H overlapping naphthyl), 8.17 (t, 1H, NH, amide, *J*=5.4 Hz), 7.96-7.94 (m, 1H, naphthyl), 7.83-7.80 (m, 1H, naphthyl), 7.74-7.69 (m, 4H, NH, amides), 7.59-7.52 (m, 2H, naphthyl), 7.46-7.41 (m, 2H, naphthyl), 6.41 (s, 1H, NH, biotinyl), 6.35 (s, 1H, NH, biotinyl), 5.87 (d, 1H, 1′H, *J*=6.4 Hz), 5.48 (d, 1H, 3′OH, *J*=6.1 Hz), 5.26 (d, 1H, 2′OH, *J*=4.6 Hz), 5.19 (bs, 2H, CH_2, naphthylmethyl), 4.72-4.68 (m, 1H, 2′H), 4.31-4.28 (m, 1H, biotinyl), 4.14-4.10 (m, 1H, biotinyl), 4.05-4.02 (m, 1H, 3′H), 3.97-3.94 (m, 1H, 4′H), 3.11-3.06 (m, 1H, biotinyl), 3.00-2.96 (m, 8H, CH_2, hexanoyl), 2.83-2.79 (dd, 1H, biotinyl, *J*=5.1 Hz, *J*=12.5 Hz), 2.59 (d, 1H, biotinyl, *J*=12.5 Hz), 2.11 (t, 2H, biotinyl, *J*=7.4 Hz), 2.05-1.98 (m, 8H, CH_2, hexanoyl), 1.65-1.15 (m, 30H, 6H biotinyl overlapping 24H hexanoyl)

HRESI-MS $C_{55}H_{80}N_{12}O_9S$
MW 1085.39
$[M+Na]^+$ calcd 1107.5789
$[M+Na]^+$ found 1107.5774

5′-Deoxy-N^6-(1-naphthylmethyl)-5′-[5-(3a*S*, 4*S*, 5*S*, 6a*R*)(2,5-dioxo-octahydro-5λ^4-thieno[3,4-*d*]imidazol-4-yl)pentanoylamino]adenosine (**86**)

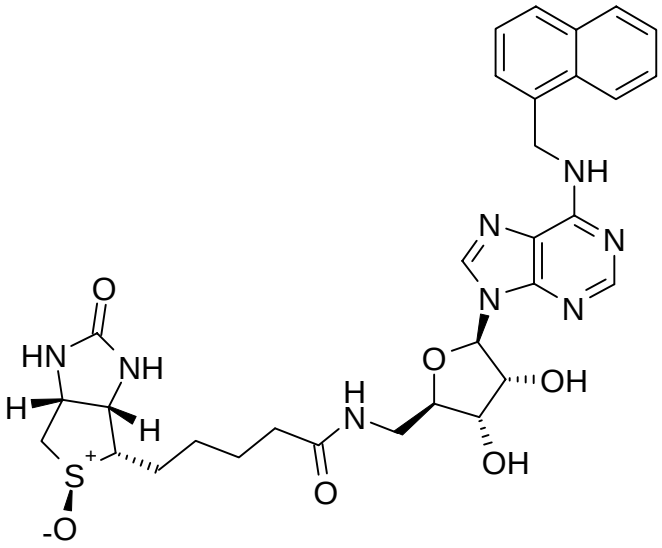

Yield 97%

^{1}H NMR (400 MHz, DMSO-d_6) = δ (ppm) 8.49 (bs, 1H, N^6H), 8.37 (bs, 1H, 8H), 8.25-8.23 (m, 2H, 2H overlapping naphthyl), 8.16 (t, 1H, NH, amide, *J*=5.6 Hz), 7.96-7.94 (m, 1H, naphthyl), 7.83-7.80 (m, 1H, naphthyl), 7.59-7.52 (m, 2H, naphthyl), 7.46-7.41 (m, 2H, naphthyl), 6.78 (s, 1H, NH, biotinyl), 6.67 (s, 1H, NH, biotinyl), 5.88 (d, 1H, 1′H, *J*=6.4 Hz), 5.46 (d, 1H, 3′OH, *J*=6.1 Hz), 5.24 (d, 1H, 2′OH, *J*=4.8 Hz), 5.19 (bs, 2H, CH_2, naphthylmethyl), 4.72-4.67 (m, 1H, 2′H), 4.45-4.41 (m, 1H, biotinyl), 4.33-4.29 (m, 1H, biotinyl), 4.07-4.03 (m, 1H, 3′H), 3.98-3.95 (m, 1H, 4′H), 2.93-2.84 (m, 2H, biotinyl), 2.15 (t, 2H, biotinyl, *J*=7.4 Hz), 1.73-1.33 (m, 6H, biotinyl)

HRESI-MS $C_{31}H_{36}N_8O_6S$
MW 648.75
$[M+H]^+$ calcd 649.2558
$[M+H]^+$ found 649.2561

5′-Deoxy-N^6-(1-naphthylmethyl)-5′-{4-[5-(3a*S*, 4*S*, 5*S*, 6a*R*)(2,5-dioxo-octahydro-5λ^4-thieno[3,4-*d*]imidazol-4-yl)pentanoylamino]butanoylamino}-adenosine (**87**)

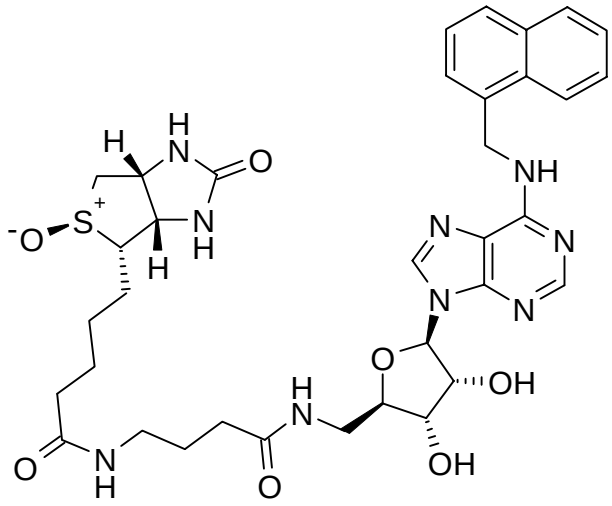

Yield 97%

^{1}H NMR (400 MHz, DMSO-d_6) = δ (ppm) 8.51 (bs, 1H, N^6H), 8.39 (bs, 1H, 8H), 8.25-8.20 (m, 3H, naphthyl overlapping 2H overlapping amide), 7.96-7.94 (m, 1H, naphthyl), 7.83-7.78 (m, 2H, naphthyl overlapping amide), 7.60-7.52 (m, 2H, naphthyl), 7.46-7.41 (m, 2H, naphthyl), 6.79 (s, 1H, NH, biotinyl), 6.69 (s, 1H, NH, biotinyl), 5.87 (d, 1H, 1′H, *J*=6.6 Hz), 5.45 (d, 1H, 3′OH, *J*=6.1 Hz), 5.27 (d, 1H, 2′OH, *J*=4.6 Hz), 5.19 (bs, 2H, CH_2, naphthylmethyl), 4.72-4.68 (m, 1H, 2′H), 4.45-4.41 (m, 1H, biotinyl), 4.32-4.28 (m, 1H, biotinyl), 4.05-4.02 (m, 1H, 3′H), 3.97-3.94 (m, 1H, 4′H), 3.04-2.99 (m, 2H, CH_2, butanoyl), 2.92-2.87 (m, 2H, biotinyl), 2.13 (t, 2H, biotinyl, *J*=7.4 Hz), 2.05 (t, 2H, CH_2, butanoyl, *J*=7.3 Hz), 1.64-1.32 (m, 8H, 6H biotinyl overlapping 2H butanoyl)

HRESI-MS $C_{35}H_{43}N_9O_7S$
MW 733.85
$[M+H]^+$ calcd 734.3085
$[M+H]^+$ found 734.3093

5′-Deoxy-N^6-(1-naphthylmethyl)-5′-{6-[5-(3a*S*, 4*S*, 5*S*, 6a*R*)(2,5-dioxo-octahydro-5λ^4-thieno[3,4-*d*]imidazol-4-yl)pentanoylamino]hexanoylamino}-adenosine (**88**)

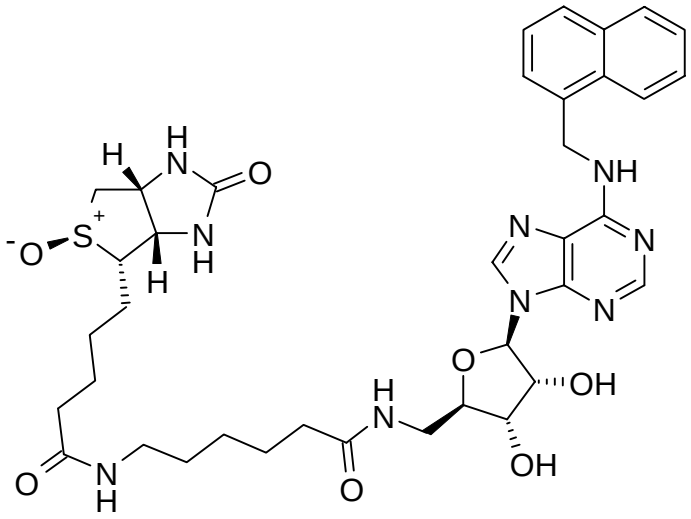

Yield 95%

^{1}H NMR (400 MHz, DMSO-d_6) = δ (ppm) 8.51 (bs, 1H, N^6H), 8.39 (bs, 1H, 8H), 8.25-8.23 (m, 2H, naphthyl overlapping 2H), 8.18 (t, 1H, NH, amide, *J*=5.4 Hz), 7.96-7.94 (m, 1H, naphthyl), 7.83-7.81 (m, 1H, naphthyl), 7.74 (t, 1H, NH, amide, *J*=5.6 Hz), 7.60-7.52 (m, 2H, naphthyl), 7.47-7.41 (m, 2H, naphthyl), 6.80 (s, 1H, NH, biotinyl), 6.69 (s, 1H, NH, biotinyl), 5.88 (d, 1H, 1′H, *J*=6.4 Hz), 5.20 (bs, 2H, CH_2, naphthylmethyl), 4.72-4.70 (m, 1H, 2′H), 4.47-4.43 (m, 1H, biotinyl), 4.34-4.30 (m, 1H, biotinyl), 4.05-4.03 (m, 1H, 3′H), 3.98-3.96 (m, 1H, 4′H), 3.02-2.97 (m, 2H, CH_2, hexanoyl), 2.98-2.86 (m, 2H, biotinyl), 2.12 (t, 2H, biotinyl, *J*=7.4 Hz), 2.05 (t, 2H, CH_2, hexanoyl, *J*=7.4 Hz), 1.55-1.18 (m, 12H, 6H biotinyl overlapping 6H hexanoyl)

HRESI-MS $C_{37}H_{47}N_9O_7S$
MW 761.91
$[M+H]^+$ calcd 762.3398
$[M+H]^+$ found 762.3397

N^6-{2-[2-(2-{11-[5-(3a*S*, 4*S*, 5*S*, 6a*R*)(2,5-dioxo-octahydro-5λ^4-thieno[3,4-*d*]imidazol-4-yl)-pentanoylamino]undecanoylamino}ethoxy)ethoxy]ethyl}-adenosine (**89**)

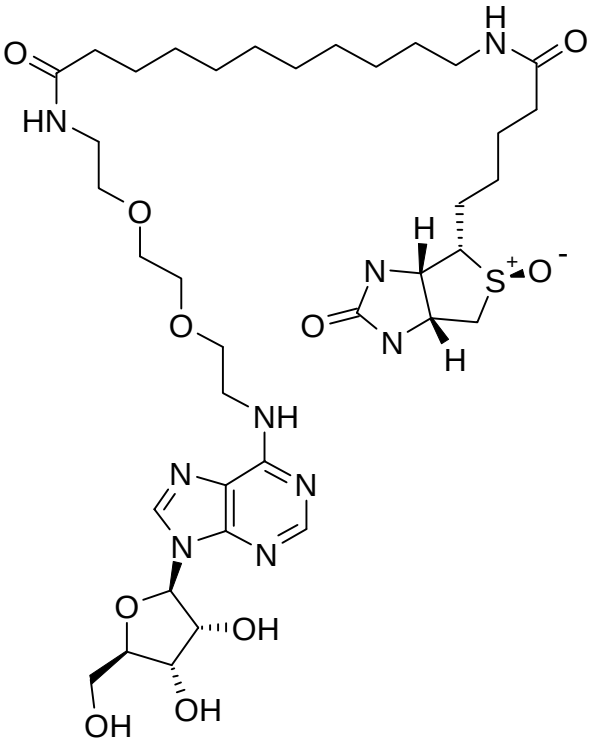

Yield 80%

^{1}H NMR (400 MHz, DMSO-d_6) = δ (ppm) 8.36 (s, 1H, 8H), 8.22 (s, 1H, 2H), 7.81 (t, 1H, NH, *J*=5.6 Hz), 7.78 (bs, 1H, NH), 7.73 (t, 1H, NH, *J*=5.3 Hz), 6.79 (s, 1H, NH, biotinyl), 6.69 (s, 1H, NH, biotinyl), 5.89 (d, 1H, 1´H, *J*=6.4 Hz), 5.45 (d, 1H, 3´OH, *J*=6.4 Hz), 5.41-5.38 (m, 1H, 5´OH), 5.20 (d, 1H, 2´OH, *J*=4.6 Hz), 4.62-4.58 (m, 1H, 2´H), 4.47-4.42 (m, 1H, biotinyl), 4.34-4.30 (m, 1H, biotinyl), 4.16-4.13 (m, 1H, 3´H), 3.97-3.95 (m, 1H, 4´H), 3.70-3.48 (m, 8H, 5´CH_2 overlapping CH_2 1,8-diamino-3,6-dioxa-octyl), 3.39-3.35 (m, 2H, CH_2, 1,8-diamino-3,6-dioxaoctyl), 3.19-3.14 (m, 2H, CH_2, 1,8-diamino-3,6-dioxa-octyl), 3.02-2.97 (m, 2H, CH_2, 1,8-diamino-3,6-dioxa-octyl), 2.94-2.86 (m, 2H, biotinyl), 2.08-2.01 (m, 4H, biotinyl overlapping CH_2 undecanoyl), 1.78-1.70 (m, 2H, CH_2, undecanoyl), 1.57-1.34 (m, 6H, biotinyl), 1.22 (s, 16H, CH_2, undecanoyl)

HRESI-MS $C_{37}H_{61}N_9O_{10}S$ $[M+Na]^+$ calcd 897.4057
MW 824.02 $[M+Na]^+$ found 897.4069

5′-Deoxy-N^6-(1-naphthylmethyl)-5′-(6-{6-[5-(3a*S*, 4*S*, 5*S*, 6a*R*)(2,5-dioxo-octahydro-5λ^4-thieno[3,4-*d*]imidazol-4-yl)-pentanoylamino]hexanoyl-amino}hexanoylamino)adenosine (**90**)

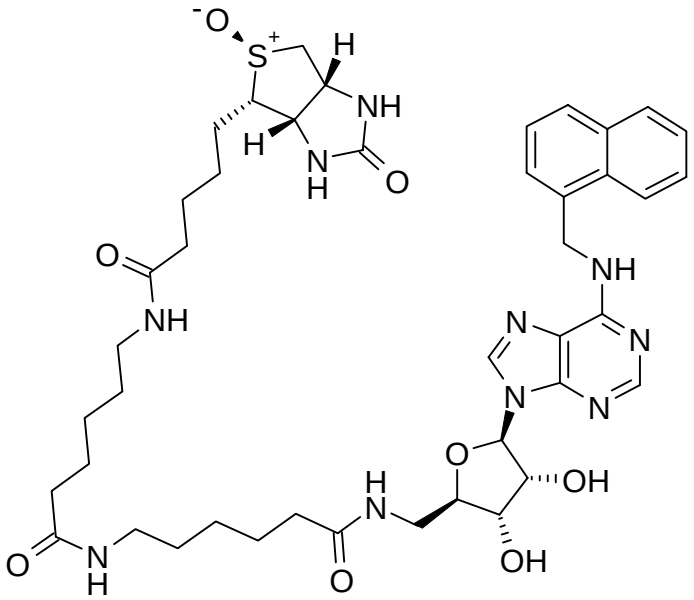

Yield 91%

^{1}H NMR (400 MHz, DMSO-d_6) = δ (ppm) 8.51 (bs, 1H, N^6H), 8.38 (bs, 1H, 8H), 8.24-8.17 (m, 3H, naphthyl overlapping 2H overlapping amide), 7.96-7.94 (m, 1H, naphthyl), 7.83-7.81 (m, 1H, naphthyl), 7.75-7.69 (m, 2H, NH, amides), 7.60-7.53 (m, 2H, naphthyl), 7.46-7.41 (m, 2H, naphthyl), 6.79 (s, 1H, NH, biotinyl), 6.69 (s, 1H, NH, biotinyl), 5.87 (d, 1H, 1′H, *J*=6.4 Hz), 5.49 (d, 1H, 3′OH, *J*=5.6 Hz), 5.26 (bs, 1H, 2′OH), 5.18 (bs, 2H, CH_2, naphthylmethyl), 4.72-4.68 (m, 1H, 2′H), 4.46-4.43 (m, 1H, biotinyl), 4.34-4.30 (m, 1H, biotinyl), 4.04-4.03 (m, 1H, 3′H), 3.97-3.94 (m, 1H, 4′H), 3.00-2.86 (m, 6H, CH_2, 2H biotinyl overlapping 4H hexanoyl), 2.11 (t, 2H, biotinyl, *J*=7.4 Hz), 2.08-1.98 (m, 4H, CH_2, hexanoyl), 1.55-1.15 (m, 18H, 6H biotinyl overlapping 12H hexanoyl)

HRESI-MS $C_{43}H_{58}N_{10}O_8S$
MW 875.07
$[M+Na]^+$ calcd 897.4057
$[M+Na]^+$ found 897.4069

N^6-[2-(6-{2-(2*S*)-[5-(3a*S*, 4*S*, 5*S*, 6a*R*)(2,5-dioxo-octahydro-5λ^4-thieno[3,4-*d*]imidazol-4-yl)pentanoylamino]-3-phenylpropionylamino}hexanoylamino)-ethyl]adenosine (**91**)

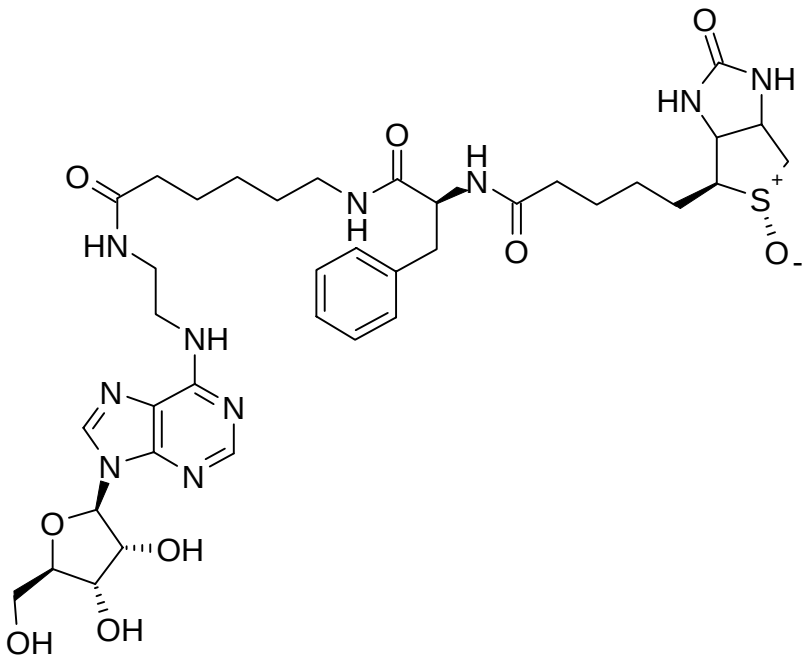

Yield 71%

^{1}H NMR (400 MHz, DMSO-d_6) = δ (ppm) 8.36 (s, 1H, 8H), 8.22 (s, 1H, 2H), 8.03 (d, 1H, NH, *J*=8.7 Hz), 7.94-7.86 (m, 3H, NH, amides), 7.27-7.15 (m, 5H, phenyl), 6.79 (s, 1H, NH, biotinyl), 6.70 (s, 1H, NH, biotinyl), 5.89 (d, 1H, 1´H, *J*=6.1 Hz), 5.45-5.40 (m, 2H, 3´OH overlapping 5´OH), 5.38-5.36 (dd, 2H, CH_2, phenylalanyl, *J*=2.1 Hz, 6.0 Hz), 5.20 (d, 1H, 2´OH, *J*=4.6), 4.63-4.58 (m, 1H, 2´H), 4.48-4.43 (m, 2 H, biotinyl overlapping phenylalanyl), 4.33-4.28 (m, 1H, biotinyl), 4.16-4.13 (m, 1H, 3´H), 3.98-3.95 (m, 1H, 4´H), 3.70-3.65 (m, 1H, 5´CH_2), 3.58-3.52 (m, 3H, 5´CH_2 overlapping CH_2 1,2-diaminoethyl), 3.06-2.85 (m, 4H, CH_2 hexanoyl overlapping 2H biotinyl), 2.08-2.01 (m, 4H, CH_2 hexanoyl overlapping 2H biotinyl), 1.48-1.11 (m, 12H, CH_2 hexanoyl overlapping 6H biotinyl)

HRESI-MS $C_{37}H_{52}N_{10}O_9S$
MW 812.95
$[M+H]^+$ calcd 813.3718
$[M+H]^+$ found 813.3726

N-Benzyl-3-nitro-4-{3-[2-(2-{3-[5-(3a*S*, 4*S*, 5*S*, 6a*R*)(2,5-dioxo-octahydro-5λ^4-thieno[3,4-*d*]imidazol-4-yl)pentanoylamino]propoxy}ethoxy)ethoxy]-propylamino}benzamide (**94**)

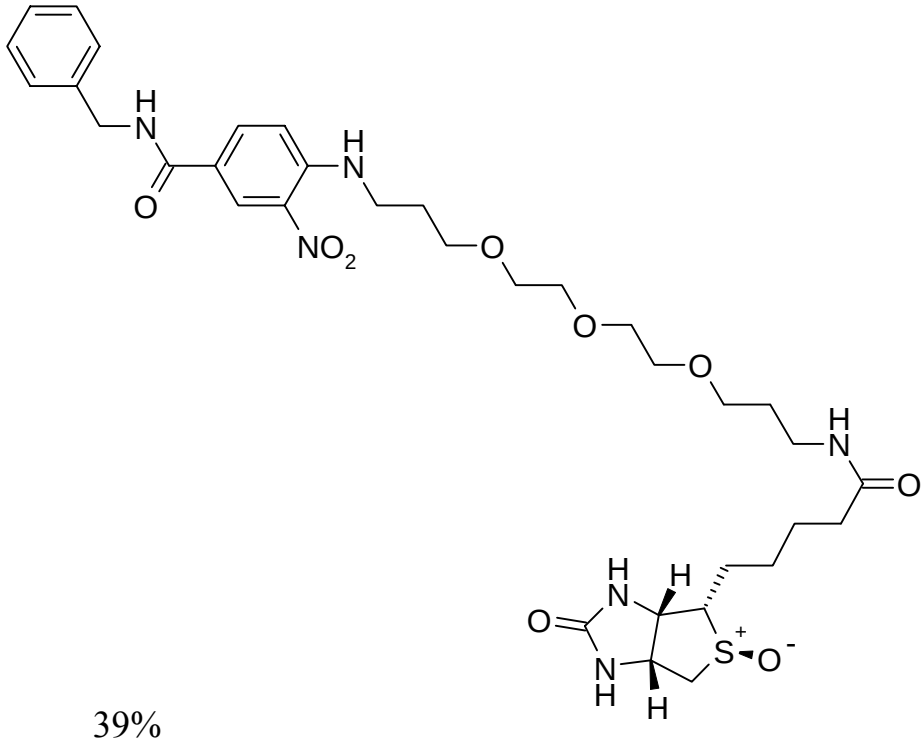

Yield 39%

^{1}H NMR (400 MHz, DMSO-d_6) = δ (ppm) 9.07 (t, 1H, NH, *J*=5.9 Hz), 8.71 (d, 1H, 4-amino-3-nitrobenzoyl, *J*=2.3 Hz), 8.52 (t, 1H, NH, *J*=5.3 Hz), 8.05-8.03 (m, 1H, 4-amino-3-nitrobenzoyl), 7.74 (t, 1H, NH, *J*=5.5 Hz), 7.35-7.30 (m, 4H, phenyl), 7.27-7.22 (m, 1H, phenyl), 7.14 (d, 1H, 4-amino-3-nitrobenzoyl, *J*=9.2 Hz), 6.78 (s, 1H, NH, biotinyl), 6.68 (s, 1H, NH, biotinyl), 4.47-4.43 (m, 3H, CH_2 benzyl overlapping 1H biotinyl), 4.34-4.30 (m, 1H, biotinyl), 3.55-3.45 (m, 14H, CH_2, 1,13-diamino-4,7,10-trioxatridecyl), 3.08-3.03 (m, 2H, CH_2, 1,13-diamino-4,7,10-trioxatridecyl), 2.94-2.86 (m, 2H, biotinyl), 2.06 (t, 2H, biotinyl, *J*=7.4 Hz), 1.91-1.85 (m, 2H, CH_2, 1,13-diamino-4,7,10-trioxatridecyl), 1.77-1.70 (m, 2H, CH_2, 1,13-diamino-4,7,10-trioxatridecyl), 1.63-1.33 (m, 6H, biotinyl)

HRESI-MS $C_{34}H_{48}N_6O_9S$ $[M+Na]^+$ calcd 739.3101
MW 716.86 $[M+Na]^+$ found 739.3079

N-Benzyl-3-nitro-4-{9-[5-(3a*S*, 4*S*, 5*S*, 6a*R*)(2,5-dioxo-octahydro-5λ^4-thieno[3,4-*d*]imidazol-4-yl)pentanoylamino]nonyl-1-amino}benzamide (**95**)

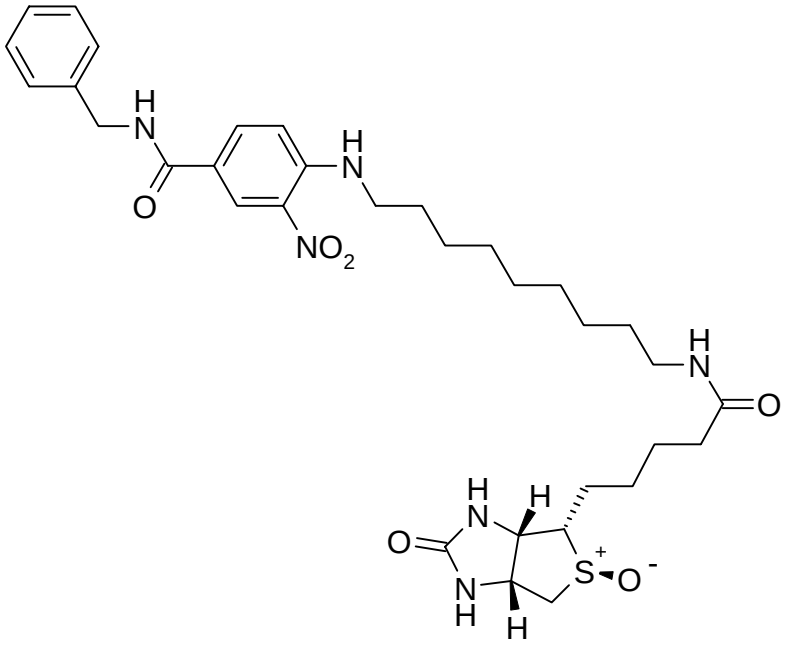

Yield 29%

^{1}H NMR (400 MHz, DMSO-d_6) = δ (ppm) 9.07 (t, 1H, NH, *J*=5.9 Hz), 8.70 (d, 1H, 4-amino-3-nitrobenzoyl, *J*=2.0 Hz), 8.38 (t, 1H, NH, *J*=5.5 Hz), 8.05-8.02 (m, 1H, 4-amino-3-nitrobenzoyl), 7.73 (t, 1H, NH, *J*=5.3 Hz), 7.33-7.22 (m, 5H, phenyl), 7.13 (d, 1H, 4-amino-3-nitrobenzoyl, *J*=9.2 Hz), 6.79 (s, 1H, NH, biotinyl), 6.69 (s, 1H, NH, biotinyl), 4.47-4.43 (m, 3H, CH_2 benzyl overlapping 1H biotinyl), 4.34-4.30 (m, 1H, biotinyl), 3.03-2.98 (m, 2H, CH_2, 1,9-diaminononyl), 2.94-2.86 (m, 2H, biotinyl), 2.06 (t, 2H, biotinyl, *J*=7.4 Hz), 1.77-1.70 (m, 2H, CH_2, 1,9-diaminononyl), 1.66-1.26 (m, 20H, 6H biotinyl overlapping 14H 1,9-diaminononyl)

HRESI-MS $C_{33}H_{46}N_6O_6S$
MW 654.84
$[M+Na]^+$ calcd 677.3097
$[M+Na]^+$ found 677.3087

N-Benzyl-3-nitro-4-{8-[5-(3a*S*, 4*S*, 5*S*, 6a*R*)(2,5-dioxo-octahydro-5λ^4-thieno[3,4-*d*]imidazol-4-yl)pentanoylamino]octyl-1-amino}benzamide (**96**)

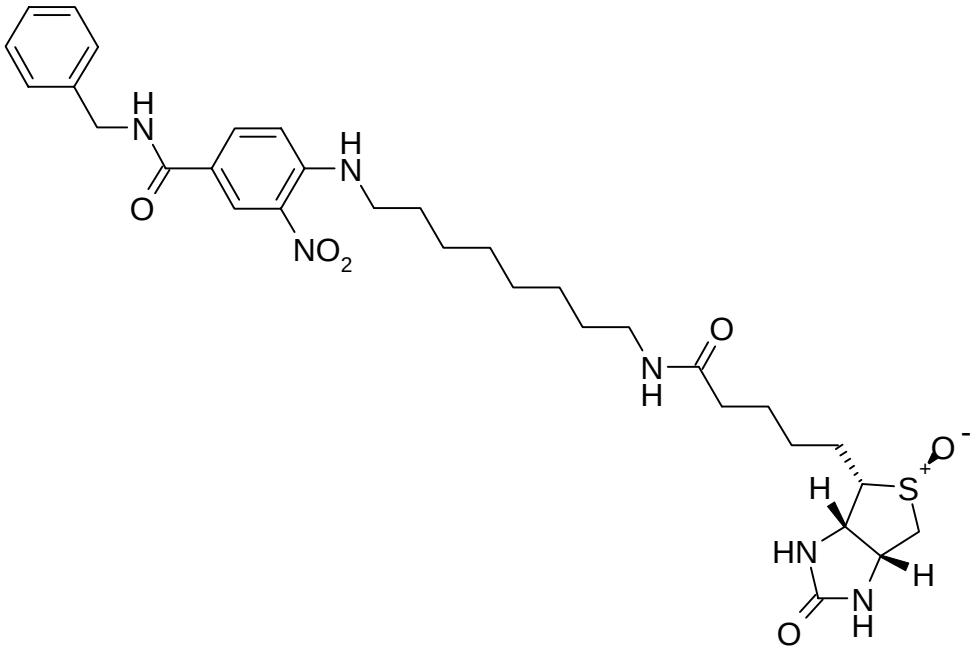

Yield 43%

^{1}H NMR (400 MHz, DMSO-d_6) = δ (ppm) 9.07 (t, 1H, NH, *J*=5.9 Hz), 8.70 (d, 1H, 4-amino-3-nitrobenzoyl, *J*=2.0 Hz), 8.38 (t, 1H, NH, *J*=5.7 Hz), 8.05-8.02 (m, 1H, 4-amino-3-nitrobenzoyl), 7.74 (t, 1H, NH, *J*=5.6 Hz), 7.35-7.30 (m, 4H, phenyl), 7.26-7.22 (m, 1H, phenyl), 7.14 (d, 1H, 4-amino-3-nitrobenzoyl, *J*=9.2 Hz), 6.79 (s, 1H, NH, biotinyl), 6.69 (s, 1H, NH, biotinyl), 4.47-4.43 (m, 3H, CH_2 benzyl overlapping 1H biotinyl), 4.34-4.30 (m, 1H, biotinyl), 3.03-2.99 (m, 2H, CH_2, 1,8-diamino-octyl), 2.94-2.86 (m, 2H, biotinyl), 2.06 (t, 2H, CH_2, biotinyl, *J*=7.4 Hz), 1.77-1.70 (m, 2H, CH_2, 1,8-diamino-octyl), 1.66-1.27 (m, 18H, 6H biotinyl overlapping 12H 1,8-diamino-octyl)

HRESI-MS $C_{32}H_{44}N_6O_6S$
MW 640.81
$[M+Na]^+$ calcd 663.2941
$[M+Na]^+$ found 663.2918

5′-Deoxy-N^6-(1-naphthylmethyl)-5′-{3-nitro-4-[8-(3a*S*, 4*S*, 5*S*, 6a*R*)(2,5-dioxo-octahydro-5λ^4-thieno[3,4-*d*]imidazol-4-yl)pentanoylamino]octyl-1-aminobenzoylamino}adenosine (**97**)

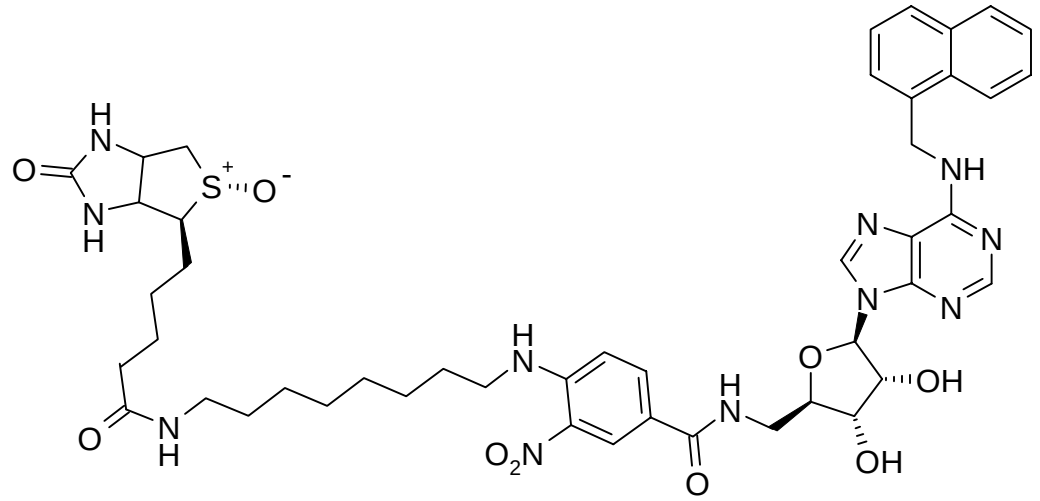

Yield 21%

^{1}H NMR (400 MHz, DMSO-d_6) = δ (ppm) 8.70 (t, 1H, NH, *J*=5.5 Hz), 8.65 (d, 1H, 4-amino-3-nitrobenzoyl, *J*=2.0 Hz), 8.44-8.35 (m, 3H, N^6H overlapping 8H overlapping NH), 8.24-8.22 (m, 1H, naphthyl), 8.18 (s, 1H, 2H), 8.00-7.94 (m, 2H, 4-amino-3-nitrobenzoyl overlapping naphthyl), 7.83-7.80 (m, 1H, naphthyl), 7.73 (t, 1H, NH, amide, *J*=5.6 Hz), 7.59-7.52 (m, 2H, naphthyl), 7.46-7.40 (m, 2H, naphthyl), 7.11 (d, 1H, 4-amino-3-nitrobenzoyl, *J*=9.4 Hz), 6.78 (s, 1H, NH, biotinyl), 6.68 (s, 1H, NH, biotinyl), 5.90 (d, 1H, 1′H, *J*=6.1 Hz), 5.48 (d, 1H, 3′OH, *J*=6.1 Hz), 5.28 (d, 1H, 2′OH, *J*=4.8 Hz), 5.18 (bs, 2H, CH_2, naphthylmethyl), 4.79-4.77 (m, 1H, 2′H), 4.47-4.43 (m, 1H, biotinyl), 4.34-4.31 (m, 1H, biotinyl), 4.21-4.18 (m, 1H, 3′H), 4.09-4.05 (m, 1H, 4′H), 3.66-3.51 (m, 2H, CH_2, 1,8-diamino-octyl), 3.03-2.98 (m, 2H, 1,8-diamino-octyl), 2.94-2.86 (m, 2H, biotinyl), 2.06 (t, 2H, biotinyl, *J*=7.4 Hz), 1.63-1.60 (m, 2H, CH_2, 1,8-diamino-octyl), 1.53 (t, 2H, CH_2, 1,8-diamino-octyl, *J*=7.4 Hz), 1.46-1.23 (m, 14H, 6H biotinyl overlapping 8H 1,8-diamino-octyl)

HRESI-MS $C_{46}H_{57}N_{11}O_9S$
MW 940.10
$[M+H]^+$ calcd 940.4139
$[M+H]^+$ found 940.4152

N-Benzyl-4-[3-(2-{2-[3-(bis-cyanomethyl-amino)propoxy]ethoxy}ethoxy)-propylamino]-3-nitrobenzamide (**98**); side-product of **94**

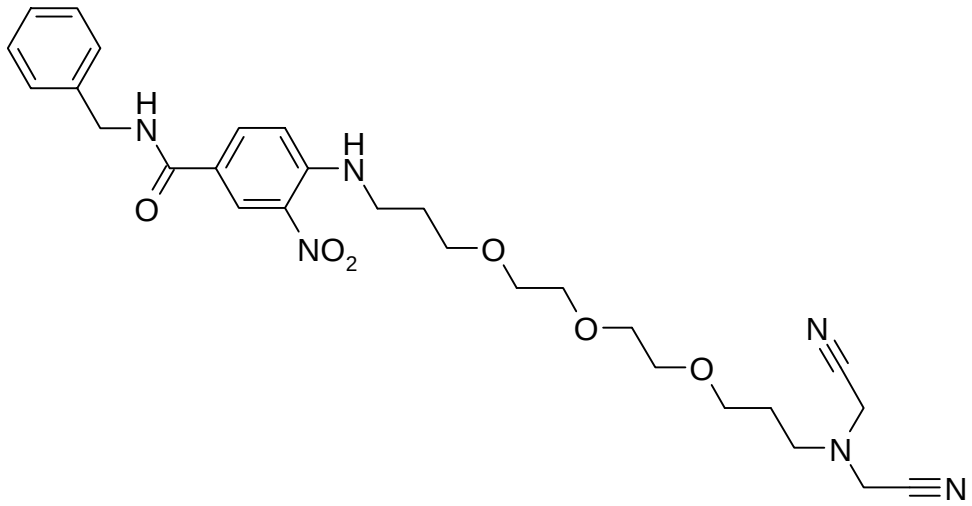

Yield 12%

^{1}H NMR (400 MHz, DMSO-d_6) δ (ppm) = 9.06 (t, 1H, NH, *J*=5.9 Hz), 8.71 (d, 1H, 4-amino-3-nitrobenzoyl, *J*=2.3 Hz), 8.52 (t, 1H, NH, *J*=5.3 Hz), 8.06-8.03 (m, 1H, 4-amino-3-nitrobenzoyl), 7.35-7.22 (m, 5H, phenyl), 7.14 (d, 1H, 4-amino-3-nitro-benzoyl, *J*=9.2 Hz), 4.47 (d, 2H, CH_2 benzyl, *J*=5.9 Hz), 3.83 (s, 4H, cyanomethyl), 3.55-3.46 (m, 14H, CH_2, 1,13-diamino-4,7,10-trioxatridecyl), 2.62 (t, 2H, CH_2, 1,13-diamino-4,7,10-trioxatridecyl, *J*=7.2 Hz), 1.91-1.85 (m, 2H, CH_2, 1,13-diamino-4,7,10-trioxatridecyl), 1.70-1.61 (m, 2H, CH_2, 1,13-diamino-4,7,10-trioxatridecyl)

HRESI-MS $C_{28}H_{36}N_6O_6$
MW 552.64
$[M+Na]^+$ calcd 575.2594
$[M+Na]^+$ found 575.2617

5′{4-[8(Bis-cyanomethyl-amino)octylamino]-3-nitrobenzoylamine}-5′-deoxy-N^6-(1-naphthylmethyl)adenosine (**99**); side-product of **97**

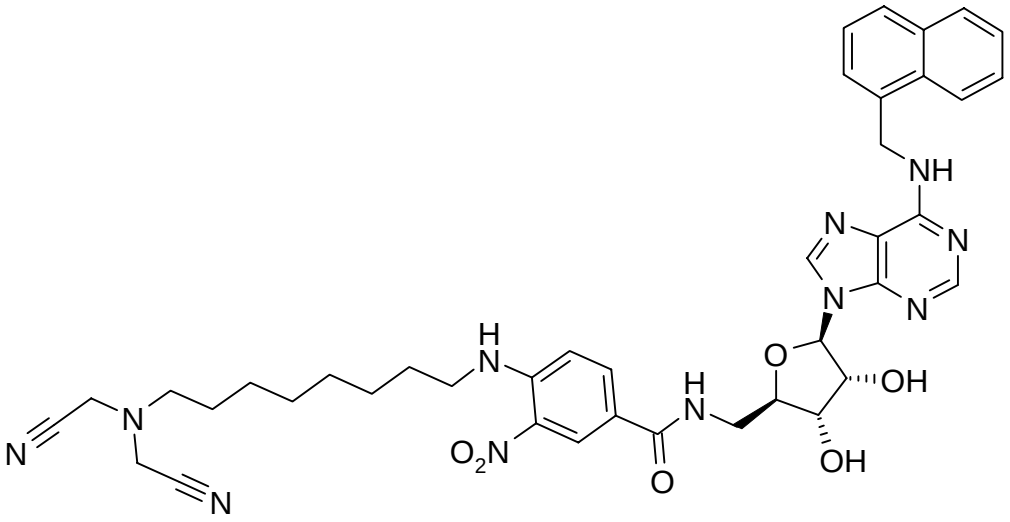

Yield 29%

^{1}H NMR (400 MHz, DMSO-d_6) δ (ppm) = 8.70 (t, 1H, NH, *J*=5.9 Hz), 8.65 (d, 1H, 4-amino-3-nitrobenzoyl, *J*=2.0 Hz), 8.44-8.35 (m, 3H, N^6H overlapping 8H overlapping NH), 8.24 (d, 1H, naphthyl, *J*=7.6 Hz), 8.18 (s, 1H, 2H), 8.00-7.96 (m, 2H, 4-amino-3-nitrobenzoyl overlapping naphthyl), 7.83-7.81 (m, 1H, naphthyl), 7.59-7.52 (m, 2H, naphthyl), 7.44-7.41 (m, 2H, naphthyl), 7.11 (d, 1H, 4-amino-3-nitrobenzoyl, *J*=9.2 Hz), 5.90 (d, 1H, 1′H, *J*=5.9 Hz), 5.48 (d, 1H, 3′OH, *J*=6.1 Hz), 5.28 (d, 1H, 2′OH, *J*=4.6 Hz), 5.19 (bs, 2H, CH_2, naphthyl-methyl), 4.79-4.77 (m, 1H, 2′H), 4.21-4.20 (m, 1H, 3′H), 4.09-4.06 (m, 1H, 4′H), 3.82 (s, 4H, cyanomethyl), 3.65-3.51 (m, 4H, CH_2, 1,8-diamino-octyl), 1.62 (t, 2H, CH_2, 1,8-diamino-octyl, *J*=6.9 Hz), 1.43 (t, 2H, CH_2, 1,8-diamino-octyl, *J*=6.9 Hz), 1.37-1.23 (m, 8H, CH_2, 1,8-diamino-octyl)

HRESI-MS $C_{40}H_{45}N_{11}O_6$
MW 775.87
$[M+Na]^+$ calcd 798.3452
$[M+Na]^+$ found 798.3451

Biotin Labeling of Other Molecules Bearing an Amino Functionality-*N*-{4-[4-(2-Methoxyphenyl)piperazin-1-yl]butyl}biotinamide (**101**)

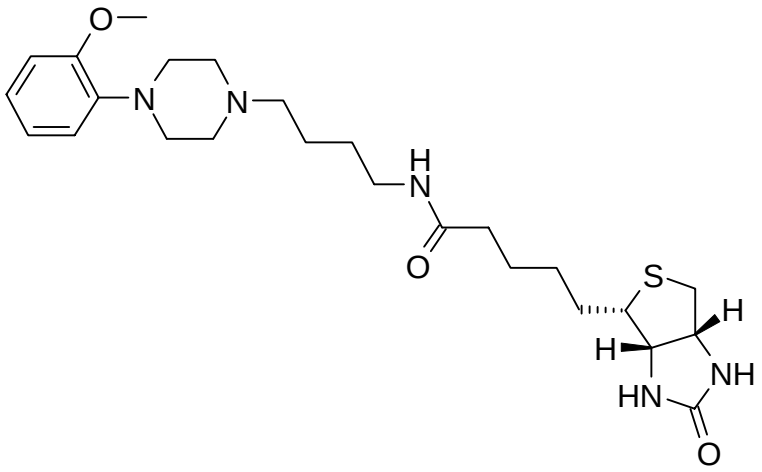

101 was obtained following **general procedures F**, **C_1**, and **D_1** (for **72**, **78-80**, and **85**) described above.

Yield 90%

^{1}H NMR (400 MHz, DMSO-d_6) = δ (ppm) 7.75 (t, 1H, NH, amide, *J*=5.5 Hz), 6.96-6.90 (m, 2H, phenyl), 6.88-6.84 (m, 2H, phenyl), 6.40 (bs, 1H, NH, biotinyl), 6.34 (bs, 1H, NH, biotinyl), 4.31-4.28 (m, 1H, biotinyl), 4.14-4.11 (m, 1H, biotinyl), 3.76 (s, 3H, methoxy), 3.12-3.08 (m, 1H, biotinyl), 3.07-3.02 (m, 2H, CH_2, butyryl), 2.94 (bs, 4H, CH_2, piperazinyl), 2.84-2.79 (dd, 1H, biotinyl, *J*=5.1 Hz, 12.5 Hz), 2.59 (d, 1H, biotinyl, *J*=12.5 Hz), 2.48 (bs, 4H, CH_2, piperazinyl), 2.30 (t, 2H, CH_2, butyryl, *J*= 6.6 Hz), 2.05 (t, 2H, CH_2, biotinyl, *J*=7.4 Hz), 1.66-1.24 (m, 10H, 6H biotinyl overlapping 4H butyryl)

^{13}C NMR (101 MHz, DMSO-d_6) = δ (ppm) 173.60, 163.92, 152.84, 142.02, 123.48, 121.80, 118.86, 112.74, 61.98, 60.10, 58.48, 56.30, 56.18, 53.74, 50.78, 40.62, 39.35, 39.20, 36.11, 31.13, 29.09, 28.86, 27.88, 26.21, 24.33

HRESI-MS $C_{25}H_{39}N_5O_3S$ $[M+H]^+$ calcd 490.2825
MW 489.69 $[M+H]^+$ found 490.2849

5′-Azido-5′-deoxyguanosine (**106**)

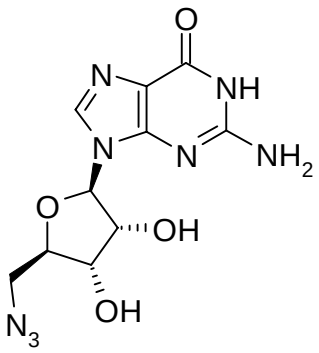

To a stirred solution of guanine-9-β-D-ribofuranoside (10.0 g, 35 mmol) in anhydrous acetone (215 mL) 2,2-dimethoxypropane (21.4 mL, 175 mmol) and p-toluensulfonic acid monohydrate (6.7 g, 35 mmol) were added[16]. After 4 h, additional 2,2-dimethoxypropane (2 mL, 16 mmol) was added to the reaction mixture, because of incomplete conversion of **102** to **103**. After 24 h the resulting solution was poured slowly into stirred aqueous 0.5 M $NaHCO_3$ (108 mL). The obtained suspension was concentrated in vacuo and extracted with trichloromethane (4 times 30 mL). The combined layers were washed with brine (20 mL), dried with Na_2SO_4, and finally evaporated in vacuo yielding a white solid of 2′,3′-*O*-isopropylidene-guanosine (**103)**. Yield 55%.

103 (4.1 g, 12.5 mmol) was suspended in pyridine abs. (62.5 mL). Over a time period of 15 min tosylchloride was added stepwise to the stirred reaction mixture. After 20 min the solution (light yellow) turned into a highly viscous gel. The gel was further stirred for 30 min at ambient temperature and subsequently stored in the refrigerator for 4 d. Pyridine was evaporated in vacuo[17]. The resulting solid was suspended in saturated $NaHCO_3$ solution, filtered off and washed with $NaHCO_3$ solution, water, EtOH, and ether providing 2′,3′-*O*-isopropylidene-5′-*O*-tosylguanosine (**104**) as a white solid. Yield 88%.

104 was suspended in 50% formic acid and stirred for 7 d at ambient temperatures[17]. The obtained solution was evaporated in vacuo. The resulting resin like slurry was suspended in EtOH and stored for 3 d in the refrigerator. The corresponding white solid was filtered off and washed with ethanol and ether furnishing 5′-deoxy-5′-*O*-tosylguanosine (**105**). Yield 86%.

To a solution of **105** (1.73 g, 4 mmol) in DMF (45 mL) NaN_3 (1.3 g, 20 mmol) was added. The resulting reaction mixture was stirred for 3 d at

ambient temperature. The reaction was monitored by TLC and IR. Evaporation of the solvent and purification over silica gel with THF yielded **106** (white, amorphous solid). Due to solubility problems of **106**, traces of residual tosylate remained in the sample.

Yield 108% (including traces of residual tosylate)

^{1}H NMR (400 MHz, DMSO-d_6) = δ (ppm) 10.65 (s, 1H, NH, purine), 7.91 (s, 1H, 8H), 7.49 (d, 0.7H, tosyl, *J*=8.1 Hz), 7.13 (d, 0.7H, tosyl, *J*=7.9 Hz), 6.51 (bs, 2H, NH_2, purine), 5.73 (d, 1H, 1´H, *J*=5.9 Hz), 5.56 (d, 1H, 3´OH, *J*=5.9 Hz), 5.33 (d, 1H, 2´OH, *J*=4.6 Hz), 4.60-4.56 (m, 1H, 2´H), 4.08-4.05 (m, 1H, 3´H), 4.00-3.97 (m, 1H, 4´H), 3.69-3.64 (m, 1H, 5´CH_2), 3.54-3.50 (m, 1H, 5´CH_2), 2.29 (s, 1.1H, tosyl)

HRESI-MS $C_{10}H_{12}N_8O_4$
MW 308.26
$[M+Na]^+$ calcd 331.0879
$[M+Na]^+$ found 331.0876

5´-Amino-5´-deoxyguanosine (**107**)

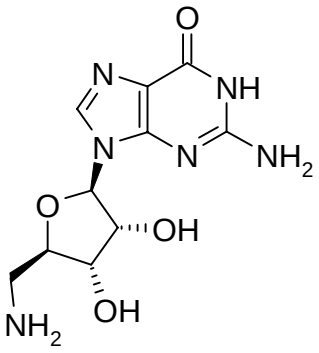

To a solution of **106** (1.3 g, 4.2 mmol) in THF/H_2O (v/v 70/30) palladium on charcoal (100 mg) was added. H_2-gas was introduced while stirring for 2 h. The catalyst was removed by filtration and the resulting solution subsequently evaporated in vacuo. The obtained solid was purified over Dowex® OH^- with MeOH/H_2O gradients yielding 5´-amino-5´-deoxy-guanosine (**107**). **107** was evaluated by NMR and high-resolution MS. Data obtained are comparable to those reported[17]. Again, traces of residual tosylate remained in the sample due to solubility problems of **107**.

5′-{2-[2-(2-Amino-ethoxy)ethoxy]ethylamino}-5′-deoxyguanosine (**108**)

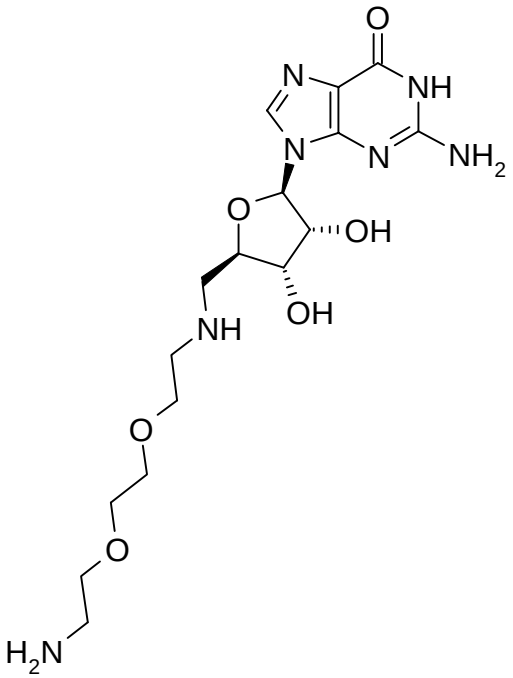

2-[2-(2-Amino-ethoxy)ethoxy]ethylamine (20 mL) was added to **105** (1.0 g, 2.3 mmol) and stirred for 7 d at ambient temperature. The resulting solution was evaporated in vacuo and purified over Dowex® OH^- with MeOH/H_2O gradients yielding **108** as a brownish, crystallized solid.

Yield 32%

^{1}H NMR (400 MHz, DMSO-d_6) = δ (ppm) 7.88 (s, 1H, 8H), 6.59 (bs, 2H, NH_2, purine), 5.67 (d, 1H, 1′H, *J*=5.9 Hz), 4.46 (t, 1H, 2′H, *J*=5.5 Hz), 4.05 (t, 1H, 3′H, *J*=4.5 Hz), 3.91-3.88 (m, 1H, 4′H), 3.76 (bbs, 2H, NH_2), 3.46 (t, 4H, CH_2, 1,8-diamino-3,6-dioxa-octyl, *J*=5.6 Hz), 3.39 (t, 4H, CH_2, 1,8-diamino-3,6-dioxa-octyl, *J*=5.6 Hz), 2.82-2.67 (m, 6H, 5′CH_2 overlapping CH_2 1,8-diamino-3,6-dioxa-octyl)

^{13}C NMR (101 MHz, DMSO-d_6) = δ (ppm) 158.04, 156.81, 153.73, 151.29, 135.58, 86.37, 83.71, 72.97, 71.33, 71.30, 69.99, 69.47, 51.17, 48.82, 40.05

HRESI-MS $C_{16}H_{27}N_7O_6$
MW 413.44
$[M+H]^+$ calcd 414.2101
$[M+H]^+$ found 414.2107

5′-[4-(2,4-Dichlorophenoxy)butanamido]-5′-deoxyguanosine (**109**)

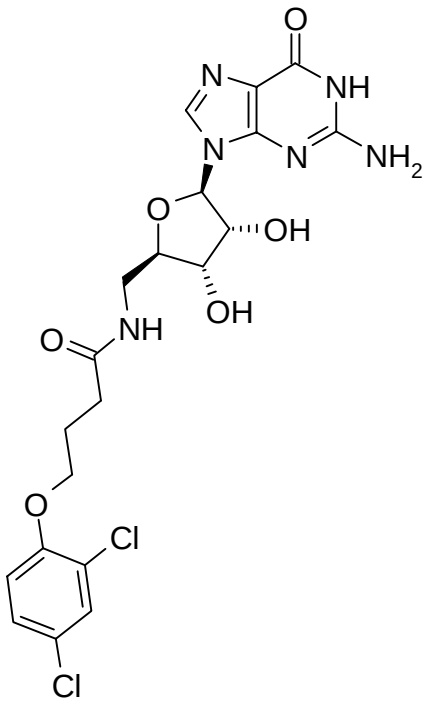

4-(2,4-Dichlorophenoxy)butyric acid was attached via the Kenner safety-catch linker to aminomethylated polystyrene (see **general procedure A** for the synthesis of simple polymer-supported acids, chapter 2.6). The polymer-bound acid residue was then activated and chemoselectively transferred to the guanosine template **107** as described above (see **general procedure C_1** and **general procedure D_2** (for compounds **72**, **78**-**80**, and **85**)).

Yield 89%

^{1}H NMR (400 MHz, DMSO-d_6) = δ (ppm) 10.63 (bs, 1H, NH, purine), 8.04 (t, 1H, NH, amide, *J*=5.6 Hz), 7.90 (s, 1H, 8H), 7.55 (d, 1H, phenyl, *J*=2.3 Hz), 7.35-7.32 (dd, 1H, phenyl, *J*=2.5 Hz, 8.9 Hz), 7.15-7.12 (m, 1H, phenyl), 6.46 (bs, 2H, NH_2, purine), 5.68 (d, 1H, 1′H, *J*=6.1 Hz), 5.42 (d, 1H, 3′OH, *J*=5.9 Hz), 5.15 (d, 1H, 2′OH, *J*=4.8 Hz), 4.43-4.39 (m, 1H, 2′H), 4.04 (t, 3H, 3′H overlapping CH_2 butyryl, *J*=6.1 Hz), 3.87-3.83 (m, 1H, 4′H), 3.49-3.42 (m, 1H, 5′CH_2), 2.28 (t, 2H, CH_2, butyryl, *J*=7.1 Hz), 1.97 (m, 2H, CH_2, butyryl)

HRESI-MS $C_{20}H_{22}Cl_2N_6O_6$ $[M+Na]^+$ calcd 535.0876
MW 513.34 $[M+Na]^+$ found 535.0873

For the biotinylation of guanosine templates spacer-modified biotin labels were prepared, activated and introduced into the nucleoside template **108** according to **general procedures E**, **F**, **C_1**, and **D_2** described above providing **110** and **111** as ivory solids. **112** and **113** (obtained as brownish, sticky solids) according to **general procedures E**, **F**, **C_1**, and **D_2** with the following deviation. The nucleoside scaffold **108** was dissolved in 1 mL DMSO, subsequently added to a slurry of 400 mg of the appropriate polymer-bound biotin label in 4 mL NMP and treated as described.

5′-(6-Biotinylamido-hexanoylamino)-5′-deoxyguanosine (**110**)

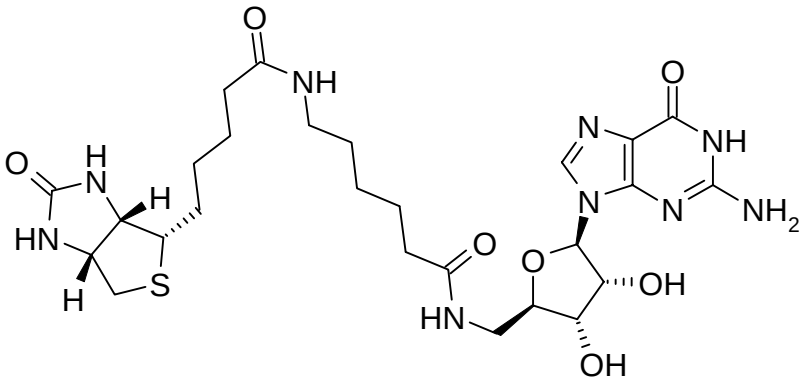

Yield 89% (including traces of tosylate)

^{1}H NMR (400 MHz, DMSO-d_6) = δ (ppm) 10.62 (bs, 1H, NH, purine), 7.94-7.87 (m, 2.5H, 8H overlapping tosyl), 7.72-7.67 (m, 1.4H, tosyl), 7.41 (t, 1H, NH, amide, *J*=7.4 Hz), 7.32 (t, 1H, NH, *J*=7.4 Hz), 6.45 (bs, 2H, NH_2, purine), 6.40 (s, 1H, NH, biotinyl), 6.34 (s, 1H, NH, biotinyl), 5.67 (d, 1H, 1′H, *J*=5.9 Hz), 5.42-5.40 (m, 1H, 3′OH), 5.14-5.12 (m, 1H, 2′OH), 4.43-4.38 (m, 1H, 2′H), 4.21-4.18 (m, 1H, biotinyl), 4.14-4.11 (m, 1H, biotinyl), 4.04-4.00 (m, 1H, 3′H), 3.85-3.81 (m, 1H, 4′H), 3.47-3.42 (m, 1H, 5′CH_2), 3.11-3.07 (m, 1H, biotinyl), 3.02-2.94 (m, 2H, CH_2, hexanoyl), 2.84-2.79 (m, 1H, biotinyl), 2.60 (d, 1H, biotinyl, *J*=12.5 Hz), 2.29 (s, 0.6H, CH_3, tosyl), 2.09-2.02 (m, 4H, CH_2 hexanoyl overlapping CH_2 biotinyl), 1.64-1.19 (m, 12H, 6H hexanoyl overlapping 6H biotinyl)

HRESI-MS $C_{26}H_{39}N_9O_7S$ $[M+Na]^+$ calcd 644.2591
MW 621.72 $[M+Na]^+$ found 644.2598

5′-(11-Biotinylamido-undecanoylamino)-5′-deoxyguanosine (**111**)

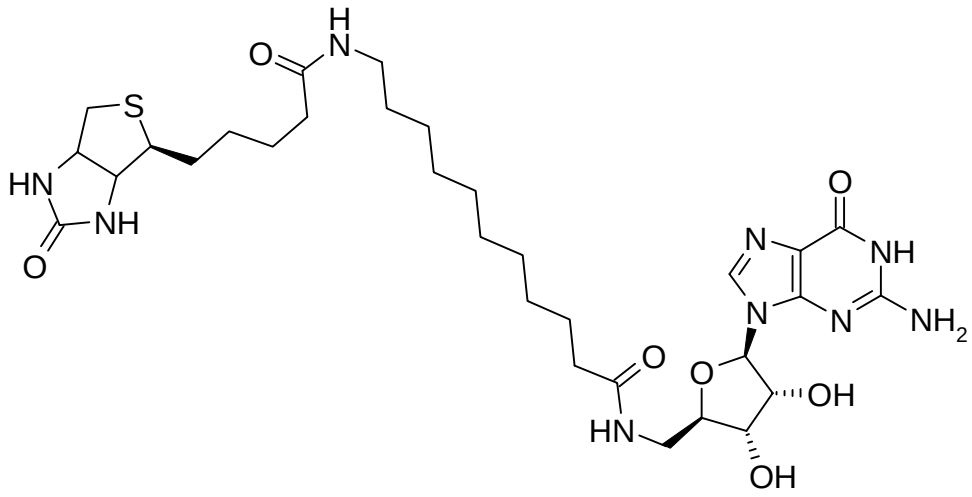

Yield 92% (including traces of tosylate)

^{1}H NMR (400 MHz, DMSO-d_6) = δ (ppm) 10.61 (bs, 1H, NH, purine), 7.92-7.87 (m, 2.2H, 8H overlapping tosyl), 7.72-7.67 (m, 1.4H, tosyl), 7.41 (t, 1H, NH, amide, *J*=7.5 Hz), 7.32 (t, 1H, NH, *J*=7.5 Hz), 6.45 (bs, 2H, NH_2, purine), 6.40 (bs, 1H, NH, biotinyl), 6.34 (bs, 1H, NH, biotinyl), 5.67 (d, 1H, 1′H, *J*=6.1 Hz), 5.41 (d, 1H, 3′OH, *J*=6.1 Hz), 5.13 (d, 1H, 2′OH, *J*=4.8 Hz), 4.42-4.38 (m, 1H, 2′H), 4.32-4.28 (m, 1H, biotinyl), 4.14-4.11 (m, 1H, biotinyl), 4.03-4.00 (m, 1H, 3′H), 3.85-3.81 (m, 1H, 4′H), 3.47-3.40 (m, 1H, 5′CH_2), 3.11-3.06 (m, 1H, biotinyl), 3.02-2.97 (m, 2H, CH_2, undecanoyl), 2.84-2.79 (dd, 1H, biotinyl, *J*=5.1 Hz, 12.5 Hz), 2.59 (d, 1H, biotinyl, *J*=12.5 Hz), 2.29 (s, 0.5H, CH_3 tosyl), 2.08-2.02 (m, 4H, CH_2, undecanoyl overlapping CH_2 biotinyl), 1.54-1.22 (m, 22H, 16H undecanoyl overlapping 6H biotinyl)

HRESI-MS $C_{31}H_{49}N_9O_7S$
MW 691.86
$[M+Na]^+$ calcd 692.3554
$[M+Na]^+$ found 692.3553

5′-(2-{2-[2-(6-Biotinylamido-hexanoylamino)ethoxy]ethoxy}ethylamino)-5′-deoxyguanosine (**112**)

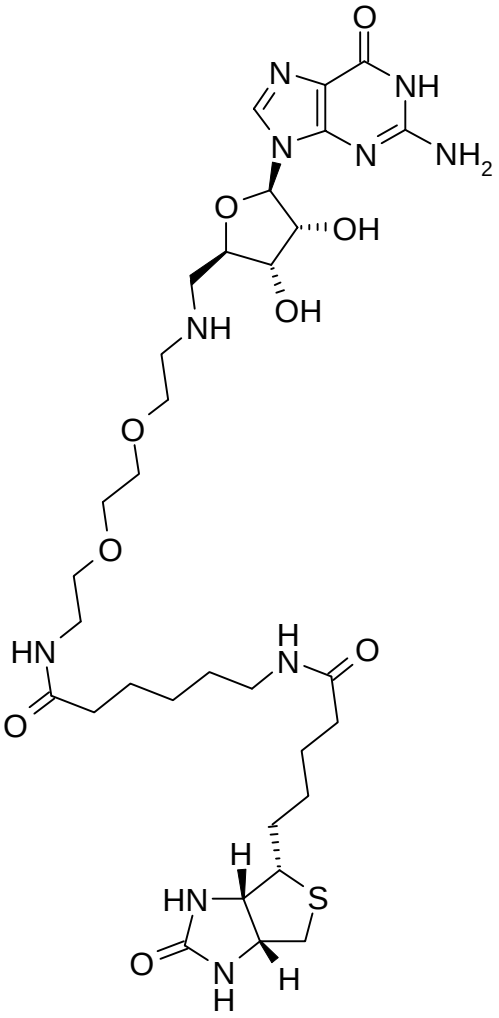

Due to solubility problems of the template **108** and the final compound **112**, **112** could not be obtained in sufficient purity for analytical evaluation. However, ^{1}H NMR revealed characteristic peaks for the purine and the sugar moiety as well as for the biotin and biotin sulfoxide moiety. MS analysis proved that a mixture of the biotin and biotin sulfoxide labeled guanosine derivative was obtained.

Yield 103% (mixture of biotin and biotin sulfoxide derivatives)

HRESI-MS $C_{32}H_{52}N_{10}O_{10}S$ (biotin sulfoxide derivative)
MW 768.90
$[M+Na]^+$ calcd 769.3667
$[M+Na]^+$ found 769.3662

5′-(2-{2-[2-(11-Biotinylamido-undecanoylamino)ethoxy]ethoxy}-ethylamino]-5′-deoxyguanosine (**113**)

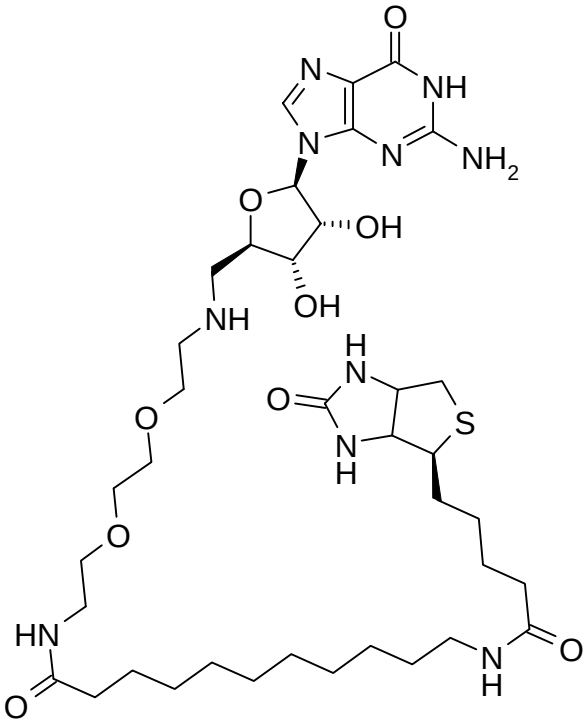

Due to solubility problems of the template **108** and the final compound **113**, **113** could not be obtained in sufficient purity for analytical evaluation. However, ^{1}H NMR revealed characteristic peaks for the purine and sugar moiety as well as for the biotin and biotin sulfoxide moiety. MS analysis proved that a mixture of the biotin and biotin sulfoxide labeled guanosine derivative was generated.

Yield 101% (mixture of biotin and biotin sulfoxide derivatives)

HRESI-MS $C_{37}H_{62}N_{10}O_9S$ (biotin derivative)
MW 823.03
$[M+Na]^+$ calcd 823.4500
$[M+Na]^+$ found 823.4500

4.7 References

(1) Wilchek, M.; Bayer, E. A. *Anal. Biochem.* **1988**, *171*, 1-32.

(2) Sakai, T.; Naidenko, O. V.; Iijima, H.; Kronenberg, M.; Koezuka, Y. *J. Med. Chem.* **1999**, *42*, 1836-1841.

(3) Shinohara, Y.; Kim, M.; Shimizu, M.; Goto, M.; Tosu, Y.; Hasegawa, Y. *Eur. J. Biochem.* **1994**, *223*, 189-194.

(4) Shinohara, Y.; Sota, H.; Kim, F.; Shimizu, M.; Gotoh, M.; Tosu, M.; Hasegawa, Y. *J. Biochem. (Tokyo)* **1995**, *117*, 1076-1082.

(5) Anzai, J.-I.; Hoshi, T.; Osa, T. *Trends Anal. Chem.* **1994**, *13*, 205-210.

(6) Karlsson, R.; Stahlberg, R. *Anal. Biochem.* **1995**, *228*, 274-280.

(7) Lackmann, M. *Methods Mol. Biol.* **2001**, *124*, 335-359.

(8) Weimar, T. *Angew. Chem. Int. Ed.* **2000**, *39*, 1219-1221.

(9) O'Shannessy, D. J.; Brigham-Burke, M.; Peck, K. *Anal. Biochem.* **1992**, *205*, 132-136.

(10) Johnsson, B.; Lofas, S.; Lindquist, G.; Edstrom, A.; Muller Hillgren, R. M.; Hansson, A. *J. Mol. Recognit.* **1995**, *8*, 125-131.

(11) Hashimoto, M.; Yang, J.; Holman, G. D. *ChemBioChem* **2001**, *2*, 52-59.

(12) Katoh, M.; Sodeoka, M. *Bioorg. Med. Chem. Lett.* **1999**, *9*, 881-884.

(13) Dubber, M.; Lindhorst, T. K. *J. Org. Chem.* **2000**, *65*, 5275-5281.

(14) Golisade, A.; Herforth, C.; Wieking, K.; Kunick, C.; Link, A. *Bioorg. Med. Chem. Lett.* **2001**, *11*, 1783-1786.

(15) Liu, F.-T.; Leonard, N. J. *J. Am. Chem. Soc.* **1979**, *101*, 996-1013.

(16) Kappler, F.; Hampton, A. *J. Med. Chem.* **1990**, *33*, 2545-2551.

(17) Schattka, K.; Jastorff, B. *Chem. Ber.* **1972**, *105*, 3824-3832.

(18) Hashimoto, M.; Liu, Y.; Fang, K.; Li, H. Y.; Campiani, G.; Nakanishi, K. *Bioorg. Med. Chem.* **1999**, *7*, 1181-1194.

5 Summary

The objective of this work was focused on the synthesis of nucleoside libraries of 5′,N^6- and 3′,N^6-disubstituted adenosines as inhibitors of the *Plasmodium falciparum* pathogen, ready for biological testing without the demand for chromatographic purification.

Novel 5′,N^6- and 3′,N^6-disubstituted adenosine derivatives with unusual substitution pattern were obtained applying an efficient (convergent) polymer-assisted solution-phase (PASP) protocol, exemplarily outlined below with the synthesis of 5′,N^6-disubstituted adenosines(*).

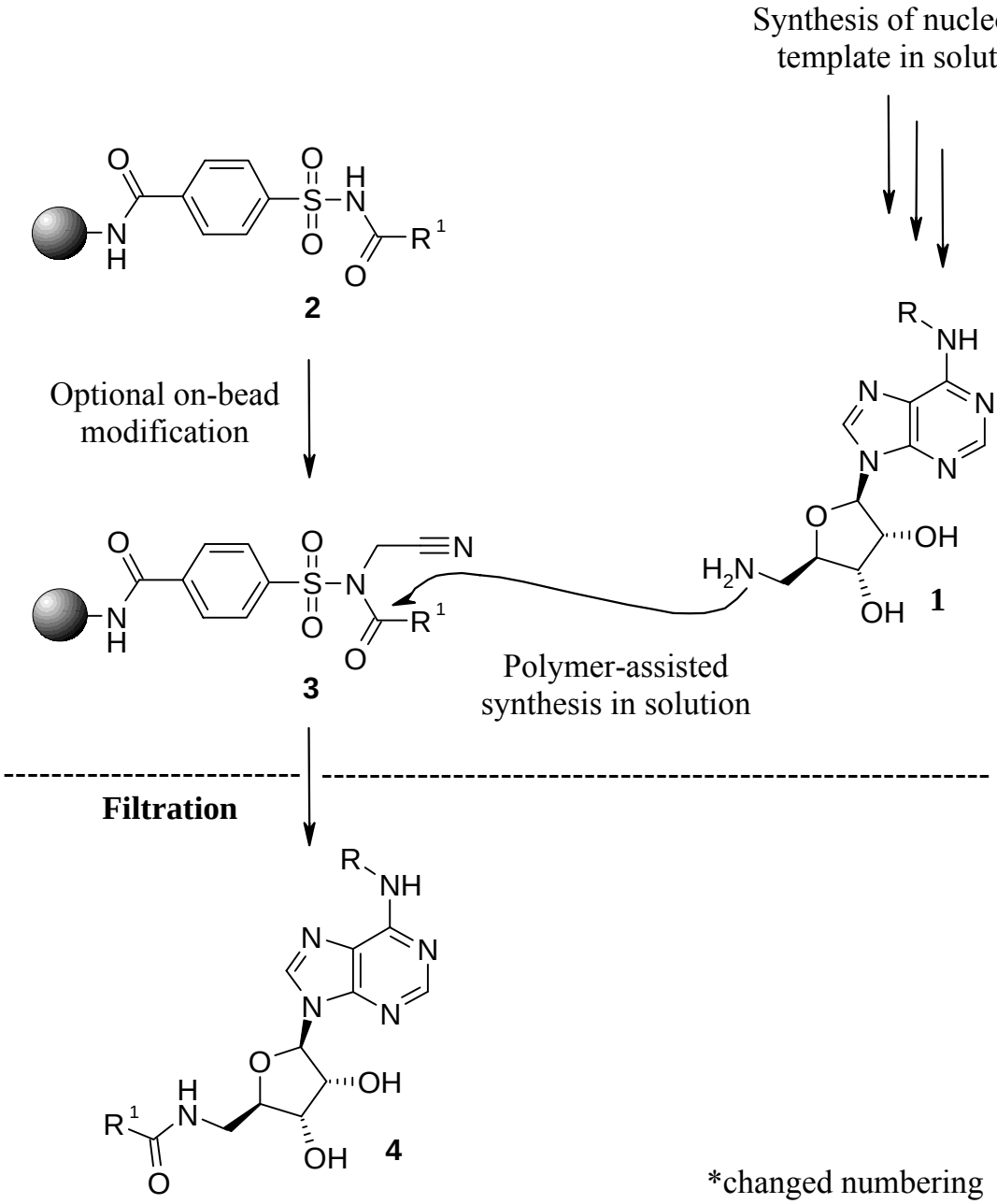

Carboxylic acid diversity fragments were connected to the polymer support via the Kenner safety-catch linker, transformed to acylating species and subsequently transferred to the amino function of appropriate nucleoside templates, obtained by conventional synthesis in solution. The chemoselective attack of weakly nucleophilic amino groups on the N-alkylated N-acylsulfonamide linker allows for the synthesis of 5′-amido-5′-deoxy-N^6-(arylmethyl)adenosines and 3′-amido-3′-deoxy-N^6-(arylmethyl)adenosines, without time-consuming protecting group operations of hydroxyl functions. The full potential of the polymer-bound acylating species can be exploited, when modifications of the carboxylic acid diversity fragment are envisioned prior to activation. Further, the polymer-bound sulfonamide linker has the added benefit of simply filtering off the polymer-bound reagent that is necessary to drive the reaction to completion, leading to final compounds in high yield and purity.
The scope and limitations of the synthetic methodology are discussed.

Biological evaluations revealed that most of the 5′,N^6- and 3′,N^6-di-substituted adenosines display moderate but significant activity against the *P. falciparum* parasite in the low-micromolar range. On molecular basis, 1-deoxy-D-xylulose-5-phosphate (DOXP) reductoisomerase utilizing an adenosyl-containing substrate was identified as a promising metabolic target.

To further explore their potential as antimalarials, selected N^6-substituted adenosine derivatives will be investigated by surface plasmon resonance (SPR) analysis, immobilized on biosensor chip surfaces via appropriate biotin labels in the 5′-position. Thus, a method for the chemoselective introduction of spacer modified biotin labels into unprotected, multi-functional amino-modified adenosine templates was established. A range of novel biotin spacer conjugates attached to a polymer-bound sulfonamide anchor was prepared. The labeled compounds are free of residual biotin and possess a custom tailored distance from the immobilization site, especially suited for the immobilization on streptavidin-functionalized dextran layers of SPR chips. The formation of biotin sulfoxides in the presence of in situ generated peroxides was investigated and is discussed.

6 Zusammenfassung

Im Mittelpunkt dieser Arbeit stand die Darstellung 5′,N^6- und 3′,N^6-modifizierter Adenosinanaloga als Inhibitoren des Malaria Erregers *Plasmodium falciparum*. Eine effiziente Synthese zur Bereitstellung von Adenosinbibliotheken zur biologischen Testung sollte, unter Umgehung aufwendiger chromatographischer Reinigung der Endsubstanzen, etabliert werden.
Mit Hilfe eines polymerunterstützten Syntheseverfahrens in Lösung wurden außergewöhnlich 5′,N^6- und 3′,N^6-disubstituierte Adenosine gewonnen; exemplarisch am Beispiel der Synthese von 5′,N^6-disubstituierten Adenosinen dargestellt(*).

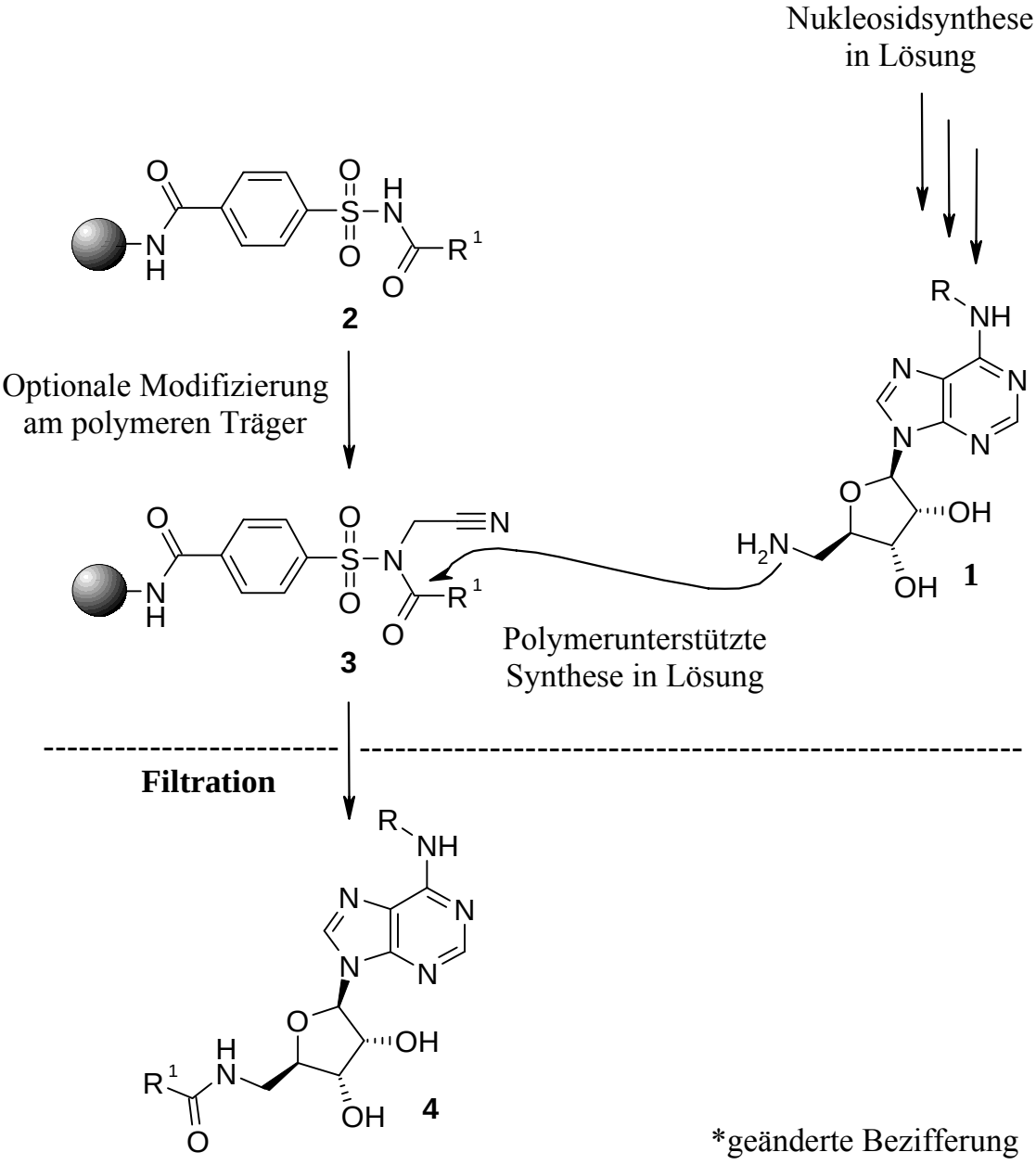

Über den ´Kenner safety-catch linker´ an aminomethyliertes Harz gebundene Carbonsäureäquivalente wurden in Acylierungsreagenzien umgewandelt und anschließend auf die Aminogruppe des Nukleosidgrundgerüsts, welches auf herkömmliche Weise in Lösung synthetisiert wurde, übertragen. Der chemoselektive Angriff der schwach nukleophilen Aminogruppe auf den N-alkylierten N-Acylsulfonamidlinker ermöglicht die schnelle Synthese von 5´-Amido-5´-desoxy-N^6-(arylmethyl)adenosinen und 3´-Amido-3´-desoxy-N^6-(arylmethyl)adenosinen; zeitaufwändige Schutzgruppenoperationen der Hydroxylgruppen des Nukleosid-Templats wurden nicht benötigt.
Das Potential des polymergebundenen Sulfonamidlinkers konnte vollständig ausgeschöpft werden, indem immobilisierte Acylbausteine optional im Sinne einer Festphasensynthese direkt am polymeren Träger modifiziert wurden. Des weiteren ermöglicht dieses Syntheseverfahren die einfache Gewinnung der Endsubstanzen, da das im Überschuß eingesetzte polymergebundene Reagenz, welches zur quantitativen Umsetzung der chemoselektiven Acylierung benötigt wird, durch einfache Filtration aus dem Reaktionsgemisch entfernt werden kann.
Möglichkeiten und Limitierungen der polymerunterstützten Synthese in Lösung zur Gewinnung von disubstituierten Adenosinderivaten werden im Rahmen dieser Arbeit beschrieben und diskutiert.

Biologische Testmodelle zeigten eine moderate aber signifikante Aktivität der synthetisierten 5´,N^6- und 3´,N^6-disubstituierten Adenosine gegenüber *P. falciparum*. Auf molekularer Ebene konnte 1-Deoxy-D-xylulose-5-phosphat (DOXP) Reduktoisomerase als mögliche metabolische Zielstruktur identifiziert werden.

Um die Bandbreite der synthetisierten Adenosinderivate als antimalaria-aktive Substanzen näher zu untersuchen, sollen in Zukunft ausgewählte biotinmarkierte N^6-substituierte Adenosine (immobilisiert an einen Streptavidin Chip) mit Hilfe von Oberflächen-Plasmonen-Resonanz (surface plasmon resonance, SPR) Experimenten untersucht werden. Infolgedessen wurde im Rahmen dieses Projektes ein weiteres polymerunterstütztes Verfahren zur chemoselektiven Einführung verschiedener Biotinmarker in die 5´-Amino-position ungeschützter N^6-substituierter Adenosine entwickelt. Eine Reihe polymergebundener Biotinmarker, die neben dem Biotinlabel ein Abstands-element zwischen Zucker- und Biotinbaustein enthalten, wurde synthetisiert. Synthetisierte biotinmarkierte Adenosinderivate waren frei von überschüs-sigem Biotin. Die Entstehung von Biotinsulfoxiden in Gegenwart von in situ generierten Peroxiden wurde untersucht und diskutiert.

Appendix

Hazard Information

No data exist about toxicological characteristics of compounds synthesized within the course of this project. Hazardous properties cannot be excluded. Thus, compounds should be treated in that manner to avoid any danger during handling that might occur due to unknown properties of substances. Physical, chemical, toxicological, and environmental characteristics of the following solvents and chemicals used are known and summarized in tables below.

Solvents	Category of Danger	Safety Phrases
acetone	F, Xi	S 9-16-26
chloroform	Xn	S 36/37
dichloromethane	Xn	S 23.2-24/25-36/37
diethylether	F^+, Xn	S 9-16-29-33
N,*N*-dimethylformamide	T	S 53-45
dimethylsulfoxide	Xi	S 26
ethanol	F	S 7-16
ethyl acetate	F, Xi	S 16-26-33
n-hexane	F, Xn, N	S 9-16-29-33-36/37-61-62
methanol	F, T	S 7-16-36/37-45
1-methylpyrrolid-2-one	Xi	S 41
pyridine	F, Xn	S 26-28.1
tetrahydrofuran	F, Xn	S 16-29-33
toluene	Xn, F	S 16-25-29-33

Chemicals	Category of Danger	Safety Phrases
acetic acid (> 90%)	C	S 23.2-26-36/37/39-45
acetic anhydride	C	S 26-36/37/39-45
ammonia (25 %)	C, N	S 26-36/37/39-45-61
di-*tert*-butyldiazocarboxylate	Xi	S 26-36
bromoacetonitrile	T, C	S 36/37/39-45
N,*N*-diisopropylcarbodiimide	T	S 26-36/37/39-45
4-dimethylaminopyridine	T	S 37-45
N,*N*,*N*-ethyldiisoproylamine	F, C	S 16-26-36/37/39-45

Chemicals	Category of Danger	Safety Phrases
hydrazine hydrate	T, N	S 53-26-36/37/39-45-60-61
hydrochloric acid (>25%)	C	S 26-36/37/39-45
isoamylnitrite	F, Xn	S 16-24-46
1-naphthylmethylamine	Xi	S 26-37/39
potassium hydroxide	C	S 26-37/39-45
1-propanol	F, Xn	S 7-16-24-26-39
propionic anhydride	C	S 26-45
sodium azide	T^+, N	S 28.1-45-60-61
tetrachloromethane	T, N	S 23.2-36/37-45-59-61
triphenylphosphine	Xn, N	S 22-24-37

Curriculum vitae

Name	Claudia Herforth
Birth date	August 02 1972
Birthplace	Hamburg

1979-1983	Albert-Schweitzer elementary school, Hamburg
1983-1992	Albert-Schweitzer high school, Hamburg
04/93-09/ 97	Pharmacy Studies at the Free University of Berlin and at the University of Hamburg
11/97-04/98	Internship at the department of Scientific & Regulatory Affairs medical, Beiersdorf AG, Hamburg
05/98-10/98	Internship at the Wolfshagen Pharmacy, Hamburg
12/98	Degree in Pharmacy (Approbation)
06/99-07/00	Research Fellowship at the department of Clinical Pharmacy at the University of California, San Francisco, CA, USA
Since 08/00	Ph.D. student at the department of Pharmaceutical Chemistry, Institute for Pharmacy, University of Hamburg

Publications

Claudia Herforth, Jochen Wiesner, Stephan Franke, Abolfasl Golisade, Hassan Jomaa, and Andreas Link: Antimalarial Activity of N^6-substituted Adenosine Derivatives (Part 2). *J. Comb. Chem.* **2002**, *4*, 302-314.

Claudia Herforth, Judith A. Stone, Anura L. Jayewardene, Terrence F. Blaschke, Fang Fang, T. Motoya, Francesca T. Aweeka. Determination of nelfinavir free drug concentrations in plasma by equilibrium dialysis and liquid chromato-graphy/tandem mass spectrometry: important factors for method optimization. *Eur. J. Pharm. Sci.* **2002**, *15*, (2), 185-195.

Abolfasl Golisade, Jochen Wiesner, Claudia Herforth, Hassan Jomaa, and Andreas Link: Anti-Malarial Activity of N^6-substituted Adenosine Derivatives. Part I. *Bioorg. Med. Chem.* **2002**, *10*, 769-777.

Abolfasl Golisade, Claudia Herforth, Ludo Quirijnen, Louis Maes, and Andreas Link: Improving an Antitrypanosomal Lead Applying Nucleophilic Substitution on a Safety Catch Linker, *Bioorg. Med. Chem.* **2002**, *10*, 159-165.

Abolfasl Golisade, Claudia Herforth, Karen Wieking, Conrad Kunick, and Andreas Link: Biotin Labelling of amines by polymer assisted solution phase synthesis. *Bioorg. Med. Chem. Lett.* **2001**, *11*, 1783-1786.

Presentations:

Claudia Herforth, Philipp Heidler, Andreas Link: Synthesis and Antimalarial Activity of Novel N^6-Substituted Adenosine Derivatives. Poster presentation. IS3NA XV International Round Table on Nucleosides, Nucleotides and Nucleic acids, Leuven, Belgium, 10.-14. September 2002, book of abstracts, abstract No. 106.

Abolfasl Golisade, Claudia Herforth, Jochen Wiesner, Hassan Jomaa, Andreas Link: Substituted Adenosines as Anti-Protozoal Agents. Poster presentation. EUFEPS Fourth European Graduate Student Meeting, Frankfurt/Main, 08.-10. February 2002, book of abstracts, abstract No. 22.
APV Award for Excellence in Pharmaceutical Research

Andreas Link, Claudia Herforth, Abolfasl Golisade: Biotinylierung durch Polymer-unterstützte Synthese in Lösung. Oral presentation. Jahreskongress der Deutschen Pharmazeutischen Gesellschaft, Halle 10.-13. Oktober 2001. *Arch. Pharm. Pharm. Med. Chem.* **2001**, *334*, Suppl. 2/01, 17 No. V1-11.

Claudia Herforth, Abolfasl Golisade, and Andreas Link: Biotin labeling of nucleoside derivatives via polymer-assisted solution-phase synthesis. Oral presentation. 222nd Meeting of the American Chemical Society 2001, 26.-30. August **2001**, Chicago, IL, U.S.A., book of abstracts, abstract No. MEDI 311.

Abolfasl Golisade, Claudia Herforth, and Andreas Link: Novel N^6-substituted adenosines: synthesis and biological evaluation as anti-malarial agents. Poster presentation. 222nd Meeting of the American Chemical Society 2001, 26.-30. August **2001**, Chicago, IL, U.S.A., book of abstracts, abstract No. MEDI 243.

Claudia Herforth, Abolfasl Golisade, and Andreas Link: High Yielding Polymer Assisted Synthesis of N^6-Alkyl-5′-Amido-5′-Deoxyadenosines Targeted at Adenosine Binding Motifs. Oral presentation. EUFEPS Third European Graduate Student Meeting, Frankfurt/Main, 23.-25 February 2001. *Arch. Pharm. Pharm. Med. Chem.* **2001**, *334*, Suppl. 2/01, 22 No. 62.